DISSERTATION

DEVELOPMENT AND APPLICATION OF MICROBIAL COMMUNITY PROFILING TECHNIQUES FOR MINE DRAINAGE BIOREMEDIATION

Submitted by

Sage Royal Hiibel

Chemical and Biological Engineering Department

In partial fulfillment of the requirements

For the Degree of Doctor of Philosophy

Colorado State University

Fort Collins, Colorado

Fall 2008

COLORADO STATE UNIVERSITY

August 4, 2008

WE HEREBY RECOMMEND THAT THE DISSERTATION PREPARED UNDER OUR SUPERVISION BY SAGE ROYAL HIIBEL ENTITLED "DEVELOPMENT AND APPLICATION OF MICROBIAL COMMUNITY PROFILING TECHNIQUES FOR MINE DRAINAGE BIOREMEDIATION" BE ACCEPTED AS FULFILLING, IN PART, REQUIREMENTS FOR THE DEGREE OF DOCTOR OF PHILOSOPHY.

Committee on Graduate Work

Dr. James C. Linden

Dr. S. Ranil Wickramasinghe

Co-Advisor: Dr. Amy Pruden

Advisor: Dr. Kenneth F. Reardon

Department Head: Dr. David S. Dandy

ABSTRACT OF DISSERTATION

DEVELOPMENT AND APPLICATION OF MICROBIAL COMMUNITY PROFILING TECHNIQUES FOR MINE DRAINAGE BIOREMEDIATION

Acid mine drainage (AMD) is a major environmental and public health issue throughout the world due to its deleterious effects on humans and the environment. AMD is the result of the oxidation of mineral surfaces exposed during mining activities, and is characterized by elevated levels of sulfate, acidity, and Fe(II). The increased acidity also mobilizes toxic trace metals, resulting in contamination of both the runoff and downstream waters. One attractive means of passively treating AMD is through sulfate-reducing bioreactors (SRBRs). These bioreactors typically contain a solid organic substrate, usually wood chips or compost, which provides a slow-release carbon substrate to support a complex anaerobic microbial community that drives remediation. The research presented in this dissertation recognizes the importance of the microbial community in AMD remediation and has focused on furthering the understanding of these communities.

A relationship between the choice of microbial inoculum and bioremediation performance was established in two separate laboratory-scale experiments. Using 16S rDNA-based profiling techniques, it was recognized that SRBRs that performed well contained a common set of three key functional groups in their microbial communities: cellulose degraders, fermenters, and sulfate-reducing bacteria (SRB). Quantitative

methods also revealed that SRB were present at concentrations near or below the detection limits of traditional 16S profiling techniques. It was therefore determined that a more appropriate biomolecular target was necessary to include the sulfate reducers in the overall microbial community profile.

Subsequent analyses of pilot- and field-scale SRBRs targeted both the 16S and the *apsA* functional gene, which catalyzes the reduction of sulfate to sulfite and is found in all SRB. The analysis of the *apsA* genes sequences provided higher resolution of the numerically small SRB subset of the overall community. Sets of *apsA* and 16S gene clone sequences were also compared with multivariate statistical analyses, allowing more objective and statistically valid conclusions to be made. Although analyses of the 16S gene sequences of the field-scale SRBRs' microbial communities did not reveal obvious differences between the two, the *apsA* gene sequences of each SRBR were significantly different. The *apsA* clone library revealed that *Thiobacillus* spp. which are species capable of oxidizing sulfur compounds to sulfate, were prevalent at the SRBR with poor remediation performance. These studies confirmed that the use of a functional gene could improve resolution of a specific subset of species, although it was also clear that the choice of targets will affect any conclusions about the microbial community.

To further improve the characterization techniques applied to the SRBRs, a novel biomolecular method, called active community profiling (ACP), was developed and validated using model one- and two-species systems. ACP identifies the active members of a mixed microbial community through the ratio of cellular rRNA to rDNA, which is known to be proportional to growth rate. The high throughput nature of ACP allows the user to evaluate microbial communities at biologically relevant time scales. When coupled with traditional physiochemical analysis, the method offers a powerful new tool to help understand community dynamics at the microbial scale.

ACP was employed to explore the effect of bioaugmentation and biostimulation on the performance and structure of microbial communities in AMD treatment systems. Two different groups of microorganisms and two different carbon sources were used to augment and stimulate column SRBRs. The performance results were unexpected, as all the columns remediated AMD to a similar level. However, ACP analysis revealed that the active members of the columns' microbial communities were distinctive, and it was determined that stimulation or augmentation at the top of the microbial carbon chain resulted in increased diversity of the active microbial species.

The research projects presented in this dissertation have emphasized the role of the microbial community associated with AMD remediation. Characterization of these microbial communities with a multitude of biomolecular tools at several scales has significantly advanced the understanding of the community's structure, function, and activity. The coupling of this microbial-level understanding with macro-level remediation performance information has also furthered the integration of microbial community dynamics with bioreactor design. The research approaches and methodologies developed in this dissertation have a wide range of application, and have provided unique and valuable contributions to the body of scientific knowledge of AMD treatment specifically and to microbial ecology and bioremediation in general.

Sage Royal Hiibel
Department of Chemical and Biological Engineering
Colorado State University
Fort Collins, CO 80523
Fall 2008

ACKNOWLEDGMENTS

I would like to acknowledge my advisors, Dr. Ken Reardon and Dr. Amy Pruden, and my committee members, Dr. Jim Linden and Dr. Ranil Wickramasinghe, for their time and input throughout the project. I would also like to thank Dr. Reardon and Dr. Pruden for their friendship, support, encouragement, and all of their guidance on everything from lab work to my professional aspirations for the last four years. Both have been instrumental in my personal and professional development, and it has been an honor and privilege to work with them.

I would like to thank Luciana Pereyra, who has been a never-ending source of information, support, and assistance as we worked side-by-side on the project. Thanks also to Claire Lavelle and Marilyn Gross for making sure I was always taken care of and all my paperwork was signed. I would also like to thank all of the members of the Reardon and Pruden labs, both past and present, for all of their support, advice, assistance, and patience through the years.

I would like to thank the financial support of the US EPA Office of Research and Development Engineering Technical Support Center, the Rocky Mountain Hazardous Substance Research Center, and the National Science Foundation. I would also like to thank David Reisman for always fitting us in the ORD budget and for all of his support of our group.

Finally, I would like to thank all my family and friends who have helped me through the ups and downs all these years. Thank you to my parents for their never ending support from the very beginning. And a very special thank you to my wife and best friend, Schyler, for all of her love and encouragement through this process.

Table of Contents

List of Figures

List of Tables

Chapter 1 Introduction and Dissertation Overview

1.1 Acid Mine Drainage

1.1.1 Description and Origin

Acid mine drainage (AMD) is characterized by elevated levels of sulfate, acidity, ferrous iron, and other metal ions. AMD is generated via a series of reactions, which are analogous to reactions involved in the natural weathering of rocks and minerals, in which sulfuric acid is produced from the oxidation of sulfidic minerals. Mining activities expose new mineral surfaces for oxidation, leading to AMD generation rates significantly greater than those associated with natural weathering (Singer and Stumm, 1970).

The generation of AMD is summarized in Equations 1.2.-1.5 (Singer and Stumm, 1970). The simplest and most prevalent sulfidic mineral, pyrite (FeS_2), is used as a representative iron disulfide mineral. Overall, pyrite, oxygen, and water react to produce ferric hydroxide ($Fe(OH)_3$) and sulfuric acid (Equation 1.1). Ferric hydroxide, also known as Yellowboy, is a solid that precipitates at pH values above 3.5 (Nordstrom and Southam, 1997) and is responsible for the red and yellow coloration typically associated with AMD.

$$FeS_2 + 3\tfrac{3}{4}\,O_2 + 3\tfrac{1}{2}\,H_2O \rightarrow Fe(OH)_{3(sol)} + 2\,H_2SO_4 \qquad \textbf{Equation 1.1}$$

The first reaction of AMD generation (Equation 1.2) is the oxidation of pyrite by oxygen. Sulfur is oxidized to sulfate and ferrous iron is released. Each mole of pyrite oxidized also results in two moles of acidity generated.

$$FeS_2 + 3\tfrac{1}{2} O_2 + H_2O \rightarrow Fe^{2+} + 2\,SO_4^{2-} + 2\,H^+ \qquad \textbf{Equation 1.2}$$

The second reaction (Equation 1.3) is the oxidation of ferrous to ferric iron. One mole of acidity is consumed per mole of pyrite initially oxidized. This reaction is considered the rate–limiting step of the overall formation of AMD under abiotic conditions (Nordstrom and Southam, 1997). However, the oxidation can also be catalyzed by certain bacteria, e.g., *Acidithiobacillus ferrooxidans* (formerly known as *Thiobacillus ferrooxidans*) and *Leptospirillum ferrooxidans* (Schrenk et al., 1998; Bond et al., 2000), which can increase the oxidation rate by up to six orders of magnitude (Nordstrom and Southam, 1997).

$$Fe^{2+} + \tfrac{1}{4} O_2 + H^+ \rightarrow Fe^{3+} + \tfrac{1}{2} H_2O \qquad \textbf{Equation 1.3}$$

The third reaction (Equation 1.4) is the hydrolysis of ferric iron. This step generates three moles of acidity per mole of initial pyrite, and is also responsible for Yellowboy formation.

$$Fe^{3+} + 3\,H_2O \rightarrow Fe(OH)_{3(sol)} + 3\,H^+ \qquad \textbf{Equation 1.4}$$

The final reaction (Equation 1.5) is the oxidation of additional pyrite by ferric iron produced in the first (Equation 1.2) and second (Equation 1.3) reactions. This step is self propagating and will occur until either the pyrite or ferric iron is consumed. The reaction does not require oxygen as an oxidizing agent. Thus, once AMD generation has begun, it may continue even under anoxic conditions.

$$FeS_2 + 14\,Fe^{3+} + 8\,H_2O \rightarrow 15\,Fe^{2+} + 2\,SO_4^{2-} + 16\,H^+ \qquad \textbf{Equation 1.5}$$

1.1.2 Environmental Impact

AMD is considered to be a multi-factor environmental pollutant with acidity and metal toxicity being its two main factors, although salinization and sedimentation/precipitation can also play key roles in surface receiving waters (Gray, 1997). The effects of AMD can be categorized as chemical, physical, biological, and ecological (Figure 1.1), with overall impacts ranging in severity from aesthetic/organoleptic to complete ecological collapse. Direct chemical effects include decreased pH and increased levels of acidity and soluble metals. Indirect chemical effects are a result of the AMD mixing with receiving waters and can include increased levels of particulate metals and an imbalance in the natural bicarbonate buffering system. The major physical effect of AMD is the adsorption of metals on sediments and other surfaces that are exposed; this sorption results in the red coloration typically associated with AMD. Other physical effects may include sedimentation, increased turbidity, and substrate modifications, depending on the conditions of the receiving water.

The combined physiochemical effects of AMD can result in biological impacts to micro- and macroscopic organisms that come in direct contact with the AMD or rely on water sources contaminated by it. The biological effects can range from behavioral changes, such as migration of species or avoidance of a water supply, to reproduction or osmoregulatory failure. These biological changes in specific species can be confounded at the ecological level by predator-prey imbalances and food chain modifications. Bioaccumulation of toxic metals in the food chains may also be a concern. Direct effects of AMD exposure can also be observed at the ecological level in the form of habitat modification that can lead to niche loss and ultimately species elimination.

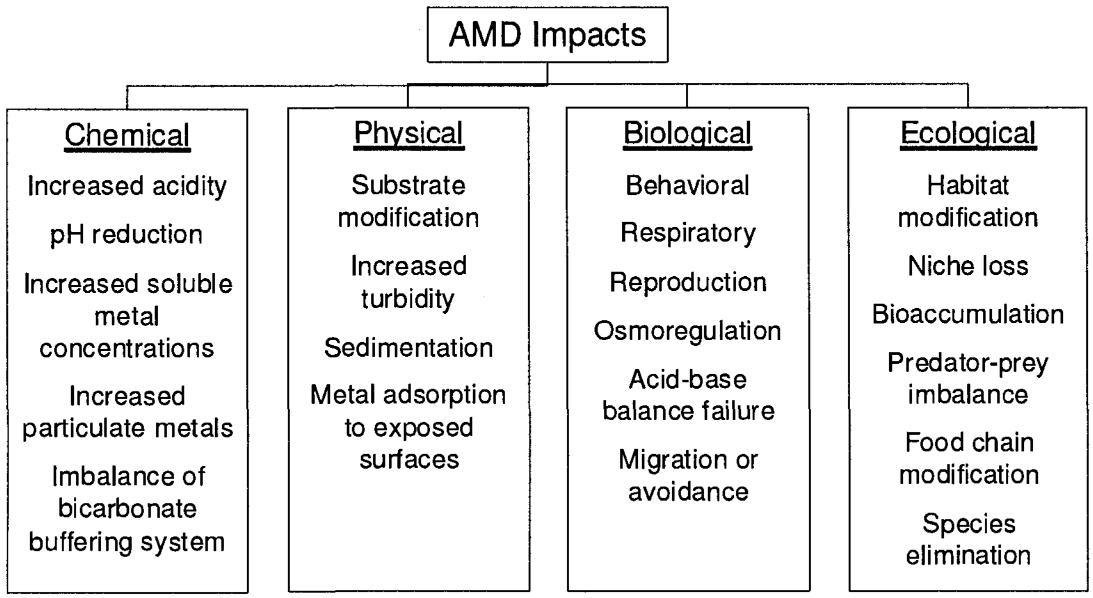

Figure 1.1 – Environmental impacts of acid mine drainage (adapted from Gray (1997)).

1.1.3 Scope of Problem

Estimating the scope of AMD contamination and clean-up costs is a challenge due to the remote geographic locations typical of mining operations, both abandoned mines from the past and those operating today. Abandoned mines are of particular concern due to the difficulties associated with locating, tracking, and then financing remediation of sites without a known responsible party. The uncertainty and difficulty of locating these abandoned sites is demonstrated by the wide range in estimates of just how many mine sites actually exist. In 1993, the United States Forest Services estimated between 20,000 and 50,000 total mine sites generating acid drainage (USDA, 1993). The same year, the Mineral Policy Center estimated 557,650 abandoned mine sites (Lyon *et al.*, 1993).

Beyond the uncertainty of the number of AMD-generating sites is the difficulty in estimating the scope of those sites and how many receiving waterways they affect. In 1993, the same USDA report (USDA, 1993) estimated that between 5,000 and 10,000 miles of streams were impacted by mine drainage; the same Mining Policy Center report (Lyon *et al.*, 1993) estimated 12,000 miles of waterways and 180,000 acres of lakes and reservoirs were contaminated by AMD.

Despite the differences in the numbers of mines reported and their impact on waterways, the enormous cost of cleanup is agreed upon by all. The U.S. Environmental Protection Agency currently has more than eighty abandoned mine sites on the National Priorities List (NPL); many of these are categorized as mega-NPL sites meaning that each will cost more than $50 million to remediate (EPA, 2005). In the U.S. alone, the total estimated remediation costs for abandoned mine sites ranges from $32 to $72 billion (EPA, 2005). Future remediation costs at currently operating mines will add to those numbers.

1.2 Current Remediation Options

Current remediation options for AMD can be divided into abiotic and biological treatments. Each of these two groups can be further split into active or passive systems. Treatments that utilize mechanized procedures for the addition or removal of chemicals or materials and require constant monitoring and maintenance are considered active. Because of this, active treatment options are generally more expensive to build and operate, but their remediation performance is more predictable. Figure 1.2 outlines some of the more common remediation systems currently in use at the pilot or full scale.

While all of the treatment options aim to decrease the acidity and metal levels in mine drainage, the abiotic methods generally do not remove sulfate. On the other hand, most of the biological treatments include microbial species that utilize sulfate as electron acceptors, thereby reducing sulfate levels in the AMD. The choice of the most appropriate method of treatment is ultimately made based on a combination of technical and economical considerations (Coulton *et al.*, 2003; Miller *et al.*, 2006). The maturity and robustness of the treatment method, as well as the site manager's confidence level in a specific method, all play roles on the technical side of the decision, while the capital, operating, and decommissioning costs dictate the economical aspect of the decision (EPA, 2005; Johnson and Hallberg, 2005).

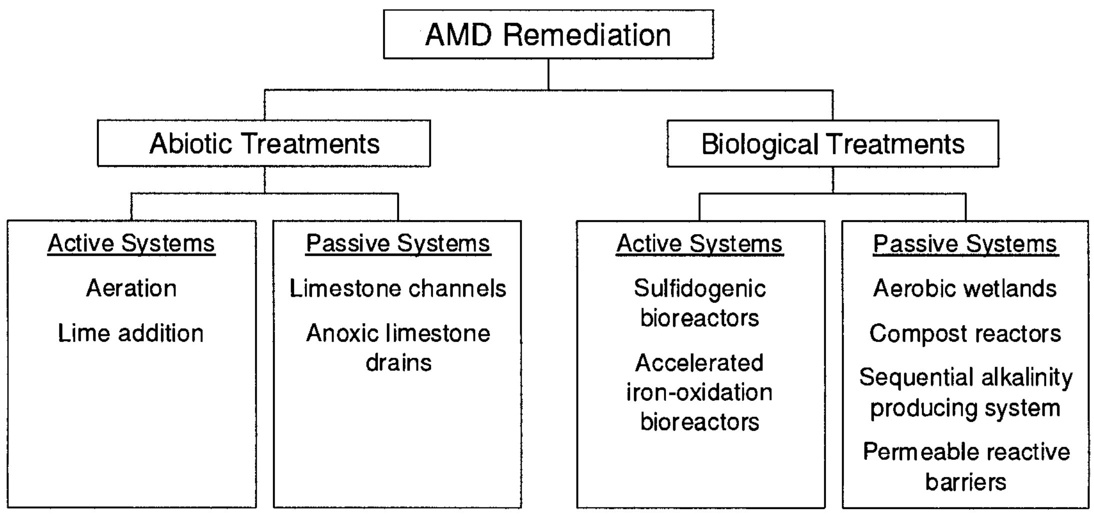

Figure 1.2 - Treatment options for AMD remediation (adapted from (Johnson and Hallberg, 2005)).

1.2.1 Abiotic Treatments

1.2.1.1 Active Methods

The most commonly used method to mitigate AMD is the addition of a low-cost chemical neutralizing agent. There are a wide variety of neutralizing agents available (Table 1.1), but a low cost alkaline material such as lime (CaO) is typically used. The alkalinity addition increases the pH and can cause the metals to precipitate as hydroxides or carbonates. Treatment takes place via two unit operations, with neutralization occurring in the first and solid separation occurring in the second. While this approach is effective at removing acidity and metals from the aqueous phase, the process byproduct is an acidic, metal-rich sludge that requires large storage capacity and further treatment before they are safe for disposal (Johnson and Hallberg, 2005).

Table 1.1 – Commonly used reagents for abiotic AMD precipitation (adapted from (Coulton et al., 2003)).

Reagent		Unit Cost ($/ton)	Theoretical		Actual		
			Dose (kg per kg Fe)	Cost (per kg Fe ($))	Efficiency (%)	Dose (kg per kg Fe)	Cost (per kg Fe ($))
Calcium oxide	CaO	197	1.00	0.20	65	1.54	0.30
Calcium hydroxide	$Ca(OH)_2$	197	1.33	0.26	65	2.05	0.41
Magnesia	MgO	433	0.72	0.31	80	0.90	0.39
Magnesium hydroxide	$Mg(OH)_2$	492	1.04	0.51	80	1.30	0.65
Sodium hydroxide	NaOH	650	1.43	0.93	95	1.50	0.98
Sodium carbonate	Na_2CO_3	384	1.89	0.73	95	2.00	0.77

At its most basic concept and implementation, chemical treatment via the addition of neutralizing agents is a low technology approach, although there have been efforts made to improve the efficiency and minimize the volume of waste generated. These improvements inherently raise the price of treatment, but those increases may be offset by cost reductions associated with storage, handling, and treatment of wastes and reduced chemical usage. One such improvement is the use of multiple neutralization/separation stages to target specific metals for removal. Because of the amphoteric behavior of many metal hydroxides (Figure 1.3) and carbonates, this type of system is especially useful if the AMD contains metals with a wide range of isoelectric points. By increasing the pH in a step-wise fashion, each metal (or group of metals) can be sequentially precipitated and removed without risk of re-solubilizing those previously precipitated. Other modifications include recycling a portion of the sludge back into the lime holding tanks for dewatering (Coulton *et al.*, 2003), using a pulsed fluidized-bed reactor setup to remove surface buildup on the limestone (Miller *et al.*, 2006), and the inclusion of aeration to oxidize metals, thus facilitating their precipitation (Klein and Neufeld, 2005).

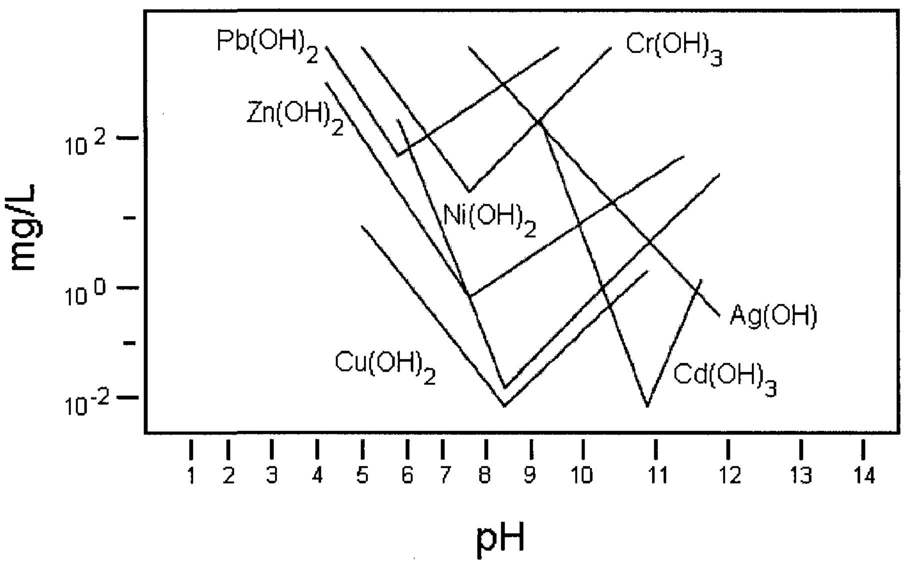

Figure 1.3 - Solubility of liquid-phase metal hydroxides at equilibrium as a function of pH (adapted from (EPA, 1980)).

1.2.1.2 Passive Methods

The same principles associated with the addition of neutralizing agents discussed above can also be implemented in a passive form via limestone channels and anoxic limestone drains (ALDs). Limestone channels are simply limestone-lined ditches or culverts through which AMD is directed elevate the pH. As a result of the elevated pH, metal removal via precipitation occurs through the length of the channel. This can give rise to an armoring effect in which the metal precipitates coat and shield the limestone surfaces from the AMD, thus hampering further remediation. To avoid armoring, limestone channels should be sloped to increase fluid velocity (Miller *et al.*, 2006).

ALDs can be thought of as packed bed reactors in which limestone rocks are used as the packing material. The systems can be implemented in a horizontal fashion, generally in the form of a lined and capped trench filled with limestone, or in a vertical fashion as gravity-fed columns. The exclusion of oxygen from these systems is important to prevent precipitation of metal hydroxides in the ALD, which would result in clogging or armoring of the limestone surfaces (Miller *et al.*, 2006). An oxidation basin immediately after the ALD allows the metals to precipitate outside of the drain (Robbins *et al.*, 1999).

1.2.2 Biological Treatment

Like abiotic treatment systems, biological methods aim to remove metals and increase the pH of AMD solutions. The most common biological approach is to use sulfate-reducing bacteria (SRB), which require an external electron donor, usually a short chain organic compound or hydrogen, and sulfate from the AMD as an electron acceptor to form hydrogen sulfide and bicarbonate (Equation 1.6). The hydrogen sulfide reacts with the dissolved divalent metals in the AMD to form insoluble metal sulfide precipitates that are retained within the barrier (Equation 1.7). Additionally, the bicarbonate reacts with free hydrogen ions in the system to neutralize the acidity (Equation 1.8). In these three reactions, the SRB can drive the removal the primary constituents associated with AMD: sulfate, metals, and acidity.

$$2\ CH_2O + SO_4^{-2} \rightarrow 2\ HCO_3^- + H_2S \qquad \textbf{Equation 1.6}$$

$$Me^{+2} + S^{-2} \rightarrow MeS_{(s)} \qquad \textbf{Equation 1.7}$$

$$HCO_3^- + H^+ \rightarrow CO_{2(g)} + H_2O \qquad \textbf{Equation 1.8}$$

1.2.2.1 Active Treatment

Sulfidogenic bioreactors are the most common active, biological remediation method. The bioreactors can be implemented in several configurations, but all use anaerobic cultures of SRB, grown in a medium formulated for the specific culture with a supplied carbon source, to produce hydrogen sulfide gas. The carbon source supplement is dictated by cost, availability, and handling ease, but is typically a small organic molecule such as acetate, lactate, ethanol, or else hydrogen in the form of a synthesis gas from an industrial operation (Sorokin et al., 2007; Muyzer and Stams, 2008). The sulfide gas produced by the SRB is then contacted with the AMD so that metal sulfide precipitation can occur as described in Equation 1.7. The metal precipitation can either occur in the same or a different unit than where SRB reside, depending on whether the H_2S is separated from the bacterial culture before being contacted with the AMD.

The remediation performance of sulfidogenic bioreactors is dependent on the hydrogen sulfide production from the SRB. When operating properly, the systems perform very well and result in high levels of metal and acidity removal. However, the costs associated with the growth medium and operation can be prohibitive. In some cases, excess sulfide is be converted to elemental sulfur for re-use or sale using sulfur-oxidizing bacteria in a second bioreactor as a way to offset the operation costs (Sorokin *et al.*, 2007).

1.2.2.2 Passive Treatment

There are two main groups of passive, biological treatment groups; sulfate-reducing bioreactors (SRBRs) and wetlands. The SRBRs operate based on the same principle as the active sulfidogenic bioreactors, but are passive systems by design and operation. A more detailed discussion of SRBRs is given in Section 1.3, below.

Wetlands can operate in one of two basic configurations; aerobic or anaerobic. Aerobic wetlands are shallow, surface flow systems with vegetation, usually cattails (*Typha latifolia*) (Brenner, 2001). The bottoms are often covered with a shallow layer of organic material to promote biologic activity and/or limestone that helps buffer the acidity to aid in precipitation and decrease toxicity to vegetation. These systems are designed to provide increased residence time and aeration so that metals can precipitate from mildly acidic or net alkaline AMD. The vegetation acts as a natural physical filter to aid in the removal of the metal precipitates, but it can also actively aid in metal removal via uptake in the root systems (Barton and Karathanasis, 1999; Brenner, 2001).

In an anaerobic wetland system, the AMD flow is subsurface through an anaerobic, solid, organic substrate with vegetation at the surface above the flow path. These systems promote contact of the drainage with the plant roots and with a microbial community associated with the organic substrate. The primary mode of remediation in these systems is chemical and biological reduction of metals, although oxidation and hydrolysis reactions near the surface and phytoremediation also play a role (Barton and

Karathanasis, 1999). The anaerobic conditions are conducive to the growth of SRB and the formation of metal sulfides and alkalinity, similar to the processes described above for sulfidogenic bioreactors (Equations 1.6-1.8).

Both aerobic and anaerobic wetlands are promising passive remediation options for AMD, and have been implemented widely throughout the world (see (Sheoran and Sheoran, 2006) for examples). Unfortunately, wetlands require large amounts of relatively flat ground to be successful, ultimately making them an unlikely option for AMD sites located in mountainous areas. Metal removal in wetlands is also hampered by a limited pH range required for vegetation growth (Barton and Karathanasis, 1999; Brenner, 2001; Miller et al., 2006).

Another passive biological remediation system that can potentially overcome the space and pH limitations of wetlands is the sequential alkalinity-producing system (SAPS), also known as vertical flow wetlands. SAPSs are multi-staged hybrids of the anaerobic wetland systems and ALDs described above. AMD flows vertically through a series of organic substrates and limestone beds. The organic layer promotes biologic growth for iron reduction and removal and for sulfate reduction for metal removal as sulfides; removal of the iron prevents armoring of the downstream limestone region (Barton and Karathanasis, 1999; Brenner, 2001; Miller et al., 2006). The vertical flow design of SAPS is an attractive alternative to wetlands because of its smaller footprint and viability in a mountainous region. Through sequential staging of the two layers, the pH of system can be raised in a step-wise fashion to remove specific metals based on their isoelectric point (see Figure 1.3). Unfortunately, SAPS systems are extremely susceptible to aluminum oxide armoring of the limestone sections, and thus prone to fail when aluminum is present in the AMD (Miller *et al.*, 2006).

1.3 Sulfate-Reducing Bioreactors

1.3.1 Description

SRBRs are a hybrid of the anaerobic wetlands and the sulfidogenic bioreactors. They are flow-through systems and are comprised of organic matter and a mixed microbial community. The systems can be implemented at the surface in a defined bioreactor volume, or can be installed in the subsurface, transverse to the flow path of the contaminated water. The surface installments are also known as biogeochemical reactors and the subsurface installments are often called sulfate-reducing permeable reactive zones (SR-PRZs). The organic matter consists of complex polymeric substances, such as wood chips containing cellulose and lignin, which act as economical slow-release carbon and energy sources for the microbes. The sulfate-reducing mixed microbial community develops from an inoculum, typically provided by an inexpensive, readily available source such as dairy manure. The inoculum is usually a generic material with high microbial density and diversity, such as dairy manure, rather than an inoculum specifically designed for a particular site. The assumption is that the microbial species necessary for remediation will be present due to the high diversity. Due to the very different environments of a cow rumen and an AMD remediation system (e.g. temperature, nutrients, and acidity), the adaptation period for microbes can be quite long.

The microbial community of SRBRs is typically represented as a carbon flow-based network consisting of four types of microorganisms (Figure 1.4). Polysaccharide-degrading species hydrolyze the organic substrate into short-chain biopolymers (e.g., cellobiose, glucose, and mannose) that are then converted to alcohols and low molecular weight organic acids by the fermentative species. These small organic molecules then act as electron donors for the SRB, which are the microbes directly responsible for the AMD remediation. Two other classes of microorganisms, acetogens and methanogens, may also be found in the microbial community. Methanogenic species, which may be present in the original dairy manure inoculum, can compete with SRB for electron donors (e.g., hydrogen and acetate), while acetogens can act as intermediates between the fermenters and SRB.

1.3.2 Design Considerations

Although SRBRs have performed as designed in the field without interruption (Blowes, 2000), other similarly designed systems either functioned poorly or failed (Benner et al., 1999; Waybrant et al., 2002). Previous research has attempted to address the poor performances through study of the organic substrates used, including straw (Bechard et al., 1994), sawdust (Wakao et al., 1979), peat (Eger and Lapakko, 1988), spent mushroom compost (Dvorak D.H., 1992), whey (Christensen et al., 1996), and oak chips (Chang, 2000). However, no clear solution has been provided.

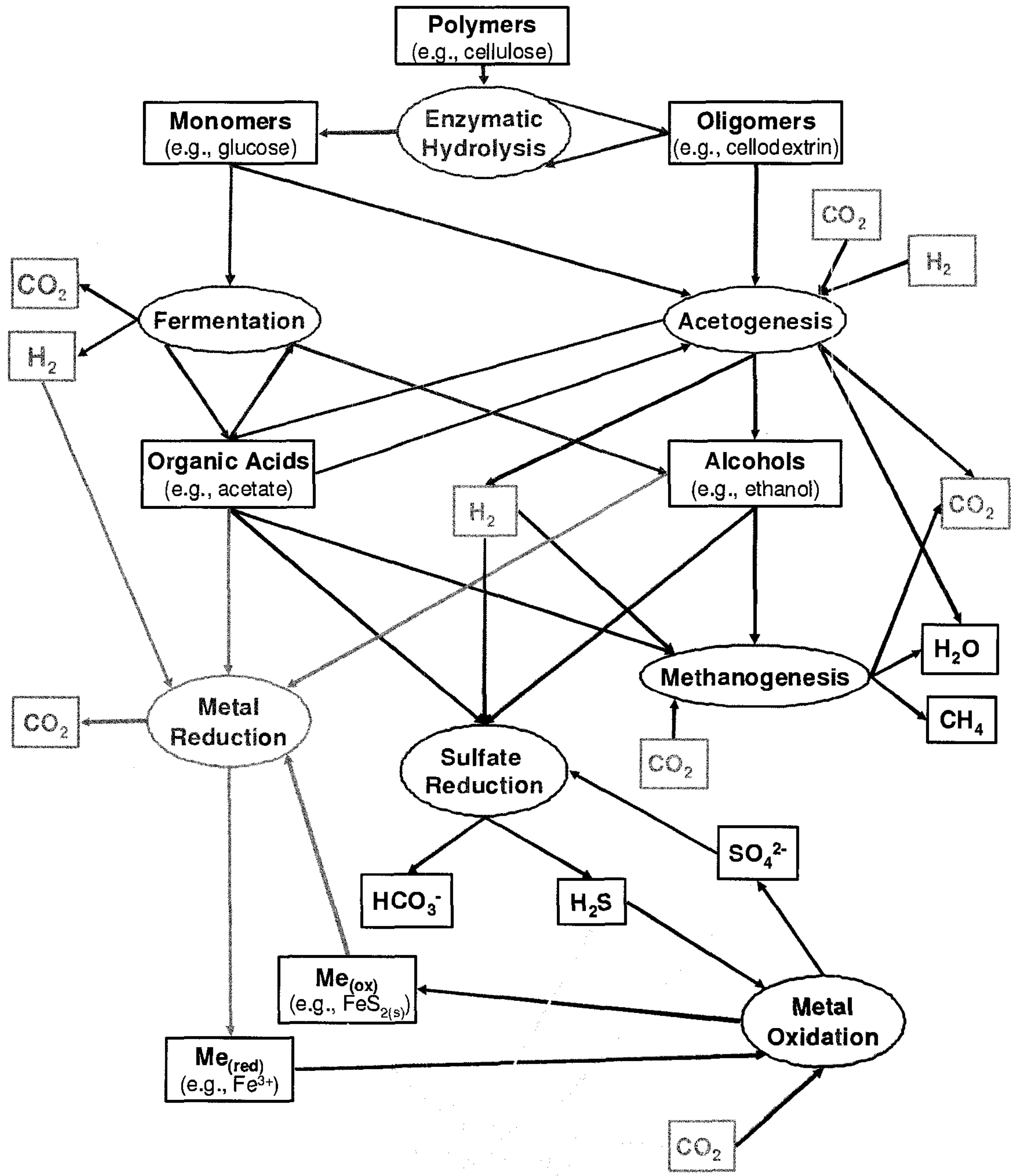

Figure 1.4 – A simplified carbon flow diagram for SRBRs.

A more likely yet relatively unexplored possibility for poor SRBR performance is the nature of the microbial inoculum. Due to a poor understanding of the fundamental microbial aspects, current efforts to improve SRBR function involve guesswork. In particular, the microorganisms actively involved in AMD remediation are not well characterized. Typically, the microbial aspect of SRBR design has been treated as a black box without consideration of the microorganisms involved. Since SRBR operation is highly dependent on microbial activity, a better understanding of the role of the mixed microbial community in these systems is needed.

1.4 Research Questions

The overall objective of this research has been to gain a better understanding of the structure and function of the microbial community associated with AMD remediation so as to better design, implement, and operate SRBRs. Lab-, pilot-, and field-scale bioreactors were studied to aid in the characterization of these microbial communities and to help elucidate the connection between the community structure and bioremediation performance. Specific research questions explored in the course of this dissertation include:

- Does the choice of microbial inoculum affect the remediation performance of an SRBR?
- Are specific microbial groups responsible for improved SRBR remediation performance?
- Does the choice of organic substrate affect the phylogenetic structure of the microbial community of an SRBR? Can the SRB be directly stimulated with ethanol?
- How do the microbial communities of field-scale SRBRs compare to one another? How do they compare to lab-scale SRBRs?

- Can functional gene analysis improve the phylogenetic resolution of a complex microbial community as compared to 16S gene analysis?
- What are the effects of biostimulation and bioaugmentation on the microbial community of an SRBR? Can overall remediation performance be improved through biostimulation or bioaugmentation?

In the process of answering the research questions above, a high-throughput method to characterize the active members of a mixed microbial community was developed. The method, termed active community profiling (ACP), was employed in the final phase of experimental work, and has potential applications in a variety of fields that use mixed microbial communities. The approaches used to address the research questions posed above and the overall dissertation layout are discussed in more detail in Chapter 2.

1.5 References

Barton, C.D., and Karathanasis, A.D. (1999) Renovation of a failed constructed wetland treating acid mine drainage. *Environmental Geology* **39**: 39-50.

Bechard, G., Yamazaki, H., Gould, W.D., and Bedard, P. (1994) Use of Cellulosic Substrates for the Microbial Treatment of Acid Mine Drainage. *Journal of Environmental Quality* **23**: 111-116.

Benner, S.G., Blowes, D.W., Gould, W.D., Herbert, R.B.J., and Ptacek, C.J. (1999) Geochemistry of a Permeable Reactive Barrier for Metals and Acid Mine Drainage. *Environmental Science and Technology* **33**: 2793-2799.

Blowes, D.W., C.J. Ptacek, S.G. Benner, C.W.T. McRae, T.A. Bennett, and R.W. Puls (2000) Treatment of inorganic contaminants using permeable reactive barriers. *Journal of Contaminant Hydrology* **45**: 123-137.

Bond, P.L., Druschel, G.K., and Banfield, J.F. (2000) Comparison of acid mine drainage microbial communities in physically and geochemically distinct ecosystems. *Applied and Environmental Microbiology* **66**: 4962-+.

Brenner, F.J. (2001) Use of constructed wetlands for acid mine drainage abatement and stream restoration. *Water Science and Technology* **44**: 449-454.

Chang, S., P.K. Shin, and B.H. Kim (2000) Biological treatment of acid mine drainage under sulphate-reducing conditions with solid waste materials as substrates. *Water Research* **34**: 1269-1277.

Christensen, B., Laake, M., and Lien, T. (1996) Treatment of Acid Mine Water by Sulfate-Reducing Bacteria: Results from Bench Scale Experiments. *Water Research* **30**: 1617-1624.

Coulton, R., Bullen, C., and Hallet, C. (2003) The design and optimization of active mine water treatment plants. *Land Contamination & Reclamation* **11**: 273-279.

Dvorak D.H., R.S.H., H.M. Edenborn, and P.E. McIntire (1992) Treatment of metal-contaminated water using bacterial sulfate reduction: results from pilot-scale reactors. *Biotechnology and Bioengineering* **40**: 609-616.

Eger, P., and Lapakko, K. (1988) Nickel and Copper Removal from Mine Drainage by a Natural Wetland. In *Mine Drainage and Surface Mine Reclamation, IC 9183* Bureau of Mines. US Department of Interior, pp. 301-309.

EPA, U.S. (1980) Control and Treatment Technology for the Metal Finishing Industry: Sulfide Precipitation. Industrial Environmental Research Laboratory, United States Environmental Protection Agency.

EPA, U.S. (2005) Mine Waste Technology Program 2005 Annual Report. U.S. Environmental Protection Agency National Risk Management Research Laboratory and U.S. Department of Energy Environmental Management Consolidated Business Center.

Gray, N.F. (1997) Environmental impact and remediation of acid mine drainage: A management problem. *Environmental Geology* **30**: 62-71.

Hallberg, K.B., and Johnson, D.B. (2005) Microbiology of a Wetland Ecosystem Constructed to Remediate Mine Drainage from a Heavy-Metal Mine. *Science of the Total Environment* **338**: 53-66.

Johnson, D.B., and Hallberg, K.B. (2005) Acid Mine Drainage Remediation Options: A Review. *Science of the Total Environment* **338**: 3-14.

Kaksonen, A.H., Plumb, J.J., Franzmann, P.D., and Puhakka, J.A. (2004) Simple Organic Electron Donors Support Diverse Sulfate-Reducing Communities In Fluidized-Bed Reactors Treating Acidic Metal- And Sulfate-Containing Waste Water. *FEMS Microbiology Ecology* **47**: 279-289.

Klein, D.B., and Neufeld, R.D. (2005) Use of a Multiple Orifice Spray Reactor to Accelerate Ferrous Iron Oxidation in Acidic Mine Waters. *Mine Water and the Environment* **24**: 186-193.

Labrenz, M., and Banfield, J.F. (2004) Sulfate-Reducing Bacteria-Dominated Biofilms That Precipitate ZnS in a Subsurface Circumneutral-pH Mine Drainage System. *Microbial Ecology* **47**: 205-217.

Logan, M.V., Reardon, K.F., Figueroa, L., McLain, J.E.T., and Ahmann, D. (2005) Microbial Community Activities During Establishment, Performance, and Decline of Bench-Scale Passive Treatment Systems for Mine Drainage. *Water Research* **39**: 4537-4551.

Lyon, J.S., Hilliard, T.J., and Bethell, T.N. (1993) *Burden of Gilt: The legacy of environmental damage from abandoned mines, and what America should do about it.* Washington, D.C.: Mineral Policy Center.

Miller, G.C., Kempton, H., Figueroa, L., and Pantano, J. (2006) Engineering Issues: Management and Treatment of Water from Hard Rock Mines. In. Office of Research and Development, N.R.M.R.L. (ed): U.S. Environmental Protection Agency.

Muyzer, G., and Stams, A.J.M. (2008) The ecology and biotechnology of sulphate-reducing bacteria. *Nature Reviews Microbiology* **6**: 441-454.

Nordstrom, D.K., and Southam, G. (1997) *Geomicrobiology of Sulfide Mineral Oxidation*. Washington, DC: Mineralogical Society of America.

Pereyra, L.P., Hiibel, S.R., Pruden, A., and Reardon, K.F. (2008) Comparison of Microbial Community Inocula Composition and Activity in Sulfate-Reducing Batch Systems Remediating Mine Drainage. *Biotechnology and Bioengineering.* In Press, DOI: 10.1002/bit.21930.

Pruden, A., Messner, N., Pereyra, L., Hanson, R.E., Hiibel, S.R., and Reardon, K.F. (2007) The effect of inoculum on the performance of sulfate-reducing columns treating heavy metal contaminated water. *Water Research* **41**: 904-914.

Robbins, E.I., Cravotta, C.A., Savela, C.E., and Nord, G.L. (1999) Hydrobiogeochemical interactions in 'anoxic' limestone drains for neutralization of acidic mine drainage. *Fuel* **78**: 259-270.

Schrenk, M.O., Edwards, K.J., Goodman, R.M., Hamers, R.J., and Banfield, J.F. (1998) Distribution of Thiobacillus ferrooxidans and Leptospirillum ferrooxidans: Implications for generation of acid mine drainage. *Science* **279**: 1519-1522.

Sheoran, A.S., and Sheoran, V. (2006) Heavy metal removal mechanism of acid mine drainage in wetlands: A critical review. *Minerals Engineering* **19**: 105-116.

Singer, P.C., and Stumm, W. (1970) Acidic Mine Drainage: The Rate-Determining Step. *Science* **167**: 1121-1123.

Sorokin, D.Y., Foti, M., Tindall, B.J., and Muyzer, G. (2007) *Desulfurispirillum alkaliphilum* gen. nov sp nov., a novel obligately anaerobic sulfur- and dissimilatory nitrate-reducing bacterium from a full-scale sulfide-removing bioreactor. *Extremophiles* **11**: 363-370.

USDA (1993) Acid Drainage from Mines on the National Forest: A Management Challenge. In: U.S. Forest Service, pp. 1-12.

Wakao, N., Takahashi, T., Sakurai, Y., and Shiota, H. (1979) A Treatment of Acid Mine Water Using Sulfate-Reducing Bacteria. *Journal of Fermentation Technology* **57**: 445-452.

Waybrant, K.R., Ptacek, C.J., and Blowes, D.W. (2002) Treatment of Mine Drainage Using Permeable Reactive Barriers: Column Experiments. *Environmental Science and Technology* **36**: 1349-1356.

Chapter 2 Research Approaches and Dissertation Overview

2.1 General Approach

The work presented in this dissertation is focused on understanding the microbial communities associated with AMD bioremediation. Existing biomolecular tools have been used and modified and new methods were developed to characterize these communities. By profiling the structure of the microbial community along with characterizing sulfate-reducing bioreactor (SRBR) remediation performance, the microorganisms that are common to well-performing bioreactors can be identified. Just as important, microorganisms unique to the bioreactors that are performing poorly can also be identified.

2.2 Research Objectives

The research objectives of this projective have all keyed on identifying correlations between AMD remediation performance and the microbial community structure, function, and activity with the goal of improving the design and performance of future bioreactors. Specific research objectives addressed in this dissertation are:

- Determine if the choice of microbial inoculum has an effect on the start-up time or remediation performance of SRBRs
- Identify specific microbial species or groups that are common to SRBRs successfully treating AMD

- Characterize the microbial communities of pilot-scale lignocellulose-based and ethanol-fed SRBRs and compare them with objective, multivariate statistical techniques
- Characterize the microbial communities of two field-scale SRBRs treating AMD of different severity and compare them to each other and to lab-scale SRBRs using objective, multivariate statistical techniques
- Develop and validate active community profiling (ACP), a high throughput technique for identifying the active members of mixed microbial communities
- Evaluate the effects of bioaugmentation and biostimulation on the active members of SRBR communities using ACP

2.3 Dissertation Overview

From initial studies (Chapters 3 & 4) targeting the 16S rRNA gene in batch and column experiments, a relationship between the choice of microbial inoculum and remediation performance was observed (Pruden, Messner et al. 2007; Pereyra, Hiibel et al. 2008). Successful SRBRs were found to have three key functional groups present in their microbial communities: cellulose degraders, fermenters, and sulfate reducers. However, quantitative measures of the SRB population indicated that this group was present at concentrations at or below the detection limits of the 16S profiling techniques used.

Pilot- and field-scale studies (Chapters 5 & 6) continued to target the 16S rRNA gene as the biomolecule for overall microbial community profiling, but also targeted the functional gene encoding adenosine 5'-phosphosulfate reductase (*apsA*) that catalyzes the reduction of sulfate to sulfite in most SRB. Analysis of the *apsA* gene allowed for higher resolution of a specific subset of the overall microbial community, in this case the sulfate reducers responsible for remediation. A decrease in SRB diversity was observed when a single carbon source was fed to pilot-scale reactor (Chapter 5). In addition, a strong connection was made between the type of *apsA* gene-containing species present and remediation performance at the field sites (Chapter 6).

These identification studies were important first steps to understanding SRBRs, but they only provided insights into which community members were present in the system. While this survey-type of information is important from an ecological perspective, knowledge of which species are actually involved (active) in the remediation process is critical from an engineering perspective. The correlation between cellular RNA content and cell growth rates is well known (Ingraham, Maaloe et al. 1983; Benthin, Nielsen et al. 1991). It has also been documented that while the total RNA tends to fluctuate depending on the growth rate of the cell, the amount of DNA in a cell remains relatively stable (Muttray and Mohn 2000). Thus, the relationship between RNA (variable) and DNA (stable) was utilized to determine which members of a mixed culture are actively growing and which microorganisms are dormant. The relative amounts of each can also be tracked over time to determine how the activities of community members change in response to environmental factors. When this information is coupled with the remediation performance of the communities, a clearer picture of which species are actively involved in the remediation process is obtained. The development of this method, known as active community profiling (ACP), is discussed in Chapter 7.

ACP was employed to explore the effect of bioaugmentation and biostimulation on the microbial communities of bioreactors treating AMD (Chapter 8). A series of columns were inoculated with dairy manure as a baseline inoculum. Bioaugmented columns also received cellulose-degrading bacteria or AMD-acclimated SRB. Biostimulated columns were fed ethanol or carboxymethyl cellulose (CMC) to stimulate the SRB and cellulose degraders, respectively. Although all of the bioreactors performed similarly, the microbial communities of the columns were distinctive, further indicating the importance of the microbes in the remediation process. Over the course of the experiment, most of the augmented cellulose-degrading species flourished in the bioreactor, indicating that bioaugmentation may be a viable option for AMD remediation sites. The activity of the microbial groups targeted in the biostimulated columns was also maintained or increased, suggesting that biostimulation may also be a viable remediation option.

The final two chapters of the dissertation, Chapters 9 & 10, offer overall project conclusions from the work presented and offer suggestions and direction for future efforts. Detailed protocols of the various chemical analyses and biomolecular procedures are given in the appendices.

2.4 References

Benthin, S., J. Nielsen, et al. (1991). "A Simple and Reliable Method for the Determination of Cellular RNA Content." Biotechnology Techniques **5**(1): 39-42.

Ingraham, J. L., O. Maaloe, et al. (1983). Growth of the Bacterial Cell. Sunderland, MA, Sinauer Associates, Inc.

Muttray, A. F. and W. W. Mohn (2000). "Quantitation of the Population Size and Metabolic Activity of a Resin Acid Degrading Bacterium in Activated Sludge Using Slot-Blot Hybridization to Measure the rRNA:rDNA Ratio." Microbial Ecology **38**: 348-357.

Pereyra, L. P., S. R. Hiibel, et al. (2008). "Comparison of Microbial Community Inocula Composition and Activity in Sulfate-Reducing Batch Systems Remediating Mine Drainage." Biotechnology and Bioengineering ***In Press,*** **DOI: 10.1002/bit.21930.**

Pruden, A., N. Messner, et al. (2007). "The effect of inoculum on the performance of sulfate-reducing columns treating heavy metal contaminated water." Water Research **Volume 41**(4): 904-914.

Chapter 3 Role of Inoculum in the Performance of Sulfate-Reducing Columns Remediating Heavy Metals

Pruden, A., Messner, N.L., Pereyra, L.P., Hiibel, S.R, Hanson, R.E., and K.F. Reardon. (2007). *Water Research.* 41 (4): 904-914

Approximate contributions of each author are as follows:
NL Messner performed 70% of the data collection and 20% of the manuscript preparation.
LP Pereyra performed 20% of the data collection, 30% of the statistical analysis, and 40% of the manuscript preparation.
SR Hiibel performed 70% of the statistical analysis and 40% of the manuscript preparation.
RE Hanson performed 10% of the data collection.
A Pruden and KF Reardon assisted with experimental design and manuscript preparation.

3.1 Abstract

Sulfate-reducing permeable reactive zones (SR-PRZs) are a passive means of immobilizing metals and neutralizing the pH of mine drainage through microbially mediated reactions. In this bench-scale study, the influence of inoculum on the performance of columns simulating SR-PRZs was investigated using chemical and biomolecular analyses. Columns inoculated from two sources (bovine dairy manure (DM) and a previous sulfate-reducing column (SRC)) and uninoculated columns (U) were fed a simulated mine drainage and compared on the basis of pH neutralization and removal of cadmium, zinc, iron, and sulfate. Cadmium, zinc, and sulfate removal was significantly higher in SRC columns than in the DM and U columns, while there was no significant difference between the DM and U columns. Denaturing gradient gel electrophoresis (DGGE) analysis revealed differences in the microbial community

composition among columns with different inocula, and indicated that the microbial community in the SRC columns was the first to reach a pseudo-steady state. In the SRC columns, a higher proportion of the DGGE band DNA sequences were related to microorganisms that carry out cellulose degradation, the rate limiting step in SR-PRZ energy flow, than was the case in the other columns. The proportion of sulfate-reducing bacteria of the genus *Desulfobacterium* was monitored using real-time quantitative PCR and was observed to be consistently higher in the SRC columns. The results of this study suggest that the inoculum plays an important role in SR-PRZ performance. This is the first report providing a detailed analysis of the effect of different microbial inocula on the remediation of acid mine drainage.

3.2 Introduction

The waters emanating from mine sites are typically characterized by low pH, high sulfate concentrations, and the presence of toxic heavy metals. Although some mine drainage issues are associated with large urban areas, many sites are located in remote areas and are subject to extreme weather conditions, which makes remediation challenging. This is particularly true in the case of abandoned mine land (AML) sites and affected streams. Researchers have estimated that there are over 200,000 AML sites and 5000 to 10,000 miles of impacted streams scattered throughout the US (EPA, 1997).

There are two general approaches for remediating mining influenced waters: active or passive. Active treatments (chemical treatment) require continuous inputs of resources to sustain the process, whereas passive treatments (biological treatment or anoxic limestone drains) require minimal inputs of resources once in operation (Johnson and Hallberg, 2005). Passive methods are preferred due to their low cost, low required maintenance, and because they produce minimal hazardous waste requiring disposal. In particular, sulfate-reducing permeable reactive zones (SR-PRZs), such as wetlands and subsurface reactive zones, are an attractive passive means of treating mine drainage. SR-PRZs contain solid organic substrates that support the growth of anaerobic microbial communities, including sulfate-reducing bacteria (SRB), which reduce sulfate in the mine drainage to sulfide. The sulfide in turn reacts with the heavy metals and immobilizes them within the zone as solid precipitates. SR-PRZs are typically inoculated with microbial communities from animal manure.

While there are many desirable aspects of SR-PRZs, there is little guidance available regarding their design. For this reason, it is not known why some have been observed to be subject to short lifetimes, low performance, and/or long startup times while others function well for several years (Benner et al., 1999, 2002; Blowes et al., 2000; Waybrant et al., 2002). Previous studies have attempted to address the issue of poor performance by focusing on the organic substrates used, and have evaluated straw (Bechard et al., 1994), sawdust (Wakao et al., 1979), peat (Eger and Lapakko, 1988), spent mushroom compost (Dvorak et al., 1992), whey (Christensen et al., 1996), and oak chips (Chang et al., 2000). However, no clear solution has been provided.

Although SR-PRZs are biologically catalyzed treatment systems, their microbial communities have not been well characterized. A few recent studies have investigated the kinds of microorganisms present in these systems using a combination of culture-based and molecular biological techniques (Benner et al., 2000; Hallberg and Johnson, 2005a; Johnson and Hallberg, 2003; Pereyra et al., 2005; Pruden et al., 2006). The results of these studies correlate well with the results of parallel research focusing on the carbon flow dynamics in these systems (Logan et al., 2005), and generally emphasize the complexity of the microbial communities responsible for remediation. Although SRB catalyze the final reaction of the SR-PRZ, they rely on the activity of anaerobic cellulolytic bacteria and fermentative bacteria to break down complex organic materials, such as cellulose from wood chips, to provide them with carbon and energy sources. Therefore, efforts to improve microbiological design criteria for SR-PRZs must consider the entire microbial community and not merely SRB.

The purpose of this study was to investigate the effect of inoculum on the performance of sulfate-reducing columns (SRC) simulating SR-PRZs. To gain a deeper understanding, denaturing gradient gel electrophoresis (DGGE) and real-time quantitative polymerase chain reaction (Q-PCR) were used to investigate the microbial community dynamics of the columns during startup and pseudo-steady-state operation. The results of this research provide insights for inoculum selection and may help improve the reliability of SR-PRZ performance in the field.

3.3 Materials and methods

3.3.1 Column specifications and packing

Six acrylic columns, 5 cm ID_15cm height, with six 34-in vertical sampling ports, were supported vertically with upward flow at an average rate of 40 mL/d. Each column was packed under a nitrogen atmosphere with 100 g dry weight of a homogenized mixture consisting of 22% beech wood chips, 2% crushed alfalfa, 11% pine shavings, 45% silica sand, 5% limestone, and 15% inoculum by weight. This mixture is typical of SR-PRZs and includes slow-release carbon and nitrogen sources (woody material and alfalfa), a source of alkalinity (limestone), and an inert material for porosity enhancement (sand) (Waybrant et al., 1998, 2002). The bottom layer (1.9 cm) of all columns was packed with a 90/10wt% mixture of silica sand/crushed pyrite to scavenge oxygen, as described by Waybrant et al. (2002). The top layer (0.6 cm) of all columns was packed with silica sand, separated from the organic layer by a stainless steel mesh to prevent organic material loss. All columns were covered in aluminum foil to inhibit photolithotrophic bacterial growth (Waybrant et al., 2002).

3.3.2 Inocula

Two inocula were compared in this study: (1) fresh bovine dairy manure (DM) collected from a dairy near Fort Collins, CO, and (2) contents from a previous column containing a sulfate-reducing community (SRC) (Logan et al., 2005). Two columns of each type (DM1, DM2, SRC1, SRC2) were prepared and compared to two uninoculated columns (U1, U2).

3.3.3 Influent composition

Columns were fed simulated mine drainage water from a common feed bottle. Due to problems with precipitation of iron in the influent bottle, the composition of the influent was variable during the initial 10 d of startup. During this time, the influent pH was adjusted from 6.0 to 5.6 and the influent $Fe(II)SO_4$ concentration was lowered from 0.49 to 0.034 g/L to reduce the extent of iron precipitation. The final influent composition was 1.32 g/L Na_2SO_4, 0.03 g/L NH_4Cl, 0.05 g/L $ZnSO_4$, 0.03 g/L $Fe(II)SO_4$, and 0.01 g/L

$CdCl_2$ at a target pH of 5.6 (adjusted with HCl and NaOH as needed). Before adding the metals, the deionized water for the influent was bubbled with nitrogen for 2 d to remove dissolved oxygen. The final influent solution was continuously bubbled with a slow stream of nitrogen (10 mL/min) to replace the headspace as the influent was pumped to the six columns. No precipitate was noted in the influent bottle for the remainder of the experiment.

3.3.4 Column and effluent sampling

Effluent was collected from the top of each column in 250-mL flasks initially containing 25mL of deionized water in which the column effluent tube was submerged to prevent entry of oxygen into the column. This initial volume was considered in the calculation of sulfate and metal concentrations. Column material (approx. 0.5 g) was removed weekly from the middle sampling port of the DM and SRC columns for the first 6 weeks to monitor microbial community development. The uninoculated columns were sampled only at Week 6. Columns were disconnected from the flow system and manipulated under a nitrogen atmosphere during sampling.

3.3.5 Analytical methods

Sulfate was quantified using the turbidimetric SulfaVers 4 method (Hach Co., Loveland, CO) with an Odyssey DR/2500 spectrophotometer (Hach Co.). After collection, aqueous samples were immediately filtered through 0.2-mm syringe tip filters and diluted with deionized water to achieve a concentration within the detection range of 2–70 mg/L. In order to verify that characteristics of the samples did not interfere with the turbidimetric method, samples were spiked with standard sulfate solutions. Based on these tests, no matrix effects were found.

Metals were analyzed by inductively coupled plasma absorbance emission spectroscopy (ICP-AES) (Thermo Jarrell Ash IRIS Advantage). Aqueous samples were filtered through 0.2-mm syringe-tip filters, diluted with deionized water, and acidified with trace metals-grade nitric acid (Mallinckrodt, Hazelwood, MO). The acidified solution was then boiled down to one-tenth of the initial volume and diluted to 50mL with deionized water for direct analysis by ICP-AES. Detection limits were 0.01 mg/L for iron and zinc, and 0.005 mg/L for cadmium. In every independent set of measurements, a deionized water blank was also measured. The calibration of the ICP-AES instrument was checked every 10 runs.

To determine the distribution of metals in the solid substrate of the columns at the end of operation, the column contents were divided approximately in thirds by volume into top, middle, and bottom sections. The material of these sections was well mixed and subsequently digested in a CEM microwave digester (MS-2000, Mathews, NC) per EPA Method SW-3015. The digested material was analyzed by ICP-AES as described above.

3.3.6 DNA extraction

DNA extractions were carried out using the FastDNAs Spin Kit for Soil (Q-BIOGene, Irvine, CA) according to the manufacturer's protocol using approximately 0.5 g of homogenized column material (the exact amount was recorded for quantification). Concentrations of DNA were determined spectrophotometrically (Hewlett Packard 8452A diode array spectrophotometer, Houston, TX) by measuring the absorbance at 260 nm. All DNA extracts were diluted 1:3 with sterile deionized water in preparation for polymerase chain reaction (PCR).

3.3.7 PCR amplification of 16S rDNA

A nested PCR approach was used to amplify the variable V3 region of the 16S rDNA molecule using primers 8F and 1492R (Weisburg et al., 1991) followed by I341F and I533R (Watanabe et al., 2001). The reaction (total volume 25 mL) included 12.9 mL purified water, 2.5 mL 10X Taq Reaction Buffer, 5.0 mL TaqMaster PCR Enhancer (Eppendorf, Hamburg, Germany), 5 pM of each dNTP, 0.25pM of each primer, 0.25 mL formamide, 1.75U Taq DNA polymerase (Eppendorf), and 1 mL DNA template. The temperature conditions for PCR were those described by Weisburg et al. (1991) for 8F and 1492R primers and by Watanabe et al. (2001) for I341F and I533R primers.

3.3.8 Denaturing gradient gel electrophoresis (DGGE)

Gels (8% acrylamide/bisacrylamide 19:1, BioRad) were cast using a denaturing gradient of 20–55%, with 100% denaturant defined as 7M urea and 20% v/v formamide. A standard prepared with a mixture of DNA from pure cultures was loaded in all gels to verify the gradient. Gels were exposed to at 45V for 20h at 57.5 1C and stained with SybrGold nucleic acid stain (Molecular Probes, Inc., Eugene, OR). Gels were documented using a UVP BioChem gel documentation system and images were analyzed using Labworks software (UVP, Upland, CA). This software was used to identify the bands in the gels and to obtain the intensity profiles for each of the lanes. The intensity profiles were used to assess the degree of similarity between replicates at different times. The relative diversity was calculated using the Shannon diversity index (Equation 3.1)

$$H = -\sum\left[\frac{n_i}{N}\log\left(\frac{n_i}{N}\right)\right] \qquad \textbf{Equation 3.1}$$

where n_i is the intensity of the individual bands and N is the sum of the intensity of all the bands (Cox, 1972; Xia et al., 2005). Representative visible DGGE bands (33 total) were excised with sterile razor blades and stored in 2-mL tubes with 36 mL of sterile water.

3.3.9 DNA sequence analysis

DNA present in the DGGE bands was PCR amplified and purified for sequencing using the GeneClean Spin Kit (Q-BIOGene). Sequencing of the 200 bp product was performed by Davis Sequencing (Davis, CA). The closest matches to known microorganisms available in the National Center for Biotechnology Information database were determined using the BLAST alignment tool (http://www.ncbi.nlm.nih.gov/BLAST/). A literature survey was conducted to characterize the properties of the closest matches with respect to substrate utilization and sulfate reduction.

3.3.10 Cloning

Eighteen of the 33 cut DGGE bands resulted in mixed sequences. To separate these, the excised bands were PCR amplified using primers I341F and I533R as described above, purified using the GeneClean Spin Kit (Q-BIOGene), and cloned into Escherichia coli using the TOPO TA Cloning Kit for Sequencing (Invitrogen, Carlsbad, CA) according to the manufacturers' protocols. Inserts were PCR amplified directly from colonies using M13F and M13R primers. At least three clones per band were analyzed. PCR products were purified using the GeneClean Spin Kit (Q-BIOGene) and sequenced by Davis Sequencing (Davis, CA).

3.3.11 Real-time Q-PCR

Q-PCR targeting the 16S rDNA of total bacteria and the SRB genus *Desulfobacterium* (DSB), which has commonly been identified in mine drainage systems (Hallberg and Johnson, 2005b; Morales et al., 2005), was performed using a Cepheid SmartCycler (Sunnyvale, CA). Primers were designed for the DSB subgroup in the δ-proteobacteria subdivision using FastPCR software (Kalendar, 2005). The sequences of the DSB primers were 5'-AGT ARA GTG GCG YAC GGG TGA G for the forward primer (HDBM52f) and 5'-WTC AYY CAC GCG GCG TYG CTG C for the reverse primer (HDBM372r), yielding a product of approximately 320 bp. The specificity of the primers was verified both by a BLAST search and by shotgun cloning and sequencing of amplified products. Qiagen SybrGreen MasterMix (Valencia, CA) was used to adapt the primers to Q-PCR. The template used for calibration was purified 16S rDNA PCR product obtained from *Desulfobacterium autotrophicum* ATCC43914D (American Type Culture Collection, Rockville, MD). Calibration curves were constructed using six points with four replicates for each point. In every Q-PCR run, three standards were included. The Ct values of these standards were compared to the corresponding values in the calibration curve, and if the difference was more than 75%, the data from that run were discarded. The limit of quantification of the DSB assay was 917 copies per reaction. For total bacteria, the conditions described by Suzuki et al. (2000) were used, including universal 16S rDNA primers and probe. A six-point calibration curve was generated using amplified 16S rDNA from a sample collected from a sulfate-reducing bioreactor as the template, with four replicates in two independent runs for each point. For both assays, a dilution series was performed on all samples and analyzed by Q-PCR to identify the linear range unaffected by inhibitors. A dilution of 1:20 was sufficient for most samples.

3.3.12 Statistical and mathematical analyses

Mixed linear regressions were fit to all data sets using the PROC MIXED function of SAS 9.1 (SAS Institute Inc., Cary, NC). Log transformation of all data sets was required to achieve homoscedasticity, and all comparisons were made in log scale. Degrees-of-freedom calculations were performed using the Kenward–Roger method with repeated time measurements. Significance was defined by a Type III p-value p0.05. Dixon's Extreme Value test was used to test for statistical outliers.

Column pore volume was estimated using the ratio of pore volume to empty column volume based on Logan et al. (2005) as similar column materials and packing techniques were utilized in the present study. The pore volume was found to be 166cm3 with a residence time of 4 d at an average flow rate of 40 mL/d.

For cumulative sulfate and metal removal analyses, cubic splines were fit to the effluent concentrations and flow rate data and then interpolated for direct comparison with the discrete influent data. Splines and interpolation were performed with the 'cspline' and 'interp' functions of MathCAD 12 (Mathsoft Engineering & Education, Inc., Cambridge, MA).

3.4 Results

3.4.1 Qualitative observations

Between the first and seventh weeks of operation, the color of the column material changed only slightly (from dark to light green) in the columns inoculated with DM (DM1, DM2), and there was some darkening (from light brown to gray) in the uninoculated columns (U1, U2). By contrast, the columns inoculated with preacclimated column substrate (SRC1, SRC2) changed markedly from light brown to black. Hydrogen sulfide odor was also detectable in the effluents of the SRC columns after 2 wk, whereas this odor was not apparent in the effluents of the other two sets of columns.

3.4.2 Cumulative sulfate removal

Cumulative sulfate removal (Figure 3.1) was negligible in the DM and U columns until Day 30, while sulfate was removed at low rates in the SRC columns during this period. After this time, an increase in the rate of removal was observed in all columns, with the highest sustained rates occurring in the SRC columns. The DM and U columns maintained the higher removal rate for approximately 60 d, while the SRC columns maintained the rate for an additional 30 d (through Day 120). Significantly greater cumulative sulfate removal was observed in the SRC columns than in the DM ($p = 0.004$) and U columns ($p < 0.001$), and no statistical difference was determined between the DM and U columns ($p = 0.2731$).

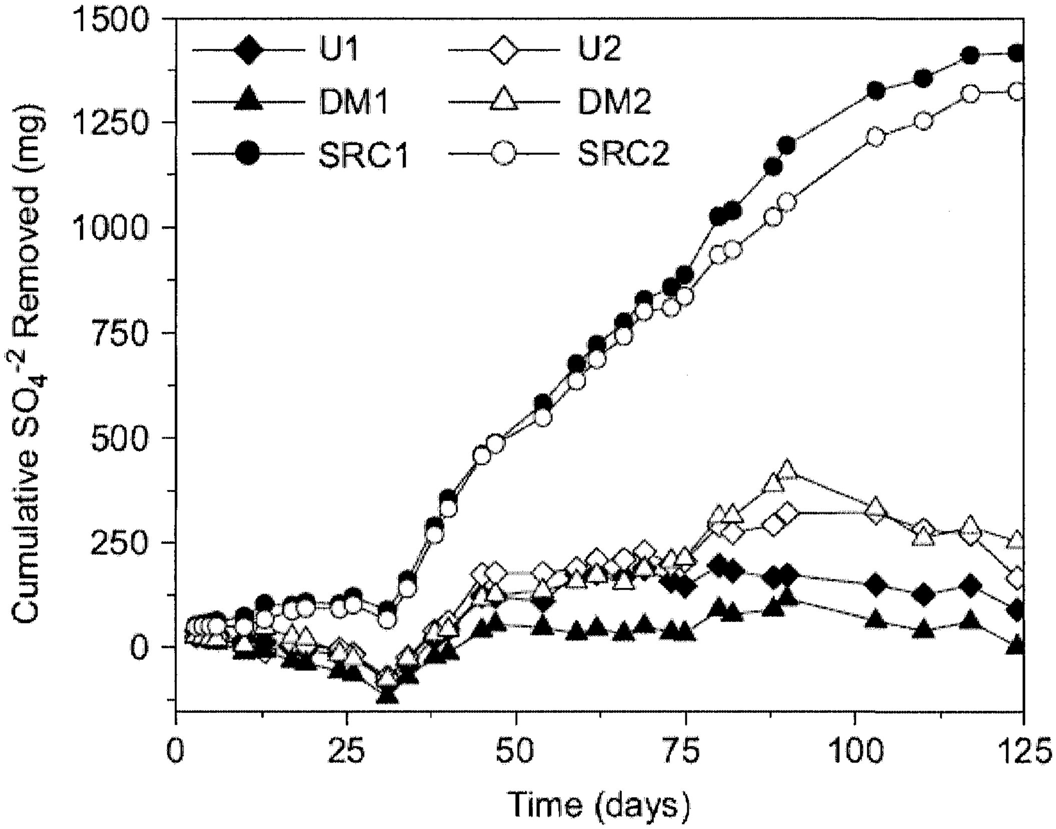

Figure 3.1 – Cumulative sulfate removal in duplicate SR-PRZ columns that were uninoculated (U) or inoculated with an acclimated culture (SRC) or with bovine dairy manure (DM). Cubic splines were fit to the effluent sulfate concentrations and flow rate data and then interpolated for direct comparison with the discrete influent data using a residence time of 4 d. The negative cumulative removal values for the DM and U columns during the first 30 d can be attributed to the variable influent concentrations at the beginning of the experiment and to the propagation of error associated with the mathematical treatment of the minimal sulfate removal during this time.

3.4.3 pH

The effluent pH varied significantly with startup, followed by a gradual increase in all columns throughout the experiment. Between 40 and 125 d of operation, the pH of the SRC column effluent was consistently higher than that of the DM or U columns and fluctuated near pH 8 after Day 60. However, due to the fluctuation of the influent pH, no statistically valid distinction could be made among the columns. Because the influent was not buffered, a consistent pH in the influent was not attained (pH range 4–8, with an average and standard deviation of 5.61 ± 1.06). However, the buffering capacity was increased by the column contents, yielding a relatively stable effluent pH.

3.4.4 Cumulative metal removal

Calculated cumulative mass removals (Figure 3.2) revealed that the total mass of cadmium and zinc removed by the SRC columns was greater than that removed by the DM ($p < 0.001$ for both metals) and U columns ($p < 0.0001$ for both metals). No statistical difference in cumulative cadmium removal was observed between the U and DM columns ($p = 0.552$), and cumulative zinc removal in the DM columns was statistically greater than the removal in the U columns ($p = 0.002$). For the duration of the experiment, the rate of removal for both cadmium and zinc was greater in the SRC columns than in the DM and U columns. In the case of iron (data not shown), cumulative removal in the SRC and U columns was significantly higher than in the DM columns ($p < 0.001$ for both column sets) but no significant differences in removal were observed between SRC and U columns ($p = 0.972$).

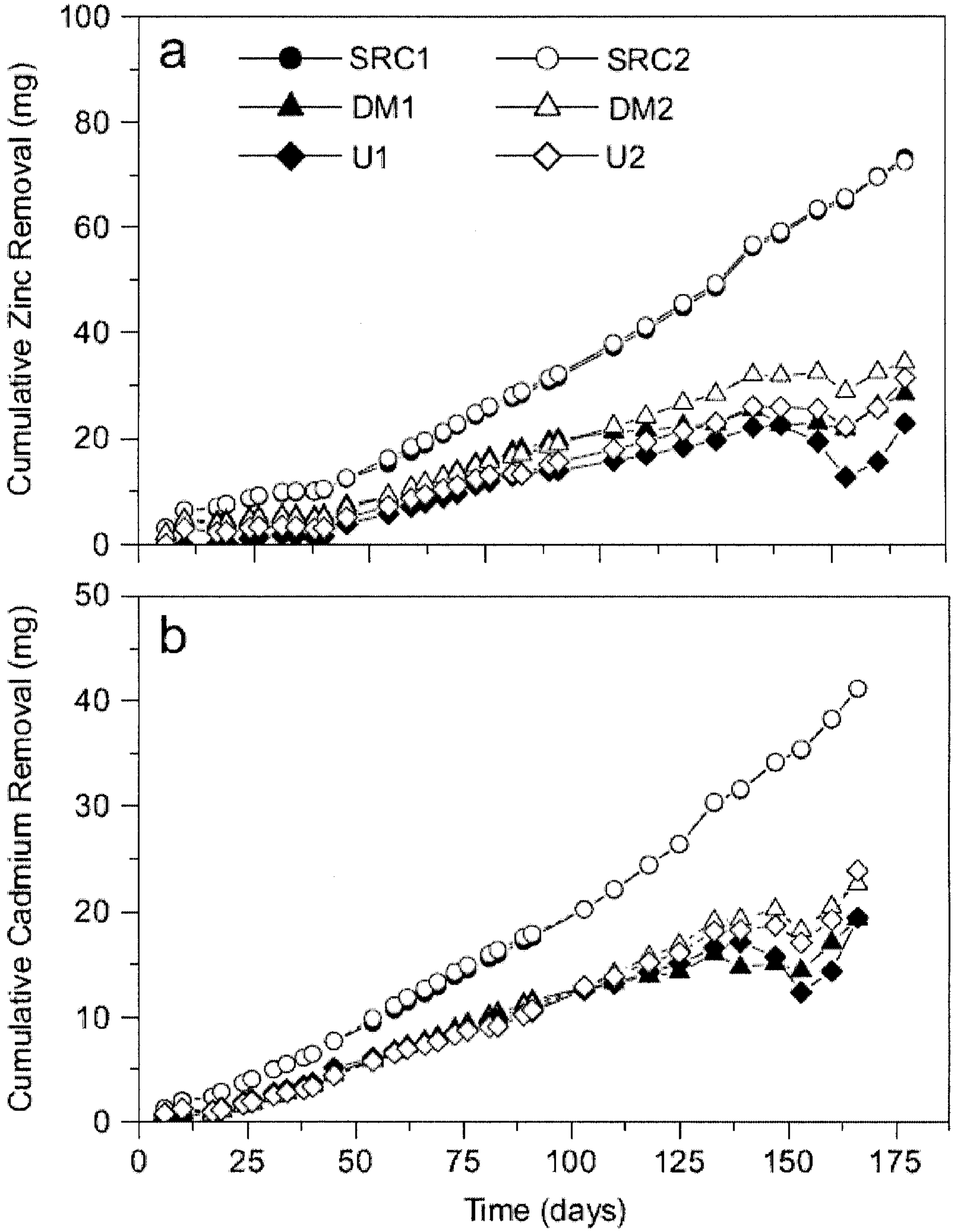

Figure 3.2 – Cumulative zinc (a) and cadmium (b) removal in the uninoculated columns (U) and columns inoculated with an acclimated inoculum (SRC) or with bovine dairy manure (DM). Cubic splines were fit to the effluent metal concentrations and flow rate data and then interpolated for direct comparison with the discrete influent data using a residence time of 4 d.

3.5. Distribution of metals within the columns

In the solids of the DM1 and U2 columns, the cadmium and zinc concentrations did not differ between the top, middle, and bottom ($p > 0.1$) (Figure 3.3). In the DM2 columns, the concentrations of these metals were slightly lower in the bottom (inlet) portion. In the SRC columns, concentrations of cadmium and zinc were lower in the upper section than in the middle and bottom. However, in the SRC1 column, most of the cadmium and zinc was near the inlet, whereas these metals were equally concentrated in the bottom and middle of the SRC2 column.

Iron concentrations were highest in the inlet section of the DM and U columns (data not shown). In the SRC columns, however, the iron concentrations were more equally distributed among the three portions of the columns, with the highest concentration in the middle (SRC2) or in the bottom (SRC1).

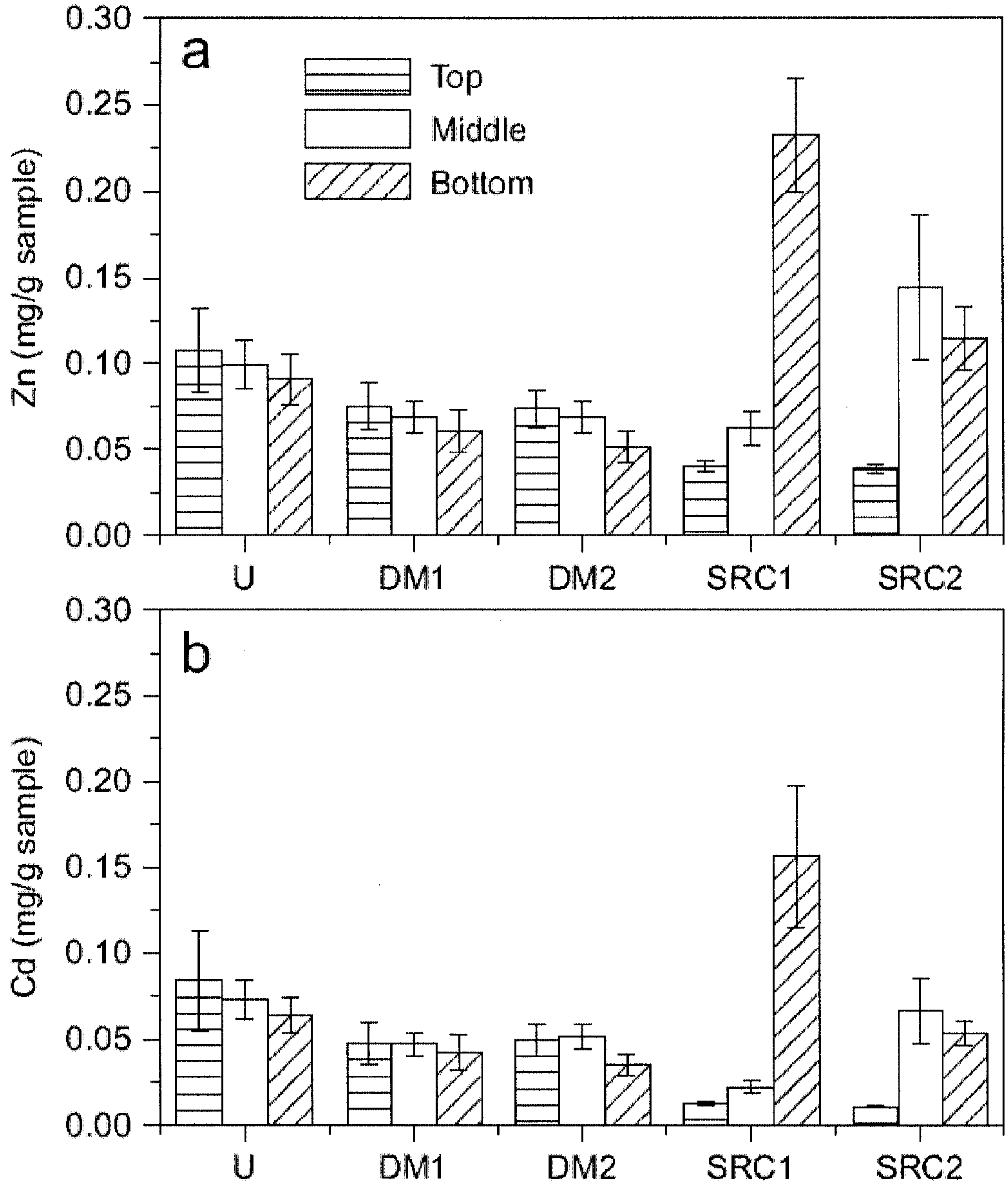

Figure 3.3 – Distribution of (a) cadmium and (b) zinc in the columns determined by ICP-AES analysis of digested column material collected from the top, middle, and bottom sections of each column after 170 d of operation. The influent entered the columns from the bottom. Results for only one uninoculated column are shown because the second was used for a tracer test. Error bars represent standard deviations of the means of five replicates.

3.6. DGGE of column microbial communities

Using the criterion that a microbial community reached a pseudo-steady state when no new DGGE bands were detected and no existing bands disappeared, the microorganisms in the SRC columns formed a stable community (after Week 2) before the other columns (Figure 3.4a). By contrast, the DM columns still had new detectable bands at Week 4, while three bands faded gradually after this time in the DM1 column (Figure 3.4b). More bands were observed in the DGGE gels for SRC columns than in the gels for DM or U columns. However, the Shannon diversity indices for the SRC and DM columns were not significantly different ($p = 0.136$). Diversity indices for the two SRC columns were highly similar and ranged from a value of $H = 1$ at the beginning of the experiment to $H = 1.37$ at Week 6. Diversity indices for column DM2 were consistently lower than those for column DM1 until Week 6, at which time the index values for both columns converged. Diversity index for column DM2 increased from an initial value of $H = 0.5$ to a value of $H = 1.12$ at Week 6. The initial average diversity index in column DM1 was $H = 1.26$. This index decreased to an average value of $H = 1.08$ by Week 1 and remained constant at all other sampling points.

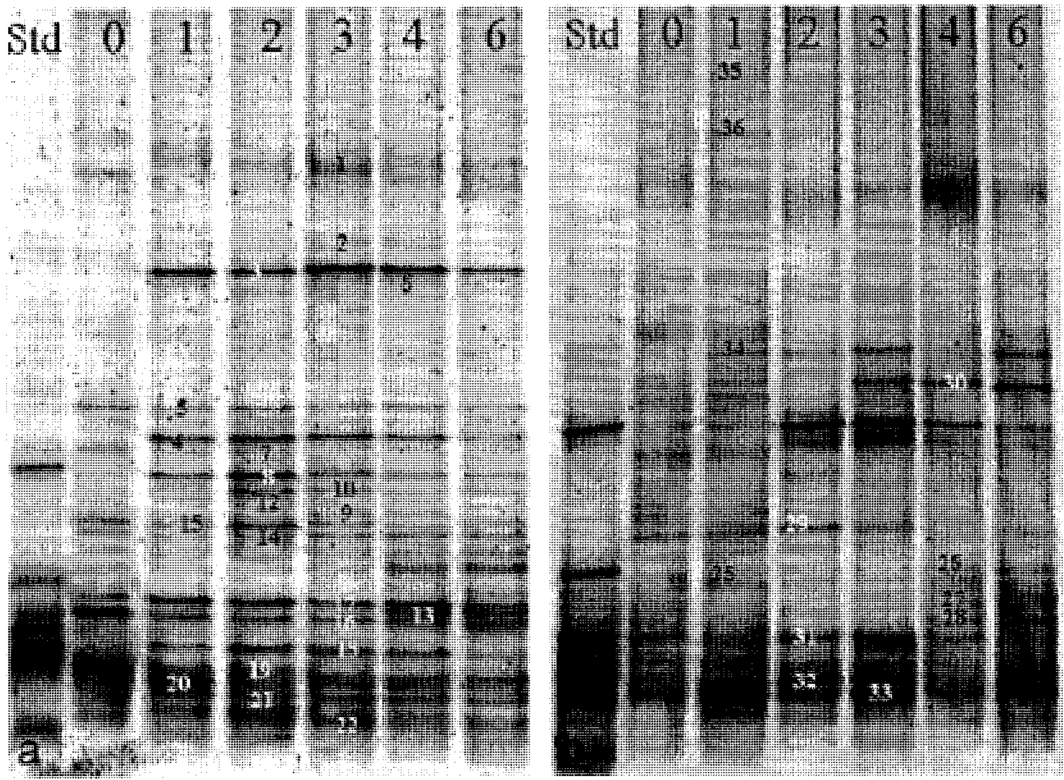

Figure 3.4 – DGGE gel image of nested I341F and I533R PCR products of DNA extracted from (a) column SRC1 and (b) column DM1 during the first 6 wk. Lane numbers correspond to the sampling week. 'std' is the positive control. Twenty-three of the labeled bands were sequenced and their identities are indicated in Table 3.1.

Table 3.1 summarizes the results obtained by sequencing DGGE bands. Of the 30 unique bands of the SRC columns, 15 were sequenced, while eight of 27 unique bands were sequenced from the DM columns. Several cellulose-degrading bacteria belonging to the *Eubacterium*, *Clostridium*, and *Bacteroides* genera were found in the SRC columns. Fermentative bacteria in SRC columns were related to the classes Enterobacteria, Clostridia, and Bacteroidetes. In DM columns, the majority of the fermenters and the one cellulose degrader identified were related to members of the genus *Clostridium.* An SRB was identified in the SRC columns, and an SRB was also detected in one of the U columns (data not shown). No SRB were detected in the eight sequenced DGGE bands from the DM columns.

Table 3.1 – Characterization of microorganisms represented by DGGE bands.

Band[+]	Highest Match (GenBank accession number)	% Match	A*	B*	C*	D°	Ref.
		SRC					
1	*Clostridium indolis* strain DSM 755(Y18184) *Clostridium celerecrescens* strain EIB 5 (AY458859)	99% 99%	- +	+ -	+ +	- -	(Dworkin, 2000; Holt, 1984; Leschine, 1995; Palop et al., 1989)
2	Uncultured bacterium BTCE-T2 1F 16S ribosomal RNA gene (AY217446)	96%					
3	*Clostridium fimetarium* (AF126687)	99%	-	-	+	-	(Kotsyurbenko et al., 1995)
4	*Eubacterium cellulosolvens* strain Ce2 (AY178842)	100%	+	+	+	-	(Bryant et al., 1958)
6	*Bacteroides* sp. 253c (AY082449)	94%	+	+	+	-	(Dworkin, 2000)
7	*Desulfovibrio vulgaris* strain I5 (AY362360)	96%	-	-	-	+	
8	*Clostridium longisporum* strain DSM 8431	98%	+	+	+	-	(Varel, 1989)
10	Uncultured bacterium clone BCf5-21 (AB062828) that was 92% similar to an uncultured *Clostridiaceae* bacterium (AB089033)	91%					
12	*Klebsiella pneumoniae* (AY369139)	92%	-	-	+	-	(Dworkin, 2000)
13	Uncultured isopod gut bacterium clone RKPsAM (AF395327) that was 93.6% similar to an unidentified *Bacteroides* spp. (AF150715)	88%	+	+	+	-	
14	Uncultured *Clostridiaceae* bacterium clone:Rs-Q69 (AB089029)	96%			+		(Dworkin, 2000)
16	*Clostridium longisporum* strain DSM 8431 (X76164)	99%	+	+	+	-	(Varel, 1989)
20	*Escherichia vulneris* (AF530476)	87%	-	-	+	-	(Brenner et al., 1982)
21	*Clostridium longisporum* strain DSM 8431 (X76164)	99%	+	+	+	-	(Varel, 1989)
22	*Escherichia senegalensis* (AY217654)	93%	-	-	+	-	(Dworkin, 2000)
		DM					
25	Uncultured bacterium RSa32 (AJ289204). Related to *Clostridium polysaccharolyticum* (X77839)	99%	+	+	+	-	(Holt, 1984; Vangylswyk, 1980)
26	Uncultured bacterium clone HuCB56 (AJ409006) that was 94% similar to *Eubacterium xylanophilum* (L34628).	99%	-	+	+	-	(Vangylswyk and Vandertoorn, 1985)
27	*Clostridiaceae* bacterium 80Kb (AB084627) that was 91.5% Similar to *Clostridium leptum* (AF262239)	95%	-	-	+	-	(Holt, 1984; Moore et al., 1976)
28	*Sporomusa malonica* strain DSM 5090 (AJ279799)	81%	-	-	+	-	(Dehning et al., 1989)
29	*Clostridium indolis* strain DSM 755 (Y18184)	95%	-	+	+	-	(Dworkin, 2000; Holt, 1984)
32	Uncultured bacterium clone Thompsons76 (AY854354)	88%					
34	*Clostridium butyricum* strain EIB 3-4 (AY458857)	94%	-	+	+	-	(Dworkin, 2000; Holt, 1984)
35	*Clostridium lituseburense* strain EIB 6 (AY458860)	82%	-	-	+	-	(Holt, 1984)

3.4.5 Q-PCR

Although the total bacterial population in the DM columns was initially larger than that in the SRC columns, it rapidly decreased during the first 3 wk and was similar to the SRC columns for the remainder of the experiment (data not shown). At Week 6, the final sampling point, the bacterial populations of DM and SRC columns were not significantly different in size from those of the U columns.

Overall, the DSB populations in the SRC columns were significantly larger than in the DM columns ($p = 0.027$) (Figure 3.5a). The number of DSB 16S rRNA gene copies increased in the SRC columns at Week 2 while it decreased in the DM columns. At Week 6, the DSB populations in the U columns were significantly smaller than those in the SRC ($p = 0.021$) and the DM ($p = 0.010$) columns.

The DSB population also constituted a much larger fraction of the bacterial community in the SRC columns than in the DM and U columns (Figure 3.5b). At the beginning of the experiment, the ratio of DSB to total bacteria was smaller in the DM columns ($p = 0.022$). By Week 2, this ratio had increased in the SRC columns while it did not change in the DM columns. The ratios of DSB to bacteria in the SRC and DM columns were significantly different ($p < 0.001$). The higher ratios for the SRC columns are in agreement with the superior metal and sulfate removal observed for these columns.

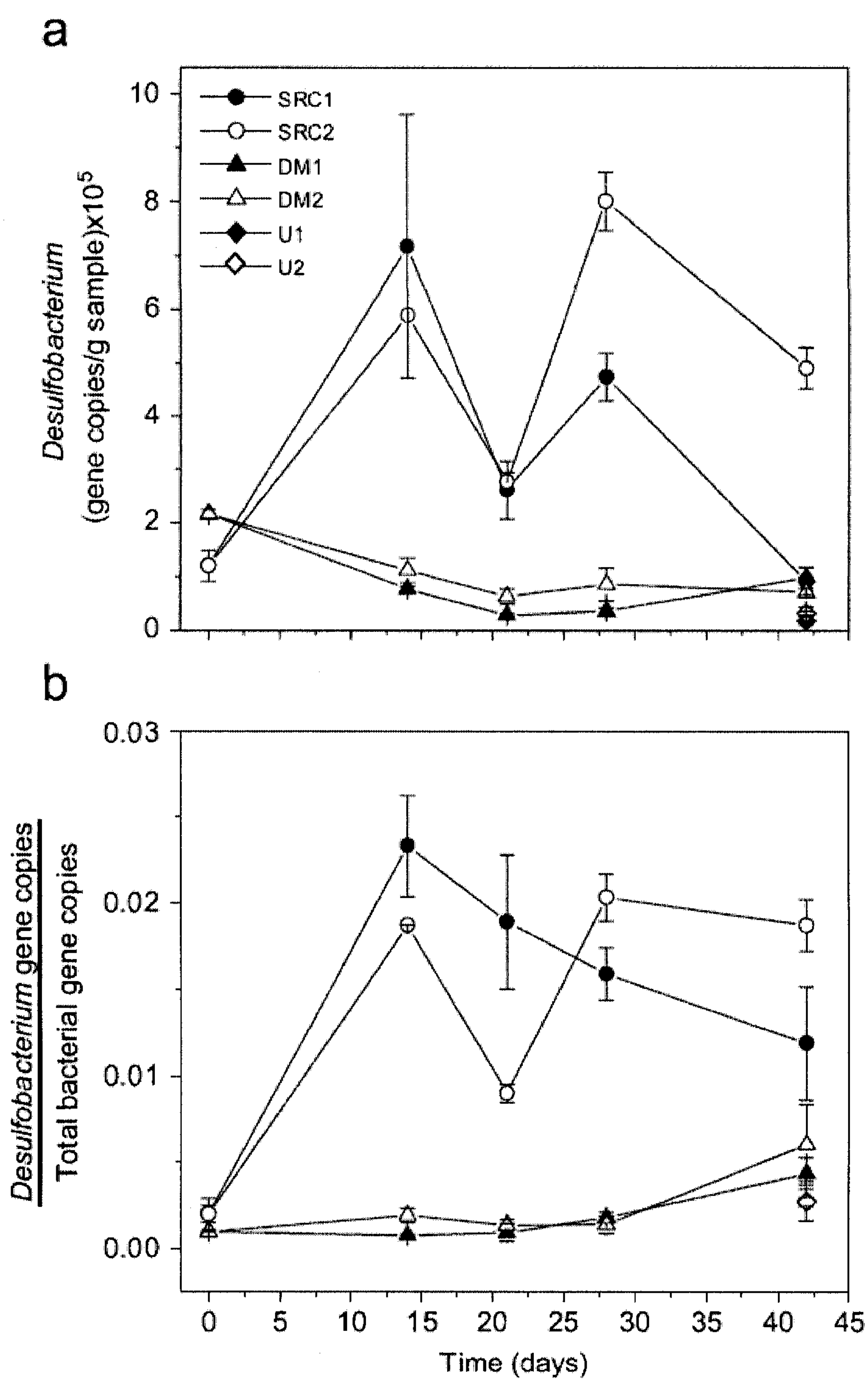

Figure 3.5 – Quantification of *Desulfobacterium* with time by QPCR for SRC, DM, and U columns (a) normalized to mass of sample used for DNA extraction and (b) normalized to total bacteria. Error bars represent standard deviations of the means of two to six replicates.

3.5 Discussion

3.5.1 Effect of inoculum on column performance

Metal removal, pH neutralization, and sulfate removal can be used as indicators of column performance. This work indicates that the microbial inoculum significantly affects the performance of columns remediating acid mine drainage (AMD). The rates of removal of sulfate and metals in the SRC columns were superior to those in the DM and U columns (except in the case of iron, which was removed by both the SRC and U columns better than by the DM columns). Interestingly, the columns inoculated with DM, a common source of inoculum (Castro et al., 1999; Christensen et al., 1996), did not perform better than the uninoculated columns. This suggests that the 'wrong' inoculum may not provide an advantage over no inoculum at all.

In addition to remediation performance, the startup time and duration of active remediation (pseudo-steady state) are important parameters in determining the overall column performance. For comparison, startup time was taken as the point when sulfate or metal removal was observed, independent of removal rate, and pseudo-steady state was considered as the time during which the rate of removal was constant. Cadmium and zinc removal was observed in all columns from the start of the study, indicating an immediate startup to a pseudo-steady state. The pseudo-steady state was maintained throughout the experiment in the SRC columns, while the DM and U columns displayed a decline in removal rate after Days 125 and 133 for zinc and cadmium, respectively, indicating the end of the pseudo-steady state period. The startup was also immediate in terms of sulfate removal in the SRC columns, but required more than 4wk for the DM and U columns. Pseudo-steady state did not begin until Day 30 for all columns. The active remediation lasted for 90 d (through Day 120) in the SRC columns at a significantly higher removal rate than the DM and U columns, which remained in pseudo-steady state for only 60 d (through Day 90). These results suggest that the type of inoculum does not affect the startup time for metal removal (which may have been achieved partly by sorption in the first several days); however, inoculation with a preacclimated culture resulted in a shorter startup time for sulfate removal and maintenance of remediation capabilities for a longer period than the use of DM or no inoculum. A longer experiment would be required to fully simulate operation times in the field, which vary from 2 to 20 years (Benner et al., 1999, 2002; Blowes et al., 2000; Waybrant et al., 2002).

These findings agree with results of other studies that show an effect of microbial inoculum on system performance. Moreno et al. (2005a) found that inoculating a submerged filter for biological denitrification with a pure culture of denitrifying bacteria increased system stability and performance indicators compared to inoculation with a mixed culture from a wastewater treatment plant's activated sludge. In the same system, Moreno et al. (2005b) also showed that the choice of microbial inoculum can also influence startup time. Pereira et al. (2001) verified that the degradation of oleic acid in anaerobic filters was improved by inoculating the system with acclimated biomass compared to nonacclimated biomass.

3.5.2 Spatial distribution of metal removal

Analysis of cadmium, zinc, and iron in the column material revealed spatial heterogeneity in the SRC columns (Figure 3.3). In particular, zinc and cadmium concentrations in the bottom and middle portions of the SRC columns may have been higher because the higher levels of sulfate reduction in the SRC columns precipitated the metals more efficiently near the inlet, preventing them from reaching the upper layers at high concentration.

3.5.3 Microbial community composition and dynamics

Microbial community profiling by DGGE provided data to determine the time required to reach a pseudo-stable microbial community, to identify microorganisms, and to compare the relative diversity. Based on DGGE, the microbial communities in the SRC columns achieved a stable composition sooner than the populations in the DM and U columns. This correlates well with the performance data, and is a promising suggestion that the composition of the microbial inoculum can influence the startup time of a SR-PRZ, an issue that is significant for field operation. In a bench-scale study of AMD treatment using microbial-driven sulfate reduction, Christensen et al. (1996) demonstrated that inoculating the system with SRB shortened the initial lag phase.

The majority of the bands sequenced from the SRC columns corresponded to microorganisms that degrade cellulose and other polysaccharides, such as pectin and starch, and ferment the products of the hydrolysis (e.g., *Clostridium longisporum* and *Eubacterium cellulosolvens*). Sequences related to *Bacteroides* spp. were found only in SRC columns. *Bacteroides* spp. are saccharolytic microorganisms and, as a group, are able to utilize a wide variety of compounds as carbon and energy sources, including cellulose, hemicellulose, starch, and pectin (Dworkin, 2000). The mechanisms of polysaccharide digestion in *Bacteroides* spp. are highly effective (Dworkin, 2000). By contrast, only one of the sequences from the DM columns (DGGE Band 25) was confirmed to be related to a cellulose degrader. In the DM columns, 88% of the sequenced bands corresponded to microorganisms that ferment di- and/or monosaccharides and 57% of these microorganisms were also able to degrade polysaccharides such as starch and pectin. Since the degradation of cellulose has been shown to be the rate-limiting step in the carbon flow dynamics in SR-PRZs of the type tested here (Logan et al., 2005), the presence of *Bacteroides* spp. together with a diverse population of additional polysaccharide fermenters in the SRC columns might have constituted an advantage of these columns over the DM columns.

Although sulfate was removed by the DM columns, no SRB were found in the sequenced DGGE bands. In the SRC columns, the sequence from Band 7 showed 96% similarity to the sulfate reducer *Desulfovibrio vulgaris* strain I5. This band was detected by DGGE in Week 2. Both *Desulfovibrio* spp. and DSB spp., which were quantified by Q-PCR, have been identified as major SRB in AMD treatment systems (Hallberg and Johnson, 2005a; Labrenz and Banfield, 2004). SRB have been observed to represent a relatively low proportion of the microbial community in other sulfate-reducing mine drainage treatment systems (Hallberg and Johnson, 2005b; Johnson and Hallberg, 2003; Morales et al., 2005). This may explain why more SRB were not detected by DGGE and is corroborated by the low proportion of DSB (0.1–2%) detected by Q-PCR in all of the columns. This also supports the hypothesis of the importance of the upstream microorganisms that provide SRB with carbon substrates for growth (cellulose degraders and fermenters). A higher proportion of SRB in the SRC columns together with a variety of microorganisms capable of degrading complex organic materials might have caused the increased metal removal and pH neutralization observed in these columns compared to the DM columns.

Q-PCR analysis also revealed that the DM columns initially contained more total bacteria than the SRC columns. The decrease in total bacteria in DM columns in the following weeks could be an indication that the conditions were not favorable for a large portion of the original microbial community. This is not surprising considering the stark contrast in environmental conditions between the columns and the thermophilic lower intestinal tract of a dairy cow. It is also possible that the nutrient availability at the beginning of the experiment (especially the presence of readily available soluble organics) caused competition of different microbial groups that ultimately lead to the survival of only those that were better at procuring these nutrients, but not necessarily better at the activities that lead to heavy metal precipitation.

3.6 Conclusions

The results of this study demonstrate that the nature of the inoculum influences the performance of sulfate-reducing systems treating heavy metal contaminated water. An inoculum previously acclimated to sulfate-reducing conditions and complex organic substrates outperformed DM, a typical SR-PRZ inoculum. The application of biomolecular tools provided deeper insights into the composition and overall dynamics of the microbial communities in the columns. The results of this study provide justification and basic information needed to support future efforts in the development of SR-PRZ inocula for improving reliability and performance in the field.

3.7 Acknowledgments

The authors thank EPA STAR Grant number R8395101-0 for funding this project and the Hazardous Substance Research Center at Colorado State University. Financial assistance was also provided by the National Science Foundation Research Experience for Undergraduates program in Water Research at Colorado State University. The authors would like to thank Ruoting Pei, HyunSuk Hong, Carmen Sans, and Santiago Esplugas for their help in performing effluent tests and substrate extractions, and Tom Sale and Dave Gilbert for providing assistance in column design and laboratory space for experiments.

3.8 References

Bechard, G., Yamazaki, H., Gould, W.D., Bedard, P., 1994. Use of cellulosic substrates for the microbial treatment of acid-mine drainage. J. Environ. Qual. 23 (1), 111–116.

Benner, S.G., Blowes, D.W., Gould,W.D., Herbert, R.B.J., Ptacek, C.J., 1999. Geochemistry of a permeable reactive barrier for metals and acid mine drainage. Environ. Sci. Technol. 33, 2793–2799.

Benner, S.G., Gould, W.D., Blowes, D.W., 2000. Microbial populations associated with the generation and treatment of acid mine drainage. Chem. Geol. 169 (3–4), 435–448.

Benner, S.G., Blowes, D.W., Ptacek, C.J., Mayer, K.U., 2002. Rates of sulfate reduction and metal sulfide precipitation in a permeable reactive barrier. Appl. Geochem. 17 (3), 301–320.

Blowes, D.W., Ptacek, C.J., Benner, S.G., McRae, C.W.T., Bennett, T.A., Puls, R.W., 2000. Treatment of inorganic contaminants using permeable reactive barriers. J. Contam. Hydrol. 45 (1–2), 123–137.

Brenner, D.J., McWhorter, A.C., Knutson, J.K.L., Steigerwalt, A.G., 1982. *Escherichia vulneris* - a new species of *Enterobacteriaceae* associated with human wounds. J. Clin. Microbiol. 15 (6), 1133–1140.

Bryant, M.P., Small, N., Bouma, C., Robinson, I.M., 1958. Characteristics of ruminal anaerobic cellulolytic cocci and *Cillobacterium cellulosolvens* n. sp. J. Bacteriol. 76 (5), 529–537.

Castro, J.M., Wielinga, B.W., Gannon, J.E., Moore, J.N., 1999. Stimulation of sulfate-reducing bacteria in lake water from a former open-pit mine through addition of organic wastes. Water Environ. Res. 71 (2), 218–223.

Chang, S., Shin, P.K., Kim, B.H., 2000. Biological treatment of acid mine drainage under sulphate-reducing conditions with solid waste materials as substrates. Water Res. 34 (4), 1269–1277.

Christensen, B., Laake, M., Lien, T., 1996. Treatment of acid mine water by sulfate-reducing bacteria: results from bench scale experiments. Water Res. 30 (7), 1617–1624.

Cox, G.W., 1972. Laboratory Manual of General Ecology. W.C. Brown, Dubuque, IA, pp. 120–124.

Dehning, I., Stieb, M., Schink, B., 1989. *Sporomusa malonica* sp. nov., a homoacetogenic bacterium growing by decarboxylation of malonate or succinate. Arch. Microbiol. 151 (5), 421–426.

Dvorak, D.H., Hedin, R.S., Edenborn, H.M., McIntire, P.E., 1992. Treatment of metal-contaminated water using bacterial sulfate reduction: results from pilot-scale reactors. Biotechnol. Bioeng. 40, 609–616.

Dworkin, M. (Ed.), 2000. The Prokaryotes: An Evolving Electronic Resource for the Microbiological Community. Springer, New York. <http://141.150.157.117:8080/prokPUB/index.htm>.

Eger, P., Lapakko, K., 1988. Nickel and copper removal from mine drainage by a natural wetland. Bureau of Mines, US Department of Interior.

Hallberg, K.B., Johnson, D.B., 2005a. Microbial populations of compost wetlands constructed to remediate acidic coal spoil drainage. In: Harrison, S.T.L., Rawlings, D.E., Peteren, J. (Eds.), The 16th International Biohydrometallurgy Symposium (IBS), Cape Town, South Africa, pp. 713–722.

Hallberg, K.B., Johnson, D.B., 2005b. Microbiology of a wetland ecosystem constructed to remediate mine drainage from a heavy-metal mine. Sci. Total Environ. 338, 53–66.

Holt, J.H. (Ed.), 1984. Bergey's Manual of Systematic Bacteriology, vol. 2. Williams & Wilkins, Baltimore.

Johnson, D.B., Hallberg, K.B., 2003. The microbiology of acidic mine waters. Res. Microbiol. 154 (7), 466–473.

Johnson, D.B., Hallberg, K.B., 2005. Acid mine drainage remediation options: a review. Sci. Total Environ. 338 (1–2), 3–14.

Kalendar, R., 2005. FastPCR: PCR primer design, DNA and protein tools, repeats and own database searches program. <http://www.biocenter.helsinki.fi/bi/programs/fastpcr.htm>.

Kotsyurbenko, O.R., Nozhevnikova, A.N., Osipov, G.A., Kostrikina, N.A., Lysenko, A.M., 1995. A new psychoactive bacterium *Clostridium fimetarium*, isolated from cattle manure digested at low temperature. Microbiology 64 (6), 681–686.

Labrenz, M., Banfield, J.F., 2004. Sulfate-reducing bacteria-dominated biofilms that precipitate ZnS in a subsurface circumneutral-pH Mine drainage system. Microb. Ecol. 47, 205–217.

Leschine, S.B., 1995. Cellulose degradation in anaerobic environments. Ann. Rev. Microbiol. 49, 399–426.

Logan, M.V., Reardon, K.F., Figueroa, L., McLain, J.E.T., Ahmann, D., 2005. Microbial community activities during establishment, performance, and decline of bench-scale passive treatment systems for mine drainage. Water Res. 39, 4537–4551.

Moore, W.E.C., Johnson, J.L., Holdeman, L.V., 1976. Emendation of *Bacteroidaceae* and *Butyrivibrio* and descriptions of *Desulfomonas* gen. nov. and 10 new species in genera *Desulfomonas*, *Butyrivibrio*, *Eubacterium*, *Clostridium*, and *Ruminococcus*. Int. J. Syst. Bacteriol. 26 (2), 238–252.

Morales, T.A., Dopson, M., Athar, R., Herbert Jr., R.B., 2005. Analysis of bacterial diversity in acidic pond water and compost after treatment of artificial acid mine drainage for metal removal. Biotechnol. Bioeng. 90 (5), 543–551.

Moreno, B., Gómez, M.A., González-López, J., Hontoria, E., 2005a. Inoculation of a submerged filter for biological denitrification of nitrate polluted groundwater: a comparative study. J. Hazardous Mater. 117 (2–3), 141–147.

Moreno, B., Gomez, M.A., Ramos, A., Gonzalez-Lopez, J., Hontoria, E., 2005b. Influence of inocula over start up of a denitrifying submerged filter applied to nitrate contaminated groundwater treatment. J. Hazardous Mater. 127 (1–3), 180–186.

Palop, M.L., Valles, S., Pinaga, F., Flors, A., 1989. Isolation and characterization of an anaerobic, cellulolytic bacterium, *Clostridium celerecrescens* sp. nov. Int. J. Syst. Bacteriol. 39 (1), 68–71.

Pereira, A., Mota, M., Alves, M., 2001. Degradation of oleic acid in anaerobic filters: the effect of inoculum acclimatization and biomass recirculation. Water Environ. Res. 73 (5), 612–621.

Pereyra, L.P., Hanson, R.E., Hiibel, S.R., Pruden, A., Reardon, K.F., 2005. Comparison of Inocula Applied in the Remediation of Acid Mine Drainage by Sulfate Reduction. American Society for Mining and Reclamation (ASMR), Breckenridge CO.

Pruden, A., Pereyra, L.P., Hiibel, S.R., Reardon, K.F., 2006. Microbiology of sulfate-reducing passive treatment systems. In: Seventh International Conference on Acid Rock Drainage (ICARD), St. Louis, MO.

Suzuki, M.T., Taylor, L.T., DeLong, E.F., 2000. Quantitative analysis of small-subunit rRNA genes in mixed microbial populations via 50-nuclease assays. Appl. Environ. Microbiol. 66 (11), 4605–4614.

US EPA, 1997. EPA's national hardrock mining framework. United States Environmental Protection Agency Office of Water.

Vangylswyk, N.O., 1980. A *Fusobacterium polysaccharolyticum* sp. nov., gram-negative rod from the rumen that produces butyrate and ferments cellulose and starch. J. Gen. Microbiol. 116, 157–163.

Vangylswyk, N.O., Vandertoorn, J.J.T.K., 1985. *Eubacterium uniforme* sp. nov. and *Eubacterium xylanophilum* sp. nov., fiber-digesting bacteria from the rumina of sheep fed corn stover. Int. J. Syst. Bacteriol. 35 (3), 323–326.

Varel, V.H., 1989. Reisolation and characterization of *Clostridium longisporum*, a ruminal sporeforming cellulolytic anaerobe. Arch. Microbiol. 152 (3), 209–214.

Wakao, N., Takahashi, T., Sakurai, Y., Shiota, H., 1979. A treatment of acid mine water using sulfate-reducing bacteria. J. Ferment. Technol. 57 (5), 445–452.

Watanabe, K., Kodama, Y., Harayama, S., 2001. Design and evaluation of PCR primers to amplify bacterial 16S ribosomal DNA fragments used for community fingerprinting. J. Microbiol. Methods 44 (3), 253–262.

Waybrant, K.R., Blowes, D.W., Ptacek, C.J., 1998. Selection of reactive mixtures for use in permeable reactive walls for treatment of mine drainage. Environ. Sci. Technol. 32 (13), 1972–1979.

Waybrant, K.R., Ptacek, C.J., Blowes, D.W., 2002. Treatment of mine drainage using permeable reactive barriers: column experiments. Environ. Sci. Technol. 36, 1349-1356.

Weisburg, W.G., Barns, S.M., Pelletier, D.A., Lane, D.J., 1991. 16S ribosomal DNA amplification for phylogenetic study. J. Bacteriol. 173 (2), 697–703.

Xia, S.Q., Shi, Y., Fu, Y.G., Ma, X.M., 2005. DGGE analysis of 16S rDNA of ammonia-oxidizing bacteria in chemical-biological flocculation and chemical coagulation systems. Appl. Microbiol. Biotechnol. 69 (1), 99–105.

Chapter 4 Microbial Community Inocula Composition and Activity in Sulfate-Reducing Batch Systems Remediating Mine Drainage

Pereyra, L.P., Hiibel, S.R., Pruden, A., and K.F. Reardon. (2008). Comparison of. *Biotechnology and Bioengineering*. (In Press, DOI: 10.1002/bit.21930)

Approximate contributions of each author are as follows:

LP Pereyra performed 60% of experimental setup, 50% of the analytical measurements, 50% of the DNA extractions, 60% of the PCR amplification, 60% of the DGGE, 40% of the DNA sequence analysis, 100% of the Q-PCR, 40% of the statistical analyses, and 60% of the manuscript preparation.

SR Hiibel performed 40% of experimental setup, 50% of the analytical measurements, 50% of the DNA extractions, 40% of the PCR amplification, 40% of the DGGE, 60% of the DNA sequence analysis, 100% of the Q-PCR, 60% of the statistical analyses, and 40% of the manuscript preparation.

A Pruden and KF Reardon assisted with experimental design and manuscript preparation.

4.1 Abstract

Five microbial inocula were evaluated for the ability to remediate for mine drainage in batch tests. Twice-acclimated inoculum (ACC), dairy manure (DM), anaerobic digester sludge (ADS) and substrate from the Luttrell (LUTR) and Peerless Jenny King (PJK) sulfate-reducing permeable reactive zones (SR-PRZs) were compared in terms of sulfate and metal removal and pH neutralization. The microbial communities were characterized over 14 weeks using denaturing gradient gel electrophoresis (DGGE) and quantitative polymerase chain reaction (Q-PCR) analysis targeting sulfate-reducing bacteria (SRB) of the genus *Desulfovibrio*. The cultures inoculated with the LUTR, PJK, and DM materials demonstrated significantly higher rates of sulfate and metal removal, and contained all the microorganisms necessary for the desired functioning of SR-PRZs (i.e.,

polysaccharide degraders, fermenters, and sulfate reducers) as well as a relatively high proportion of *Desulfovibrio* spp. These results demonstrate that inoculum influences performance and also provide insights into key aspects of inoculum composition that impact performance. This is the first systematic examination of the relationship between microbial community composition and mine drainage remediation capabilities.

4.2 Introduction

Mine drainage (MD) is a critical environmental problem, with treatment costs estimated in the tens of billions of dollars (Benner *et al.*, 1997). It is formed by the chemical and biological oxidation of sulfide minerals, which results in highly acidic to mildly alkaline waters enriched in sulfate and heavy metals (Benner *et al.*, 1997; Johnson & Hallberg, 2002).

Passive treatment options for MD based on biogeochemical processes are gaining ground over traditional (active) techniques such as limestone addition, which are expensive and require extensive operation and maintenance to function properly (Johnson & Hallberg, 2002). Passive alternatives such as sulfate-reducing permeable reactive zones (SR-PRZs) are minimal-maintenance, low-cost, *in situ* technologies that produce minimal hazardous waste (Johnson & Hallberg, 2002). SR-PRZs are installed in the flow path of the contaminated groundwater and contain a mixture of relatively biodegradable and recalcitrant materials that supply electron donors to a consortium of anaerobic microorganisms responsible for the remediation of the MD (Blowes *et al.*, 2000). The principle mode of function of SR-PRZs is metal sulfide precipitation due to bacterial dissimilatory sulfate reduction. Sulfate-reducing bacteria (SRB) use sulfate as an electron acceptor and reduce it to hydrogen sulfide, which reacts with divalent dissolved metals to form insoluble metal sulfides that precipitate in the barrier. Thus, the activity of the SRB results in decreased sulfate and metal concentrations and an increase in alkalinity and pH due to the production of bicarbonate (Johnson & Hallberg, 2005). Despite the advantages, passive MD treatment systems have been implemented in the field and at laboratory scale with mixed success. Many perform as designed (Benner *et al.*, 1997) while others fail to remove contaminants to the required levels (Barton & Karathanasis, 1999; Johnson & Hallberg, 2002).

Cellulosic materials such as straw, mushroom compost and sawdust are used to provide a long-term source of carbon and energy for the SR-PRZ microorganisms (Johnson & Hallberg, 2002). These complex polymeric compounds cannot be directly degraded by SRB, which only utilize simple organic acids or molecular hydrogen as electron donors. As a consequence, a complex microbial community is responsible for MD remediation in SR-PRZs (Logan *et al.*, 2005). This microbial community includes cellulose-degrading and fermenting bacteria that hydrolyze cellulose and other polymeric compounds and transform the degradation products into simpler organic compounds that can be utilized by the SRB (Logan *et al.*, 2005).

The controlling influence of microbial inoculum on the treatment of MD (Chang *et al.*, 2000; Jong & Parry, 2003; Pruden *et al.*, 2007) as well as on the bioremediation of other contaminants such as nitrate (Moreno *et al.*, 2005), hydrocarbons (Juteau *et al.*, 2003), chlorinated aliphatics (Hourbron *et al.*, 2000) and polychlorinated biphenyls (Fava & Bertin, 1999) has been demonstrated. However, no studies have systematically examined the relationship between the microbial composition of several types of inocula and their ability to remediate MD. Thus, the main objective of the study was to identify key characteristics of microbial inocula for optimizing SR-PRZ performance and reliability using a combination of biomolecular tools and multivariate statistics. The composition and activities of five inocula were compared in batch tests with respect to sulfate and metal removal and pH neutralization. Batch tests are simple to perform in large numbers and, while not exact analogs of the continuous-flow SR-PRZs, they serve as a valuable tool to evaluate and compare several conditions in parallel. The composition of the microbial community over time was monitored with denaturing gradient gel electrophoresis (DGGE) and quantitative polymerase chain reaction (Q-PCR) targeting all bacteria and *Desulfovibrio* spp.. The UniFrac algorithm (Lozupone *et al.*, 2006) was used to compare the microbial communities and identify microorganisms that contributed to major differences among the cultures.

4.3 Materials and Methods

4.3.1 Inocula

Five inocula were investigated: twice-acclimated inoculum (ACC), dairy manure (DM), anaerobic digester sludge (ADS), and substrate collected from two SR-PRZs operating at field sites (Luttrell (LUTR) and Peerless Jenny King (PJK), near Helena, MT). The ACC material was collected from a column simulating a SR-PRZ (Pruden *et al.*, 2007) that had been inoculated with contents from a column containing a sulfate-reducing community (Logan *et al.*, 2005). The dairy manure was obtained from a dairy in Wellington, CO and was included in this study for comparison purposes as it is an inoculum type commonly used in field SR-PRZs (Johnson & Hallberg, 2005). The ADS material was provided by the Drake Water Reclamation Facility of the City of Fort Collins, CO.

4.3.2 Batch Tests Setup

Inoculum, simulated mine water, solid organic substrate, and limestone were added to serum bottles (125 mL) in an anaerobic hood under a nitrogen atmosphere. To avoid inoculation with material that could have been exposed to oxygen, each inoculum was sampled from the core of its storage container. The organic substrate added to each bottle consisted of 7.27 g of beech wood chips (particle size 2.00 mm – 13.33 mm), 0.66 g of pulverized alfalfa (particle size < 0.85 mm), and 3.64 g of pine shavings (particle size 2.00 mm – 9.42 mm). Limestone (1.65 g per bottle, particle size 0.29 mm – 0.85 mm) was added as a source of alkalinity. The simulated mine water was a solution with pH between 5.5 and 6.0 containing: 1.32 g/L $MgSO_4$; 0.03 g/L NH_4Cl; 0.09 g/L $ZnSO_4 \cdot 7H_2O$; 0.06 g/L $FeSO_4 \cdot 7H_2O$, and 0.01 g/L $CdCl_2$ in deionized water purged with nitrogen. Ammonium was included to ensure that microbial growth was not nitrogen limited. Ninety milliliters of simulated acidic MD were added to each bottle. The amount of inoculum added to each bottle was such that all the bottles would initially have the same number of viable bacterial cells (2×10^{10} cells per bottle), as determined by total phospholipid quantification (Findlay *et al.*, 1989). ACC bottles received 80% fewer cells than the other bottles due to limited availability of this inoculum. Uninoculated bottles ("Control") were also tested. Silica sand (particle size 0.42 mm – 0.85 mm) was used to reach the target weight of 33 g per bottle. The bottles were capped with ¼-inch butyl rubber septa (Bellco Glass Inc., Vineland, NJ), sealed with aluminum crimp seals, and maintained upside down in the dark.

Thirteen bottles were prepared for each type of inoculum and two bottles of each type were sacrificed after 0, 2, 4, 9, and 14 weeks. The liquid from the sacrificed bottles was collected in 60-mL Nalgene® bottles and stored at 4 °C. The solid material was stored in 50-mL sterile centrifuge tubes at -80 °C.

4.3.3 Analytical Methods

Sulfate was measured using the SulfaVer® 4 method (Hach Company, Loveland, CO) and a DR/3000 spectrometer (Hach Company). Aqueous samples were filtered through 0.45-μm filters and diluted with deionized water to achieve a concentration within the detection range of 2-70 mg/L. To verify that the characteristics of the samples did not interfere with the method, samples were spiked with standard sulfate solutions. No matrix effects were found.

To determine the metal concentrations, 10 mL of the filtered liquid phase were digested in a CEM microwave digester model MS-2000 (Matthews, NC) using EPA Method SW-3015 and analyzed by inductively coupled plasma atomic emission spectroscopy (ICP-AES) with a Thermo Jarrell Ash IRIS Advantage ICP (Thermo Electron Corp., Milford, MA). Detection limits were 0.01 mg/L for zinc, 0.005 mg/L for cadmium, and 0.01 mg/L for magnesium.

The pH in the liquid phase was measured with an Accumet® AB15 Basic pH meter (Fisher Scientific, Pittsburgh, PA).

4.3.4 DNA Extraction

DNA extractions were carried out on the substrate of the sacrificed bottles using the Ultraclean™ Soil DNA kit (MO BIO, Carlsbad, CA) according to the manufacturer's protocol. Approximately 0.5 g of material was used per extraction and the extracted DNA was PCR amplified and then analyzed by DGGE. For Q-PCR analysis, eight independent DNA extractions were performed and the extracts were pooled together.

4.3.5 PCR Amplification

The variable V3 region of the 16S rDNA was amplified using primers I341F (with a GC clamp) and I533R (Watanabe *et al.*, 2001). The master mix composition and temperature conditions for PCR were described by Pruden et al.(2007) and Watanabe et al. (2001), respectively. The PCR products were quantified using Low DNA Mass™ Ladder (Invitrogen, Carlsbad, CA) in a 1.2% agarose gel.

4.3.6 Denaturing Gradient Gel Electrophoresis (DGGE)

Gels (8% acrylamide/bisacrylamide 19:1, BioRad) were cast using a denaturing gradient of 20 to 55% (PJK, LUTR, and DM samples) or 30 to 50% (ADS and ACC samples), with 100% denaturant defined as 7 M urea and 20% v/v formamide. Electrophoresis was performed at 45 V for 20 hours at 57.5 °C and gels were stained with SybrGold nucleic acid stain (Molecular Probes, Inc., Eugene, OR). For each inoculum, the PCR products corresponding to the different time points sampled were loaded in the same DGGE gel. In each gel, equal masses of the PCR products were loaded in each lane to allow for a semi-quantitative comparison among lanes. The PCR product from one of the LUTR samples was also loaded in the DGGE gels with the ACC and ADS samples to characterize gel-to-gel variations. Gel images were captured using a UVP BioChemi Gel Documentation System (UVP, Upland, CA) and analyzed using Labworks software (UVP). Representative visible DGGE bands were excised with sterile razor blades and stored in 0.5-mL tubes with 36 μL of sterile water. A total of 9, 10, 12, 7, and 13 DGGE bands from the PJK, LUTR, DM, ADS, and ACC gels were sequenced, respectively.

Labworks software was used to identify the bands in the gels and to quantify their relative proportion in each lane. The relative diversity of the microbial community in each sample was calculated using the Shannon Diversity Index (Equation 4.1) (Cox, 1972; Xia *et al.*, 2005):

$$H = -\sum\left[\frac{n_i}{N}\log\left(\frac{n_i}{N}\right)\right] \qquad \textbf{Equation 4.1}$$

where n_i is the intensity of the individual bands and N is the sum of the intensity of all the bands in the lane.

4.3.7 DNA Sequence Analysis

DNA present in the DGGE bands was re-amplified with primers I341F and I533R as described above and the ~200 bp PCR product was sequenced by SeqWright DNA Technology Services (Houston, TX). The closest matches to known microorganisms available in the National Center for Biotechnology Information database were determined using the BLAST alignment tool (http://www.ncbi.nlm.nih.gov/BLAST/). A literature survey was conducted to characterize the properties of the closest matches with respect to substrate utilization and sulfate reduction.

A phylogenetic tree was constructed with the DGGE sequences and 39 reference bacterial sequences belonging to *Prevotella, Bacteroides, Lactobacillus, Anoxibacillus, Sulfurospirillum, Acetobacterium, Flavobacterium, Acinetobacter, Spirochaetaceae, Enterobacteriaceae* and Clostridia. The sequences were aligned with ClustalX (Thompson *et al.*, 1997). The phylogenetic tree was estimated by the neighbor-joining method using PAUP* 4.0 Beta Trial Version (Swofford, 2002) and was analyzed with the UniFrac application (Lozupone *et al.*, 2006). UniFrac was used to compare the different cultures as well as the microbial community in each culture over time to determine if there were significant differences (UniFrac significance test), to identify the microorganisms that led to major differences (lineage-specific analysis), and to find patterns of similarity (principal coordinate analysis (PCoA)) . The comparisons made by these three tests were based on the phylogenetic distances among the samples.

4.3.8 Quantitative PCR (Q-PCR)

Q-PCR targeting the 16S rDNA of total bacteria (B) and the SRB genus *Desulfovibrio* (DSV) was performed using a 7300 Real-Time PCR System (Applied Biosystems, Foster City, CA). The primers used to quantify DSV were described by Daly et al. (2000). For the DSV primers, Q-PCR amplification was performed in a 25 µL reaction mixture using 1X *Power* SYBR® Green PCR Master Mix (Applied Biosystems), 0.30 µM of each primer, 0.2 mM $Mg(OAc)_2$, and 1µL of template with a temperature program of 10 min at 95 °C followed by 60 cycles of 15 s at 95 °C, 37 s at 64 °C, and 60 s at 72 °C. TaqMan® Universal PCR Master Mix (Applied Biosystems) was used to quantify total bacterial 16S rDNA using the conditions, universal 16S rDNA primers and probe described by Suzuki et al. (2000). For each sample and set of primers, a suppression factor that takes into account the impact of PCR inhibitors in the DNA extract was determined as described in Pei et al. (2006).

4.3.9 Statistical Analyses

Mixed linear regressions were fit to the data sets using the PROC MIXED function of SAS 9.1 (SAS Institute Inc., Cary NC). Log transformation of all data sets was required to achieve homoscedasticity, and thus all comparisons were made in log scale. Degrees-of-freedom calculations were performed using the Kenward-Roger method. Significance was defined by a pair-wise comparison p-value ≤ 0.05.

4.4 Results

4.4.1 Effect of Inoculum on Performance

4.4.1.1 Sulfate removal

Liquid-phase sulfate concentrations decreased 46-66% in the LUTR, DM, and PJK bottles. No significant removal was observed in the ADS, ACC, or Control bottles, which were not statistically different from each other (Figure 4.1). The highest extent of sulfate removal occurred in the LUTR bottles, in which nearly 70% of the sulfate had been removed by Week 9.

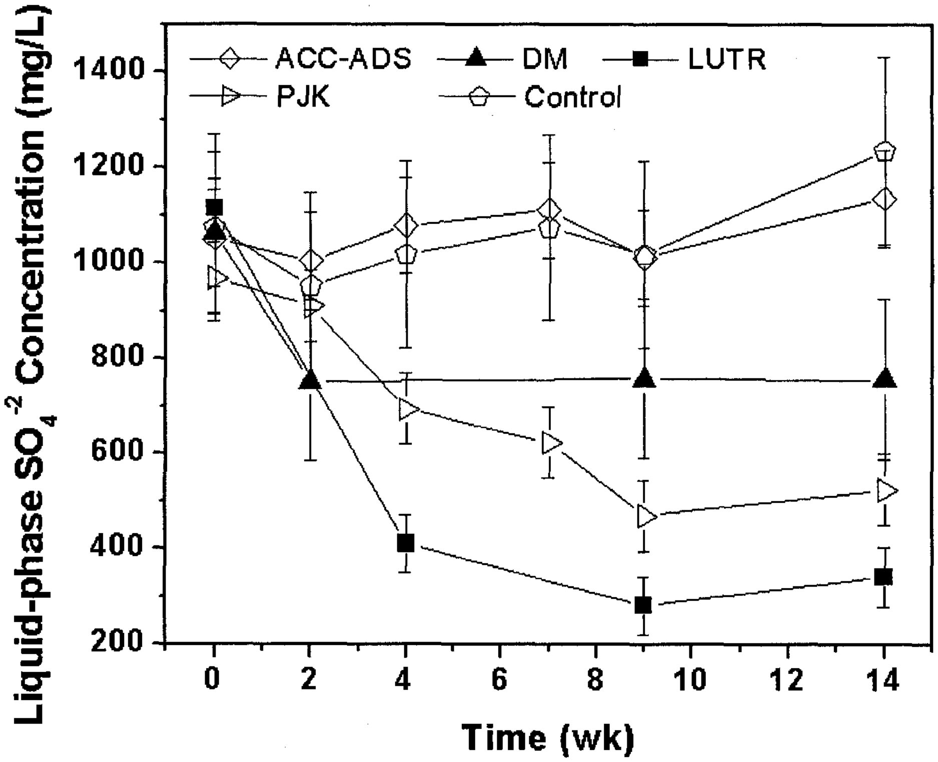

Figure 4.1 – Sulfate concentration in the liquid phase of the bottles. Data points represent the average of technical triplicates and biological duplicates, and error bars correspond to the pooled standard error. Since ACC and ADS bottles were not significantly different, one curve is shown to represent the trend observed in both types of inocula.

The sulfate concentrations in the liquid phase of the bottles sacrificed at Weeks 2 and 9 were also measured two weeks before the sacrifice in order to calculate the average rates of sulfate removal in these two periods (Figure 4.2). At Week 2, the removal rates in the LUTR and DM bottles were significantly higher than those in the other bottles. At Week 9, the rates in the LUTR and DM bottles had decreased and there were no significant differences among the different bottles.

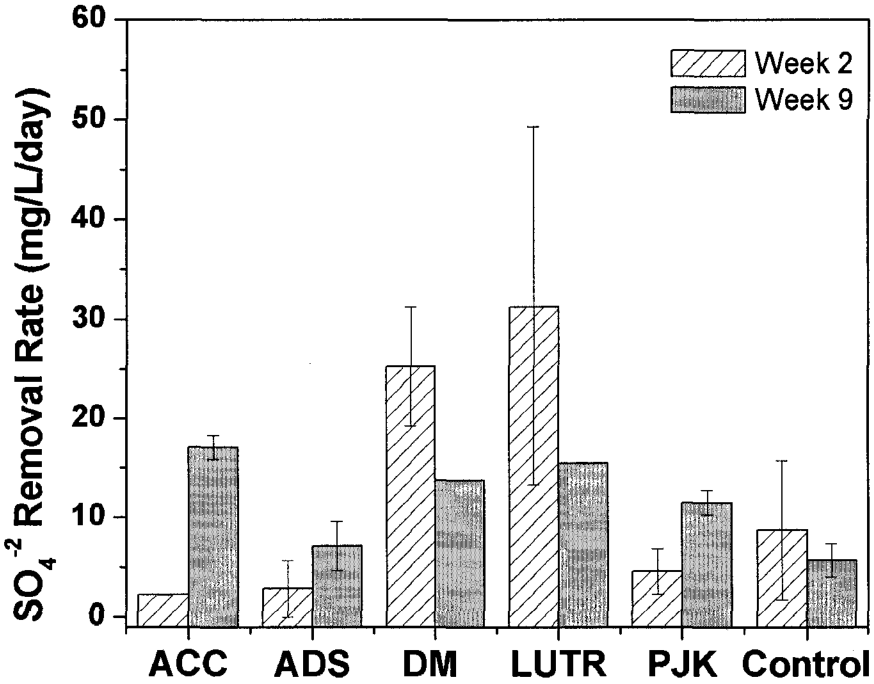

Figure 4.2 – Rate of sulfate removal observed at Weeks 2 and 9 of the experiment. Column heights are the average of biological duplicates, and the error bars are the corresponding pooled standard error.

4.4.1.2 Metal Removal

With respect to the extent of zinc removal, two significantly different groups were observed: zinc removal was high (80-100%) in LUTR- and DM-inoculated bottles, and low (20-40%) in the others (Figure 4.3). A similar trend was observed in cadmium removal (data not shown). Within each group there were no significant differences among bottles ($p>0.05$). In all bottles, the highest rates of removal occurred in the first two weeks. Due to difficulties during the acid digestion of the substrate, no zinc data were obtained for the PJK bottles. Magnesium removal was minimal in all bottles (data not shown).

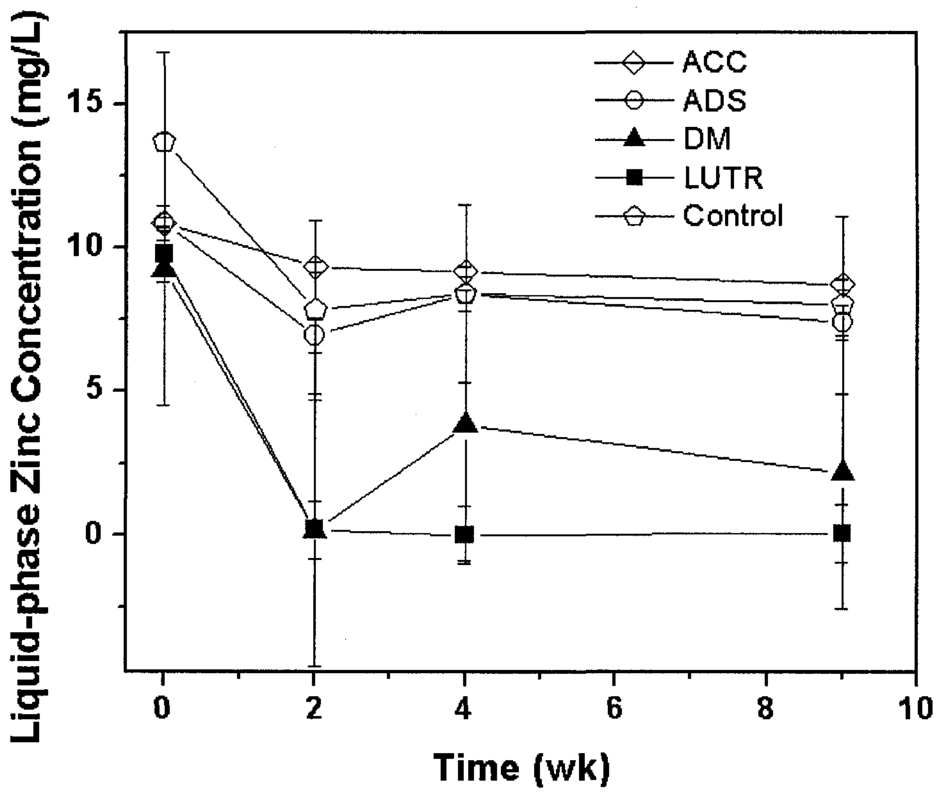

Figure 4.3 – Concentration of soluble zinc in the bottles determined by ICP-AES analysis of digested liquid-phase material. Data points represent the average of technical triplicates and biological duplicates, and error bars correspond to the pooled standard error. PJK data could not be obtained due to technical difficulties with the acid digestion.

4.4.1.3 pH

The initial pH in the bottles was 5.25-5.75 (Figure 4.4). Over the course of the experiment, the pH in the LUTR and PJK bottles was significantly higher than the pH in the other bottles, and no significant differences were found among the others. The pH increased until Week 9 in all bottles except those inoculated with the ADS material, in which the pH decreased during the first four weeks.

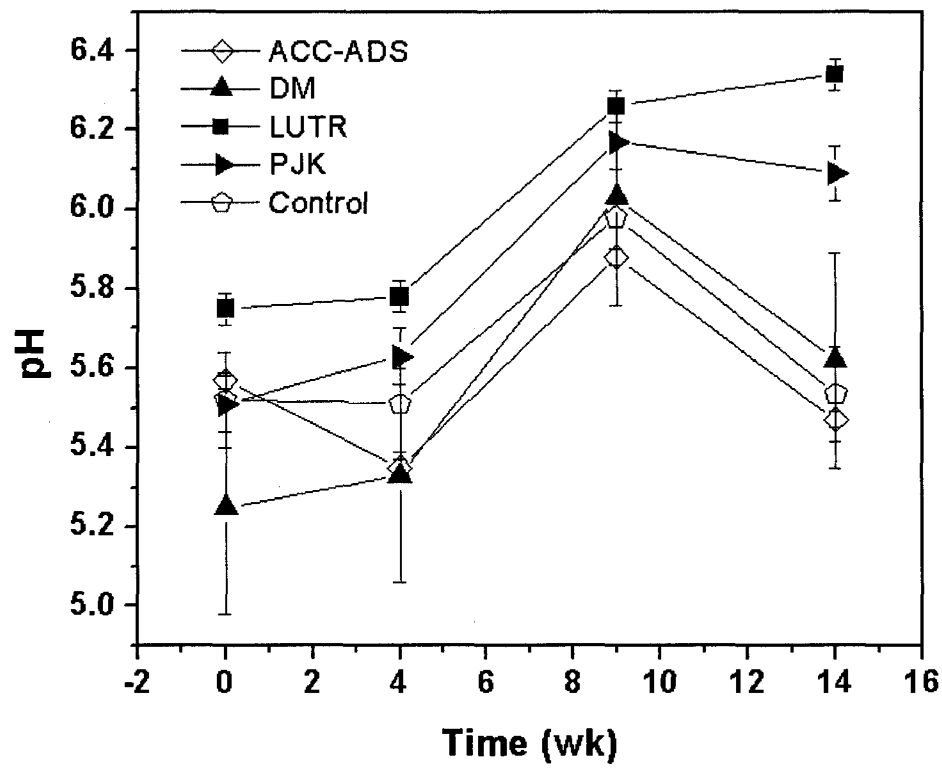

Figure 4.4 – pH in the liquid phase of the bottles. Data points represent the means of biological duplicates, and error bars correspond to the pooled standard error. Since ACC and ADS bottles were not significantly different, one curve is shown to represent the trend observed in both types of inocula.

4.4.2 Microbial Community Composition

4.4.2.1 Microbial Diversity

In the ADS, ACC, and PJK cultures, the DGGE banding patterns changed with time with more bands being detected by the end of the experiment. In the LUTR cultures, the DGGE banding pattern between Weeks 2 and 14 also changed with time but approximately the same number of bands was detected at each time point. In the DM cultures, there was a high similarity in the DGGE banding patterns between Weeks 2 and 14. Values of the Shannon Diversity Index in DM and LUTR cultures remained constant throughout the experiment (H = 0.82 ± 0.05 for DM cultures and 0.86 ± 0.05 for LUTR cultures). In the ADS and ACC cultures, diversity increased between Weeks 0 and 2 and then remained constant at H values of 1.07 ± 0.10 and 1.10 ± 0.19, respectively. The Shannon Diversity Index of the PJK culture increased until Week 4 and then remained constant at 1.12 ± 0.05. A comparison of Shannon Diversity Index values among different cultures was not carried out because of apparent gel-to-gel variations. However, cloning of 16S rDNA (data not shown) indicated that the initial microbial diversity was higher in the LUTR, DM, and PJK cultures than in the ADS culture.

4.4.2.2 Microbial Composition of the Cultures

Sequencing of DGGE bands revealed the identity of some of the members of the microbial communities and gave insight into their function (Table 4.1). The majority of the DNA sequences were related to *Bacteroides, Prevotella,* Spirochaetes and *Clostridium.* In the DM cultures, an uncultured microorganism whose closest cultured phylogenetic relative is the SRB *Desulfosalina propionicus* was detected during Weeks 0, 2, and 14. A microorganism that produces H_2S (*Sulfurospirillum*) from sulfur or thiosulfate (MacRae *et al.*, 2007) was detected in the LUTR culture during Weeks 4, 9, and 14.

Table 4.1 - Characterization of major constituents of the microbial communities in the cultures represented by DGGE bands.

	Highest Match (GenBank accession number) /number of matching DGGE bands/	WK*	% Match	Closest Cultured Relative (GenBank accession number) % Match	C*	P*	F*
PJK	Uncultured bacterium clone anNSG06 (EF034865) /1/	0,2,4,9,14	95	*Bacteroides ovatus* (X83952) 93%	-	+	+
	Uncultured bacterium clone ASG2 (AJ514430) /3/	0,2,4,9,14	90-99	*Prevotella albensis* (AJ011683) 90%	-	+	+
	Uncultured *Bacteroidaceae* bacterium clone dgD-135 (AB264075) /2/	2,4,9,14	86-99	*Bacteroides vulgatus* (M58762) 99%	-	+	+
	Uncultured bacterium clone up.21 (AY212542) /2/	0,2,4,9,14	97-98	*Prevotella bryantii* (AJ006457) 87%	-	+	+
	Uncultured bacterium clone CFT214H12 (DQ456399) /1/	2,4,9	83	*Bacteroides vulgatus* (CP000139) 97%	±	±	+
LUTR	Uncultured bacterium clone ASG2 (AJ514430) /3/	2,4,9,14	97-100	*Prevotella albensis* (AJ011683) 90%	-	+	+
	Uncultured *Sulfurospirillum* sp. clone KB-1 16S ribosomal RNA (AY780560) /1/	4,9,14	92	*Sulfurospirillum multivorans* (X82931) 98%	-	-	-
	Clostridium fimetarium (AF126687)/1/	0,2,4,9	86		-	-	+
	Uncultured bacterium clone CFT214H12 (DQ456399) /1/	2,4,9,14	97	*Bacteroides vulgatus* (CP000139) 97%	±	±	±
	Uncultured Bacteroidetes bacterium clone edNE10 (DQ886174) /2/	2,4,9,14	98-99	*Bacteroides eggerthii* (AB050107) 92%	-	+	+
	Acetobacterium sp. LS2 (DQ767880)/1/	0,2,4,14	98		-	-	+
	Flavobacterium xanthum strain R-9010 (AJ601392) /1/	0,4,9,14	96			-	-
DM	Uncultured bacterium clone ASG2 (AJ514430) /2/	0,2,4,9,14	92-97	*Prevotella albensis* (AJ011683) 90%	-	+	+
	Bacteroides pectinophilus (DQ497993)/3/	0,2,4,9,14	90-98		-	+	+
	Uncultured bacterium clone: 1-H07 (AB107581) /2/	0,2,4,9,14	96-99	*Clostridium ramosum* (M23731) 89%	-	-	+
	Uncultured *Treponema* sp. clone LO008 (AY739142) /1/	0,2,4,9,14	98	*Treponema primitia* (AF093252) 88&	-	+	+
	Uncultured *Treponema* sp. clone MgMjD-083 (AB234369) /1/	0,2,4,9,14	98	*Treponema primitia* (AF093251) 88%	-	+	+
	Uncultured delta proteobacterium clone ESB8 (EF061191)/1/	0,2,14	94	*Desulfosalina propionicus* (DQ067422) 81%	-	-	±
	Clostridium botulinum strain F550 (EF030541) /1/	0,2,4,9,14	84		-	-	+
	Clostridium fimetarium (AF126687)/1/	0,2,9,14	88		-	-	+
ADS	Uncultured bacterium clone H2-2D.74 (DQ423665) /1/	0,4,9,14	83	*Roseiflexus castenholzii* (CP000804) 78%	-	-	-
	Lactobacillus curvatus subsp. *curvatus* (AY204894) /1/	0,2,9	94		-	-	+
	Lactobacillus bifermentans (LBARR16SH) /1/	0,2,4,9,14	97		-	-	+
	Uncultured bacterium clone ASG2 (AJ514430) /4/	0,2,4,9,14	88-98	*Prevotella albensis* (AJ011683) 90%	-	+	+
	Uncultured Bacteroidetes bacterium clone edNE14a (EF152337) /1/	0,2,4,9,14	97	*Bacteroides intestinalis* (AB214329) 91%	±	±	±
ACC	Uncultured bacterium clone ASG2 (AJ514430) /3/	0,2,4,9,14	85-98	*Prevotella albensis* (AJ011683) 90%	-	+	+
	Lachnospira pectinoschiza isolate M56 (AY699283) /1/	0,2,4	94		-	+	-
	Brevundimonas sp. 28/28 (DQ310472) /1/	0,14	97		-	-	-
	Bacteroides helcogenes strain: JCM 6927 (AB200227) /1/	0,2,4,9,14	97		-	+	+
	Uncultured bacterium G1Clone107 (EF149120) /4/	0,2,4,9,14	86-97	*Prevotella bryantii* (AF396925) 92%	-	+	+
	Uncultured bacterium clone: 1-H07 (AB107581) /1/	0,2,4,9,14	96	*Clostridium ramosum* (M23731) 89%	-	-	+
	Uncultured Bacteroidetes bacterium clone edNE65a (EF152339) /2/	0,2,4,9,14	89-99	*Prevotella oulora* (L16472) 92%	-	+	+

*WK: weeks of the experiment in which the band was detected on the DGGE gel; C: cellulose degradation P: Degradation of polysaccharides other than cellulose (pectin, starch, xylan); F: Fermentation *of monosaccharides* (and/or *disaccharides*); +: *function is present*, -: *function is absent*, ±: *function might be present*. Where more than one sequence had the same similarity with the DGGE sequence, all the results corresponding to the highest matches are presented. When the DGGE band sequence corresponded to an uncultured bacterium the function of the microorganism was assigned based on the functions of the closest known relative.

4.4.2.3 Analysis of Microbial Community Differences and Temporal Changes

An overall comparison of the cultures using the UniFrac Significance test revealed that the microbial communities were significantly different (p=0.00). According to the UniFrac lineage-specific analysis, the main differences among cultures were due to the presence of *Treponema* spp. and *Bacteroides pectinophilus* in the DM culture, *Lactobacillus* spp. and an uncultured bacterium (NCBI Accession Number DQ423665) in the ADS cultures, and *Lachnospira pectinophila* in the ACC culture. PCoA did not identify any clear clustering of the communities (Figure 4.5a). The changes in the clustering at the beginning and end of the experiment were also examined with PCoA and no significant differences were found (Figure 4.5b).

The UniFrac lineage-specific analysis and PCoA were also used to study the changes in the microbial community in the same culture over time (Figure 4.5). In the LUTR cultures, Bacteroidetes, Clostridia, *Acetobacterium*, *Sulfurospirillum*, and *Flavobacterium spp.* were abundant at Week 9, and differences in the culture at this point vs. all other times was captured by the first principal coordinate, which explained 61.3% of the variability observed in the data. In the DM cultures, PCoA revealed that there was a high similarity among the microbial communities at Weeks 2, 4, and 9 with *Bacteroides pectinophilus* as the dominant microorganism. In the PJK cultures, the PCoA clustering suggested that the microbial communities in Weeks 4, 9, and 14 were more similar to each other than they were to the communities present at Weeks 0 and 2. An uncultured bacterium (NCBI Accession number AY212542) that is related to *Prevotella bryantii* was dominant during Weeks 9 and 14 and an uncultured bacterium related to *Bacteroides vulgatus* was dominant at Week 4. In the ACC cultures, the initial microbial community was different from the community at all other times and *Bacteroides* spp. were dominant in Weeks 2, 4, and 9 but not initially. In the ADS bottles, the microbial communities at Weeks 0 and 2 were different from each other and from the communities at Weeks 4, 9, and 14. *Lactobacillus* spp. were dominant during Weeks 2 and 9 and an uncultured bacterium (NCBI Accession number DQ423665) was dominant at the beginning of the experiment.

4.4.2.4 Quantification of Total Bacteria and SRB

Throughout the experiment, the lowest numbers of bacterial 16S rDNA gene were observed in the LUTR and Control cultures and the highest numbers in the DM and PJK cultures (Figure 4.6a). In the LUTR culture, the concentration of bacterial 16S rDNA copies did not change significantly for the duration of the experiment.

Desulfovibrio spp. were detected by Q-PCR in all the cultures at the five time points analyzed. Among the ACC, ADS, and Control cultures, there were no significant differences in the ratio of *Desulfovibrio* to total bacteria, which ranged from $1x10^{-6}$ to 0.002 (Figure 4.6b). In the PJK and LUTR cultures, this ratio was higher, ranging from 0.025 to 0.3. Only in the LUTR culture was a continuous increase in the proportion of *Desulfovibrio* observed (6.5-fold increase by Week 14). In the DM culture, the ratio of *Desulfovibrio* to total bacteria at Weeks 0, 4, and 9 was comparable to that of the ACC, ADS, and Control cultures while at Weeks 2 and 14 the ratio was higher and comparable to that of the PJK and LUTR cultures.

The average sulfate removal rates observed at Weeks 2 and 9 were compared to the corresponding values of *Desulfovibrio* normalized to total bacteria. A direct relationship was found only in the ACC and PJK bottles.

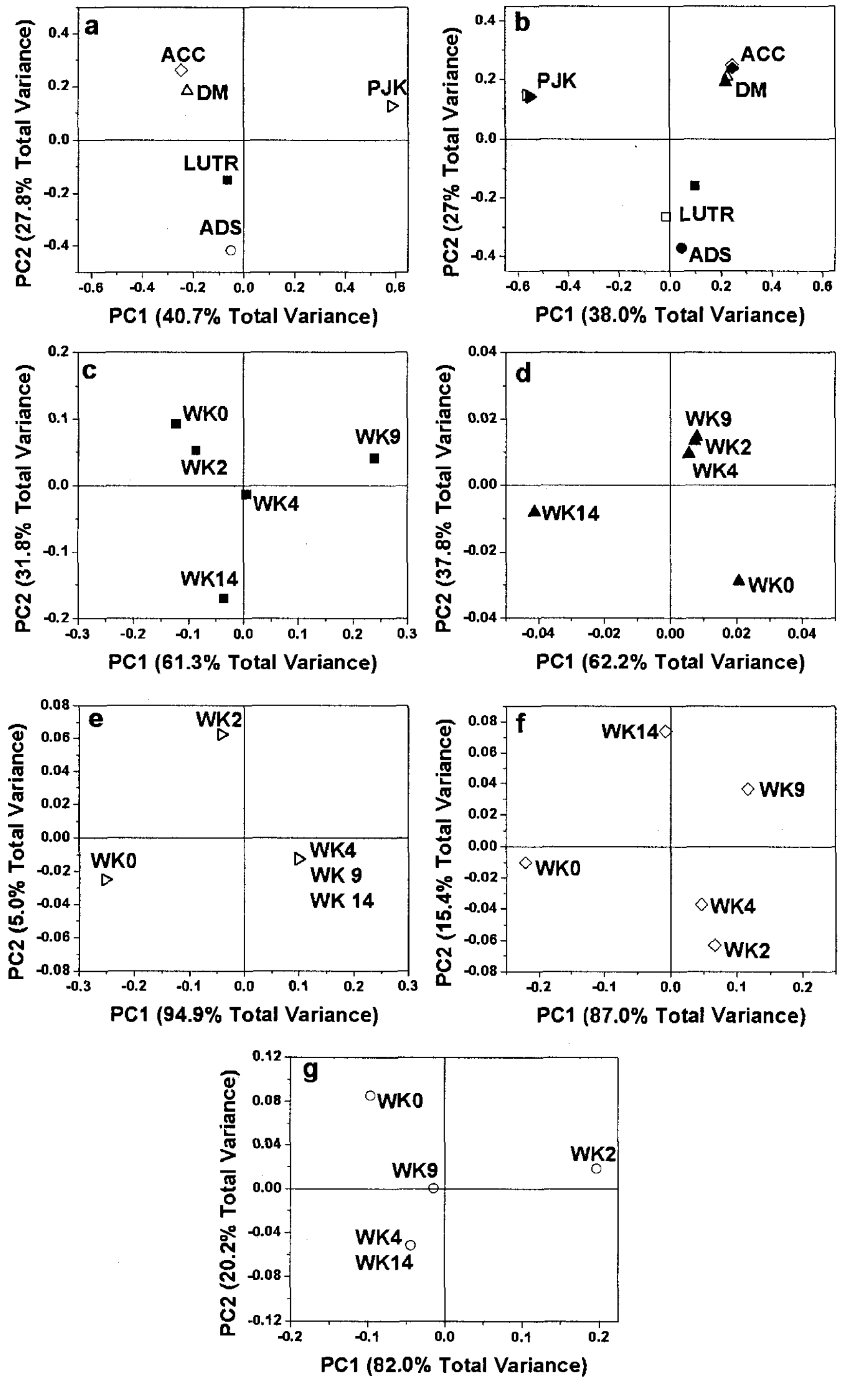

Figure 4.5 - Principal coordinates analysis of the microbial communities in the bottles. Bottles inoculated with different materials, overall comparison (a), and at Weeks 0 (solid symbols) and 14 (open symbols) (b), and LUTR (c), DM (d), PJK (e), ACC (f), and ADS (g) bottles over time.

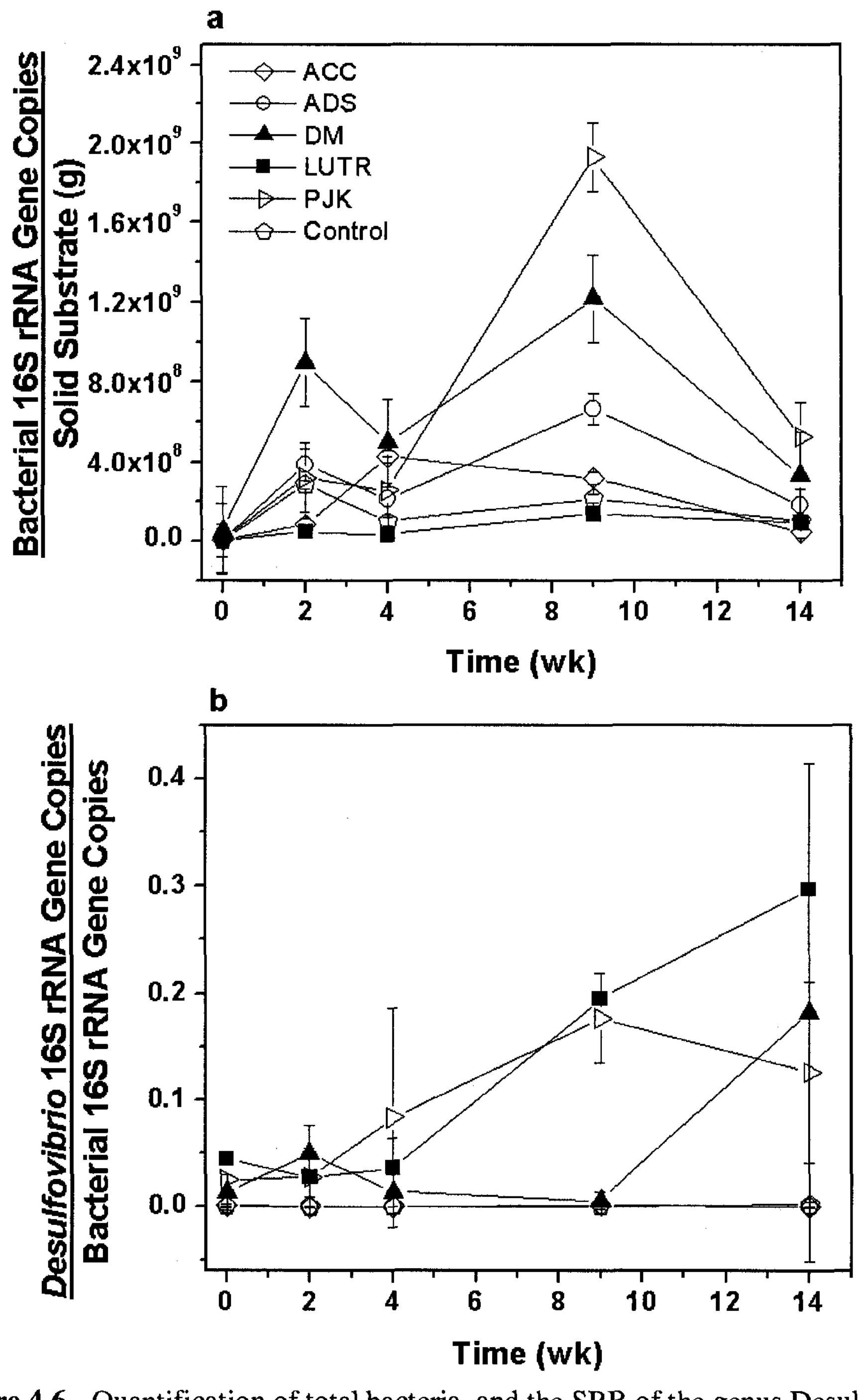

Figure 4.6 - Quantification of total bacteria, and the SRB of the genus Desulfovibrio with time by Q-PCR. Total bacterial 16S rRNA gene copies normalized to mass of substrate (a), and total Desulfovibrio 16S rRNA gene copies normalized to total bacteria (b). Data points are the average of technical triplicates and biological duplicates. The error bars represent the pooled standard error.

4.5 Discussion

4.5.1 Effect of Inoculum on Performance

The results of this study demonstrate that inoculum affected performance based on sulfate removal, zinc removal, and pH neutralization. The best performance was observed in the bottles inoculated with the LUTR, DM, and PJK materials. Performance in the ADS and ACC bottles was poor and was comparable to that of the uninoculated Control bottles.

The major differences in sulfate and zinc removal rates occurred in the first two weeks of the experiment, when these chemical species were removed at higher rates in the DM and LUTR bottles. This suggests that the type of inoculum influences the startup time and is consistent with results from a previous study in columns simulating SR-PRZs (Pruden *et al.*, 2007). The minimal removal of Mg in all the bottles is presumably due to the high solubility product of MgS and is consistent with results obtained by Jong and Parry (2003).

In LUTR and PJK bottles, pH neutralization was higher than in the other bottles. Since all of the bottles received an equivalent dose of limestone, the differences in pH response among them can be attributed to the buffering effect of the bicarbonate generated due to microbial activity. Reduction of the acidity of the water helps improve its quality and also favors microbial activity. For example, cellulose hydrolysis is particularly sensitive to acidic conditions (Weimer, 1992). Thus, low pH in the liquid phase of the cultures might slow cellulose degrading organisms and affect downstream microbial processes, resulting in a deleterious effect on the ability to remediate MD.

4.5.2 Microbial Community Composition and Performance

SRB typically represent a small fraction of the microbial community in the systems treating MD (Hong *et al.*, 2007; Morales *et al.*, 2005; Pruden *et al.*, 2007) and, as a consequence, they are likely to be difficult to detect with DGGE (Muyzer *et al.*, 1993a). For these reasons, DGGE was used here to study only the major constituents of the microbial communities while the SRB were studied with Q-PCR.

Bacteroides, Prevotella, Treponema, and *Clostridium* were the major constituents of the microbial community in the different cultures. This is consistent with the findings of other studies (Labrenz & Banfield, 2004; Pruden *et al.*, 2007). In the PJK and DM cultures, comparison of the PCoA plots and performance data revealed that in each culture the microbial communities were highly similar during the periods of greatest sulfate removal. However, this relationship between PCoA clustering and sulfate removal was not evident in the LUTR culture, in which sulfate removal was also significant. Interestingly, the points in the PCoA plots for the ACC and ADS cultures were spread across the x- and y-axes, and no clear clustering of the communities in relation to the performance was observed. This suggests that the microbial communities in these cultures changed with time without being able to adapt to the environmental conditions.

The microbial communities in the cultures at the beginning and end of the experiment were compared to determine whether the cultures became more similar over time. The convergence of communities to the same composition from different starting conditions has been observed in fixed-film reactors treating aromatic hydrocarbons (MassolDeya *et al.*, 1997) and in soil contaminated with aromatic hydrocarbons (Greene *et al.*, 2000). In this study, however, the microbial communities did not seem to become more similar, suggesting that a variety of communities with different compositions can be active in the remediation of MD and that the inoculum composition plays a significant role in driving this.

4.5.3 Potential Indicators of Inoculum Suitability for MD Remediation

Demonstration of the impact of the inoculum source on performance leads to the question of precisely which inoculum characteristics predict performance. This knowledge may help guide enrichment of inocula known to have the desired microorganisms.

4.5.3.1 Inoculum Source

In this study, it appears that pre-acclimated material from a SR-PRZ (e.g., LUTR or PJK) is ideal while ADS is not recommended. Our previous column study also indicated that acclimated material is associated with superior performance (Pruden *et al.*, 2007). However, because of variability, caution is necessary in this approach. For example, the performance of systems inoculated with dairy manure was poor in a previous study (Pruden *et al.*, 2007) but good in the present study. Although dairy manure is a common source of inoculum for SR-PRZs, its microbial activity and composition are variable and depend on many factors such as animal species, feed composition, manure pH, and manure handling (Leggett *et al.*, 1998). Since a different source of manure was used in both studies, it is likely that the manure microbial composition had an effect. Therefore, while general inoculum sources might provide some guide, more specific information about the inoculum composition is needed.

Handling and storage of the inoculum are also important aspects that must be taken into account. For example, the poor performance of the ACC bottles was unexpected because the ACC inoculum came from a column that was actively removing sulfate and metals from MD (Pruden *et al.*, 2007). Despite the fact that 80% fewer cells were inoculated to the ACC bottles, it was expected that the "MD-adapted" microorganisms in this inoculum would quickly increase in number and remove sulfate at high rates. The poor performance of this culture might be due to extensive manipulation prior to use in this study, including exposure to air.

4.5.3.2 Overall Biomass and Diversity

While higher total biomass concentrations should relate to higher microbial activity, no such trend was apparent. This emphasizes the need for a suitable microbial community composition rather than overall number of bacteria.

Diversity has also been considered to potentially correlate with performance. Von Canstein et al. (2002) reported that species diversity correlated with the efficiency of a mercury-reducing biofilm, and Kaksonen et al. (2004) suggested that diversity and flexibility of the microbial community may enhance the robustness of sulfate-reducing reactors. The microbial communities in LUTR and DM bottles, which performed well, were the most functionally and phylogenetically diverse on the basis of the DGGE analysis. In these cultures, diversity did not change throughout the experiment, whereas the initial diversity of the poorly performing cultures was low and increased later in the experiment.

4.5.3.3 Presence of Key Functional Groups

Cellulose degraders, polysaccharide degraders, fermenters, and sulfate reducers play key roles in SR-PRZ function (Logan *et al.*, 2005) and therefore are of particular interest. In this study, the best performing cultures had in common the presence of microorganisms from all levels of the carbon flow. For example, the LUTR bottles had reached their maximum sulfate removal at Week 9 and the corresponding microbial community contained a variety of microorganisms, including cellulose degraders and fermenters (*Bacteroides* spp. and Clostridia) and H_2S producers (*Sulfurospirillum* and *Desulfovibrio spp.*).

4.5.3.3.1 Cellulose and Other Polysaccharide Degraders:

Members of *Clostridium*, a genus known to include highly efficient cellulose-degrading bacteria, were found only in LUTR and DM cultures. Since cellulose was the major constituent of the carbon substrate in the bottles, and its degradation has been reported to be the rate-limiting step in SR-PRZs (Logan *et al.*, 2005), the presence of *Clostridium* may be a desirable characteristic of the inocula (Labrenz & Banfield, 2004). Clostridia were also found in high-performing sulfate-reducing columns in a previous study (Hong *et al.*, 2007). *Bacteroides* spp., which were detected in all the cultures, are extremely versatile in terms of their growth substrate and they can ferment several poly-, oligo-, and monosaccharides (Holt, 1984a). Some *Bacteroides* spp. are able to ferment cellulose.

Microorganisms that hydrolyze polysaccharides other than cellulose were detected in some cultures. Examples of these microorganisms are *Bacteroides pectinophilus* and spirochetes of the genus *Treponema* found in the DM culture, *Prevotella bryantii* detected in the PJK culture and an uncultured bacterium (NCBI Accession Number AJ514430) related to *Prevotella albensis* that was detected in all the cultures. Some *Treponema* spp. can degrade hemicellulosic material such as xylan, the main component of hemicellulose (Leschine, 1995). *B. pectinophilus* uses pectin, a polysaccharide of high molecular weight, as the only fermentable substrate for growth (Jensen & Canaleparola, 1986). *Prevotella* spp. can utilize plant polysaccharides such as starch, pectins and xylan (Avgustin *et al.*, 1997). The activity of these polysaccharide degraders may benefit cellulose-degrading bacteria by rendering cellulose more accessible (Weimer, 1992) and/or by keeping a low concentration of the products of cellulose hydrolysis (Leschine, 1995).

In general, the best performing cultures contained a variety of polysaccharide-degrading microorganisms that do not degrade cellulose, but that form close associations with cellulose degraders. These microorganisms may be used as indicators of the suitability of the inoculum for MD remediation.

4.5.3.3.2 Fermenters

While all of the cellulose and polysaccharide degraders described above are also capable of fermentation, microorganisms with metabolism restricted to fermentation of simpler molecules were also found in all cultures (Table 4.1). Although the presence of fermentative bacteria is crucial to supply electron donors to the SRB, not all fermenters might be beneficial to the SRB. For example, *Lactobacillus curvatus* and *L. bifermentans* were present throughout the experiment in the poorly performing ADS culture. Lactic acid, the main product of the fermentative metabolism of Lactobacilli (Holt, 1984b), has been reported to inhibit cellulolytic activity in the rumen (Weimer, 1992). Thus, it is possible that *Lactobacillus spp.* have an inhibitory effect on the desired functioning of the microbial food chain, reducing the supply of simple organic compounds to SRB and resulting in a reduction of the sulfate and metal removal rates of these cultures.

4.5.3.3.3 Sulfate Reducers

Desulfovibrio spp. have been identified as major SRB in MD treatment systems (Labrenz & Banfield, 2004) suggesting that they play a role in remediation. In this study, Q-PCR data indicated that the cultures with better performance generally had a higher fraction of *Desulfovibrio* spp. over time.

The ACC and PJK cultures reduced sulfate at rates proportional to the fraction of *Desulfovibrio* in the microbial community, which suggests that, for these cultures, the SRB population limited the rate of sulfate reduction. For the other cultures, different factors (e.g., slow cellulose hydrolysis) may have influenced the rate of sulfate reduction. This observation, along with the fact that the SRB are generally a small fraction of the total bacterial community, emphasizes the need to also consider other members of the microbial community.

4.6 Conclusions

This study demonstrates the influence of microbial inoculum on the remediation of MD and supports our previous findings from column experiments (Pruden *et al.*, 2007) by examining a wider range of inocula and combining biomolecular analyses with multivariate statistical analyses to identify key characteristics. Batch cultivation proved to be a viable experimental format that enabled higher throughput testing than column experiments. The best overall performance with respect to sulfate and zinc removal and pH neutralization was observed in systems inoculated with LUTR, PJK, and DM materials, which contained fermentative and sulfate-reducing bacteria and a variety of polysaccharide degraders. The results of this study suggest that enrichment of inocula known to have the desired microorganisms is a promising low cost means of improving the performance of SR-PRZs.

4.7 Acknowledgements

We are grateful for funding through EPA STAR Grant R 8395101-0, which supported the Rocky Mountain Regional Hazardous Substance Research Center and this project. Additional funding was provided by the National Science Foundation Award CBET-0651947. We also thank Rachel Hanson, Nella Kashani, and April Tischer for laboratory assistance.

4.8 References

Avgustin G, Wallace RJ, Flint HJ. 1997. Phenotypic diversity among ruminal isolates of *Prevotella ruminicola*: Proposal of *Prevotella brevis* sp nov, *Prevotella bryantii* sp nov, and *Prevotella albensis* sp nov and redefinition of *Prevotella ruminicola*. Int. J. Syst. Bacteriol. 47(2):284-288.

Barton CD, Karathanasis AD. 1999. Renovation of a failed constructed wetland treating acid mine drainage. Environ. Geol. 39(1):39-50.

Benner SG, Blowes DW, Ptacek CJ. 1997. A full-scale porous reactive wall for prevention of acid mine drainage. Ground Water Monit. Rem. 17(4):99-107.

Blowes DW, Ptacek CJ, Benner SG, McRae CWT, Bennett TA, Puls RW. 2000. Treatment of inorganic contaminants using permeable reactive barriers. J. Contam. Hydrol. 45(1-2):123-137.

Chang IS, Shin PK, Kim BH. 2000. Biological treatment of acid mine drainage under sulphate-reducing conditions with solid waste materials as substrate. Water Res. 34(4):1269-1277.

Cox GW. 1972. Laboratory Manual of General Ecology. Brown WC, editor. Dubuque, IA. 120-124 p.

Daly K, Sharp RJ, McCarthy AJ. 2000. Development of oligonucleotide probes and PCR primers for detecting phylogenetic subgroups of sulfate-reducing bacteria. Microbiology-(UK) 146:1693-1705.

Dworkin M, editor. 2000. The Prokaryotes: An Evolving Electronic Resource for the Microbiological Community. New York: Springer.

Fava F, Bertin L. 1999. Use of exogenous specialized bacteria in the biological detoxification of a dump site-polychlorobiphenyl-contaminated soil in slurry phase conditions. Biotechnol. Bioeng. 64(2):240-249.

Fields MW, Russell JB, Wilson DB. 1998. The role of ruminal carboxymethylcellulases in the degradation of beta-glucans from cereal grain. FEMS Microbiol. Ecol. 27(3):261-268.

Findlay RH, King GM, Watling L. 1989. Efficacy of phospholipid analysis in determining microbial biomass in sediments. Appl. Environ. Microbiol. 55(11):2888-2893.

Foti M, Sorokin DY, Lomans B, Mussman M, Zacharova EE, Pimenov NV, Kuenen JG, Muyzer G. 2007. Diversity, activity, and abundance of sulfate-reducing bacteria in saline and hypersaline soda lakes. 73(7):2093-2100.

Greene EA, Kay JG, Jaber K, Stehmeier LG, Voordouw G. 2000. Composition of soil microbial communities enriched on a mixture of aromatic hydrocarbons. Appl. Environ. Microbiol. 66(12):5282-5289.

Hanada S, Takaichi S, Matsuura K, Nakamura K. 2002. *Roseiflexus castenholzii* gen. nov., sp nov., a thermophilic, filamentous, photosynthetic bacterium that lacks chlorosomes. 52:187-193.

Holt JG, editor. 1984a. Bergey's Manual of Systematic Bacteriology. Baltimore, MD: Williams & Wilkins.

Holt JG, editor. 1984b. Bergey's Manual of Systematic Bacteriology. Baltimore, MD: Williams & Wilkins.

Hong H, Pruden A, Reardon KF. 2007. Comparison of CE-SSCP and DGGE for monitoring a complex microbial community remediating mine drainage. J. Microbiol. Methods 69:52-64.

Hourbron E, Escoffier S, Capdeville B. 2000. Trichloroethylene elimination assay by natural consortia of heterotrophic and methanotrophic bacteria. Water Sci. Technol. 42(5-6):395-402.

Jensen NS, Canaleparola E. 1986. *Bacteroides pectinophilus* sp. nov. and *Bacteroides galacturonicus* sp. nov. 2 pectinolytic bacteria from the human intestinal tract. Appl. Environ. Microbiol. 52(4):880-887.

Johnson DB, Hallberg KB. 2005. Acid mine drainage remediation options: a review. Sci. Total Environ. 338(1-2):3-14.

Johnson DJ, Hallberg KB. 2002. Pitfalls of passive mine water treatment. Rev. Environ. Sci. Biotechnol. 1(4):335-343.

Jong T, Parry DL. 2003. Removal of sulfate and heavy metals by sulfate reducing bacteria in short-term bench scale upflow anaerobic packed bed reactor runs. Water Res. 37(14):3379-3389.

Juteau P, Bisaillon JG, Lepine F, Ratheau V, Beaudet R, Villemur R. 2003. Improving the biotreatment of hydrocarbons-contaminated soils by addition of activated sludge taken from the wastewater treatment facilities of an oil refinery. Biodegradation 14(1):31-40.

Kaksonen AH, Plumb JJ, Franzmann PD, Puhakka JA. 2004. Simple organic electron donors support diverse sulfate-reducing communities in fluidized-bed reactors treating acidic metal- and sulfate-containing wastewater. FEMS Microbiol. Ecol. 47(3):279-289.

Kotsyurbenko OR, Nozhevnikova AN, Osipov GA, Kostrikina NA, Lysenko AM. 1995. A new psychoactive bacterium *Clostridium fimetarium*, isolated from cattle manure digested at low temperature. Microbiology 64(6):681-686.

Labrenz M, Banfield JF. 2004. Sulfate-reducing bacteria-dominated biofilms that precipitate ZnS in a subsurface circumneutral-pH mine drainage system. Microb. Ecol. 47(3):205-217.

Leggett JA, Lanyon LE, Graves RE. 1998. Biological manipulation of manure: Getting what you want from animal manure. University Park, PA.: The Pennsylvania State University. Department of Agricultural and Biological Engineering. PSU/96.

Leschine SB. 1995. Cellulose degradation in anaerobic environments. Annu. Rev. Microbiol. 49:399-426.

Logan MV, Reardon KF, Figueroa LA, McLain JET, Ahmann DM. 2005. Microbial community activities during establishment, performance, and decline of bench-scale passive treatment systems for mine drainage. Water Res. 39(18):4537-4551.

Lozupone C, Hamady M, Knight R. 2006. UniFrac - An online tool for comparing microbial community diversity in a phylogenetic context. BMC Bioinformatics 7.

MacRae JD, Lavine IN, McCaffery KA, Ricupero K. 2007. Isolation and characterization of NP4, arsenate-reducing *Sulfurospirillum*, from Maine groundwater. J. Environ. Eng.-ASCE 133(1):81-88.

MassolDeya A, Weller R, RiosHernandez L, Zhou JZ, Hickey RF, Tiedje JM. 1997. Succession and convergence of biofilm communities in fixed-film reactors treating aromatic hydrocarbons in groundwater. Appl. Environ. Microbiol. 63(1):270-276.

Matsui H, Ogata K, Tajima K, Nakamura M, Nagamine T, Aminov RI, Benno Y. 2000. Phenotypic characterization of polysaccharidases produced by four *Prevotella* type strains. Curr. Microbiol. 41(1):45-49.

Morales TA, Dopson M, Athar R, Herbert RB. 2005. Analysis of bacterial diversity in acidic pond water and compost after treatment of artificial acid mine drainage for metal removal. Biotechnol. Bioeng. 90(5):543-551.

Moreno B, Gomez MA, Gonzalez-Lopez J, Hontoria E. 2005. Inoculation of a submerged filter for biological denitrification of nitrate polluted groundwater: a comparative study. J. Hazard. Mater. 117(2-3):141-147.

Muyzer G, Dewaal EC, Uitterlinden AG. 1993. Profiling of complex microbial populations by denaturing gradient gel electrophoresis analysis of polymerase chain reaction-amplified genes coding for 16S rRNA. Appl. Environ. Microbiol. 59(3):695-700.

Pei RT, Kim SC, Carlson KH, Pruden A. 2006. Effect of River Landscape on the sediment concentrations of antibiotics and corresponding antibiotic resistance genes (ARG). Water Res. 40(12):2427-2435.

Pruden A, Messner N, Pereyra L, Hanson RE, Hiibel SR, Reardon KF. 2007. The effect of inoculum on the performance of sulfate-reducing columns treating heavy metal contaminated water. Water Res. 41(4):904- 914.

Russell JB, Rychlik JL. 2001. Factors that alter rumen microbial ecology. Science 292(5519):1119-1122.

Suzuki MT, Taylor LT, DeLong EF. 2000. Quantitative analysis of small-subunit rRNA genes in mixed microbial populations via 5 '-nuclease assays. Appl. Environ. Microbiol. 66(11):4605-4614.

Swofford DL. 2002. PAUP*: Phylogenetic Analysis Using Parsimony (and Other Methods) 4.0 Beta, 4.0b10. Sinauer Associates I, editor. Sinauer Associates, Inc.

Thompson JD, Gibson TJ, Plewniak F, Jeanmougin F, Higgins DG. 1997. The CLUSTAL_X windows interface: flexible strategies for multiple sequence alignment aided by quality analysis tools. Nucleic Acids Res. 25(24):4876-4882.

von Canstein H, Kelly S, Li Y, Wagner-Dobler I. 2002. Species diversity improves the efficiency of mercury-reducing biofilms under changing environmental conditions. Appl. Environ. Microbiol. 68(6):2829-2837.

Watanabe K, Kodama Y, Harayama S. 2001. Design and evaluation of PCR primers to amplify bacterial 16S ribosomal DNA fragments used for community fingerprinting. J. Microbiol. Methods 44(3):253-262.

Weimer PJ. 1992. Cellulose degradation by ruminal microorganisms. Crit. Rev. Biotechnol. 12(3):189-223.

Xia SQ, Shi Y, Fu YG, Ma XM. 2005. DGGE analysis of 16S rDNA of ammonia-oxidizing bacteria in chemical-biological flocculation and chemical coagulation systems. Appl. Microbiol. Biotechnol. 69(1):99-105.

Chapter 5 Effect of Organic Substrate on the Microbial Community Remediating Acid Mine Drainage: National Tunnel, Colorado Pilot Study

Pereyra, L.P., Hiibel, S.R., Prieto, M.V., Figueroa, L.A., Reisman, D.J., Reardon, K.F., and A. Pruden

(*in preparation for submission to* Applied and Environmental Microbiology)

Approximate contributions of each author are as follows:

LP Pereyra performed 50% of the sample collection, 100% of the Q-PCR, 75% of the Q-PCR data analysis, 20% of the sequence BLASTing, 25% of the PCoA, and 40% of the manuscript preparation.

SR Hiibel performed 50% of the sample collection, 25% of the Q-PCR data analysis, 20% of the 16S cloning, 100% of the *apsA* cloning, 50% of the sequence BLASTing, 75% of the PCoA, and 40% of the manuscript preparation.

MV Prieto performed 100% of the DNA extractions, 80% of the 16S cloning, 30% of the sequence BLASTing, and 20% of the manuscript preparation.

LA Figueroa assisted with experimental design.

DJ Reisman assisted with experimental design and manuscript preparation.

KF Reardon and A Pruden assisted with manuscript preparation.

5.1 Abstract

Acid mine drainage (AMD) is acidic, metal-rich water formed when sulfide minerals react with oxygen and water. There are various options for the treatment of AMD; however, passive biological systems such as sulfate-reducing bioreactors (SRBRs) are promising because of their low cost and maintenance requirements. The purpose of this study was to explore the effect the choice of organic substrates had on the microbial communities present in pilot-scale SRBRs treating AMD in order to better understand how substrate-microbe interactions drive performance. Three organic substrates were evaluated: ethanol (ETOH); and two lignocellulose-based mixtures: hay and wood chips

(HYWD), and corn stover and wood chips (CSWD). The microbial community compositions were characterized by cloning of 16S rRNA genes and *apsA* genes associated with sulfate reduction. Quantitative polymerase chain reaction (Q-PCR) was applied to quantify *Desulfovibrio-Desulfomicrobium* spp. and methanogens. Results revealed distinct differences in microbial community compositions and relative quantities of total and sulfate-reducing bacteria (SRB) among the SRBRs. In particular, the greatest proportion of SRBs was observed in the ETOH SRBRs, but the total number of bacteria was low. The HYWD and CSWD SRBRs had highly similar bacterial communities, which were complex in composition in comparison to the ETOH SRBRs. Methanogens were found to be present in all SRBRs at low levels and were the highest in the lignocellulose-based SRBRs. This study demonstrates that the choice of organic substrate influences microbial community composition and diversity, which may play an important role in performance and reliability.

5.2 Introduction

Acid mine drainage (AMD) is acidic, metal-rich water formed when sulfide minerals from abandoned or active mines are exposed to and react with oxygen and water. AMD represents a worldwide concern due to its potential to cause contamination of drinking water systems, disruption of growth and reproduction of aquatic life, and other problems related to its toxicity. Because most remediation sites are remote or associated with abandoned mines, treatment systems that are efficient and cost-effective are of great importance.

A variety of abiotic and biological remediation systems have been developed and used for the treatment of AMD. Abiotic methods usually involve the addition of neutralizing agents or other chemicals and thus can require an impractically high level of operation and maintenance. Alternatively, bioremediation offers promise because of the low cost of maintenance and low external energy requirements. In particular, sulfate-reducing biochemical reactors (SRBRs) have been applied with some success, but reports from the field are variable in terms of their overall performance and reliability (Benner et al. 1997; Barton and Karathanasis 1999; Johnson and Hallberg 2002). The basic principle of SRBRs is the cultivation of sulfate-reducing bacteria (SRB) that reduce the sulfate in the mine drainage to sulfide, which then reacts with heavy metals and precipitates them as metal sulfides. Metal sulfides are immobilized within the SRBR and thus removed from the water (Johnson and Hallberg, 2005). Significant levels of alkalinity are also produced, which helps neutralize the acidity.

A significant aspect of SRBR design is the choice of organic substrate. Relatively simple substrates, such as organic acids or alcohols, have the advantage in that they provide a carbon and energy source that SRB can utilize directly for growth. The disadvantage, however, is that organic acids and alcohols are used quickly and cannot be retained within the system, which increases the cost and maintenance requirements. Alternatively, complex lignocellulosic organic material, such as wood chips, provides a slow-release source of carbon and energy that can be retained within the system. Because SRB cannot directly utilize cellulosic material, they must rely on the activities of anaerobic cellulose degraders and fermenters to break the complex material down into simpler components that they can utilize (Logan et al., 2005).

The purpose of this study was to explore how microbial communities in parallel pilot-scale SRBRs treating AMD were affected by the choice of organic substrate they received. Recent studies applying molecular biological tools have revealed the complexity of microbial communities in lignocellulose-based SRBRs (Pruden et al., 2007; Johnson and Hallberg, 2005); however, a side-by-side comparison of the microbial communities resulting from complex versus simple carbon substrates has not been determined previously. Since microbes are the primary catalysts of SRBR function, the composition of the microbial community potentially plays a highly important role in SRBR performance. For example, complex versus simple substrate SRBRs are likely to drive the development of distinct microbial communities. The relative levels of microorganisms that compete with SRB for hydrogen, acetate, and other available electron donors, such as methanogens, may have a negative overall impact (Daly et al., 2000). Distinct kinds of SRB may also result, which may then differ in their susceptibilities to toxins or their abilities to tolerate various stressors, such as low temperatures or shifts in pH or metal concentrations. Currently, the ability to recover from such stress events as well as the overall lifespan of performance are major challenges to SRBR design and operation.

In this study, six pilot-scale SRBRs were operated in Black Hawk, Colorado, and were fed with discharge from the National Tunnel, which is a major contributor of contaminants to this area (Buccambuso et al., 2007). Three organic substrate conditions were compared in duplicate: ethanol (ETOH 1,2), hay and wood chips (HYWD 3,4), and corn stover and wood chips (CSWD 5,6). Microbial populations within these conditions were characterized by cloning of 16S genes, which are conserved in all bacteria, and the adenosine-5'-phosphosulfate reductase (*apsA*) gene, which is a functional gene present in SRB. In addition, quantitative polymerase chain reaction (Q-PCR) was performed targeting total bacteria, the *Desulfovibrio* and *Desulfomicrobium* genera of SRB, and methanogens, in order to obtain a quantitative understanding of these groups within the community. The overall effect of substrate on SRBR performance is described further elsewhere (Venot et al., 2008). Thus the broader goal of this project is to better understand the role of substrate-microbe interactions in SRBR performance. With this understanding of SRBR microbial and organic substrate composition, better criteria may be developed for their design, operation, and overall success.

5.3 Materials and Methods

5.3.1 Sample Site and Collection

The bioreactors in this study are located in Black Hawk, Colorado, under the Mill Street Bridge, within the Central City Clear Creek Superfund site. They are fed with a water discharge from the National Tunnel that contains elevated levels of sulfate and heavy metals (zinc, copper, manganese, cadmium, lead, and arsenic) resulting from historic gold mining. Four organic substrate conditions were studied in duplicate (further details are provided in Venot et al., 2008):

- Ethanol-fed SRBRs (ETOH 1 & 2): Each of these vertical-down flow reactors consists of one non-metallic 55-gallon drum packed with limestone (~3/4 in) and a zero-valence iron (ZVI) slag layer on the top. The reactors were inoculated with approximately 5 lb of fresh horse manure layered on top of the limestone, and are constantly fed with ethanol and AMD from the National Tunnel.

- Solid-substrate SRBRs (HYWD 3 & 4 and CSWD 5 & 6): These 55-gal non-metallic drums contain mixed wood chips, limestone, horse manure, and hay or corn stover (Table 5.1), and are also fed with AMD from the National Tunnel with a vertical-down flow.

Table 5.1 - Proportion of solid substrate components in the HYWD and CSWD SRBRs.

	Percentage (%)	
Component	HYWD	CSWD
Wood Chips	50	35
Limestone	30	20
Horse Manure	10	15
Hay	10	0
Corn Stover	0	30

Five removable mesh bags were filled with the respective substrate and stacked in the center of each reactor within a vertically placed perforated PVC pipe to facilitate sampling. For sample collection, one mesh bag from each reactor (second from the topmost) was removed and placed on ice for immediate transport to the laboratory where they were then stored at -80 °C for subsequent analyses. Random grab samples were also collected from the main portion of the SRBRs about 1 inch below the surface, in order to determine the representativeness of the mesh bags for sampling.

5.3.2 DNA Extraction

DNA was extracted from approximately 5 g of each of the collected samples using the PowerMax Soil DNA Isolation Kit (MO BIO, Carlsbad, CA) according to the manufacturer's protocol, and stored at -80 °C for subsequent studies. The exact mass of material used in each extraction was determined and recorded for downstream quantification purposes.

5.3.3 Real-Time Quantitative Polymerase Chain Reaction (Q-PCR)

The 16S rDNA assays were targeted to quantify total bacteria and the SRB genera *Desulfovibrio* and *Desulfomicrobium.* Methanogens were quantified by targeting the gene that encodes the alpha subunit of the methyl coenzyme-M reductase (*mcrA*), an enzyme unique to methanogens.

All reactions were performed in a 7300 Real-Time PCR cycler (Applied Biosystems, Foster City, CA). Reactions were performed in triplicate using 1X Power SYBR Green PCR Master Mix (Applied Biosystems, Foster City, CA) with primers DSV230f and DSV838r (Daly et al., 2000) to target the 16S rDNA of *Desulfovibrio* and *Desulfomicrobium* species or the *mcrA* primers designed by Luton et al. (2002) to target methanogens. TaqMan Universal PCR Master Mix (Applied Biosystems, Foster City, CA) and primers 1369f and 1492r (Suzuki et al., 2000) were used to target the 16S rDNA of total bacteria. A calibration curve was constructed for each set of primers using serial dilutions of PCR amplified 16S rDNA (for total bacteria and *Desulfovibrio /Desulfomicrobium* Q-PCR) previously purified and quantified (standards) or serial dilutions of genomic DNA (for the methanogens Q-PCR). An environmental sample consisting of DNA extracted from the CSWD6 sample was used as standard for the total bacteria Q-PCR, and a *Desulfovibrio salexigens* pure culture was used as standard for the *Desulfovibrio/Desulfomicrobium* Q-PCR. Genomic DNA from *Methanococcus maripaludis* (ATCC 43000D) served as standard for the methanogens Q-PCR.

5.3.4 16S rDNA and apsA PCR Amplification and Cloning

To characterize the overall composition of the bacterial community and to identify dominant bacteria, cloning of 16S rDNA was performed. In order to directly target SRB, *apsA* gene cloning was also performed. The 16S rRNA gene and *apsA* gene (Friendrich, 2002) were PCR-amplified using primer sets 341F and 1492R (Weisburg *et al.*, 1991) and 7F and 8R (Friedrich (2002)), respectively. PCR products were cloned with the TOPO TA Cloning Kit (Invitrogen, Carlsbad, CA) according to the manufacturer's protocol. Amplified rDNA restriction analysis (ARDRA) was performed visually from MspI (Promega, Madison, WI) digested PCR-amplified (using vector specific primers) inserts. 16S gene clones with ARDRA patterns appearing two or more times and all *apsA* gene clones with unique ARDRA patterns were sequenced. Because of the labor and cost associated with cloning of the 16S rDNA gene, and because it has already been applied in other studies (Johnson and Hallberg, 2005; Hiibel et al., in press), cloning of 16S rDNA was performed on only one of each of the duplicate SRBRs.

5.3.5 Sequence analyses

The DNA sequences obtained from cloning were aligned to the sequences of the closest identified microorganisms by the Basic Local Alignment Search Tool (BLAST) (http://www.ncbi.nlm.nih.gov/BLAST/) and the Ribosomal Database Project II (RDP) (http://rdp.cme.msu.edu/). A literature review involving the microorganisms identified was used to assign a putative function to the identified bacteria. A phylogenetic tree was constructed using the 16S gene sequences of each of the unique clones identified, and 16S rDNA sequences of related organisms obtained from BLAST results.

5.3.6 Principal Coordinate Analysis (PCoA)

The phylogenetic trees representing the two genes were analyzed directly using PCoA and the UniFrac significance tests of the UniFrac algorithm (Lozupone & Knight, 2005; Lozupone et al., 2006; Lozupone et al., 2007). PCoA differs from principal component analysis (PCA) in that the input data are the phylogenetic distances between each pair of sampling locations rather than the number of times each clone sequence was observed at each location. The UniFrac significance test is used to determine whether two microbial communities are significantly different. Communities are considered different if the fraction of the phylogenetic tree unique to one is greater than would be expected by chance (Lozupone & Knight, 2005). For all analyses, the non-normalized abundance data, based on the ARDRA screening, were incorporated in the UniFrac significance test; reference strains used to construct the phylogenetic trees were not included. The raw p-values from the UniFrac significance tests are reported, with p-value ≤ 0.05 considered to be statistically significant.

5.4 Results

5.4.1 Microbial community diversity and composition

Rarefaction analysis of ARDRA patterns revealed that the overall bacterial diversity of a lignocellulose-based SRBR (CSWD 5) was significantly higher than that of an ethanol-fed SRBR (ETOH 2) (Figure 5.1). The overall diversity of the HYWD 3 reactor was similar to that of the ETOH 2 reactor. However, it should be noted that the HYWD 3 reactor encountered significant operational problems in which the substrate material was inadvertently exposed to oxygen.

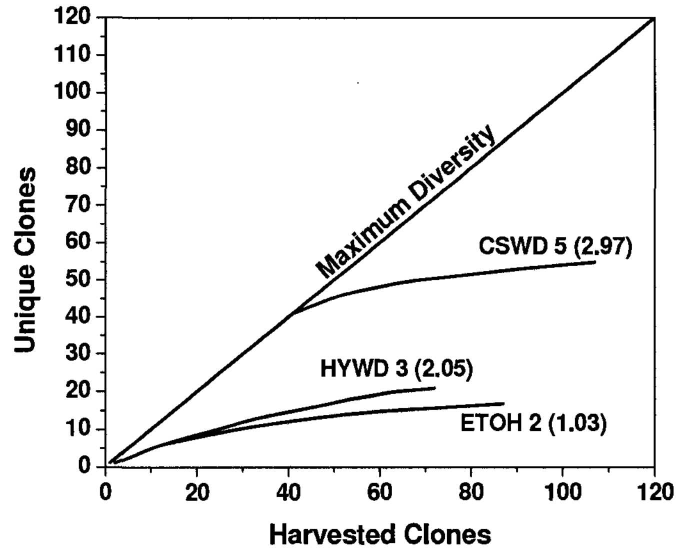

Figure 5.1 - Relative diversity of the ETOH 2, HYWD 3, and CSWD 5 SRBRs determined by cloning of the 16S gene. Shannon diversity indices for each SRBR are indicated in parenthesis and were calculated based on the frequency of each clone in the clone library.

Analysis of the 16S rDNA sequences of the dominant clones also revealed differences among the SRBRs. Notably, the proportion of SRB in the ETOH 2 reactor was almost 70%, whereas SRB were only 2-5% in the HYWD 3 and CSWD 6 reactors (Figure 5.2). Other putative functional groups, such as cellulose degraders, were identified in the lignocellulose-based reactors but not in the ETOH reactor. Fermenters were estimated at 25-30% of the lignocellulose-based communities and only 5% of the ETOH community.

ApsA gene profiling revealed some overlaps and some differences between the lignocellulose and ETOH SRBRs (Figure 5.3). An SRB most closely related to

Desulfovibrio sp. JD160 and *Desulfovibrio aerotolerans* was found in all of the SRBRs. A *Desulfomicrobium baculatum* relative was only found in the two SRBRs, ETOH 1 and HYWD 3. In the lignocellulose SRBRs, additional bacteria carrying the *apsA* gene were found: an uncultured bacterium that was present at about 10% in the three properly functioning SRBRs (HYWD 4, CSWD 5, and CSWD 6), *Thiobacillus* spp. (only in HYWD 3), *D. desulfuricans*, and *D. burkinensis*. *Thiobacillus* spp. have been recognized in the literature as aerobic organisms that reverse the process of sulfate reduction.

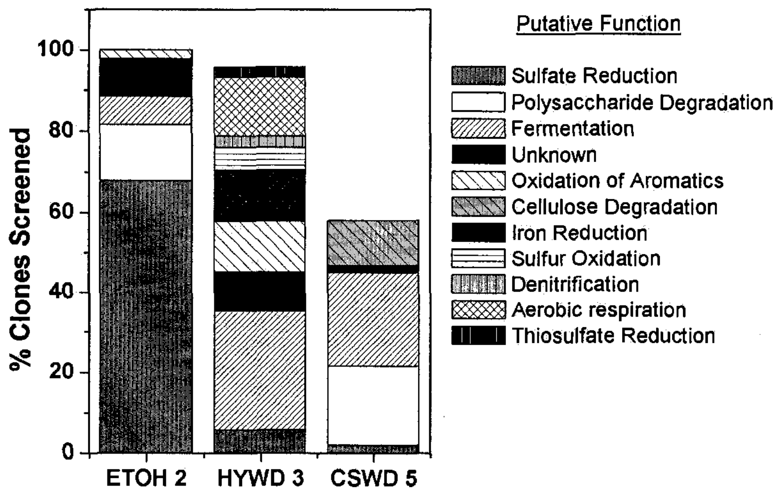

Figure 5.2 - Distribution of microbial functions in each SRBR based on the identity of the microorganisms identified through 16S gene cloning and DNA sequencing.

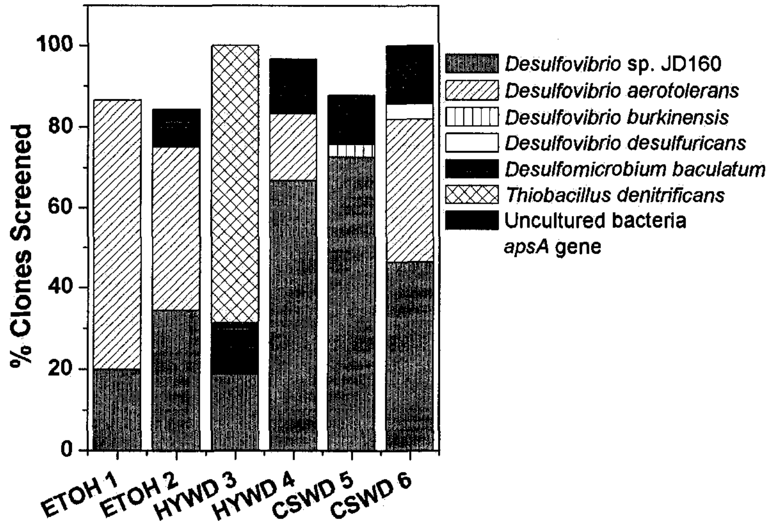

Figure 5.3 - Identity and percentages of *apsA*-containing microorganisms in ETOH, HYWD, and CSWD SRBRs.

PCoA provided a means to statistically compare the microbial communities and identify similarities and differences (Figure 5.4). PCoA analysis of 16S rDNA revealed that the ETOH 2, HYWD 3, and CSWD 6 communities were distinct across both coordinates. PCoA analysis of *apsA* genes, however, indicated that all of the SRBRs except HYWD 3 were relatively similar along the second coordinate, but distinct along the first coordinate, although the ETOH SRBRs were near to each other along the first coordinate as were the lignocellulose-based SRBRs.

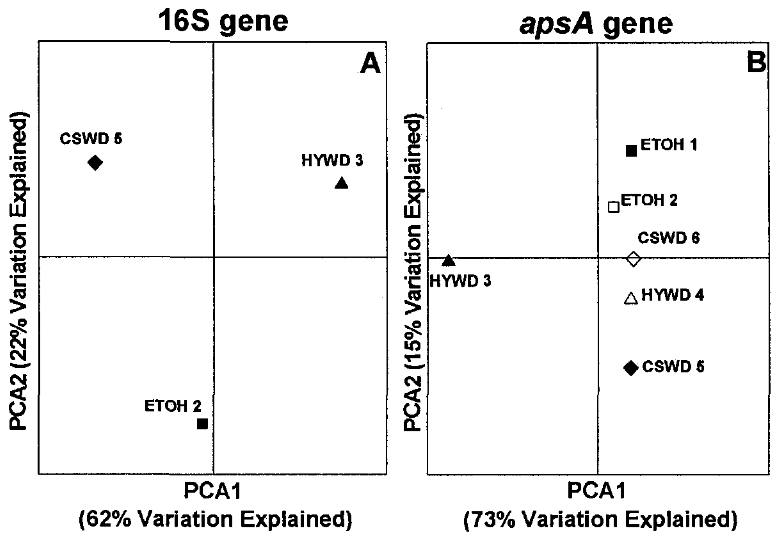

Figure 5.4 - Principal coordinate analyses (PCoA) of the (A) total bacterial community based on 16S rRNA gene sequences and the (B) *apsA* gene-containing community based on *apsA* gene sequences.

5.4.2 Quantification of total bacteria, SRB, and methanogens

Q-PCR results targeting the 16S rDNA of total bacteria and the SRB genus *Desulfovibrio-Desulfomicrobium* provided a concentration of these genes per uL of DNA. These concentrations, related to the initial mass of the sample used for DNA extractions, yielded an estimate of the amount of 16S rDNA genes per gram of sample as well as the normalized ratios of 16S rDNA of *Desulfovibrio-Desulfomicrobium* species and methanogens with respect to total bacteria (Figure 5.5). It was found that the ETOH 1 SRBR contained a very high percentage of SRB (94±15%), which was in agreement with the ARDRA sequence analysis. However, the total concentration of bacteria was much lower in both ETOH SRBRs than the lignocellulose reactors. Methanogens were found to be present at lower levels in the ETOH reactors than in the lignocellulose SRBRs, especially in the ETOH SRBR that was exposed to oxygen due to operational problems (ETOH 1).

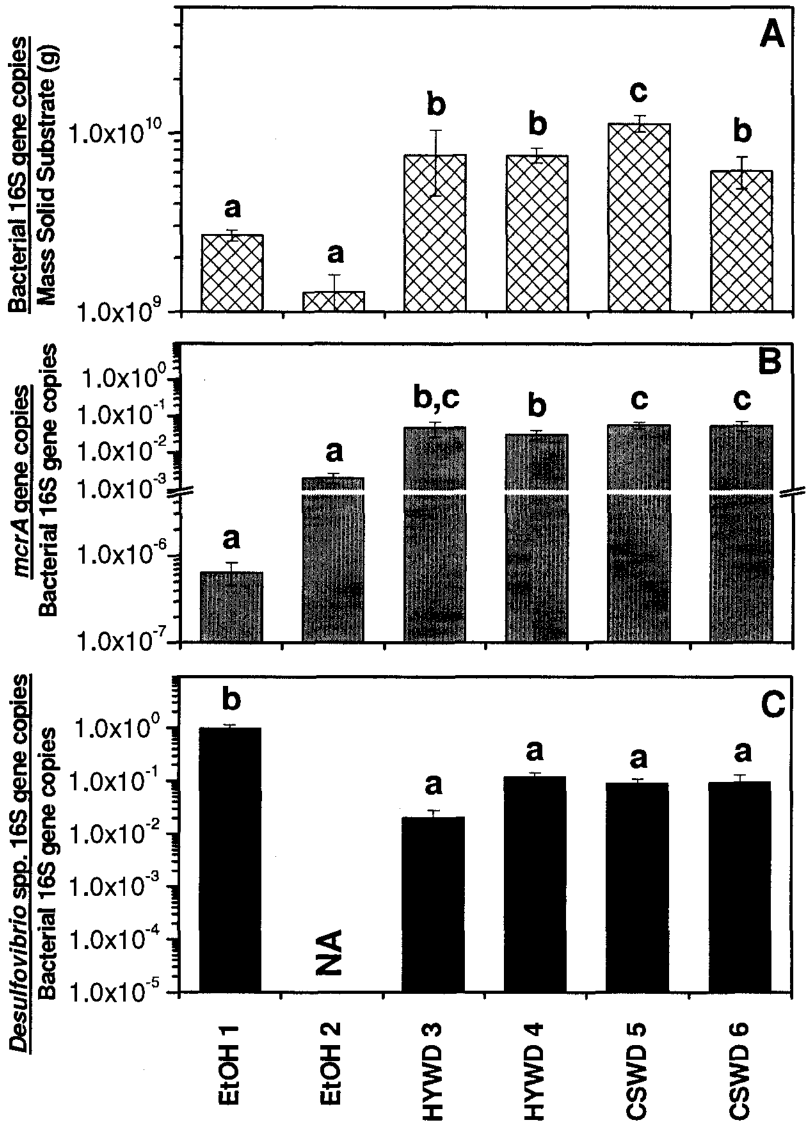

Figure 5.5 - Quantification of total bacteria, the SRB of the genus *Desulfovibrio* and methanogenic bacteria for the ETOH, HYWD, and CSWD SRBRs by Q-PCR. Total bacteria 16S rDNA copies normalized to mass of substrate (A), total Desulfovibrio spp. 16S rDNA copies normalized to total bacteria (B), and mcrA genes normalized to total bacteria (C). Bars with the same letter are not significantly different at the 0.05 level. NA – not analyzed.

5.5 Discussion and Conclusions

This study investigated the effect of organic substrate on microbial communities present in SRBRs treating AMD. Our central hypothesis was that complex substrate conditions require complex communities of cellulolytic and fermentative microbes to break down the organic matter into simple substrates that SRB can utilize (Logan et al., 2005), and thus different organic substrates would yield distinct communities. The results provided strong support for this hypothesis.

One of the most notable differences among the communities was the much higher proportion of SRB in the community in the ETOH SRBR than in the lignocellulosic SRBRs, as determined by ARDRA and Q-PCR. The low levels of SRB in the lignocellulosic SRBRs were typical of what has been observed by others (Pruden et al., 2007; Hong et al., 2007; Johnson and Hallberg, 2005). The diversity levels of the SRB in the SRBRs were similar, with 3-4 different SRB identified in the lignocellulosic bioreactors, and 2-3 different SRB in the ETOH bioreactors. These SRB may vary from one another in terms of substrate utilization capabilities, kinetics, and other characteristics such as tolerance to oxygen exposure and other stresses (Warren et al., 2005). Such difference could have a significant impact on SRBR performance. Although the proportion of SRB was higher in ETOH SRBRs, the total bacterial community was smaller, likely due to the lower surface area of the limestone as compared to the lignocellulosic material.

The overall diversity of bacteria was found to be much higher in the lignocellulose-based SRBRs. This was likely a result of the complexity of the substrate in the lignocellulose-based SRBRs, which required a broader array of functional groups for its breakdown than ethanol. This difference may represent an important advantage to these systems in terms of resilience to stress. For example, redundancy within each functional group may have provided a competitive advantage because this increased the likelihood of individual species that tolerated the stress. This factor would have important implications towards improving the design of SRBRs for stress tolerance.

The proportion of methanogens was found to be lowest in the ETOH SRBRs, especially in ETOH 1, which was exposed briefly to oxygen. Assuming that methanogens had an overall negative impact on SRBR performance due to their competitive relationship with SRB, this may have indicated an advantage of ethanol-based SRBRs. However, methanogens may play a positive role as well. For example, some SRB are inhibited by high concentrations of acetate, which is removed easily by methanogens (Raskin et al., 1996).

It was also of interest that different microbial communities were found in SRBRs that experienced operational problems resulting in exposure of the bioreactor contents to oxygen. For example, *Thiobacillus* spp. were only found in the HYWD 3 SRBR, which was unintentionally exposed to oxygen due to operational difficulties. *Thiobacillus* spp. are aerobic or denitrifying organisms that convert sulfides to sulfates (Holt, 1984; Beller *et al.*, 2006), thus reversing the process applied in remediation. This provided additional validation to the observed results and is consistent with results obtained in the field SRBR at the Peerless Jenny King site, where *Thiobacillus* spp. were found to be the dominant *apsA*-containing species (Hiibel et al., 2008).

Interestingly, the metal removal performance of the six SRBRs was comparable (Buccambuso et al., 2007), although the sulfate removal in the ETOH SRBRs was consistently greater than in the lingocellulosic SRBRs (Venot et al., 2008). It can be concluded that ethanol bioreactors can be useful in situations where ethanol is readily available as a substrate and provided at low feed rates, because it directly supports the

SRB performing the AMD treatment. Lignocellulose-based SRBRs still represent a less expensive and lower maintenance option since the organic substrate is made up of waste material that can indirectly support the SRB via a complex microbial community, without having to be constantly replenished. The results of this study suggest that there may be advantages of lignocellulose-based SRBRs in terms of the overall diversity of the microbial community, which may aid in providing resilience to stress. Future research exploring this hypothesis, as well as the effects of other substrates, could be helpful in improving design and performance of SRBRs.

5.6 Acknowledgements

Financial assistance was provided by the EPA Office of Research and Development's Engineering Technical Support Center, under contract with Golder Associates, Inc., Contract # GS-10F00130N DO #1101 (David Reisman, Project Officer; reisman.david@epa.gov); and by the Water Research Experience for Undergraduates program at CSU sponsored by the National Science Foundation. This research has undergone EPA peer and policy review, and has been cleared for publication. Mention of commercial products does not constitute endorsement by the Agency.

5.7 References

Barton CD, Karathanasis AD. 1999. Renovation of a failed constructed wetland treating acid mine drainage. Environmental Geology. 39(1):39-50.

Beller, H.R., Letain, T.E., Chakicherla, A., Kane, S.R., Legler, T.C., and Coleman, M.A. (2006) Whole-genome transcriptional analysis of chemolithoautotrophic thiosulfate oxidation by *Thiobacillus denitrificans* under aerobic versus denitrifying conditions. *J Bacteriol* 188:7005–7015.

Benner SG, Blowes DW, Ptacek CJ. 1997. A full-scale porous reactive wall for prevention of acid mine drainage. Ground Water Monitoring and Remediation. 17(4):99-107.

Buccambuso, E., Ruhs, A., Figueroa, L., Gusek, J. J., Wildeman, T., Holmes, M. & Reisman, D. Presented June 2-7, 2007. National Meeting of the American Society of Mining and Reclamation, Gillete WY.

Daly, K., Sharp, R., and McCartey, A. 2000. Development of oligonucleotide probes and PCR primers for detecting phylogenetic subgroups of sulfate-reducing bacteria. Microbiology 146, 1693-1705.

Hiibel, S.R., Pereyra, L.P., Inman, L.Y., Tischer, A., Reisman, D.J., Reardon, K.F., and A. Pruden. Microbial Community Analysis of Two Field-Scale Sulfate-Reducing Bioreactors Treating Mine Drainage. Environmental Microbiology (*accepted March, 2008*).

Holt, J.H. (ed.). (1984) *Bergey's Manual of Systematic Bacteriology.* Baltimore, MD, USA: Williams & Wilkins.

Hong, H., Inman, L.Y., Pruden, A., and K.F. Reardon. 2007. Comparison of CE-SSCP and DGGE for Monitoring a Complex Microbial Community Remediating Mine Drainage. Journal of Microbiological Methods 69,52–64.

Johnson DJ, Hallberg KB. 2002. Pitfalls of passive mine water treatment. Reviews in Environmental Science and Biotechnology. 1(4):335-343.

Johnson, D. B. & Hallberg, K. B. 2005. Acid mine drainage remediation options: a review. Science of the Total Environment 338, 3-14.

Logan, M. V., Reardon, K. F., Figueroa, L., McLain, J. E. T. & Ahmann, D. 2005. Microbial community activities during establishment, performance, and decline of bench-scale passive treatment systems for mine drainage. Water Research 39, 4537-4551.

Lozupone, C. & Knight, R. 2005. UniFrac: a new phylogenetic method for comparing microbial communities. Applied and Environmental Microbiology 71, 8228-8235.

Lozupone, C., Hamady, M. & Knight, R. 2006. UniFrac - An online tool for comparing microbial community diversity in a phylogenetic context. BMC Bioinformatics 7.

Lozupone, C. A., Hamady, M., Kelley, S. T. & Knight, R. 2007. Quantitative and Qualitative beta Diversity Measures Lead to Different Insights into Factors That Structure Microbial Communities. Applied Environmental Microbiology 73, 1576-1585.

Luton, P. E., Wayne, J. M., Sharp, R. J. & Riley, P. W. 2002. The *mcrA* gene as an alternative to 16S rRNA in the phylogenetic analysis of methanogen populations in landfill. Microbiology 148, 3521-3530.

Muyzer, G., Dewaal, E. C., & Uitterlinden, A. G. 1993. Profiling of complex microbial populations by denaturing gradient gel electrophoresis analysis of polymerase chain reaction-amplified gene coding for 16S rRNA. Applied and Environmental Microbiology 59, 695-700

Pruden, A., Messner, N., Pereyra, L., Hanson, R. E. , Hiibel, S. R. & Reardon, K. F. 2007. The effect of inoculum on the performance of sulfate-reducing columns treating heavy metal contaminated water. Water Research 41, 904-914.

Raskin, L., Rittman, B. E., & Stahl, D. A. 1996. Competition and Coexistence of Sulfate-Reducing and Methanogenic Populations in Anaerobic Biofilms. Applied and Environmental Microbiology 62, 3847-3857.

Suzuki, M. T., Taylor, L. T., & DeLong, E. F. 2000. Quantitative analysis of small subunit rRNA genes in mixed microbial populations via 5'-nuclease assays. Applied and Environmental Microbiology 66, 4605-4614.

Venot, C., Figueroa, L., Wildeman, T.R., Reisman, D., & Holmes, M. 2008. Pilot-scale evaluation of solid and liquid phase organic substrates used in biochemical reactors for the treatment of mining influenced water, Paper was presented at the 2008 National Meeting of the American Society of Mining and Reclamation, Richmond VA, *New Opportunities to Apply Our Science* June 14-19, 2008. R.I. Barnhisel (Ed.) Published by ASMR, 3134 Montavesta Rd., Lexington, KY 40502.

Warren, A. Y., Citron, D. M., Merriam, C. V., & Goldstein, E. J. 2005. Biochemical Differentiation and comparison of Desulfovibrio species and other phenotypically similar genera. Journal of Clinical Microbiology 43, 4041-4045.

Weisburg, W. G., Barns, S. M., Pelletier, D. A. and Lane, D. J. 1991. 16S ribosomal DNA amplification for phylogenetic study. Journal of Bacteriology 173, 697-703.

Chapter 6 Microbial Community Analysis of Two Field-Scale Sulfate-Reducing Bioreactors Treating Mine Drainage

Hiibel, S.R., Pereyra, L.P., Inman, L.Y., Tischer, A., Reisman, D.J., Reardon, K.F., and A. Pruden. (2008). *Environmental Microbiology.* 10(8), 2087-2097.

Approximate contributions of each author are as follows:

SR Hiibel performed 25% of the DNA extraction, 60% of the cloning, 70% of the sequence BLASTing, 100% of the sequence data analysis, 25% of the Q-PCR data analysis, and 60% of the manuscript preparation.

LP Pereyra performed 25% of the DNA extraction, 10% of the sequence BLASTing, 100% of the Q-PCR, 75% of the Q-PCR data analysis, and 40% of the manuscript preparation.

LY Inman performed 10% of the DNA extractions, 10% of the cloning, and 5% of the sequence BLASTing.

A Tischer performed 40% of the DNA extractions, 30% of the cloning, and 15% of the sequence BLASTing.

DJ Reisman, KF Reardon, and A Pruden assisted with manuscript preparation.

6.1 Abstract

The microbial communities of two field-scale pilot sulfate-reducing bioreactors treating acid mine drainage (AMD), Luttrell and Peerless Jenny King (PJK), were compared using biomolecular tools and multivariate statistical analyses. The two bioreactors were well suited for this study because their geographic locations and substrate compositions were similar while the characteristics of influent AMD, configuration and degree of exposure to oxygen were distinct. The two bioreactor communities were found to be functionally similar, including cellulose degraders, fermenters and sulfate-reducing bacteria (SRB). Significant differences were found between the two bioreactors in phylogenetic comparisons of cloned 16S rRNA genes and adenosine 5-phosphosulfate

reductase (*apsA*) genes. The *apsA* gene clones from the Luttrell bioreactor were dominated by uncultured SRB most closely related to *Desulfovibrio* spp., while those of the PJK bioreactor were dominated by *Thiobacillus* spp. The fraction of the SRB genus *Desulfovibrio* was also higher at Luttrell than at PJK as determined by quantitative real-time polymerase chain reaction analysis. Oxygen exposure at PJK is hypothesized to be the primary cause of these differences. This study is the first rigorous phylogenetic investigation of field-scale bioreactors treating AMD and the first reported application of multivariate statistical analysis of remediation system microbial communities applying UniFrac software.

6.2 Introduction

Acid mine drainage (AMD), characterized by low pH and elevated concentrations of sulfate and heavy metals, is typically a result of mining activities that expose sulfide minerals to air and water. The cost of treatment worldwide is estimated to be in the tens of billions of US Dollars (1999) and, in the USA alone, there are between 5,000 and 10,000 miles of impacted streams (EPA, 1997).

Passive treatment systems are preferred for AMD remediation because of their low cost, low required maintenance and minimal production of hazardous waste (Berghorn and Hunzeker, 2001; Waybrant *et al.*, 2002). Sulfate-reducing bioreactors provide an attractive passive treatment approach because they are typically inexpensive to construct and require a minimal input of resources once in operation (Benner *et al.*, 1999; Johnson and Hallberg, 2005a). These bioreactors contain solid organic materials, such as wood chips, which provide a slow release carbon substrate, supporting a complex anaerobic microbial community that drives remediation. The community includes microorganisms that degrade the organic substrate, releasing electron donors usable by sulfate-reducing bacteria (SRB), which reduce sulfate to sulfide and also produce bicarbonate. The sulfide reacts with heavy metal cations to form stable metal sulfides that are immobilized in the bioreactor while the bicarbonate buffers the acidity (Johnson and Hallberg, 2005b; Logan *et al.*, 2005).

As sulfate-reducing bioreactors are microbiologically driven, an improved understanding of the microbial community involved is fundamental for improved design and performance (Kaksonen *et al.*, 2004; Labrenz and Banfield, 2004; Hallberg and Johnson, 2005a). In the 1990s, researchers began to investigate the microbiology of the systems using culture-based techniques (Lyew *et al.*, 1994; Hard *et al.*, 1997; Benner *et al.*, 2000; Labrenz and Banfield, 2004; Hallberg and Johnson, 2005a) and, more recently, biomolecular techniques (Clarke *et al.*, 2004; Kaksonen *et al.*, 2004; Labrenz and Banfield, 2004; Hallberg and Johnson, 2005a; Morales *et al.*, 2005; Bruneel *et al.*, 2006; Chandler *et al.*, 2006; Geets *et al.*, 2006; Knotek-Smith *et al.*, 2006; Nicomrat *et al.*, 2006a,b; Pruden *et al.*, 2007). A relationship between performance and the type of microbial inoculum has recently been demonstrated (Pruden *et al.*, 2007), providing evidence that the role of the microbial community is important for design and operation. However, thorough field-scale analyses are still required to verify lab results and to help understand the spatial and temporal behaviors of the scaled-up systems.

The goal of this study was to apply DNA-based techniques and statistical analyses to compare the microbial communities of two active pilot sulfate-reducing bioreactors operating in the field. The two bioreactors serve as highly suitable model systems for this study because they share a common geographic location and environmental conditions, but vary in their configuration, exposure to oxygen and the severity of AMD treated. The microbial populations were compared by targeting the 16S rRNA gene and the *apsA* gene, a functional gene that encodes the adenosine 5′-phosphosulfate reductase a-subunit. This protein is responsible for the reduction of sulfate to sulfite and is thought to be present in all SRB, along with several microbes associated with the sulfur cycle, such as *Thiobacillus* spp. (Friedrich, 2002). Statistical comparisons were made based on the phylogenetic relatedness using the newly developed, web-based UniFrac software (Lozupone and Knight, 2005; Lozupone *et al.*, 2006; 2007). Comparisons were made at the ribosomal and functional gene levels between the two sites, and spatially within each site to examine the effect of operating conditions. This research is the first to comprehensively compare two field-scale treatment systems at both the sampling and statistical levels and is one of the first to apply biomolecular tools to the analysis of field-scale reactors.

6.3 Results

6.3.1 Microbial composition of the bioreactors

Sequences of 16S rRNA gene clones were compared with the GenBank and Ribosomal Database Project II (RDP) databases to identify the microorganisms with the highest similarity. The number of clones screened, the percentage of those screened that were assigned a putative function and the qualitative proportions of three main functional groups associated with AMD-treating sulfate-reducing bioreactors are presented in Table 6.1. All sampling locations from both bioreactors yielded clones corresponding to fermentative organisms. Each of the Luttrell sampling locations also yielded clones assigned as cellulose degraders or cellulose degraders and fermenters, while these were not found at the 1mT and 4T sampling locations at Peerless Jenny King (PJK). Sulfate-reducing capabilities were associated with sequences from the Luttrell 2T and PJK 1fT, 3B and 4B sampling locations.

Table 6.1 – Presence/absence of putative functions associated with sulfate-reducing bioreactors as determined by 16S rRNA gene sequences.

	Luttrell						PJK							
	1B	1T	2B	2T	3B	3T	1fB	1fT	1mB	1mT	3B	3T	4B	4T
Cellulose degradation	+++	++++	+++	++++	+	+	++	+++	+	–	+	+++	++	–
Fermentation	++++	++	+++++	++++	+++	++++	+	++	–	+++++	++	++	++	++
Sulfate reduction	–	–	–	++	–	–	–	+	–	–	++	–	++	–
Number of clones screened	120	123	109	104	111	105	113	108	109	106	188	149	109	103
Clones assigned putative function (%)[a]	21	20	46	28	10	22	7	13	2	26	11	11	11	4

a. Percentages based on ARDRA of all clones screened.
–, $x = 0\%$; +, $0\% < x \leq 3\%$; ++, $3\% < x \leq 5\%$; +++, $5\% < x \leq 10\%$; ++++, $10\% < x \leq 20\%$; +++++, $x > 20\%$.

Cloned *apsA* gene sequence results are presented in Figure 6.1. The dominant clone in all of the Luttrell sampling locations had high similarity to an uncultured SRB (GenBank ID: DQ825786) originally sequenced from a wetland remediating AMD, accounting for at least 80% of the *apsA* clones screened. Three other clones with high similarity to other uncultured SRB obtained from the same wetland (DQ825784, DQ825788 and DQ825789) made up the remaining fraction of uncultured organisms identified by the *apsA* gene in the Luttrell bioreactor. The majority of sequences obtained from all sampling locations at PJK were closely related to *Thiobacillus denitrificans* (AY296750), and uncultured *Thiobacillus* spp. and a smaller proportion of the same uncultured SRB observed at Luttrell were also found. The top of PJK 3 also yielded a sequence with high similarity to *Desulfobulbus rhabdoform* (AF418110), the only non-*Desulfovibrio* or uncultured SRB species identified.

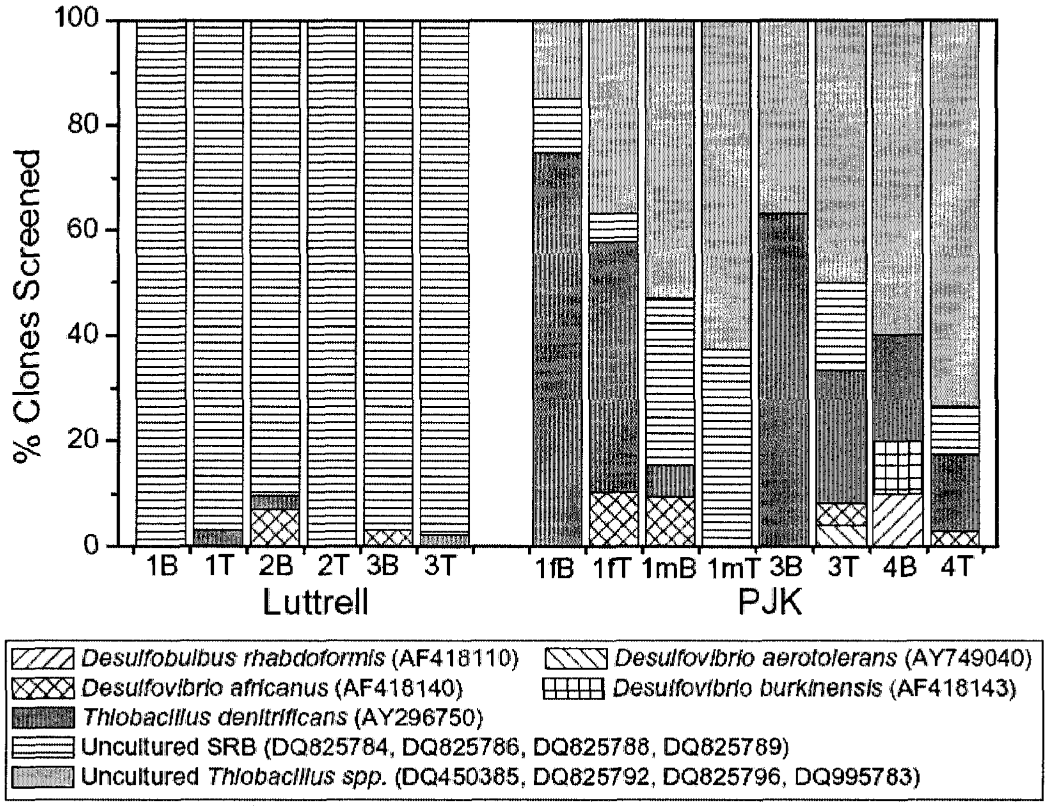

Figure 6.1 – Identification and percentages of *apsA* gene sequences at the Luttrell and PJK sites based on BLAST results. GenBank accession numbers listed in parenthesis.

6.3.2 Principal co-ordinates analysis comparison of PJK and Luttrell

Principal co-ordinates analysis (PCoA) was performed to determine whether the various populations were distributed along any easily interpreted axes of variation. PCoA of the overall microbial community based on the 16S rRNA gene sequences revealed that more than 45% of the total variance could be explained by the first two principal co-ordinates (Figure 6.2a). No obvious grouping of sequences from specific sampling locations of the bioreactors could be identified, although the sampling locations within each bioreactor loosely clustered together. However, the PJK 1fB sampling location appeared to be more similar to Luttrell sampling locations than other PJK locations along the first principle co-ordinate.

Analysis of the *apsA* gene-containing community revealed strongly bimodal clustering (Figure 6.2b). All six sampling locations from the Luttrell field site were grouped tightly, while the eight sampling locations from the PJK bioreactors were grouped separately. This separation was clearly along the first principal co-ordinate, which explained 82% of the variance in the data. The PJK populations were not grouped as tightly as those from Luttrell, but their variance was predominantly in the direction of the second principal co-ordinate, which accounted for only 5.25% of the variance in the sequences.

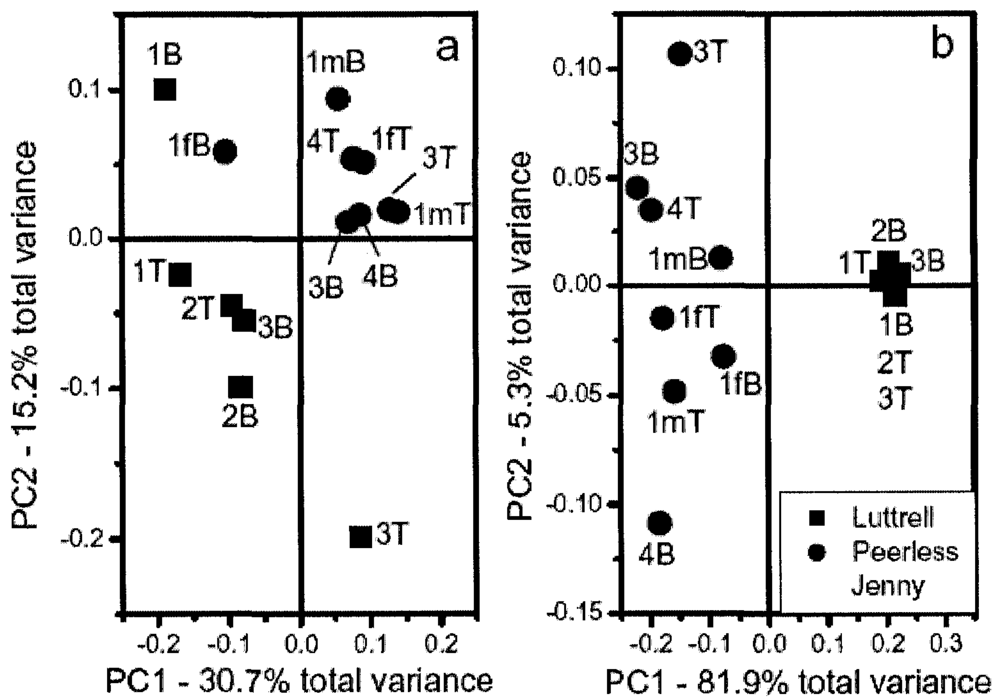

Figure 6.2 - PCoA of the (a) total bacterial community based on 16S rRNA gene sequences and the (b) sulfate-reducing bacterial community based on *apsA* gene sequences.

6.3.3 Significance testing

The UniFrac significance test was applied to each of the sampling locations as pair-wise comparisons. Differences between many individual sampling locations were found to be statistically significant at the *P*-value = 0.05 level (Table 6.2). In general, it appeared that there was more difference in 16S rRNA gene sequences between the PJK and Luttrell bioreactors than within each bioreactor. This trend is especially apparent in examining the overall pattern of *P*-values in

Table 6.2. The *P*-values from comparisons of PJK sampling locations with Luttrell sampling locations generally trended lower than within reactor comparisons, except for the PJK 1fB location versus Luttrell locations. The PJK 1fB sampling location appears to be the anomaly, with higher *P*-values characterizing its similarity to all Luttrell sampling locations except 3T, which itself is distinct from all other Luttrell locations. For complex environmental data sets typical of the UniFrac significance test, a *P*-value between 0.05 and 0.1 is considered 'suggestive' (Lozupone and Knight, 2005).

Table 6.2 - Pair-wise comparison *P*-values from the UniFrac significance testing on the 16S rRNA gene sequences.

		Luttrell					PJK							
		1T	2B	2T	3B	3T	1fB	1fT	1mB	1mT	3B	3T	4B	4T
Luttrell	1B	0.78	0.02	0.15	0.20	0.00	0.29	0.00	0.03	0.00	0.00	0.00	0.00	0.01
	1T		0.34	0.63	0.74	0.00	0.44	0.00	0.06	0.00	0.00	0.00	0.00	0.02
	2B			0.76	1.00	0.01	0.33	0.02	0.13	0.01	0.00	0.00	0.02	0.03
	2T				1.00	0.00	0.81	0.11	0.58	0.04	0.04	0.00	0.08	0.27
	3B					0.01	0.58	0.20	0.52	0.04	0.15	0.04	0.17	0.45
	3T						0.00	0.00	0.00	0.00	0.00	0.00	0.01	0.00
PJK	1fB							0.02	0.42	0.01	0.01	0.00	0.06	0.09
	1fT								0.56	0.55	0.07	0.04	0.30	0.60
	1mB									0.36	0.09	0.12	0.79	0.66
	1mT										0.09	0.11	0.25	0.09
	3B											0.40	0.05	0.64
	3T												0.01	0.46
	4B													0.22

Shaded values indicate a significant difference (*P*-value < 0.05).

A stronger trend is seen in the analysis of the *apsA* gene sequences. In the case of *apsA*, all of the sampling locations at the PJK bioreactor were significantly different from all of the samples from the Luttrell bioreactor (P-value < 0.03) (Table 6.3). Additionally, the top and bottom of Luttrell 1 were significantly different (P-value = 0.00), as were the tops of the front of PJK Cell 1 and Cell 3 (P-value = 0.05). When all of the sampling locations were combined within each bioreactor, the differences between the two bioreactor communities based on both the 16S rRNA gene and the *apsA* gene sequences were significant (P-value = 0.00). The microbial populations in the front and back sampling locations within each bioreactor were not significantly different based on the 16S rRNA gene (P-value = 1.00 for PJK and P-value = 0.71 for Luttrell) or the *apsA* gene (P-value = 0.89 for PJK and P-value = 0.97 for Luttrell). In addition, the sampling locations of the PJK bioreactors originally hypothesized to be more consistently anaerobic were not found to be significantly different from those sampling locations that experience obvious aerobic conditions based on either the 16S rRNA gene (P-value = 0.16) or the *apsA* gene (P-value = 0.93). However, the 16S rRNA gene sequences of one of the PJK sampling locations originally classified as anaerobic, 1fB, was found to be the most distinct as compared with the other PJK sampling locations, being statistically different from four out of seven locations at a P-value of 0.05 and six out of seven locations at the suggestive P-value of 0.1 (Table 6.2).

Table 6.3 - Pairwise comparison *P*-values from the UniFrac significance testing on the *apsA* gene sequences.

		Luttrell					PJK							
		1T	2B	2T	3B	3T	1fB	1fT	1mB	1mT	3B	3T	4B	4T
Luttrell	1B	0.00	0.51	0.61	0.15	0.64	0.00	0.00	0.00	0.00	0.00	0.00	0.00	0.00
	1T		0.89	0.43	0.61	0.53	0.00	0.00	0.00	0.00	0.00	0.00	0.00	0.00
	2B			0.96	0.98	0.97	0.00	0.00	0.00	0.00	0.00	0.00	0.00	0.00
	2T				0.96	0.99	0.00	0.00	0.00	0.00	0.00	0.00	0.00	0.00
	3B					0.95	0.00	0.00	0.01	0.03	0.00	0.00	0.00	0.00
	3T						0.00	0.00	0.00	0.01	0.00	0.00	0.00	0.00
PJK	1fB							0.39	0.30	0.42	0.45	0.23	0.74	0.83
	1fT								0.24	0.33	0.22	0.05	0.60	0.64
	1mB									0.95	0.12	0.38	0.19	0.41
	1mT										0.23	0.68	0.65	0.69
	3B											0.18	0.19	0.88
	3T												0.88	0.67
	4B													0.87

Shaded values indicate a significant difference (*P*-value < 0.05).

6.3.4 Quantitative real-time polymerase chain reaction quantification of total bacteria and SRB

The concentrations of total bacteria and the SRB genus *Desulfovibrio* at each sampling location were quantified using quantitative real-time polymerase chain reaction (Q-PCR). The sizes of the total bacterial population at the different sampling locations in the two reactors differed, with 11 Fisher's least significant difference (LSD) groupings (LSD = 1.61 ± 107) among the 14 locations. PJK 1fB had a significantly larger total bacterial population than all other PJK and Luttrell locations. The L1T and L1B populations were significantly larger than those of the remaining Luttrell locations. The PJK populations decreased from the front to the end of the bioreactor, with significantly larger concentrations at the bottom locations than at the top except at the middle of Cell 1 (Figure 6.3a). The SRB populations of the genus *Desulfovibrio* (normalized to total bacteria) were generally higher in the Luttrell sampling locations than the PJK sampling locations. Luttrell locations 1 and 2 revealed significantly (LSD = 0.045) larger proportions of *Desulfovibrio* than all other locations. Only three PJK sampling locations, 1fT, 1mB and 1mT, yielded *Desulfovibrio* levels above the detection limit, and these were statistically similar in concentration to the L3B and L3T levels (Figure 6.3b).

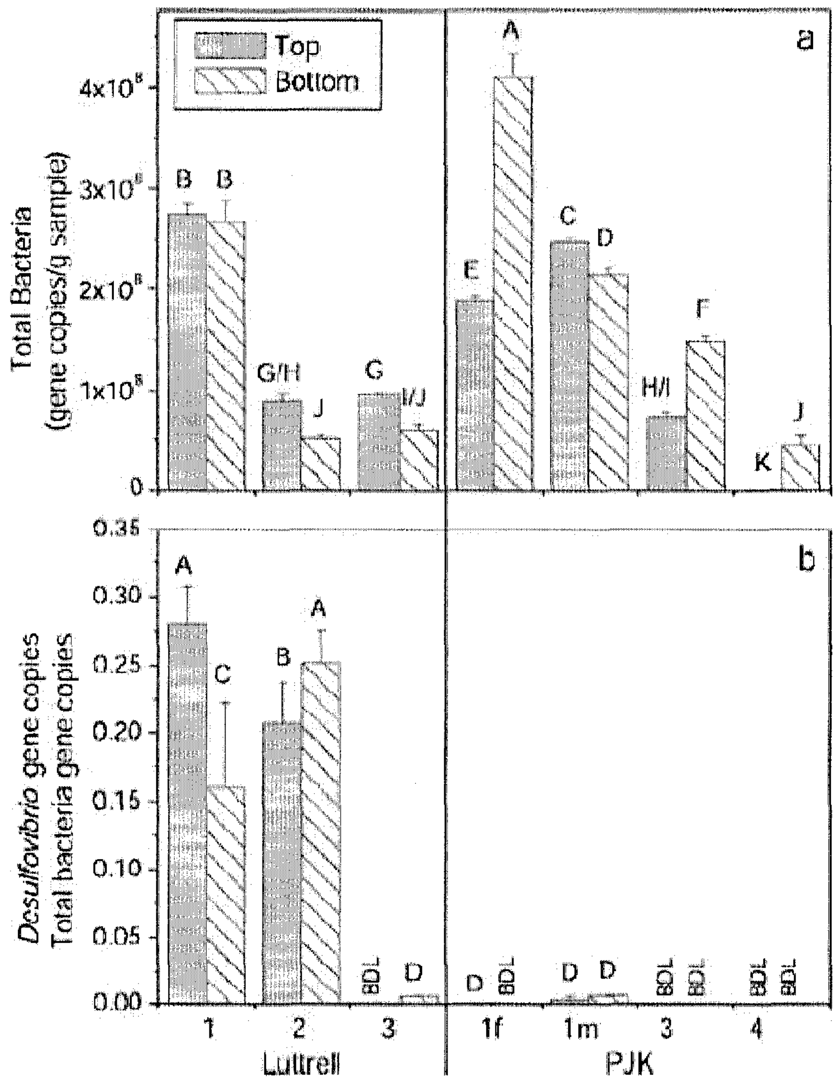

Figure 6.3 – Q-PCR results targeting (a) total bacteria and (b) the *Desulfovibrio* genus normalized to total bacteria. Capital letters above each bar represent Fisher's LSD groupings (BDL – below detection limit). Error bars are standard deviations of triplicate Q-PCR analyses.

6.3.5 Diversity estimates

Shannon Diversity Indices were determined based on the 16S rRNA gene amplified rDNA restriction analysis (ARDRA) for the Luttrell (1.86 ± 0.14) and PJK (1.87 ± 0.11) bioreactors (Figure 6.S1). The average indices suggest that there is no significant difference in the overall microbial diversity between the two reactors. It was not possible to determine diversity indices based on DNA sequence similarities because DNA sequences were only available for a subset of the community chosen based on ARDRA frequencies.

6.4 Discussion

6.4.1 Microbial community comparisons between and within sites

Luttrell and PJK are ideal field-scale systems for comparative study because of their similar geographic location and climate. Furthermore, both bioreactors were constructed with the same organic material and were inoculated with manure from the same source, and thus the starting microbial communities at each site were highly similar. The differences between the two sites include the quantity and quality of influent AMD, the configuration of the bioreactors (horizontal flow at PJK versus vertical top-down flow at Luttrell) and the degree of exposure to aerobic conditions.

Sequence analysis of the cloned *apsA* gene revealed a strong contrast between the subcommunities of the two bioreactors and notable homogeneity of the species carrying this gene within each bioreactor (Figures 6.1-6.3). BLAST comparisons against the GenBank database indicate a population dominated by species similar to uncultured SRB most closely related to *Desulfovibrio* spp. in the Luttrell bioreactor, and by *T.*

denitrificans and uncultured *Thiobacillus* spp. in the PJK bioreactor (Figure 6.1). Quantification of total bacteria and one genus of SRB revealed significant differences between the two bioreactors, with PJK generally associated with lower totals and fractions than Luttrell (Figure 6.3). Thus, it appears that conditions at Luttrell better selected for SRB than the conditions at PJK. The SRB detected with the 16S rRNA gene were also different between the bioreactors, with species similar to *Desulfovibrio* detected at Luttrell and *Desulfosporosinus* and *Desulfobulbus* detected at PJK (data not shown). Interestingly, two of the three total SRB clones recovered from PJK had high similarity to *Desulfosporosinus* spp., which are spore-forming SRB (Holt, 1984), suggesting habitual stress at PJK, perhaps from oxygen exposure.

The PCoA based on the phylogenetic alignment of the 16S rRNA gene sequences yielded two broad groupings defining the two bioreactors (Figure 6.2). Pair-wise comparisons between each of the sampling locations at the two bioreactors supported this observation (Table 6.2). This distinction was especially strong when the comparison was made based on the *apsA* gene (Figure 6.3, Table 6.3). Thus, analysis of the 16S and *apsA* genes provided different taxonomic resolution, which had an effect on the overall representation of the community. Targeting other key functional genes may help clarify whether differences such as these are generally a result of comparing functional versus ribosomal genes or whether analyzing a specific subgroup rather than the whole community leads to more statistical sensitivity.

Clone sequences from both sites had high similarity to organisms associated with the three main functional groups important to sulfate-reducing bioreactor function: cellulose degraders, fermenters and SRB. However, organisms with high similarity to cellulose degraders and fermenters were consistently present in the clone libraries from all of the Luttrell sampling sites and generally at higher levels than from the PJK sampling sites (Table 6.1). In particular, cellulose degraders have been observed to perform a potentially rate-limiting step in substrate degradation (Logan *et al.*, 2005).

Together, these results suggest that environmental and operating conditions had a corresponding effect on the overall bacterial community. Furthermore, the PJK sampling location with the population the most similar on the 16S rRNA gene level to populations at Luttrell (1fB, Figure 6.2, Table 6.2) was also most similar in terms of consistent water saturation and thus low oxygen exposure. Whether similar microbial community structure could also have been achieved with different initial inocula would be of interest in guiding the design and operation of sulfate-reducing bioreactors in the field. Currently, design criteria for inoculum selection do not exist for sulfate-reducing bioreactors. Inoculation design could prove to be a very simple and effective engineering tool, as suggested by Pruden and colleagues (2007).

6.4.2 Evidence of oxygen exposure and its implications

As a result of seasonal flow fluctuations and its design, several locations within the PJK bioreactor are known to have experienced periodic aerobic conditions. It was hypothesized that this exposure to oxygen would result in differences in the PJK microbial community compared with that of the more consistently anaerobic Luttrell bioreactor, namely the presence of aerobic, facultative aerobic or aerotolerant species.

Despite carrying the *apsA* gene, no known *Thiobacillus* spp. can perform sulfate reduction (Holt, 1984). *Thiobacillus denitrificans* is a facultative aerobe known to use oxygen or nitrate as electron acceptors (Beller *et al.*, 2006), and all known *Thiobacillus* spp. can oxidize inorganic Fe(II) and sulfur compounds (Holt, 1984). The combined presence of *Thiobacillus*-like species and oxygen could potentially reverse the desired outcome of sulfate-reducing bioreactors. The observed prevalence of *Thiobacillus* spp., as well as the aerotolerant SRB *Desulfovibrio aerotolerans* (Mogensen *et al.*, 2005) (Figure 6.1) and spore-formers, suggested the presence of oxygen at PJK, which is consistent with site observations. Interestingly, these bacteria were detected throughout the bioreactor, indicating that transiently aerobic conditions were not necessarily concentrated in PJK Cells 1 and 4 as initially hypothesized, but may have been widespread throughout the reactor.

Repeated oxygen exposure may have several negative impacts in addition to the toxic effects of oxygen on some SRB. One consequence may be the enrichment of counterproductive microorganisms, such as *Thiobacillus* spp. Perhaps even more critical is the potential for loss of carbon substrate via aerobic biodegradation, which results in the production of CO2 rather than electron donors for SRB. Logan and colleagues presented evidence that cellulose degradation, rather than sulfate reduction, can be the rate-limiting step in these types of sulfate-reducing bioreactors (Logan *et al.*, 2005). The high concentrations of SRB found in the Luttrell bioreactor (Figure 6.3) and the greater sulfate removal (Table 6.4) may indicate that the sulfate reduction in Luttrell is less cellulose degradation-limited than in the PJK bioreactor. Similarly, the poor sulfate removal at PJK may be a result of loss of cellulosic material via aerobic degradation. This hypothesis is supported by the observation that the ratio of cellulose and hemicellulose to lignin was lower in the PJK bioreactor than in the Luttrell bioreactor (Place *et al.*, 2006) at the time of sampling.

Table 6.4 - Water chemistry and removal data for the Luttrell and PJK field-scale bioreactors treating AMD.

	Influent		Effluent			
Luttrell field site	Week[a]	Long term[b]	Week[a]	Long term[b]		
Flow (l/D)	30 091	4168	30 091	4168		
pH	5.24	3.64	5.99	6.07		
Temp (C)	5.6	10.9	5.4	11.4		
			Percent removal		Average removal rate (mg/l/day)	
			Week[a]	Long term[b]	Week[a]	Long term[b]
Sulfate (mg l^{-1})	988	3776	73	64	3.0×10^{-2}	2.2×10^{0}
Fe (mg l^{-1})	n.a.	61.59	n.a.	86	n.a.	4.8×10^{-2}
Al (mg l^{-1})	n.a.	67.15	n.a.	100	n.a.	6.1×10^{-2}
Zn (mg l^{-1})	n.a.	204.53	n.a.	99	n.a.	1.9×10^{-1}
Cu (mg l^{-1})	n.a.	15.81	n.a.	100	n.a.	1.4×10^{-2}
Cd (mg l^{-1})	n.a.	1.39	n.a.	99	n.a.	1.3×10^{-3}
Mn (mg l^{-1})	n.a.	195.40	n.a.	59	n.a.	1.1×10^{-1}
Ni (mg l^{-1})	n.a.	0.52	n.a.	0	n.a.	0.0×10^{0}

	Influent		Effluent			
PJK field site	Week[a]	Long term[b]	Week[a]	Long term[b]		
Flow (L/d)	204 390	116 170	181 498	88 108		
pH	6.35	6.89	6.55	6.69		
Temp (C)	6.7	10.3	7.8	12.6		
			Percent removal		Average removal rate (mg/l/day)	
			Week[a]	Long term[b]	Week[a]	Long term[b]
Sulfate (mg l^{-1})	98.0	87.1	28	37	7.7×10^{-3}	5.5×10^{-1}
Fe (mg l^{-1})	0.10	0.23	11	18	3.2×10^{-6}	6.9×10^{-4}
Al (mg l^{-1})	0.02	0.07	11	46	6.4×10^{-7}	5.4×10^{-4}
Zn (mg l^{-1})	1.95	0.64	41	−11	2.3×10^{-4}	-1.2×10^{-3}
Cu (mg l^{-1})	0.03	0.01	70	24	6.0×10^{-6}	4.1×10^{-5}
Cd (mg l^{-1})	0.01	0.01	11	24	3.2×10^{-7}	4.1×10^{-5}
Mn (mg l^{-1})	4.19	1.51	41	2	5.0×10^{-4}	5.3×10^{-4}
Ni (mg l^{-1})	0.01	0.01	11	24	3.2×10^{-7}	4.1×10^{-5}

a. Average values the week prior to sampling.
b. Average lifetime values (2002–2005 for Luttrell, 2003–2005 for PJK).
n.a., data not available.

6.4.3 Bioreactor performance

The results of this study indicate correlations between microbial populations and remediation performance, suggesting that microbial communities play an important role in determining the success of the treatment process. Over their lifetimes, the Luttrell bioreactor has removed more than 60% of the influent sulfate compared with the less than 40% removed at PJK. Luttrell also has a higher lifetime sulfate removal rate than PJK

(2.2 mg l-1/day versus 0.55 mg l-1/day, Table 6.4). These performance differences may be partially the result of the shorter residence times and lower sulfate concentrations at PJK, as sulfate reduction rate is a function of sulfate concentration and hydraulic residence time. However, a recent review by Neculita and colleagues (2007) documented a wide range of sulfate removal rates for passive sulfate-reducing systems treating AMD and operating under a variety of conditions, configurations and scales. This wide variety of designs with no apparent trends with regard to remediation performance also suggests that the bioreactor's microbial community has a strong impact on the success of the treatment process. The 64% lifetime average sulfate removal at the Luttrell site is in the upper range of continuously operating systems with a similar sulfate load (e.g. Steed *et al.*, 2000; Boshoff *et al.*, 2004). A literature comparison for the PJK bioreactor is difficult because of the low influent sulfate concentrations (~100 mg l-1), although its 37% lifetime average sulfate removal appears to be on a par with other sites with 'low' inlet sulfate concentrations. For example, Hallberg and Johnson reported 42% removal from a wetland system treating coal mine drainage with 430 mg l-1 sulfate (Hallberg and Johnson, 2005b).

Although oxygen exposure at PJK is clearly an undesirable attribute, it is important to note that the bioreactor is still removing sulfate and metals (Table 6.4). The design and configuration of PJK also offer some advantages over Luttrell. Whereas flow at PJK goes freely through a wetland and alkaline channel, the Luttrell bioreactor is more closely controlled because flow leaves the repository and remains in piping, with the final section (~100 yards) in narrow 1 inch piping to help regulate water entering the bioreactor. Therefore, a design similar to PJK may still be an attractive approach for the remediation of large volumes of less severe AMD.

6.4.4 Insights from microbial community analyses of field-scale systems

In this study, both quantitative and qualitative biomolecular data were analyzed using multivariate statistics to characterize microbially driven treatment systems. The need for multivariate statistical analysis of 16S and other genes for comparing complex microbial communities was recently underscored in a review by Rudi and colleagues (2007). In this study in particular, this statistical approach proved to be a useful diagnostic tool, revealing the widespread effects of oxygen exposure throughout the PJK bioreactor. The utility of the diagnostic approach, however, is dependent on representative sampling; the results of this study would have likely been skewed with a small sampling set. There are also still various avenues of further study that are needed to improve the understanding of the microbiology of these systems. For example, the ratios of SRB to total bacteria in the Luttrell bioreactor were surprisingly large compared with values of 1–2% that have been previously reported in the literature (Johnson and Hallberg, 2003; Morales *et al.*, 2005; Pruden *et al.*, 2007). Of the studies that generated those values, only Pruden and colleagues (2007) used quantitative methods specifically targeting genera of SRB. Other groups used methods targeting total bacterial communities, such as 16S rRNA gene cloning (Morales *et al.*, 2005) and denaturing gradient gel electrophoresis (Johnson and Hallberg, 2003; Morales *et al.*, 2005), which have typical detection limits of 1–2% for individual species. This emphasizes the need to continue to develop quantitative biomolecular tools. Furthermore, methods targeting functional genes related to other functional groups of interest, such as fermenters and cellulose degraders, would help alleviate the burden of screening large numbers of 16S rRNA gene clones, the majority of which have unknown functions. Additional efforts are also needed in developing methods targeting other SRB specific genes as the *apsA* gene is present in some non-SRB, and thus not ideal for their study. This general approach may be beneficial to advancing the understanding of a variety of microbially driven remediation systems, taking an important step towards truly integrating microbial community dynamics with bioreactor design.

6.5 Experimental procedures

6.5.1 Sample sites

Luttrell (Figure 6.4a), constructed in 2002, is a single-cell, vertical flow bioreactor with an impermeable geotextile liner. Flow is from top to bottom through approximately 1 m of organic substrate covered with a layer of *c.* 3 cm rocks. Effluent exits the bioreactor through a series of perforated pipes at the bottom of the substrate, which consists of: 10% shredded Lodgepole pine woodchips (13–50 mm), 40% Lodgepole pine sawdust, 29% limestone, 10% alfalfa hay, 1% kiln dust and 10% dairy cow manure (fresh and stockpiled), by weight (Reisman *et al.*, 2003), and was mixed on site at the time of construction. Prior to operation, the bioreactor was saturated with AMD and the system acclimated for approximately 10 months, with less than one pore volume of metal-laden water allowed to pass through the reactor.

At PJK (Figure 6.4b), constructed in 2003, mine drainage exits the adit and flows through a pre-treatment wetland where iron oxides are precipitated. Pre-treated water passes through a limestone rock channel before entering four gravel-lined horizontal-flow bioreactor cells in series, with organic substrate depth varying from 0.7 to 1.0 m. The organic substrate mixture components and inoculum were from the same source as those in the Luttrell bioreactor. As a result of the significant seasonal flow fluctuations at the PJK site, Cell 4 has been observed to periodically dry out, resulting in aerobic conditions. In addition, the pre-treated water is oxygenated immediately before entering the bioreactor at the top of Cell 1, resulting in aerobic conditions. Unlike the Luttrell bioreactor, PJK was not allowed an acclimation period prior to continuous-flow operation.

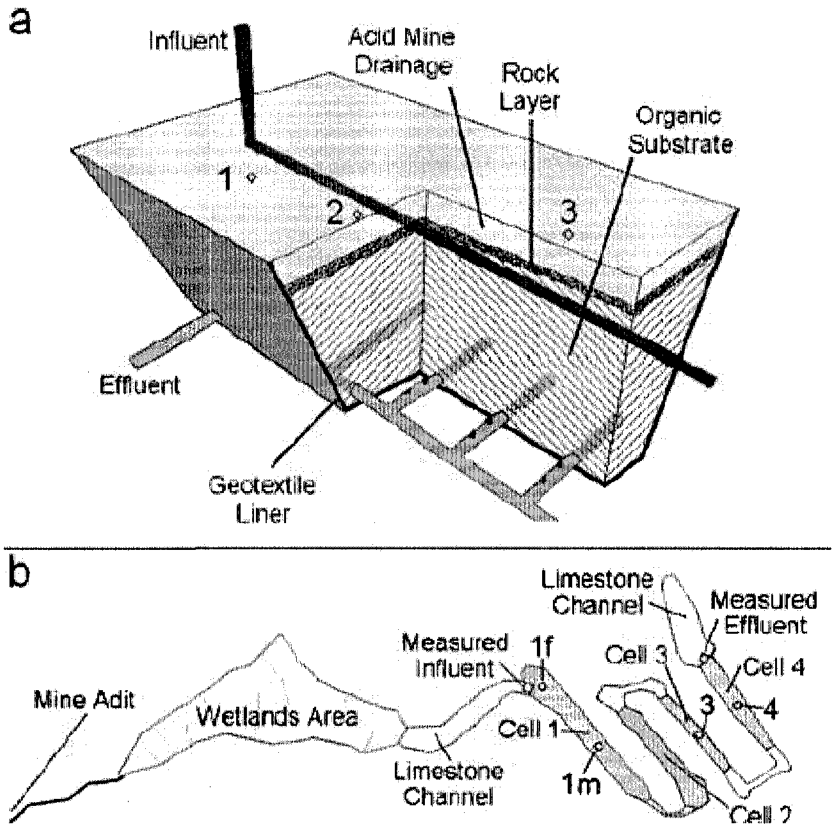

Figure 6.4 – Schematic overview of the (a) Luttrell and (b) PJK bioreactors.

The water chemistry and flow characteristics of the two field sites were analyzed during the summer months and were variable during that period (Table 6.4). In general, the PJK bioreactor treats a larger volumetric flow rate while the Luttrell bioreactor treats a more acidic and heavy metal-laden AMD.

6.5.2 Sample collection

All samples were collected 13–17 June, 2005 using a steel plate with vertically spaced sampling ports that was driven into the bioreactors and the downstream substrate and water removed. Approximately 1 kg of material was collected from the undisturbed upstream side of the plate through the sampling ports using sterile spatulas and WhirlPak sampling bags (Nasco, Modesto, CA). All samples were maintained on ice in the field, vacuum-sealed within 12 h of collection, placed on dry ice for shipment, and stored at -80°C prior to analysis.

The PJK samples were collected at two depths: 'top' (T), 2–11 cm below the surface, and 'bottom' (B), immediately above the bottom gravel layer, which varied in depth. Cells 1, 3 and 4 were sampled approximately at the horizontal midpoint (samples 1m, 3 and 4) and an additional set of samples was collected where the AMD enters the bioreactor at the front of Cell 1 (samples 1f).

Three different spatially distributed locations (1, 2 and 3) were sampled at Luttrell at two depths at each location: 'top' (T), 1–11 cm below the rock layer, and 'bottom' (B), 15–25 cm below the rock layer.

6.5.3 Microbial community analyses

6.5.3.1 DNA extraction

Genomic DNA was extracted using the MOBIO UltraClean Soil DNA Kit (Carlsbad, CA) according to the manufacturer's protocol and stored at -80°C. Eight ~1.0 g replicate extractions were conducted for each sample and combined to ensure that the heterogeneous material was well represented.

6.5.3.2 PCR amplification and cloning

The 16S rRNA gene and *apsA* gene, which target all bacteria and SRB (and others, see *Discussion*) (Friedrich, 2002; Hallberg and Johnson, 2005b), were PCR-amplified. Primer sets 8F and 1492R (Weisburg *et al.*, 1991) or 341F [Primer 1 of Muyzer and colleagues (1993)] and 1492R were used to amplify the 16S rRNA gene as described by Weisburg and colleagues (1991). The *apsA* gene was amplified using the primer sets 7F and 8R as described by Friedrich (2002). The PCR products were cloned with the TOPO TA Cloning Kit (Invitrogen, Carlsbad, CA) according to the manufacturer's protocol. ARDRA was performed visually from MspI restriction enzyme (Promega, Madison, WI)-digested PCR-amplified (using vector-specific primers) inserts; a minimum of 100 16S rRNA gene and 30 *apsA* gene clones were screened from each sampling location.

6.5.3.3 Gene quantification

The Q-PCR targeting total bacteria was performed using the BACT2 primers, probe and conditions of Suzuki and colleagues (2000). The *Desulfovibrio* genus was targeted by adapting the primers described by Daly and colleagues (2000) for Q-PCR, with an annealing temperature of 64°C. Calibration curves were developed based on published protocols (Pruden *et al.*, 2007), with *Desulfovibrio salexigens* ATCC #14944 (American Type Culture Collection, Rockville, MD) used as the template for the *Desulfovibrio* analysis. The limit of quantification for total bacteria and *Desulfovibrio* was 66 gene copies. The specificity of the *Desulfovibrio* primers was verified by cloning and sequencing PCR products from several pure cultures and environmental samples. All Q-PCR analyses were performed using an ABI 7300 Real-Time PCR System (Applied Biosystems, Foster City, CA). Fisher's LSD testing was conducted using the PROC GLM function of SAS 9.1 (SAS Institute, Cary, NC); samples below the limit of quantification were not included in the analysis.

6.5.3.4 Sequence analyses

Clones from the 16S gene analyses with ARDRA patterns appearing two or more times and all *apsA* gene clones with unique ARDRA patterns were sequenced. Sequencing was performed by Macromolecular Resources (Colorado State University, Fort Collins, CO) or SeqWright DNA Technology Services (Houston, TX). The National Center for Biotechnology Information GenBank database and the BLAST alignment tool (http://www.ncbi.nlm.nih.gov/blast/) were used to determine the similarity of DNA sequences to known microorganisms. All 16S rRNA gene matches were verified using the Sequence Match tool of RDP (http://rdp.cme.msu.edu/) (Cole *et al.*, 2007). A literature survey was performed to assign putative functional properties based on those observed for the organisms with the highest similarity with respect to substrate utilization and sulfate reduction. Not all clone sequences were assigned a function.

The 16S rRNA gene sequences were aligned using the tools available through the greengenes website (http://greengenes.lbl.gov) in the 7682-character format using the NAST alignment (DeSantis *et al.*, 2006). The aligned sequences were added to a phylogenetic tree representing a range of phylogenetic groups (Hugenholtz, 2002) using the parsimony insertion tool and the Lane mask (supplied in the same database) in the Arb software package (Ludwig *et al.*, 2004). The tree (Figure 6.S2) was exported from Arb for downstream analysis. The cloned *apsA* gene sequences, along with *apsA* genes of 60 reference taxa consisting of cultured SRB (Table 6.S1), were aligned using ClustalX (Thompson *et al.*, 1997), and a phylogenetic tree (Figure 6.S3) was created with neighbor joining with the Jukes and Cantor correction algorithm in PAUP version 4.0b10 (Swofford, 2002). The 16S rRNA gene and *apsA* gene sequence data have been submitted to the DDB/EMBL/GenBank databases under Accession Numbers EF551816-EF552051 and EF551567-EF551815 respectively.

6.5.3.5 Statistical analysis

The phylogenetic trees representing the two genes were analyzed directly using PCoA and the UniFrac significance tests of the UniFrac algorithm (Lozupone and Knight, 2005; Lozupone *et al.*, 2006; 2007). The PCoA differs from principal component analysis in that the input data are the phylogenetic distances between each pair of sampling locations rather than the number of times each clone sequence was observed at each location. The UniFrac significance test is used to determine whether two microbial communities are significantly different. Communities are considered different if the fraction of the phylogenetic tree unique to one is greater than would be expected by chance (Lozupone and Knight, 2005). For all analyses, the non-normalized abundance data, based on the ARDRA screening, were incorporated in the UniFrac significance test; reference strains used to construct the phylogenetic trees were not included. The raw *P*-values from the UniFrac significance tests are reported, with *P*-value ≤ 0.05 considered to be statistically significant.

The PCoA and UniFrac significance testing were performed using three separate environment definitions: (i) each sampling location from each bioreactor; (ii) the 'front' and the 'back' of each bioreactor and (iii) the presumed aerobic and anaerobic regions of the PJK bioreactors. Sequences from the tops and bottoms of all three sampling locations of the Luttrell bioreactor were combined to be the 'front' and 'back' respectively. For PJK, the sequences from the top and bottom of the front of Cell 1 and the top and bottom of Cell 4 were combined to be the 'front' and 'back' respectively. Based on field observations at PJK, the top influent section of Cell 1 and both top and bottom of Cell 4 were considered aerobic, and the remaining five locations were classified as anaerobic.

6.6 Acknowledgements

This research was funded by the EPA Office of Research and Development Engineering Technical Support Center (Contract #68-C-00-136; David Reisman, Project Officer) and the Rocky Mountain Hazardous Substance Research Center as part of the EPA Science to Achieve Results program under Contract Number R 8395101-0. This research was also supported by funding from the National Science Foundation CBET Award 0651947. We thank Linda Figueroa of the Colorado School of Mines, Robb Amick of Environmental Quality Management, and Jim Gusek of Golder Associates for their valuable guidance.

We also thank Nella Kashani and Kaileen Blanchard for laboratory assistance. This publication has undergone Agency review by the US Environmental Protection Agency (EPA) and is approved for publication. Mention of company names and trademarks does not constitute endorsement by the US EPA.

6.7 References

Beller, H.R., Letain, T.E., Chakicherla, A., Kane, S.R., Legler, T.C., and Coleman, M.A. (2006) Whole-genome transcriptional analysis of chemolithoautotrophic thiosulfate oxidation by *Thiobacillus denitrificans* under aerobic versus denitrifying conditions. *J Bacteriol* **188:** 7005–7015.

Benner, S.G., Blowes, D.W., Gould, W.D., Herbert, R.B.J., and Ptacek, C.J. (1999) Geochemistry of a permeable reactive barrier for metals and acid mine drainage. *Environ Sci Technol* **33:** 2793–2799.

Benner, S.G., Gould, W.D., and Blowes, D.W. (2000) Microbial populations associated with the generation and treatment of acid mine drainage. *Chem Geol* **169:** 435–448.

Berghorn, G.H., and Hunzeker, G.R. (2001) Passive treatment alternatives for remediating abandoned-mine drainage. *Remediation Journal* **11:** 111–127.

Boshoff, G., Duncan, J., and Rose, P.D. (2004) Tannery effluent as a carbon source for biological sulphate reduction. *Water Res* **38:** 2651–2658.

Bruneel, O., Duran, R., Casiot, C., Elbaz-Poulichet, F., and Personne, J.C. (2006) Diversity of microorganisms in Fe-As-Rich acid mine drainage waters of Carnoules, France. *Appl Environ Microbiol* **72:** 551–556.

Chandler, D.P., Jarrell, A.E., Roden, E.R., Golova, J., Chernov, B., Schipma, M.J., *et al.* (2006) Suspension array analysis of 16S rRNA from Fe- and SO_4^{2-}reducing bacteria in uranium-contaminated sediments undergoing bioremediation. *Appl Environ Microbiol* **72:** 4672–4687.

Clarke, A.M., Kirby, R., and Rose, P.D. (2004) Molecular microbial ecology of lignocellulose mobilization as a carbon source in mine drainage wastewater treatment. *Water SA* **30:** 658–661.

Cole, J.R., Chai, B., Farris, R.J., Wang, Q., Kulam-Syed- Mohideen, A.S., McGarrell, D.M., *et al.* (2007) The ribosomal database project (RDP-II): introducing myRDP space and quality controlled public data. *Nucleic Acids Res* **35:** D169–D172.

Daly, K., Sharp, R.J., and McCarthy, A.J. (2000) Development of oligonucleotide probes and PCR primers for detecting phylogenetic subgroups of sulfate-reducing bacteria. *Microbiology* **146:** 1693–1705.

DeSantis, T.Z., Hugenholtz, P., Keller, K., Brodie, E.L., Larsen, N., Piceno, Y.M., *et al.* (2006) NAST: a multiple sequence alignment server for comparative analysis of 16S rRNA genes. *Nucleic Acids Res* **34:** W394–W399.

EPA (1997) *EPA's National Hardrock Mining Framework: United States Environmental Protection Agency Office of Water (4203).* Washington, DC, USA: U.S. Environmental Protection Agency Office of Water (4203).

Friedrich, M.W. (2002) Phylogenetic analysis reveals multiple lateral transfers of adenosine-5′-phosphosulfate reductase genes among sulfate-reducing microorganisms. *J Bacteriol* **184:** 278–289.

Geets, J., Borrernans, B., Diels, L., Springael, D., Vangronsveld, J., van der Lelie, D., and Vanbroekhoven, K. (2006) DsrB gene-based DGGE for community and diversity surveys of sulfate-reducing bacteria. *J Microbiol Methods* **66:** 194–205.

Hallberg, K.B., and Johnson, D.B. (2005a) Microbiology of a wetland ecosystem constructed to remediate mine drainage from a heavy-metal mine. *Sci Total Environ* **338:** 53–66.

Hallberg, K.B., and Johnson, D.B. (2005b) Microbial populations of compost wetlands constructed to remediate acidic coal spoil drainage. In *16th International Biohydrometallurgy Symposium (IBS).* Harrison, S.T.L., Rawlings, D.E., and Peteren, J. (eds). Cape Town, South Africa: International Biohydrometallurgy Symposium, pp. 713–722.

Hard, B.C., Friedrich, S., and Babel, W. (1997) Bioremediation of acid mine water using facultatively methylotrophic metal-tolerant sulfate-reducing bacteria. *Microbiol Res* **152:** 65–73.

Holt, J.H. (ed.). (1984) *Bergey's Manual of Systematic Bacteriology.* Baltimore, MD, USA: Williams & Wilkins.

Hugenholtz, P. (2002) Exploring prokaryotic diversity in the genomic era. *Genome Biol* **3:** reviews0003.1–reviews0003.8.

Johnson, D.B., and Hallberg, K.B. (2003) The microbiology of acidic mine waters. *Res Microbiol* **154:** 466–473.

Johnson, D.B., and Hallberg, K.B. (2005a) Acid mine drainage remediation options: a review. *Sci Total Environ* **338:** 3–14.

Johnson, D.B., and Hallberg, K.B. (2005b) Biogeochemistry of the compost bioreactor components of a composite acid mine drainage passive remediation system. *Sci Total Environ* **338:** 81–93.

Kaksonen, A.H., Plumb, J.J., Franzmann, P.D., and Puhakka, J.A. (2004) Simple organic electron donors support diverse sulfate-reducing communities in fluidized bed reactors treating acidic metal- and sulfate-containing waste water. *FEMS Microbiol Ecol* **47:** 279–289.

Knotek-Smith, H.M., Crawford, D.L., Moller, G., and Henson, R.A. (2006) Microbial studies of a selenium-contaminated mine site and potential for on-site remediation. *J Ind Microbiol Biotechnol* **33:** 897–913.

Labrenz, M., and Banfield, J.F. (2004) Sulfate-reducing bacteria-dominated biofilms that precipitate ZnS in a subsurface circumneutral-pH mine drainage system. *Microb Ecol* **47:** 205–217.

Logan, M.V., Reardon, K.F., Figueroa, L., McLain, J.E.T., and Ahmann, D. (2005) Microbial community activities during establishment, performance, and decline of bench-scale passive treatment systems for mine drainage. *Water Res* **39:** 4537–4551.

Lozupone, C.A., Hamady, M., Kelley, S.T., and Knight, R. (2007) Quantitative and qualitative beta diversity measures lead to different insights into factors that structure microbial communities. *Appl Environ Microbiol* **73:** 1576–1585.

Lozupone, C., and Knight, R. (2005) UniFrac: a new phylogenetic method for comparing microbial communities. *Appl Environ Microbiol* **71:** 8228–8235.

Ludwig, W., Strunk, O., Westram, R., Richter, L., Meier, H., Yadhukumar, *et al.* (2004) ARB: a software environment for sequence data. *Nucleic Acids Res* **32:** 1363–1371.

Lozupone, C., Hamady, M., and Knight, R. (2006) UniFrac – an online tool for comparing microbial community diversity in a phylogenetic context. *BMC Bioinformatics* **7**. URL http://www.biomedcentral.com/1471-2105/7/371.

Lyew, D., Knowles, R., and Sheppard, J. (1994) The biological treatment of acid-mine drainage under continuous-flow conditions in a reactor. *Process Saf Environ Protect* **72:** 42–47.

Mogensen, G.L., Kjeldsen, K.U., and Ingvorsen, K. (2005) *Desulfovibrio aerotolerans* sp nov., an oxygen tolerant sulphate-reducing bacterium isolated from activated sludge. *Anaerobe* **11:** 339–349.

Morales, T.A., Dopson, M., Athar, R., and Herbert, R.B.J. (2005) Analysis of bacterial diversity in acidic pond water and compost after treatment of artificial acid mine drainage for metal removal. *Biotechnol Bioeng* **90:** 543–551.

Muyzer, G., Dewaal, E.C., and Uitterlinden, A.G. (1993) Profiling of complex microbial-populations by denaturing gradient gel-electrophoresis analysis of polymerase chain reaction-amplified genes-coding for 16s ribosomal-RNA. *Appl Environ Microbiol* **59:** 695–700.

Neculita, C.M., Zagury, G.J., and Bussière, B. (2007) Passive treatment of acid mine drainage in bioreactors using sulfate-reducing bacteria. *J Environ Qual* **36:** 1–16.

Nicomrat, D., Dick, W.A., and Tuovinen, O.H. (2006a) Microbial populations identified by fluorescence in situ hybridization in a constructed wetland treating acid coal mine drainage. *J Environ Qual* **35:** 1329–1337.

Nicomrat, D., Dick, W.A., and Tuovinen, O.H. (2006b) Assessment of the microbial community in a constructed wetland that receives acid coal mine drainage. *Microb Ecol* **51:** 83–89.

Place, D., Figueroa, L., Wildeman, T., and Reisman, D. (2006) Characterizing and tracking reactive mixture alterations: new tools for passive treatment systems design and monitoring. In *7th International Conference on Acid Rock Drainage (ICARD).* Barnhisel, R.I. (ed.). St. Louis, MO, USA: American Society of Mining and Reclamation (ASMR), pp. 1605–1619.

Pruden, A., Messner, N., Pereyra, L., Hanson, R.E., Hiibel, S.R., and Reardon, K.F. (2007) The effect of inoculum on the performance of sulfate-reducing columns treating heavy metal contaminated water. *Water Res* **41:** 904–914.

Reisman, D.J., Gusek, J.J., and Bishop, M. (2003) A pretreatability study to provide data for construction of a demonstration bioreactor In *10th International Conference on Tailings and Mine Waste.* Nelson, J.D., Foulk, C.L., Hinshaw, L.L., Ketellaper, V., Macalady, D.L., Overton, D.D., *et al.* (eds). Vail, CO, USA: Taylor & Francis, pp. 305–315.

Rudi, K., Zimonja, M., Trosvik, P., and Naes, T. (2007) Use of multivariate statistics for 16S rRNA gene analysis of microbial communities. *Int J Food Microbiol* **120:** 95–99.

Steed, V.S., Suidan, M.T., Gupta, M., Miyahara, T., Acheson, C.M., and Sayles, G.D. (2000) Development of a sulfate-reducing biological process to remove heavy metals from acid mine drainage. *Water Environ Res* **72:** 530–535.

Suzuki, M.T., Taylor, L.T., and DeLong, E.F. (2000) Quantitative analysis of small-subunit rRNA Genes in mixed microbial populations via 5′-nuclease assays. *Appl Environ Microbiol* **66:** 4605–4614.

Swofford, D.L. (2002) *PAUP*: Phylogenetic Analysis Using Parsimony (and Other Methods) 4.0 Beta.* Sunderland, MA, USA: Sinauer Associates.

Thompson, J.D., Gibson, T.J., Plewniak, F., Jeanmougin, F., and Higgins, D.G. (1997) The ClustalX windows interface: flexible strategies for multiple sequence alignment aided by quality analysis tools. *Nucleic Acids Res* **25:** 4876–4882.

Waybrant, K.R., Ptacek, C.J., and Blowes, D.W. (2002) Treatment of mine drainage using permeable reactive barriers: column experiments. *Environ Sci Technol* **36:** 1349–1356.

Weisburg, W.G., Barns, S.M., Pelletier, D.A., and Lane, D.J. (1991) 16S ribosomal DNA amplification for phylogenetic study. *J Bacteriol* **173:** 697–703.

6.8 Supplementary Material

The following supplementary material is available for this article online. This material is available as part of the online article from http://www.blackwell-synergy.com. Please note: Blackwell Publishing is not responsible for the content or functionality of any supplementary materials supplied by the authors. Any queries (other than missing material) should be directed to the corresponding author for the article.

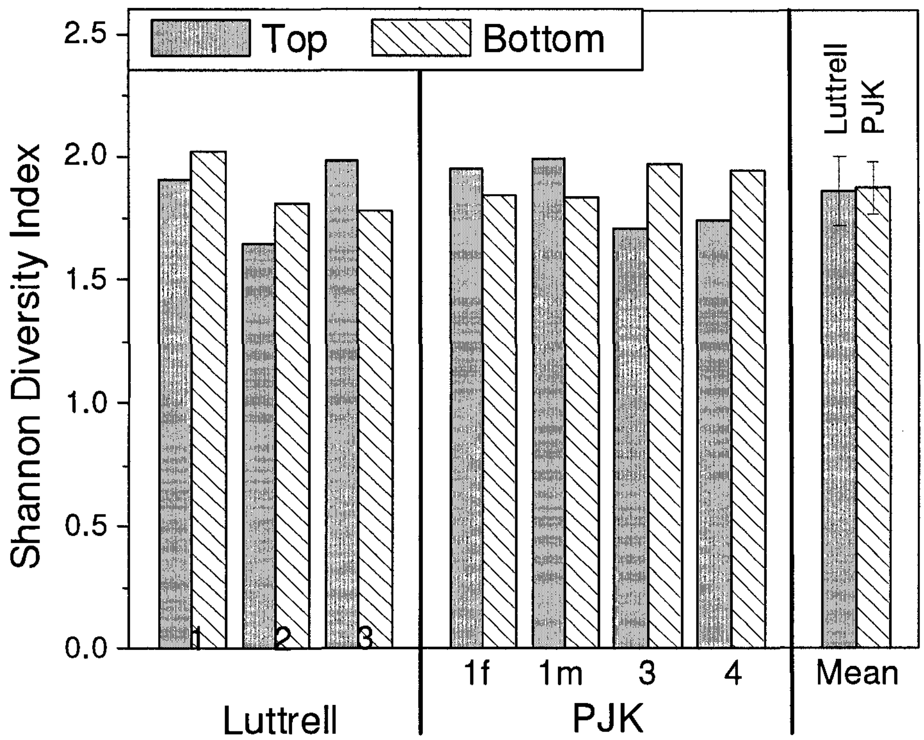

Figure 6.S1 – Shannon Diversity Indices for the Luttrell and Peerless Jenny King (PJK) bioreactors, based on the ARDRA results of the 16S rRNA gene clone library.

P1fT_323, ARB_9430
P1mT_023, ARB_70E3
P1mB_312, ARB_DCE1
P1fT_160, ARB_3DDD
P3T_123, ARB_4C65
P1mT_002, ARB_D6DD
P1mT_017, ARB_397E
P1mT_003, ARB_500E
P1mT_012, ARB_18D8
P1mT_062, ARB_62D2
P1mB_300, ARB_34A5
P1fT_156, ARB_E911
P3B_119, ARB_856A
P4B_038, ARB_3C17
P4B_073, ARB_3E48
P4B_089, ARB_9393
P4B_043, ARB_C525
P4B_071, ARB_36AF
P3T_003, ARB_C513
BurCepac, Burkholderia cepacia, M22467 M, 1445
L1B_202, ARB_7F04
P3T_077, ARB_75A9
P1fT_007, ARB_363F
L2B_038, ARB_7738
NeiGonor, Neisseria gonorrhoeae, X07714, 1544
HphTher2, Hydrogenophilus thermoluteolus, AB009828, 1459
P1fT_064, ARB_92A7
P1fT_058, ARB_6EAA
L2B_074, ARB_398F
L3T_053, ARB_A06E
P3B_251, ARB_4E0F
L2T_040, ARB_229C
P1fB_037, ARB_3698
P3B_229, ARB_F3A6
L3B_377, ARB_38F8
XanCamp7, Xanthomonas campestris , 1484
P3B_275, ARB_85B4
P3T_036, ARB_83A8
L3T_098, ARB_DF8C
P3T_134, ARB_CA99
L1T_308, ARB_3C63
L2B_013, ARB_EF50
L3T_110, ARB_D169
L3T_061, ARB_C5F8
L2B_050, ARB_AD48
L3T_043, ARB_F195
L2B_132, ARB_BD96
L2B_118, ARB_CA38
L3T_049, ARB_BDBE
L3T_073, ARB_C817
L3T_077, ARB_DAFB
L1T_105, ARB_788F
L2B_068, ARB_61BA
L2B_028, ARB_D90D
L3T_005, ARB_E885
L2B_033, ARB_DF55
L3T_069, ARB_DC11
L3T_042, ARB_8087
EscCol242, Escherichia coli, X80725, 1447
L1T_302, ARB_7551
L3T_075, ARB_4088
L3B_316, ARB_A907
L2T_322, ARB_C664
L2T_337, ARB_8588
L3B_319, ARB_9561
L2B_090, ARB_78F8
L3T_018, ARB_C765
L3T_086, ARB_A598
P1fT_300, ARB_601D
P4B_138, ARB_726C
L2B_070, ARB_D957
L3T_039, ARB_8D08
L2T_300, ARB_2EA2
P3T_080, ARB_6D7A
P4B_057, ARB_24C6
LegPneu6, Legionella pneumophila , M59157, 1501
MeyCapsu, Methylococcus capsulatus, X72770, 1457
ChrVinos, Chromatium vinosum, M26629, 1483
P1fB_005, ARB_434A
P3T_027, ARB_974F
P3B_263, ARB_D8DC
P4T_321, ARB_AF81
β-Proteobacteria
γ-Proteobacteria


P1mB_306, ARB_B6D1
P3T_070, ARB_720A
RhiLegu6, Rhizobium leguminosarum, D12782, 1427
P4T_200, ARB_234A
L3B_344, ARB_2640
P3B_118, ARB_C44B
P3B_274, ARB_C194
P1fT_001, ARB_629D
P3B_123, ARB_B970
P3T_031, ARB_5B3B
P3T_160, ARB_3904
P3B_205, ARB_83E6
P4T_068, ARB_8028
RhoCaps4, Rhodobacter capsulatus, D16428, 1386
L1B_003, ARB_5298
L1T_217, ARB_35A2
P3T_029, ARB_EABF
P3T_082, ARB_58C8
SpnPau21, Sphingomonas paucimobilis, U37337, 1414
P3B_248, ARB_B9C3
L2T_005, ARB_B822
L1B_185, ARB_3926
L2B_020, ARB_13CE
P3T_066, ARB_C97D
P3B_224, ARB_9337
P1fT_329, ARB_AB20
P3B_83, ARB_392F
P3B_135, ARB_787A
P3T_135, ARB_2A2E
P4T_043, ARB_A160
P3T_125, ARB_48EF
RhsRubru, Rhodospirillum rubrum, D30778, 1406
CauCres2, Caulobacter crescentus, M83799, 1408
P4T_044, ARB_FB35
P1fT_321, ARB_5F3D
RicProwa, Rickettsia prowazekii, M21789, 1502
P3B_005, ARB_4429
P4T_047, ARB_E587
P1fT_003, ARB_1542
2
Campylobacteraceae
P1mB_319, ARB_7154
ThiDenit, Thiomicrospira denitrificans, L40808, 1444
AlvPomp3, Alvinella pompejana epibiont, L35521, 1502
2
Helicobacteraceae
DesAceti, Desulfurella acetivorans, X72768, 1560
P3B_054, ARB_FEFF
P3T_110, ARB_7834
P3T_043, ARB_879F
P3T_061, ARB_8543
MyxXanth, Myxococcus xanthus, M34114, 1539
DenAceto, Desulfuromonas acetoxidans, M26634, 1487
DeuPostg, Desulfobacter postgatei, M26633, 1499
SytWoli2, Syntrophobacter wolinii, X70905, 1424
P1fT_347, ARB_BFFA
P4B_095, ARB_D882
BdeBact9, Bdellovibrio bacteriovorus, M59297, 1445
P1mT_104, ARB_E372
BdeStol2, Bacteriovorax stolpii, M34125, 1446
DevDesul, Desulfovibrio desulfuricans, M34113, 1550
L2T_320, ARB_46EC
5
TM6
AcbCapsu, Acidobacterium capsulatum, D26171, 1418
L2B_034, ARB_FD93
P1fT_317, ARB_C17D
UA3, soil clone UA3, AF200699, 1456
P3T_107, ARB_FCA1
P1mB_315, ARB_1F06
P3T_078, ARB_45DC
C105, soil clone C105, AF013530, 1473
32-11, soil clone 32-11, Z95711, 1550
P1mT_005, ARB_F295
P1mT_045, ARB_68F8
P1fT_075, ARB_5153
C002, forest soil clone C002, AF013515, 1462
P3T_013, ARB_97C5
P1fT_305, ARB_1217
OPB3, hot spring clone OPB3, AF027004, 1430
P3B_188, ARB_8CD8
ii3-15, soil clone ii3-15, Z95725, 1542
P4T_193, ARB_4CF0
α-Proteobacteria
ε-Proteobacteria
δ-Proteobacteria
Acidobacteria

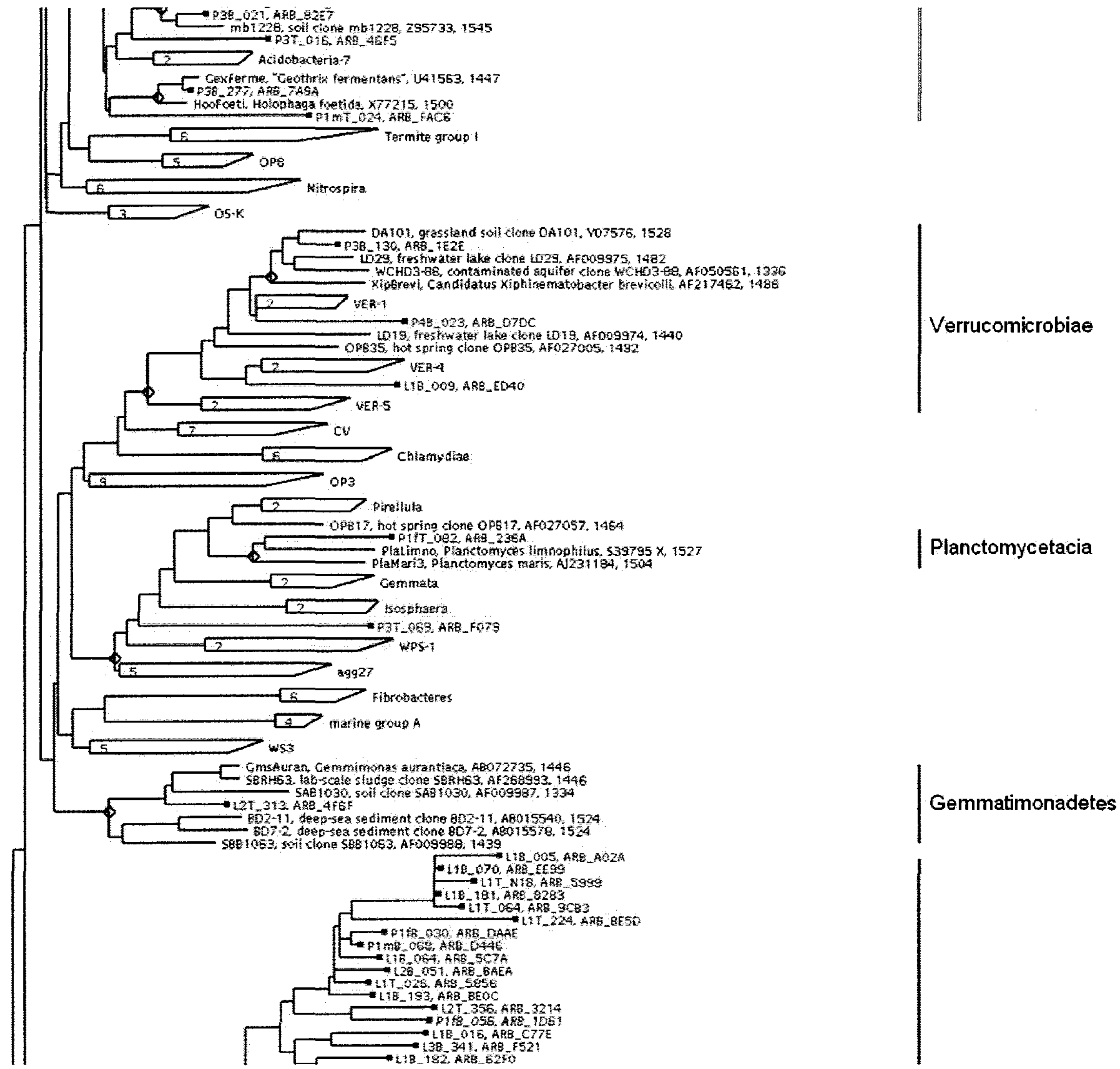
P3B_021, ARB_82E7
mb1228, soil clone mb1228, Z95733, 1545
P3T_016, ARB_46F5
Acidobacteria-7
Gexferme, "Geothrix fermentans", U41563, 1447
P3B_277, ARB_7A9A
HooFoeti, Holophaga foetida, X77215, 1500
P1mT_024, ARB_FAC6
Termite group I
OP6
Nitrospira
OS-K
DA101, grassland soil clone DA101, Y07576, 1528
P3B_130, ARB_1E2E
LD29, freshwater lake clone LD29, AF009975, 1482
WCHD3-88, contaminated aquifer clone WCHD3-88, AF050561, 1336
XipBrevi, Candidatus Xiphinematobacter brevicolli, AF217462, 1486
VER-1
P4B_023, ARB_D7DC
LD19, freshwater lake clone LD19, AF009974, 1440
OPB35, hot spring clone OPB35, AF027005, 1492
VER-4
L1B_009, ARB_ED40
VER-5
CV
Chlamydiae
OP3
Pirellula
OPB17, hot spring clone OPB17, AF027057, 1464
P1fT_082, ARB_236A
PlaLimno, Planctomyces limnophilus, S39795 X, 1527
PlaMari3, Planctomyces maris, AJ231184, 1504
Gemmata
Isosphaera
P3T_069, ARB_F079
WPS-1
agg27
Fibrobacteres
marine group A
WS3
GmsAuran, Gemmimonas aurantiaca, AB072735, 1446
SBRH63, lab-scale sludge clone SBRH63, AF268993, 1446
SAB1030, soil clone SAB1030, AF009987, 1334
L2T_313, ARB_4F6F
BD2-11, deep-sea sediment clone BD2-11, AB015540, 1524
BD7-2, deep-sea sediment clone BD7-2, AB015578, 1524
SBB1063, soil clone SBB1063, AF009988, 1439
L1B_005, ARB_A02A
L1B_070, ARB_EE99
L1T_N18, ARB_5999
L1B_181, ARB_8283
L1T_064, ARB_9CB3
L1T_224, ARB_BE5D
P1fB_030, ARB_DAAE
P1mB_068, ARB_D446
L1B_064, ARB_5C7A
L2B_051, ARB_BAEA
L1T_026, ARB_5856
L1B_193, ARB_BE0C
L2T_356, ARB_3214
P1fB_056, ARB_1D61
L1B_016, ARB_C77E
L3B_341, ARB_F521
L1B_182, ARB_62F0
Verrucomicrobiae
Planctomycetacia
Gemmatimonadetes

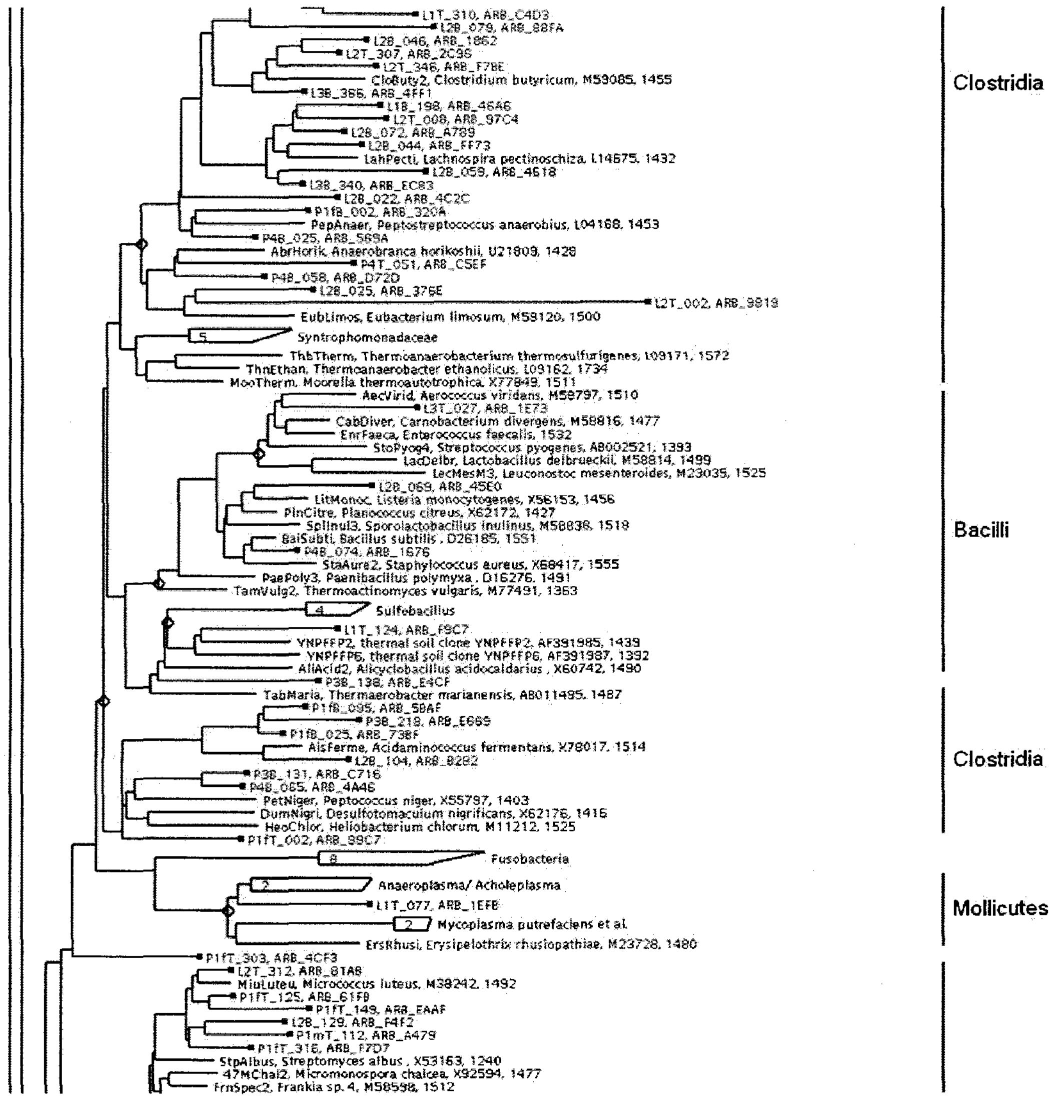
L1T_310, ARB_C4D3
L2B_079, ARB_88FA
L2B_046, ARB_1862
L2T_307, ARB_2C96
L2T_346, ARB_F78E
CloButy2, Clostridium butyricum, M59085, 1455
L3B_366, ARB_4FF1
L1B_198, ARB_46A6
L2T_008, ARB_97C4
L2B_072, ARB_A789
L2B_044, ARB_FF73
LahPecti, Lachnospira pectinoschiza, L14675, 1432
L2B_059, ARB_4618
L3B_340, ARB_EC83
L2B_022, ARB_4C2C
P1fB_002, ARB_320A
PepAnaer, Peptostreptococcus anaerobius, L04168, 1453
P4B_025, ARB_569A
AbrHorik, Anaerobranca horikoshii, U21809, 1428
P4T_051, ARB_C5EF
P4B_058, ARB_D72D
L2B_025, ARB_376E
L2T_002, ARB_9819
EubLimos, Eubacterium limosum, M59120, 1500
5
Syntrophomonadaceae
ThbTherm, Thermoanaerobacterium thermosulfurigenes, L09171, 1572
ThnEthan, Thermoanaerobacter ethanolicus, L09162, 1734
MooTherm, Moorella thermoautotrophica, X77849, 1511
AecVirid, Aerococcus viridans, M58797, 1510
L3T_027, ARB_1E73
CabDiver, Carnobacterium divergens, M58816, 1477
EnrFaeca, Enterococcus faecalis, 1532
StoPyog4, Streptococcus pyogenes, AB002521, 1393
LacDelbr, Lactobacillus delbrueckii, M58814, 1499
LecMesM3, Leuconostoc mesenteroides, M23035, 1525
L2B_069, ARB_45E0
LitMonoc, Listeria monocytogenes, X56153, 1456
PlnCitre, Planococcus citreus, X62172, 1427
SplInul3, Sporolactobacillus inulinus, M58838, 1518
BacSubti, Bacillus subtilis, D26185, 1551
P4B_074, ARB_1676
StaAure2, Staphylococcus aureus, X68417, 1555
PaePoly3, Paenibacillus polymyxa, D16276, 1491
TamVulg2, Thermoactinomyces vulgaris, M77491, 1363
4
Sulfobacillus
L1T_124, ARB_F9C7
YNPFFP2, thermal soil clone YNPFFP2, AF391985, 1439
YNPFFP6, thermal soil clone YNPFFP6, AF391987, 1392
AliAcid2, Alicyclobacillus acidocaldarius, X60742, 1490
P3B_138, ARB_E4CF
TabMaria, Thermaerobacter marianensis, AB011495, 1487
P1fB_095, ARB_58AF
P3B_218, ARB_E669
P1fB_025, ARB_738F
AisFerme, Acidaminococcus fermentans, X78017, 1514
L2B_104, ARB_8282
P3B_131, ARB_C716
P4B_065, ARB_4A46
PetNiger, Peptococcus niger, X55797, 1403
DumNigri, Desulfotomaculum nigrificans, X62176, 1416
HeoChlor, Heliobacterium chlorum, M11212, 1525
P1fT_002, ARB_99C7
8
Fusobacteria
2
Anaeroplasma/ Acholeplasma
L1T_077, ARB_1EFB
2
Mycoplasma putrefaciens et al.
ErsRhusi, Erysipelothrix rhusiopathiae, M23728, 1480
P1fT_303, ARB_4CF3
L2T_312, ARB_81A8
MiuLuteu, Micrococcus luteus, M38242, 1492
P1fT_125, ARB_61F8
P1fT_149, ARB_EAAF
L2B_129, ARB_F4F2
P1mT_112, ARB_A479
P1fT_316, ARB_F7D7
StpAlbus, Streptomyces albus, X53163, 1240
47MChal2, Micromonospora chalcea, X92594, 1477
FrnSpec2, Frankia sp. 4, M58598, 1512
Clostridia
Bacilli
Clostridia
Mollicutes

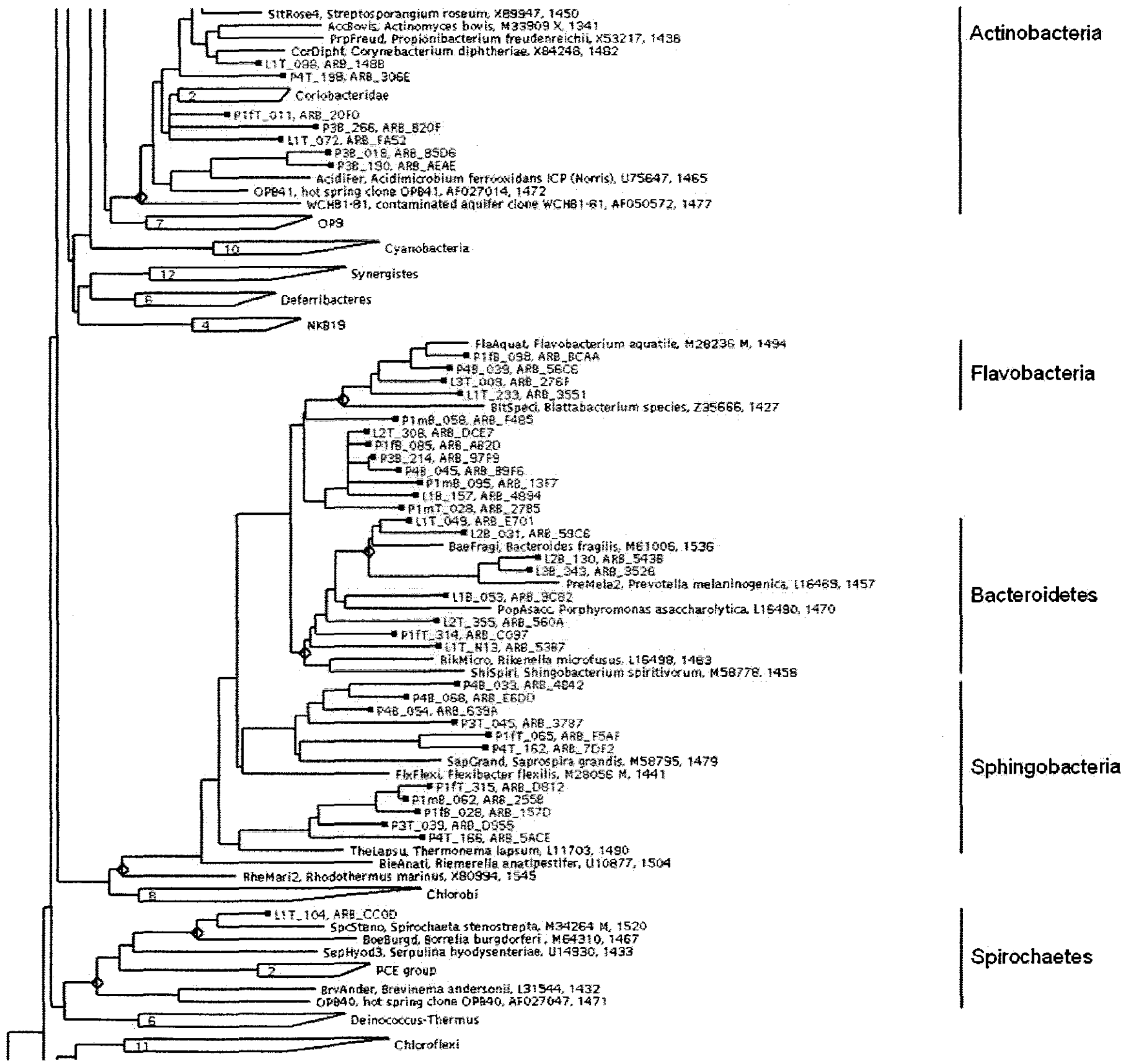
StrRose4, Streptosporangium roseum, X89947, 1450
AccBovis, Actinomyces bovis, M33909 X, 1341
PrpFreud, Propionibacterium freudenreichii, X53217, 1436
CorDipht, Corynebacterium diphtheriae, X84248, 1482
L1T_098, ARB_148B
P4T_198, ARB_306E
Coriobacteridae
P1fT_011, ARB_20F0
P3B_266, ARB_820F
L1T_072, ARB_FA52
P3B_018, ARB_85D6
P3B_190, ARB_AEAE
Acidifer, Acidimicrobium ferrooxidans ICP (Norris), U75647, 1465
OP841, hot spring clone OP841, AF027014, 1472
WCHB1-81, contaminated aquifer clone WCHB1-81, AF050572, 1477
OP9
Cyanobacteria
Synergistes
Deferribacteres
NKB19
FlaAquat, Flavobacterium aquatile, M28236 M, 1494
P1fB_098, ARB_BCAA
P4B_039, ARB_56C6
L3T_003, ARB_276F
L1T_233, ARB_3551
BltSpeci, Blattabacterium species, Z35666, 1427
P1mB_058, ARB_F485
L2T_308, ARB_DCE7
P1fB_085, ARB_AB2D
P3B_214, ARB_97F9
P4B_045, ARB_89F6
P1mB_095, ARB_13F7
L1B_157, ARB_4894
P1mT_028, ARB_2785
L1T_049, ARB_E701
L2B_031, ARB_59C6
BaeFragi, Bacteroides fragilis, M61006, 1536
L2B_130, ARB_543B
L3B_343, ARB_3526
PreMela2, Prevotella melaninogenica, L16469, 1457
L1B_053, ARB_9C82
PopAsacc, Porphyromonas asaccharolytica, L16490, 1470
L2T_355, ARB_560A
P1fT_314, ARB_C097
L1T_N13, ARB_5387
RikMicro, Rikenella microfusus, L16498, 1463
ShiSpiri, Shingobacterium spiritivorum, M58778, 1458
P4B_033, ARB_4842
P4B_068, ARB_E6DD
P4B_054, ARB_639A
P3T_045, ARB_3787
P1fT_065, ARB_F5AF
P4T_162, ARB_7DF2
SapGrand, Saprospira grandis, M58795, 1479
FlxFlexi, Flexibacter flexilis, M28056 M, 1441
P1fT_315, ARB_D812
P1mB_062, ARB_2558
P1fB_028, ARB_157D
P3T_039, ARB_D955
P4T_166, ARB_5ACE
TheLapsu, Thermonema lapsum, L11703, 1490
RieAnati, Riemerella anatipestifer, U10877, 1504
RheMari2, Rhodothermus marinus, X80994, 1545
Chlorobi
L1T_104, ARB_CC0D
SpcSteno, Spirochaeta stenostrepta, M34264 M, 1520
BoeBurgd, Borrelia burgdorferi, M64310, 1467
SepHyod3, Serpulina hyodysenteriae, U14930, 1433
PCE group
BrvAnder, Brevinema andersonii, L31544, 1432
OP840, hot spring clone OP840, AF027047, 1471
Deinococcus-Thermus
Chloroflexi
7
10
12
6
4
2
8
2
6
11
Actinobacteria
Flavobacteria
Bacteroidetes
Sphingobacteria
Spirochaetes

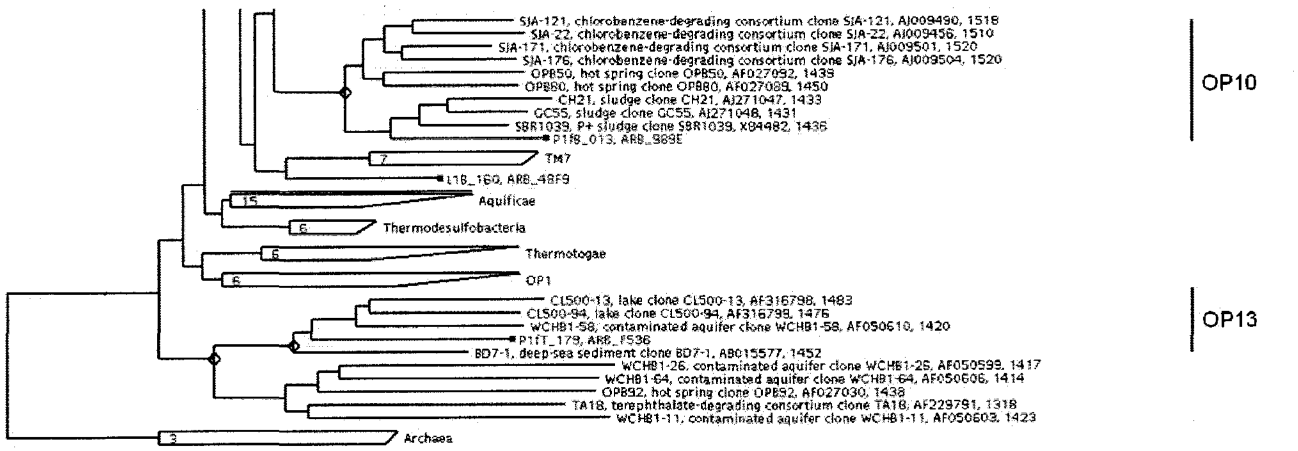

Figure 6.S2 - Phylogenetic tree for 16S rRNA gene clone sequences.

Table 6.S1 - Reference species used for sequence alignment of *apsA* gene clone sequences.

Species	Accession #	Species	Accession #
Desulfacinum hydrothermale	AF418148	*Desulforhopalus singaporensis*	AF418163
Desulfacinum infernum	AF418144	*Desulfosarcina variabilis*	AF418121
Desulfoarculus baarsii	AF418149	*Desulfospira joergensenii*	AF418116
Desulfobacter curvatus	AF418107	*Desulfotignum balticum*	AF418127
Desulfobacter postgatei	AF418157	*Desulfotomaculum acetoxidans*	AF418153
Desulfobacterium anilini	AF418158	*Desulfotomaculum aeronauticum*	AF418156
Desulfobacterium autotrophicum	AF418108	*Desulfotomaculum alkaliphilum*	AF418154
Desulfobacterium indolicum	AF418123	*Desulfotomaculum geothermicum*	AF418115
Desulfobacterium oleovorans	AF418126	*Desulfotomaculum halophilum*	AF418167
Desulfobacterium vacuolatum	AF418124	*Desulfotomaculum kuznetsovii*	AF418152
Desulfobacula toluolica	AF418128	*Desulfotomaculum nigrificans*	AF418155
Desulfobulbus elongatus	AF418146	*Desulfotomaculum putei*	AF418147
Desulfobulbus rhabdoformis	AF418110	*Desulfotomaculum ruminis*	AF418164
Desulfocapsa sulfexigens	AF418131	*Desulfotomaculum sapomandens*	AF418150
Desulfocapsa thiozymogenes	AF418166	*Desulfotomaculum thermobenzoicum*	AF418161
Desulfocella halophila	AF418117	*Desulfovibrio aerotolerans*	AY749040
Desulfococcus biacutus	AF418151	*Desulfovibrio africanus*	AF418140
Desulfococcus multivorans	AF418136	*Desulfovibrio burkinensis*	AF418143
Desulfofaba gelida	AF418118	*Desulfovibrio fructosovorans*	AF418109
Desulfofrigus oceanense	AF418145	*Desulfovibrio giganteus*	AF418141
Desulfofustis glycolicus	AF418130	*Desulfovibrio intestinalis*	AF418106
Desulfohalobium retbaense	AF418125	*Desulfovibrio profundus*	AF418133
Desulfomicrobium baculatum	AF418120	*Desulfovibrio termitidis*	AF418142
Desulfomonas pigra	AF418129	*Thermodesulfobacterium commune*	AF418114
Desulfomonile tiedjei	AF418162	*Thermodesulfobacterium hveragerdense*	AF418119
Desulfonatronovibrio hydrogenovorans	AF418111	*Thermodesulfobacterium thermophilum*	AF418112
Desulfonatronum lacustre	AF418137	*Thermodesulforhabdus norvegica*	AF418159
Desulfonema ishimotonii	AF418135	*Thermodesulfovibrio islandicus**	AF418113
Desulfonema magnum	AF418122	*Thiobacillus denitrificans*	AY296750
Desulforhabdus amnigena	AF418139		

* *Used to root phylogenetic tree*

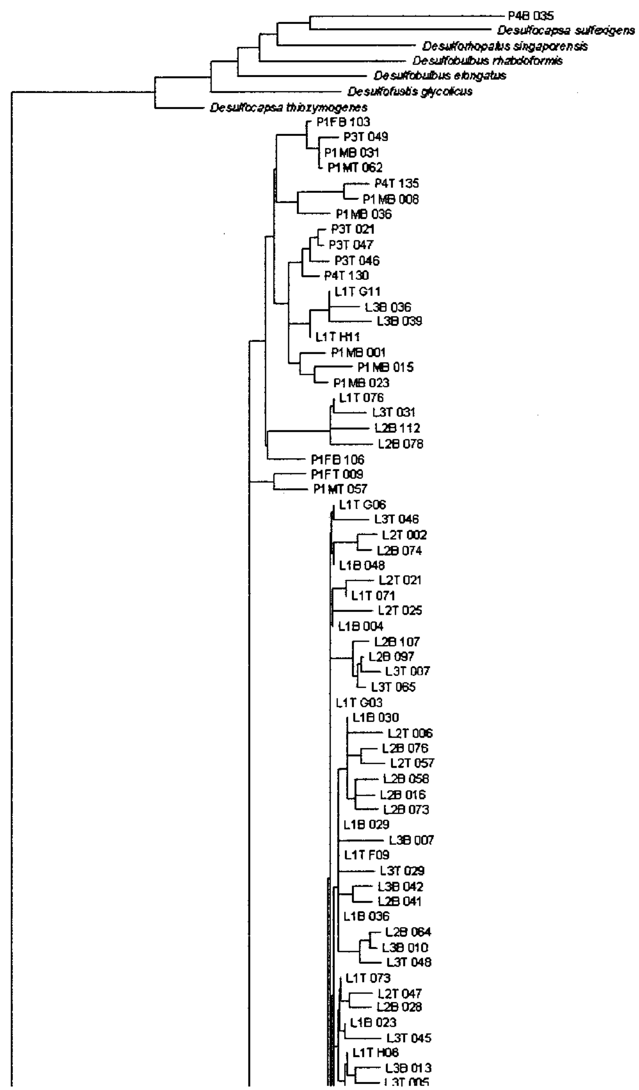

P4B 035
Desulfocapsa sulfexigens
Desulfomopalus singaporensis
Desulfobulbus rhabdoformis
Desulfobulbus elongatus
Desulfofustis glycolicus
Desulfocapsa thiozymogenes
P1FB 103
P3T 049
P1MB 031
P1MT 062
P4T 135
P1MB 008
P1MB 036
P3T 021
P3T 047
P3T 046
P4T 130
L1T G11
L3B 036
L3B 039
L1T H11
P1MB 001
P1MB 015
P1MB 023
L1T 076
L3T 031
L2B 112
L2B 078
P1FB 106
P1FT 009
P1MT 057
L1T G06
L3T 046
L2T 002
L2B 074
L1B 048
L2T 021
L1T 071
L2T 025
L1B 004
L2B 107
L2B 097
L3T 007
L3T 065
L1T G03
L1B 030
L2T 006
L2B 076
L2T 057
L2B 058
L2B 016
L2B 073
L1B 029
L3B 007
L1T F09
L3T 029
L3B 042
L2B 041
L1B 036
L2B 064
L3B 010
L3T 048
L1T 073
L2T 047
L2B 028
L1B 023
L3T 045
L1T H08
L3B 013

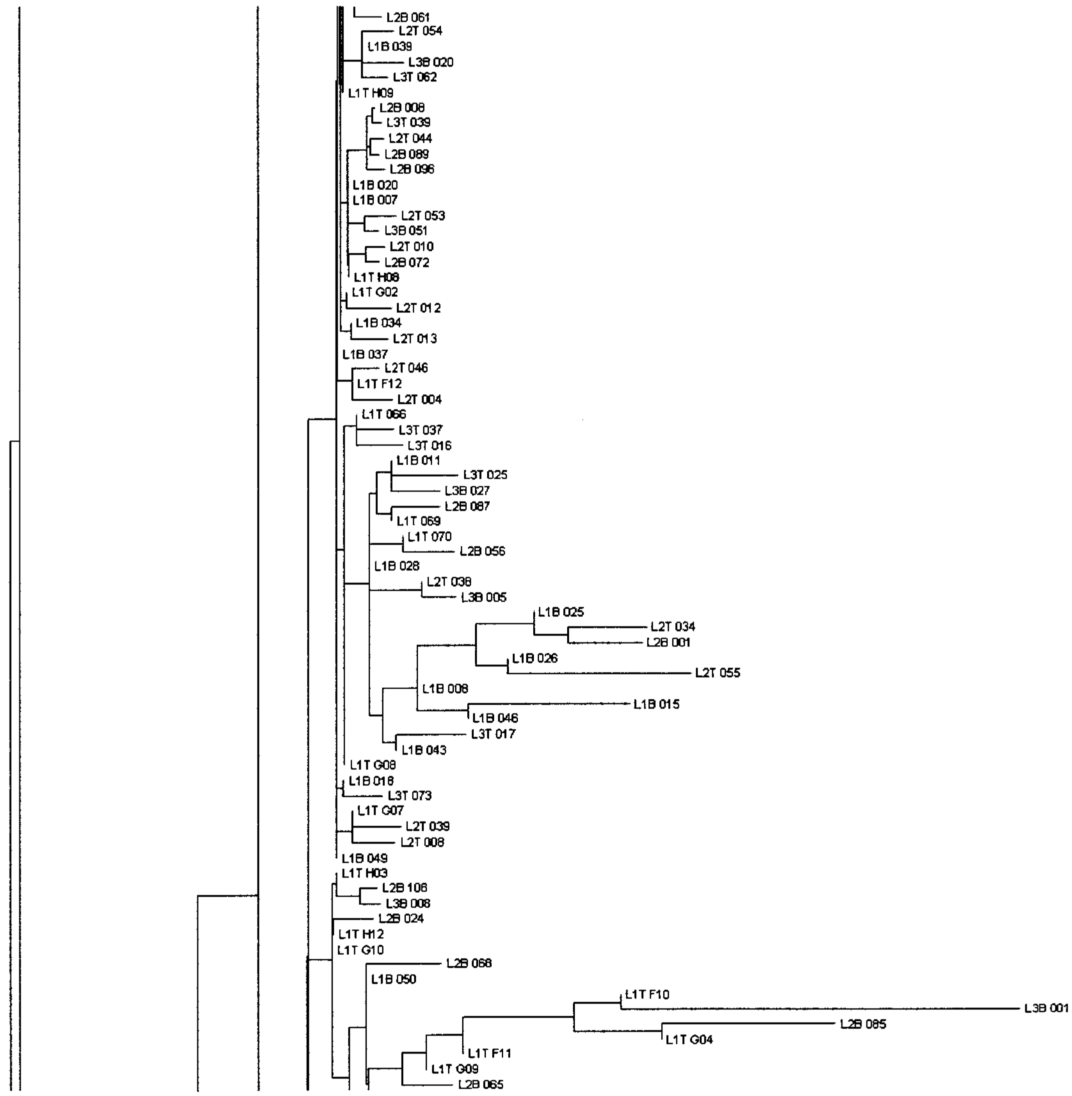
L2B 061
L2T 054
L1B 039
L3B 020
L3T 062
L1T H09
L2B 008
L3T 039
L2T 044
L2B 089
L2B 096
L1B 020
L1B 007
L2T 053
L3B 051
L2T 010
L2B 072
L1T H08
L1T G02
L2T 012
L1B 034
L2T 013
L1B 037
L2T 046
L1T F12
L2T 004
L1T 066
L3T 037
L3T 016
L1B 011
L3T 025
L3B 027
L2B 087
L1T 069
L1T 070
L2B 056
L1B 028
L2T 036
L3B 005
L1B 025
L2T 034
L2B 001
L1B 026
L2T 055
L1B 006
L1B 015
L1B 046
L3T 017
L1B 043
L1T G08
L1B 018
L3T 073
L1T G07
L2T 039
L2T 008
L1B 049
L1T H03
L2B 106
L3B 008
L2B 024
L1T H12
L1T G10
L2B 068
L1B 050
L1T F10
L3B 001
L2B 085
L1T G04
L1T F11
L1T G09
L2B 065


L1B 017
L3T 040
L1T G01
L3T 052
L1T G12
L2T 027
L3B 065
L3B 054
L2T 001
L2B 002
L2T 020
L1B 038
L1T 095
L2B 106
L2B 088
L3B 053
L1T H02
L3T 033
L1B 019
L2B 067
L3B 049
L1T G05
L3T 012
L1T 077
Desulfovibrio profundus
Desulfomonas pigra
Desulfovibrio intestinalis
Desulfovibrio termitidis
Desulfovibrio giganteus
P4B 015
P1FT 007
P3T 030
P1MB 025
P4T 114
P1FT 049
P1MB 032
P3B 111
L2B 026
L2B 048
L2B 103
Desulfovibrio africanus
P3T 039
Desulfovibrio aerotolerans
Desulfovibrio burkinensis
Desulfovibrio fructosovorans
Desulfomicrobium baculatum
Desulfonatronovibrio hydrogenovorans
Desulfonatronum lacustre
Desulfohalobium retbaense
Desulfotomaculum halophilum
Desulfotomaculum alkaliphilum
Desulfotomaculum aeronauticum
Desulfotomaculum ruminis
Desulfotomaculum nigrificans
Desulfotomaculum putei
Desulfotomaculum acetoxidans
Desulfotomaculum sapomandens
Desulfotomaculum geothermicum
Desulfomonile tiedjei
Desulfobacterium anilini
Thermodesulforhabdus norvegica
Desulforhabdus amnigena
Desulfacinum hydrothermale
Desulfacinum infernum
Desulfoarculus baarsii
Desulfotomaculum thermobenzoicum
Desulfotomaculum kuznetsovii
P3B 109
P4T 138
P4T 115
P1MT 048

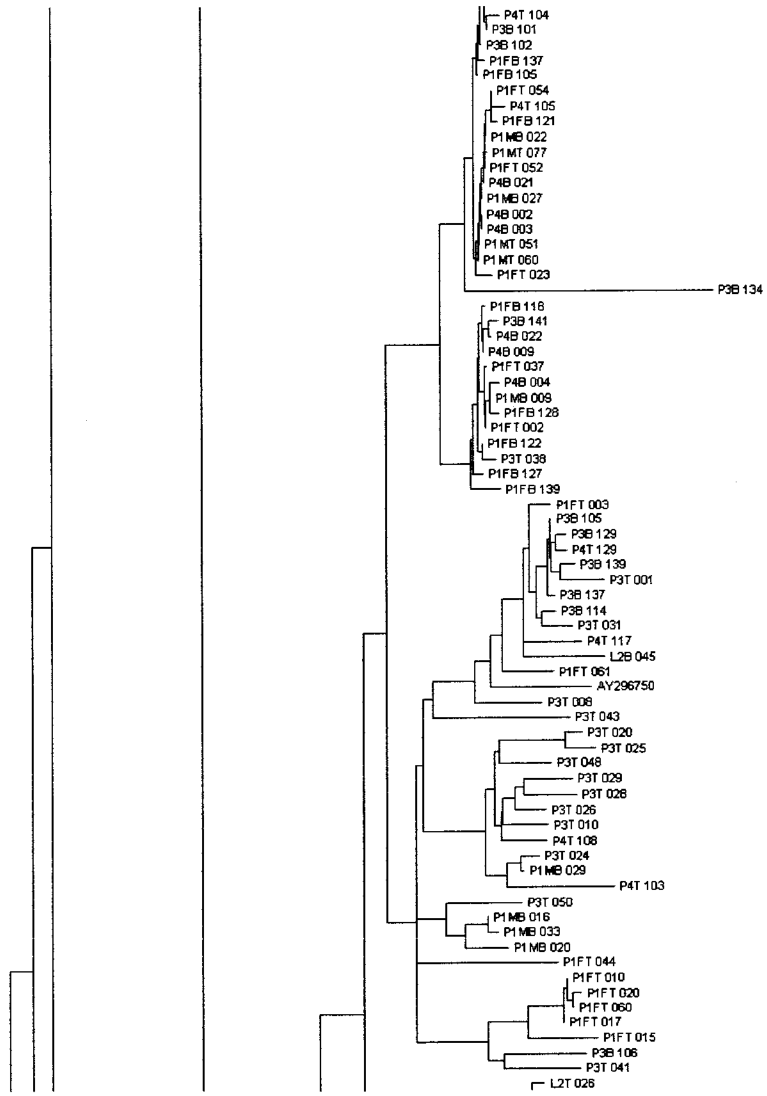
P4T 104
P3B 101
P3B 102
P1FB 137
P1FB 105
P1FT 054
P4T 105
P1FB 121
P1MB 022
P1MT 077
P1FT 052
P4B 021
P1MB 027
P4B 002
P4B 003
P1MT 051
P1MT 060
P1FT 023
P3B 134
P1FB 116
P3B 141
P4B 022
P4B 009
P1FT 037
P4B 004
P1MB 009
P1FB 128
P1FT 002
P1FB 122
P3T 038
P1FB 127
P1FB 139
P1FT 003
P3B 105
P3B 129
P4T 129
P3B 139
P3T 001
P3B 137
P3B 114
P3T 031
P4T 117
L2B 045
P1FT 061
AY296750
P3T 008
P3T 043
P3T 020
P3T 025
P3T 048
P3T 029
P3T 028
P3T 026
P3T 010
P4T 108
P3T 024
P1MB 029
P4T 103
P3T 050
P1MB 016
P1MB 033
P1MB 020
P1FT 044
P1FT 010
P1FT 020
P1FT 060
P1FT 017
P1FT 015
P3B 106
P3T 041
L2T 026

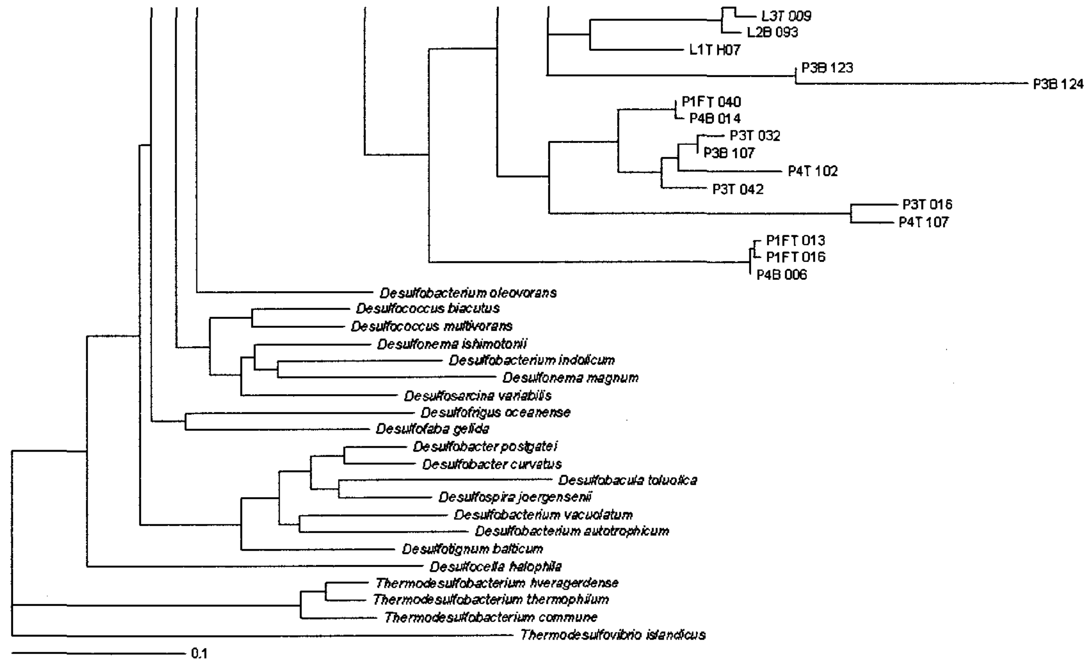

Figure 6.S3 - Phylogenetic tree for *apsA* gene clone sequences.

Chapter 7 Capillary Electrophoresis Single-Strand Conformation Polymorphism (CE-SSCP) for Active Community Profiling of Mixed Microbial Communities

Hiibel, S.R., Pruden, A., and Reardon, K.F.
(*In preparation for submission to Microbial Ecology*)

7.1 Abstract

Active community profiling (ACP), a novel, high-throughput method for fingerprinting the active members of a mixed microbial community was developed. ACP provides information on both the composition and the activity of mixed microbial cultures via comparative measurements of 16S rRNA and rDNA. Capillary electrophoresis single-strand conformational polymorphism (CE-SSCP) is used to resolve and quantify the mixed community 16S PCR products. Active members of the community are identified by elevated ratios of 16S rRNA to rDNA. This work offers proof of concept of the ACP method with defined chemostat growth studies. The correlation between growth rate and the 16S rRNA:16S rDNA ratio using ACP was first validated using a pure culture growth experiment. ACP was also used to identify the two species of a binary culture and to evaluate their activity level through a controlled stress event. ACP offers an important step forward in gaining a better understanding of complex microbial communities.

7.2 Introduction

Culture-based microbiological methods of studying microbial communities have several limitations. Current estimates of the proportion of species that can be cultured are 0.1-1% (Donachie, Foster et al. 2007), which severely limits the number of species that can be analyzed with culture-based methods. The time required for isolation and growth of culturable species also hinders throughput. Because of these limitations, culture-based methods are not sufficient when characterizing the structure of complex microbial communities, and are especially lacking when following the dynamics of the community through some event of interest.

Culture-independent methods, those which employ the direct extraction of nucleic acids from a community, circumvent the requirement of growing cultures in the lab. The extracted nucleic acids can be amplified via polymerase chain reaction (PCR) to provide sufficient DNA copies for downstream analysis. The most common PCR target has been the 16S gene, which offers conserved regions that allow for broad, kingdom-level amplification and variable regions that allow for species-level identification (Woese, Fox et al. 1975). Thus, these PCR-based approaches targeting the 16S gene can, in principle, overcome the challenge of accessing the entire microbial community. However, once amplified, the pool of 16S genes must still be separated to obtain the desired species-level information about the community. A common separation approach is to develop a clone library of the amplified community 16S genes (Pace, Stahl et al. 1985; Pace 1997). Although cloning can provide quantitative species identification and abundance, the approach can be costly and time consuming, and thus is still throughput limited. Another tactic for separating the pool of 16S gene PCR products is through the use of electrophoresis. These so-called fingerprinting methods include denaturing gel electrophoresis (DGGE) (Muyzer, Dewaal et al. 1993) and terminal restriction fragment length polymorphism (T-RFLP) (Liu, Marsh et al. 1997). By analyzing the mixed PCR product directly, throughput can be dramatically increased with these methods. Also, the fingerprints obtained provide a visual representation of the microbial composition that is convenient for side-by side comparison of multiple communities.

While overcoming the shortcomings of culture-base methods, these current community profiling techniques still fail to distinguish active from inactive members of a mixed community as they target only the 16S rDNA. The amplification of a specific species from community DNA can only verify that the species is present; the DNA of sporulated and dead species will be amplified along with that of viable cells. The DNA of lysed cells can also persist in the environment for extended periods of time (England, Holmes et al. 1998) and can later be amplified via PCR, thus contributing to the perceived community structure.

A correlation between RNA and the growth rate in pure cultures has been well documented (Ingraham, Maaloe et al. 1983; Benthin, Nielsen et al. 1991), and the cellular ratio of total RNA to DNA is known to be proportional to growth rate in a variety of organisms (Kjeldgaard and Kurland 1963; Dortch, Roberts et al. 1983). It has also been documented that while the total RNA tends to fluctuate depending on the growth rate of the cell, the amount of DNA in a cell remains relatively stable (Muttray and Mohn 2000). Several studies examining the relative amounts of RNA and DNA in various systems demonstrated that the presence of a microbial species (DNA) does not necessarily correlate to that species activity (RNA) in the system. Duthoit et al. (2005) found discrepancies between 16S RNA and DNA content of Salers cheese during the ripening process using CE-SSCP, while Moeseneder et al. (2005), using clone libraries, found α-proteobacteria to be dominant in terms of 16S DNA content and δ-proteobacteria to be dominant in terms of 16S RNA content from a marine bacterioplankton community. Using Q-PCR, Ka et al. (Ka 2001) demonstrated that the total population (16S rDNA) of a microbial community of a fuel-contaminated soil remained nearly constant while the overall metabolic activity (16S rRNA) increased substantially as a result of biostimulation.

The newly developed technique of active community profiling (ACP) takes advantage of the relationship between RNA (variable) and DNA (stable) to determine which members of a mixed culture are actively growing and which microorganisms are relatively inactive. The relative amounts of each can also be tracked over time to determine how the activities of community members change in response to environmental factors. ACP involves monitoring the composition and activity of a mixed microbial culture via comparative measurements of 16S rRNA and rDNA using capillary electrophoresis single-strand conformational polymorphism (CE-SSCP). The use of CE-SSCP for the separation of short nucleic acid fragments (~200 bp) has gained acceptance as a community profiling technique (Dabert, Fleura-Lessard et al. 2001; King, McCord et al. 2005; Zinger, Gury et al. 2007), and is considered a high-throughput method with improved resolution compared to DGGE (Hong, Pruden et al. 2007). CE-SSCP involves denaturing of double-stranded PCR products that are rapidly cooled to form unique single-stranded conformations based on their nucleic acid sequences. Capillary electrophoresis is then used to separate the conformations based on electrophoretic mobility, resulting in an electropherogram with a series of peaks representing dominant members of the microbial community. Species identification is then determined by comparing the electrophoretic mobilities of individuals from a clone library to the individual peaks of the community profile.

In this study, a pure culture chemostat growth experiment is presented in which ACP is used to characterize the correlation between growth rate and the 16S rRNA:16S rDNA ratio. The ability of ACP to differentiate between multiple species of a mixed culture is also demonstrated using a simple binary culture. In addition, the relative activity levels of the two species are tracked through a change from aerobic to anaerobic growth conditions. ACP offers an important step forward in gaining a better understanding of complex microbial communities, and this study validates ACP as a method capable of identifying and tracking the active members of mixed cultures.

7.3 Materials and Methods

7.3.1 Strains

Pure cultures of a *Escherichia coli* K12 variant (ATCC # 700926) and *Pseudomonas putida* F1 (ATCC # 700007) were used, with freezer stocks of each culture maintained at -80 °C. Overnight cultures grown on M9 minimal salts medium (BD Difco, Sparks, Maryland) were used for chemostat inoculation.

7.3.2 Chemostat Operation

A pure culture of *E. coli* was grown aerobically on M9 minimal salts medium (BD Difco) with 4.01 g/L glucose as the sole carbon source. Cultures were maintained in a New

Brunswick BioFlow III fermenter (Edison, NJ) at 37 °C and an agitation speed of 500 rpm. The pH was maintained at 6.8 +/- 0.2 by addition of 1 M NaOH or 1 M HCl, and dissolved oxygen levels kept at or above 50% by air sparging. The culture growth rate, μ, was calculated based on the chemostat dilution rate, which was varied from 0.25 to 1.0/h, by changing the medium feed rate. The reactor volume was maintained at 1 L.

A binary culture of *E. coli* and *Pseudomonas putida* F1 was grown using the same experimental system described above. Temperature was maintained at 30 °C with a growth rate of μ = 0.25/h. After reaching steady-state, as determined by OD_{600} measurements, samples were obtained and the chemostat was switched to anaerobic conditions by sparging the fermentation vessel and the feed medium with UHP nitrogen, and by the addition of a reducing agent, sterile L-cysteine*HCl (50 mg/L), to the feed medium. Samples were obtained after 2 and 5 h of anaerobic operation.

All samples were aseptically removed from the fermentation vessel using a sterile syringe, immediately divided into 1.8 mL aliquots, and snap frozen in liquid nitrogen. Samples were stored at -80 °C until further analysis.

7.3.3 Nucleic Acid Extractions and Treatment

DNA extraction was carried out using the UltraClean Microbial Isolation Kit (MoBIO, Carlsbad, CA) according to the manufacturer's protocol using 1.5 mL of liquid culture. A small portion of the extracted genomic DNA was treated for RNA contamination with RNase ONE Ribonuclease (Promega, Madison, WI). For each extract, 4 µL of genomic DNA was mixed with 4 µL of the RNase, 1 uL of nuclease free water, and 1 µL of 10X reaction buffer and incubated for 45 min at 37 °C.

RNA extraction was carried out using the RNeasy Mini Kit (Qiagen, Valencia, CA) according to the manufacturer's protocol using 1.5 mL of liquid culture. A small portion of the extracted total RNA was treated with RQ1 RNase-Free DNase (Promega, Madison, WI) for DNA contamination. For each extract, 4 μL of total RNA was mixed with 4 μL of the DNase, 1 μL of nuclease free water, and 1 μL of 10X reaction buffer and incubated for 30 min at 37 °C. After incubation, each reaction received 1 μL of DNase stop solution and was incubated for an additional 10 min at 65 °C to destroy the enzyme.

This DNase-treated RNA was reverse transcribed using AMV Reverse Transcriptase (Promega, Madison, WI). Each reaction received 3 μL of the treated RNA, 2 μL of nuclease free water, and 1 μL of the W104r (5 mM) (Brosius, Dull et al. 1981) labeled with the 5`-6FAM fluorescien (Applied Biosystems, Foster, CA) ([6FAM]-5`-TTA CCG CGG CTG GCT GGCAC-3`). The mixture was incubated at 70 °C for 5 minutes for primer annealing, followed by 5 min at 4 °C, and the 6 μL was added to the reverse transcription mix that included: 5 μL of 5X reaction buffer, 2.5 μL of dNTPs (10 uM), 2.5 μL of $Na_4P_2O_7^+$ (40 mM, at 42 °C), 7.5 μL nuclease free water, and 1.5 μL of reverse transcriptase. The solution was incubated at 50 °C for 60 min for first strand cDNA synthesis.

The treated DNA and reverse transcription product were PCR amplified targeting the highly variable V3 region of the 16S rRNA gene using primers W49f (5'- ACG GTC CAG ACT CCT ACG GG) (Brosius, Dull et al. 1981) and W104r. Each 20 μL reaction included: 12.4 μL sterile deionized water, 2.0 μL 10X *Pfu* Turbo Buffer (Stratagene, La Jolla, CA), 0.4 μL dNTP mix (10 mM, 5 Prime, Gaithersburg, MD), 2.0 μL W49f (5 uM), 2.0 μL W104r (5 uM), and 0.2 μL *Pfu Turbo®* DNA polymerase (2.5 U/ μL, Stratagene). The thermal cycling program for the PCR consisted of an initial denaturation step of 94 °C for 2 min, followed by 25 cycles of 30 sec at 94 °C, 30 sec at 61 °C, and 30 sec at 72 °C, and concluded with a final elongation period of 10 min at 72 °C. Thermal cycling was performed on an Eppendorf Mastercycler Gradient (Westbury, NY), and PCR products were verified using 1.2 wt% agarose gels.

7.3.4 CE-SSCP

For each CE-SSCP reaction, 1 μL of PCR product was added to a mixture of 18.8 μL of HiDi formamide (Applied Biosystems) and 0.2 μL ROX™ 400 (Applied Biosystems). The formamide aids in denaturation and the ROX was used as an internal standard for data alignment and normalization. The reaction mixture was heat denatured at 95 °C for 5 min in a thermal cycler, then immediately place in an ice bath for 15 min to form single-stranded conformations.

Capillary electrophoresis was performed with a Genetic Analyzer 310 with a 47 cm x 50 um ID capillary and 5.6% GeneScan polymer (Applied Biosystems, Foster City, CA). Electrophoresis run conditions were performed at 12 kV for 32 minutes at 32 °C (Hong, Pruden et al. 2007). GeneMapper 3.2 software (Applied Biosystems) (Chackhiani, Dabert et al. 2004) was used to align the electropherograms from all samples and for peak integrations. Peak areas were normalized to the ROX 220 bp peak of each run to correct for injection variation.

7.4 Results and Discussion

7.4.1 Single Species Growth

A clear correlation between growth rate and the ratio of 16S rRNA to 16S rDNA was obtained with the pure culture of *E. coli*, as determined by ACP (Figure 7.1). As expected, the ratio increased with increasing growth rate, in agreement with the trend obtained by Dortch *et al.* (1983) for several organisms. Although the ratio values of 0.15 to 2.06 for μ = 0.25 to 1.0/h, respectively, are lower than the 4 to 7.5 reported by of Dortch *et al.* (1983) for the same growth rates and *E. coli* strain, the differences can be attributed to the minimal growth medium used in this study. This pure culture experiment offers proof of concept that ACP can be used to differentiate the growth rate, and thus overall activity, of a single species.

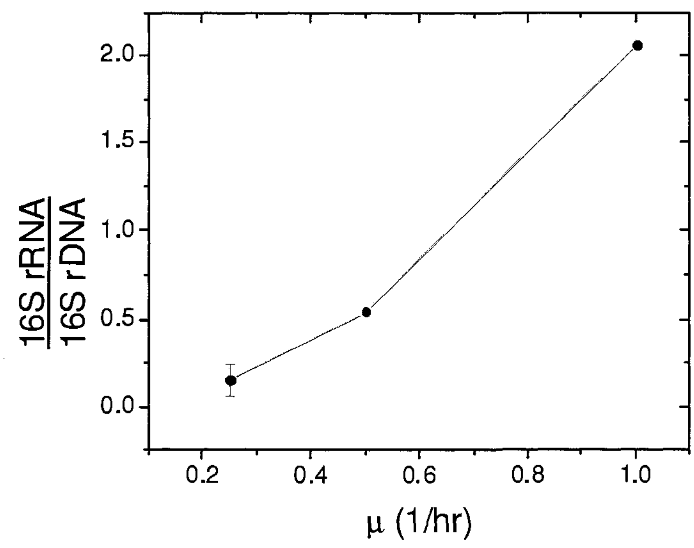

Figure 7.1 – The ratio of 16S rRNA to 16S rDNA as a function of growth rate, as determined by ACP, for a pure culture of *E. coli* grown on M9 minimal salts medium. Error bars represent the standard deviation of duplicate growth experiments and triplicate nucleic acid extractions for the same condition.

7.4.2 Binary Culture Growth

In the binary culture growth experiment, the two species were easily distinguishable form one another using CE (Figure 7.2). The 16S rRNA to 16S rDNA ratio of *P. putida* decreased dramatically when the growth conditions were changed from aerobic to anaerobic. The ratio was maintained at near zero levels through 5 hours of anaerobic operation (Figure 7.3). *P. putida* behaved as would be expected for an obligate aerobe, growing rapidly under optimal, aerobic conditions but exhibiting little or no growth under anaerobic conditions.

The *E. coli* 16S rRNA to 16S rDNA ratio followed an inverse trend compared to the *P. putida*, gradually increasing with time after oxygen was removed from the system. The lower ratio under aerobic conditions can be attributed to the growth temperature (30 °C) and to competition between *E. coli* and *P. putida* for the limited resources of the minimal medium. The influence of competition between the two is further validated by the increased 16S rRNA/16S rDNA ratio of the *E. coli*, a facultative aerobe, once the *P. putida* is inhibited by the lack of oxygen.

It is important to note that a 16S rDNA PCR product was obtained for *P. putida* at both time points under anaerobic growth. Thus, had only a traditional DNA-based profiling technique been used instead of ACP, the conclusion that would have been drawn was that both species were present during both aerobic and anaerobic growth. Under a simple binary culture, the inaccuracy of that conclusion is apparent, but in the case of an unknown complex community the interpretation may not be as clear.

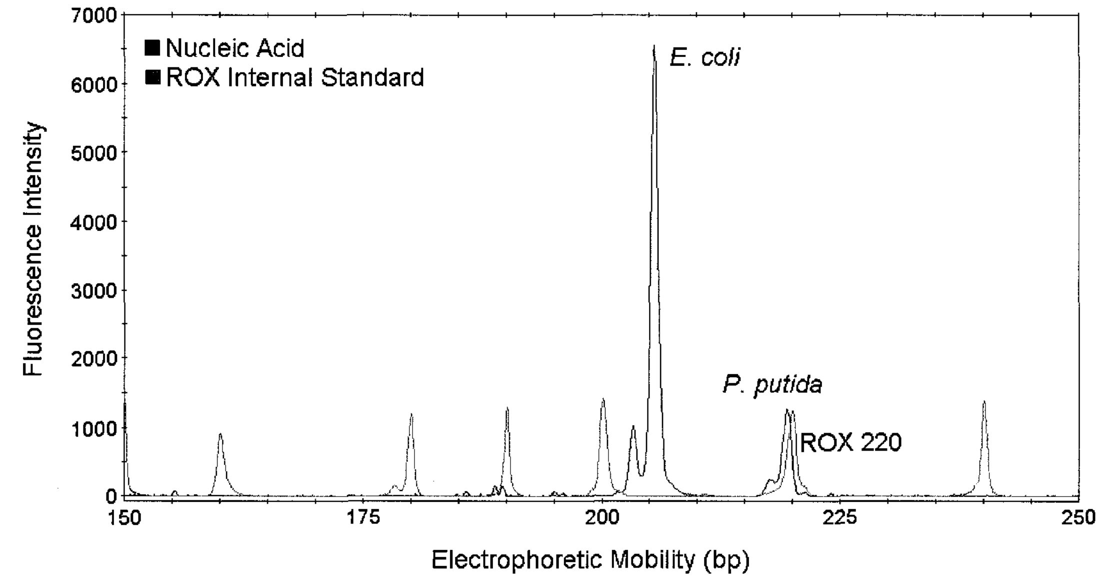

Figure 7.2 – Representative electropherogram of the *E. coli* and *P. putida* binary culture (16S rDNA after 5 h of anaerobic growth). The two species are easily distinguished in the nucleic acid trace (blue). The ROX internal standard trace (red) is used for sample alignment, and the indicated 220 bp ROX peak is used to normalize all peaks.

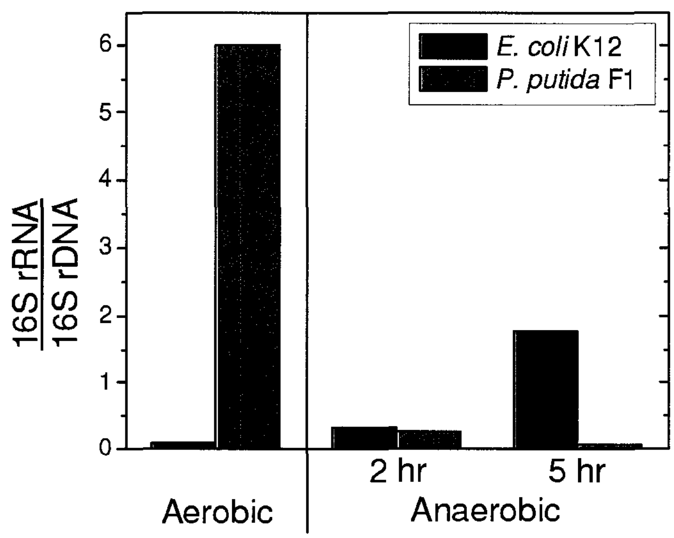

Figure 7.3 – The ratio of 16S rRNA to 16S rDNA as a function of growth rate for a binary culture of *E. coli* and *P. putida* grown on M9 minimal salts medium under aerobic and anaerobic growth conditions.

7.5 Conclusion

This study provides validation for the use of ACP as a tool to characterize the active members of mixed microbial cultures, an important advance over standard 16S rDNA community profiling techniques. The differences observed between standard 16S rDNA profiling and the newly developed rRNA-based ACP indicate that conclusions based on DNA measurements alone may not accurately represent the microbial community. Although further application of the method to more complex communities is still necessary to verify the robustness of the technique, by identifying the active species, ACP is an important step forward in gaining a deeper understanding of complex microbial communities.

7.6 Acknowledgements

Financial support for this work provided by the EPA Office of Research and Development Engineering Technical Support Center (Contract #68-C-00-136; David Reisman, Project Officer), NSF Award # 0651947, and the Rocky Mountain Hazardous Substance Research Center through the EPA Science to Achieve Results (STAR) program (Contract # R 8395101-0). The authors would also like to thank the technical assistance of Rachel E Hanson and Barbara Crimi with the capillary electrophoresis.

7.7 References

Benthin, S., J. Nielsen, et al. (1991). "A Simple and Reliable Method for the Determination of Cellular RNA Content." Biotechnology Techniques **5**(1): 39-42.

Brosius, J., T. J. Dull, et al. (1981). "Gene Organization and Primary Structure of a Ribosomal-RNA Operon from Escherichia-Coli." Journal of Molecular Biology **148**(2): 107-127.

Chackhiani, M., P. Dabert, et al. (2004). "16S rDNA characterization of bacterial and archaeal communities during start-up of anaerobic thermophilic digestion of cattle manure." Bioresource Technology **93**(3): 227-232.

Dabert, P., A. Fleura-Lessard, et al. (2001). "Monitoring of the Microbial Community of a Sequencing Batch Reactor Bioaugmented to Improve its Phosphorus Removal Capabilities." Water Science and Technology **43**(3): 1-8.

Donachie, S. P., J. S. Foster, et al. (2007). "Culture clash: challenging the dogma of microbial diversity - Commentaries." ISME Journal **1**(2): 97-99.

Dortch, Q., T. L. Roberts, et al. (1983). "Rna DNA Ratios and DNA Concentrations as Indicators of Growth-Rate and Biomass in Planktonic Marine Organisms." Marine Ecology-Progress Series **13**(1): 61-71.

Duthoit, F., L. Tessier, et al. (2005). "Diversity, Dynamics and Activity of Bacterial Populations in 'Registered Designation of Origin' Salers Cheese by Single-Strand Conformation Polymorphism Analysis of 16S rRNA Genes." Journal of Applied Microbiology **98**(5): 1198-1208.

England, L. S., S. B. Holmes, et al. (1998). "Persistence of viruses and DNA in soil." World Journal of Microbiology & Biotechnology **14**(2): 163-169.

Hong, H., A. Pruden, et al. (2007). "Comparison of CE-SSCP and DGGE for monitoring a complex microbial community remediating mine drainage." Journal of Microbiological Methods **69**(1): 52-64.

Ingraham, J. L., O. Maaloe, et al. (1983). Growth of the Bacterial Cell. Sunderland, MA, Sinauer Associates, Inc.

Ka, J. O., Z. Yu, and W.W. Mohn (2001). "Monitoring the Size and Metabolic Activity of the Bacterial Community during Biostimulation of Fuel-Contaminated Soil using Competitive PCR and RT-PCR." Microbial Ecology **42**: 267-273.

King, S., B. R. McCord, et al. (2005). "Capillary Electrophoresis Single-Strand Conformation Polymorphism Analysis for Monitoring Soil Bacteria." Journal of Microbiological Methods **60**(1): 83-92.

Kjeldgaard, N. O. and C. G. Kurland (1963). "Distribution of Soluble and Ribosomal Rna as a Function of Growth Rate." Journal of Molecular Biology **6**(4): 341-&.

Liu, W. T., T. L. Marsh, et al. (1997). "Characterization of microbial diversity by determining terminal restriction fragment length polymorphisms of genes encoding 16S rRNA." Applied and Environmental Microbiology **63**(11): 4516-4522.

Moeseneder, M. M., J. M. Arrieta, et al. (2005). "A Comparison of DNA- and RNA-Based Clone Libraries from the Same Marine Bacterioplankton Community." FEMS Microbiology Ecology **51**(3): 341-352.

Muttray, A. F. and W. W. Mohn (2000). "Quantitation of the Population Size and Metabolic Activity of a Resin Acid Degrading Bacterium in Activated Sludge Using Slot-Blot Hybridization to Measure the rRNA:rDNA Ratio." Microbial Ecology **38**: 348-357.

Muyzer, G., E. C. Dewaal, et al. (1993). "Profiling of Complex Microbial-Populations by Denaturing Gradient Gel-Electrophoresis Analysis of Polymerase Chain Reaction-Amplified Genes-Coding for 16s Ribosomal-Rna." Applied and Environmental Microbiology **59**(3): 695-700.

Pace, N. R. (1997). "A molecular view of microbial diversity and the biosphere." Science **276**(5313): 734-740.

Pace, N. R., D. A. Stahl, et al. (1985). "Analyzing Natural Microbial Populations by rRNA Sequences." American Society for Microbiology News **51**: 4-12.

Woese, C. R., G. E. Fox, et al. (1975). "Conservation of Primary Structure in 16s Ribosomal-Rna." Nature **254**(5495): 83-86.

Zinger, L., J. Gury, et al. (2007). "Improvements of polymerase chain reaction and capillary electrophoresis single-strand conformation polymorphism methods in microbial ecology: Toward a high-throughput method for microbial diversity studies in soil." Microbial Ecology **54**(2): 203-216.

Chapter 8 Tracking the Effects of Bioaugmentation and Biostimulation on a Mixed Microbial Community Treating Mine Drainage using Active Community Profiling

Hiibel, S.R., Pereyra, L.P., Perrault, E.M., Pruden, A., and Reardon, K.F.
(*in preparation for submission to* Microbial Ecology)

Approximate contributions of each author are as follows:

SR Hiibel performed 45% of experimental setup, 40% of sample collection, 100% of sulfate analysis, 5% of the metals and pH analysis, 100% of the DNA treatment, 100% of RNA extraction and treatment, 100% of ACP, and 100% of the manuscript preparation.

LP Pereyra performed 45% of experimental setup, 40% of sample collection, 50% of metals and pH analysis, and 50% of DNA extraction.

EM Perrault performed 10% of the experimental setup, 20% of sample collection, and 45% of the metals and pH analysis.

A Pruden and KF Reardon assisted with experimental design and manuscript preparation.

8.1 Abstract

The effects of bioaugmentation and biostimulation on the performance of microbial communities of sulfate-reducing bioreactors treating acid mine drainage (AMD) were evaluated using active community profiling (ACP). Column bioreactors were bioaugmented with either cellulose degraders or sulfate reducers and were biostimulated with either carboxymethyl cellulose or ethanol. The remediation performance was based on sulfate and metals removal and pH. Despite the differences in the microbial species and carbon sources added, all of the columns performed similarly from a remediation perspective, including the uninoculated control columns. However, based on ACP analysis the active members of the microbial communities of the columns were distinctly different. The diversity and number of active species in the columns augmented with

cellulose degraders and stimulated with carboxymethyl cellulose were much greater after six weeks of operation than in the starting communities. The opposite trend was observed in columns stimulated with sulfate reducers, where the number of active species in the starting community was much larger than at the end of the experiment. These results demonstrate that targeting the top level of the ecological carbon chain via either biostimulation or bioaugmentation can increase the activity of a larger portion of the microbial community than can be achieved by targeting the lower levels of the carbon chain. ACP analysis also indicated that the majority of the species bioaugmented into the columns flourished and were dominant members of the active community after six weeks, verifying the survival of the augmented species. This is the first systematic examination of the relationships between bioreactor remediation performance, the active microbial community, and the parallel use of bioaugmentation and biostimulation in AMD bioremediation systems.

8.2 Introduction

The concepts of bioaugmentation and biostimulation have been in practice for centuries in agriculture. Farmers have long known the benefits that fertilizers and soil amendments can have on crop health and yields. Nitrogen, phosphorus, and potassium (NPK) have been used extensively in the US since the early 1900's (Engelstad and Terman 1966), and it has been estimated that the application of these chemical fertilizers has improved crop yields by as much as 50% in the 20th century (Fageria, Baligar et al. 2008). Because P and K tend to accumulate in soils and N does not, nitrogen is often considered the limiting nutrient. Nature has developed mechanisms for the cycling of nitrogen into soils via nitrogen-fixing microorganisms, such as *Rhizosphere* spp. and *Frankia* spp., that are associated with the soils of plant root systems (van Veen, van Overbeek et al. 1997). Man has successfully employed the approach of nature to croplands with low or no levels of native populations of nitrogen-fixing bacteria by artificially introducing species with this ability, either in a targeted fashion via direct inoculation or as an inadvertent benefit of simple soil mixing.

More recently, the concepts of bioaugmentation and biostimulation have been applied for remediation purposes. Rather than stimulating plant growth and improving crop yields, as is the case in an agricultural context, the techniques aim to degrade or mineralize contaminants in the environment. In cases of biostimulation, nutrients are added to simulate growth of the microorganisms present in the system that are responsible for or involved in the remediation process of interest. In cases of bioaugmentation, species known to interact in a beneficial way with the contaminant of interest are applied to the impacted area. Perhaps the most well known, and most successful, case of bioaugmentation for remediation purposes involves *Dehalococcoides* spp. that are capable of degrading chlorinated solvents, such as tetrachloroethene (PCE), to ethane (MaymoGatell, Chien et al. 1997; Flynn, Loffler et al. 2000; Loffler, Sun et al. 2000; Lendvay, Loffler et al. 2003). Other groups have successfully used bioaugmentation to treat sties contaminated with BTEX (Da Silva and Alvarez 2004) and atrazine (Rousseaux, Hartmann et al. 2003), while Smith et al. (2005) used a combination of biostimulation and bioaugmentation for MTBE remediation.

Unfortunately the techniques do not always work as designed. Bouchez et al. (2000) twice attempted bioaugmentation of a nitrifying reactor with the aerobic denitrifying bacterium *Microvirgula aerodenitrificans* with no observed nitrogen removal. An overgrowth of protozoa and corresponding disappearance of free living bacteria was observed, and it was determined that the *M. aerodenitrificans* were acting as a food source for the protozoa rather than improving denitrification. Along with becoming a natural predator's prey, bioaugmented species must overcome many obstacles before thriving, and ultimately performing the function of interest, in a new environment. Many species die because of environmental incompatibility, while others fail to thrive due to limited nutrients, direct competition, or any number of other challenges (El Fantroussi and Agathos 2005).

The bioremediation of acid mine drainage (AMD) offers a unique opportunity to study the community level effect of bioaugmentation and biostimulation. AMD is formed by the oxidation of mineral surfaces exposed during mining activities and is characterized by elevated levels of acidity, sulfates, and heavy metals (1996; Benner, Blowes et al. 1997; 1998). AMD is a significant environmental problem in around the world. In the U.S. alone, the total estimated remediation costs for abandoned mine sites ranges from $32 to $72 billion (EPA 2005), and a recent Mining Policy Center report (Lyon, Hilliard et al. 1993) estimated 12,000 miles of waterways and 180,000 acres of lakes and reservoirs were contaminated by AMD. The biological treatment of AMD can be performed by sulfate-reducing bacteria (SRB) that couple the oxidation of small organic molecules with the reduction of sulfate present in the drainage to produce hydrogen sulfide and bicarbonate. The sulfides bind the heavy metals present in the AMD and precipitate as stable metal sulfides and the bicarbonate buffers the acidity (Singer and Stumm 1970).

A common bioremediation approach to AMD is through the use of sulfate-reducing bioreactors that are comprised of an organic substrate, typically wood chips or a compost-based material, and a complex microbial community that is responsible for remediation. This community includes cellulose-degrading species, fermentative species, and SRB, with the first two groups metabolizing the organic substrate into the small organic molecules used by the latter (Logan, Reardon et al. 2005; Pruden, Messner et al. 2007; Hiibel, Pereyra et al. 2008; Pereyra, Hiibel et al. 2008). The multi-leveled structure of the microbial community offers a variety of targets for biostimulation and bioaugmentation strategies to be employed.

Past biostimulation efforts have been aimed at increasing the SRB activity of the bioreactors by adding carbon sources such as methanol (Tsukamoto and Miller 1999), ethanol (Chapter 5), and lactate (Jong and Parry 2006). In all cases, SRB activity and/or AMD remediation was observed, but in each of these cases, the added electron donor was the sole carbon source for the microbial community rather than an additional, 'stimulating' nutrient. Bench-scale studies of bioaugmentation have demonstrated that inoculating a bioreactor treating AMD with SRB shortened the initial lag phase, but that overall remediation performance was not improved (Christensen, Laake et al. 1996).

This research explores the effects of bioaugmentation and biostimulation, at the top and bottom of the carbon chain, on the microbial community of sulfate-reducing bioreactors treating AMD. Cellulose-degrading bacteria and soluble cellulose were added to column bioreactors to target the top of the carbon chain; SRB and ethanol were added to columns to target the bottom of the carbon chain. The remediation performance and the microbial communities of the bioreactors were monitored over a six week period.

Active community profiling (ACP), a technique that allows for the identification of microbial species present and differentiates between metabolically active and dormant species (Chapter 7), was used to evaluate the community structure of each column. The study evaluates the feasibility of biostimulation and bioaugmentation as remediation enhancing methods for AMD.

8.3 Materials and Methods

8.3.1 Column Specifications

Twelve Schedule 40 transparent PVC columns, 10.2 cm ID x 40.5 cm operating height, were operated vertically with upward flow at an average rate of 250 mL/day and a 4.4-d hydraulic residence time. The top of each column was sealed using a monitoring well plug (Cherne Industries, Minneapolis, MN), and the bottom was cemented into a PVC flange and bolted onto an acrylic sheet to seal the column. The bottom ~12 cm and top ~4 cm of each column were filled with 1.75 kg and 0.462 kg, of clean pea gravel (0.131 – 0.187"), respectively. The influent port was located 10 cm from the column bottom and the effluent port 2 cm from the top of the column's working space. Each column also had five ¼" sampling ports, spaced 5 cm apart and starting 15 cm from the bottom of the column. The column setup is shown schematically in Figure 8.1.

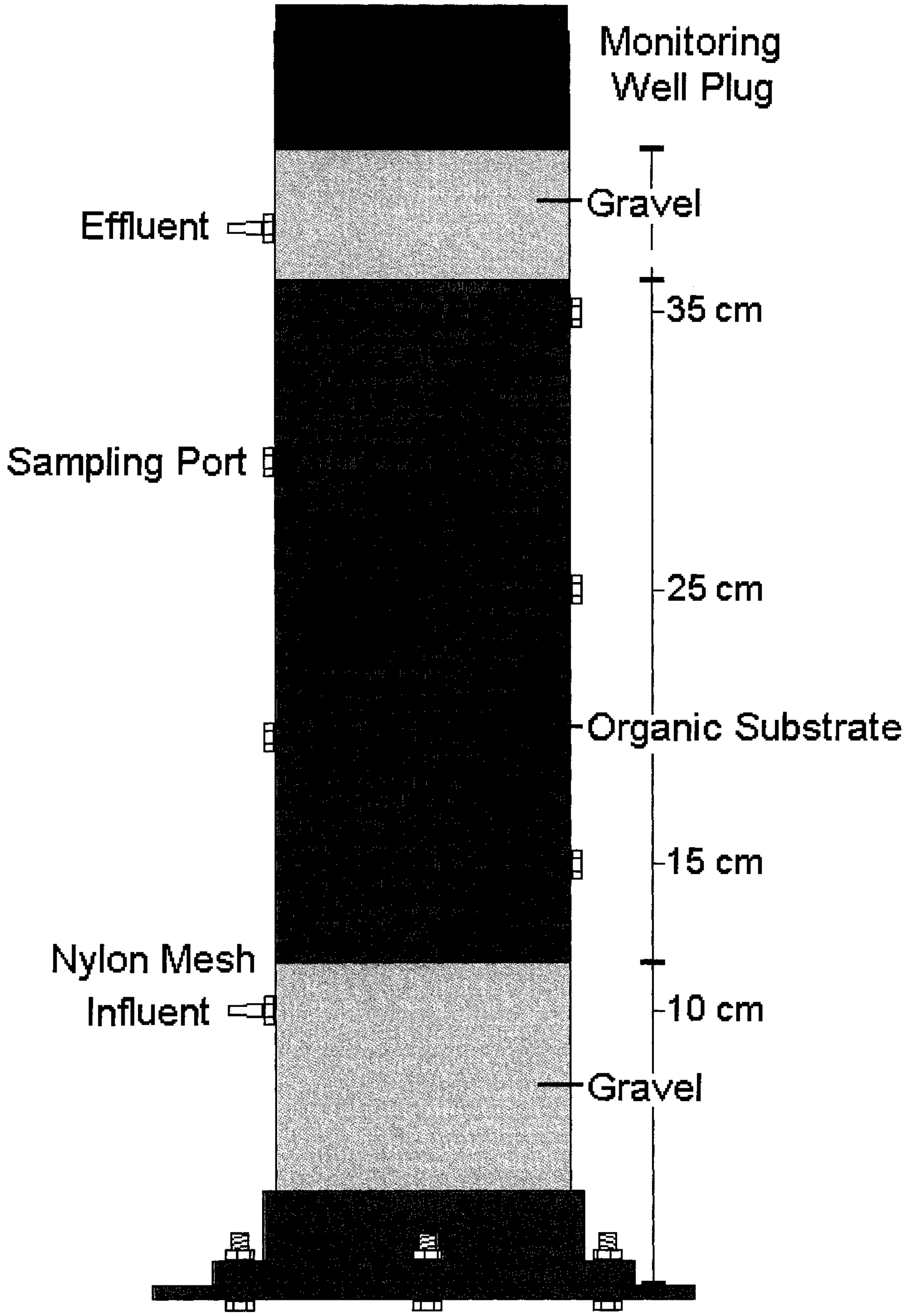

Figure 8.1 – Schematic of column setup.

The twelve columns consisted of six duplicates based on the inoculum (bioaugmented) and/or carbon source (biostimulated) that each received (

Table 8.1). The DM columns were inoculated only with the dairy manure slurry. The biostimulated columns were also inoculated only with the dairy manure slurry but were fed additional carbon sources throughout the experiment. These columns were designated as EtOH (amended with ethanol) and CMC (amended with soluble carboxymethyl cellulose). The bioaugmented columns designated SRB were inoculated with the dairy manure slurry as well as an enriched mixed culture of sulfate reducers. The bioaugmented columns designated CD were inoculated with dairy manure slurry, three pure cultures of cellulose-degrading species, and an enriched mixed culture of cellulose degraders. The control columns were not directly inoculated but were also not sterilized, thus any microorganisms associated with the dry materials used as column packing were present. Specifics of source and growth of the inocula cultures are given below.

8.3.2 Simulated Acid Mine Drainage

The simulated AMD was prepared using Nanopure deionized water (Barnstead, Dubuque, IA) and contained of 1.32 g/L Na_2SO_4, 0.03 g/L NH_4Cl, 0.089 g/L $ZnSO_4{\cdot}7H_2O$, 0.01 g/L $CdCl_2$, and $9.15x10^{-4}$ g/L $FeSO4{\cdot}7H_2O$; all reagents were analytical grade. A common tank fed ten of the twelve columns, while a separate feed tank was used for the columns biostimulated with carboxymethyl cellulose (CMC) because the CMC could not be injected directly into the feed lines due to its high viscosity. All feed solutions were adjusted to pH 5.5 and delivered to the columns via peristaltic pumps (Isamatec, Glattbrugg, Switzerland). The feed solutions were maintained anaerobic by continuously bubbling nitrogen in the feed tank.

Table 8.1 – Column designations and description of the bioaugmentation species and biostimulation sources applied.

Column Designation	Base Inoculum	Bioaumentation Species	Biostimulation Source
Control	none	none	none
DM	dairy manure	none	none
CD	dairy manure	cellulose degraders	none
SRB	dairy manure	sulfate reducers	none
CMC	dairy manure	none	carboxymethyl cellulose
EtOH	dairy manure	none	ethanol

[a] Pure cultures used for bioaugmentation
[b] Enrichment cultures used for bioaugmentation

The CMC feed also included 0.507 g/L CMC, which corresponds to the equivalents required to reduce 50% of the sulfate based on the efficiencies described by Badger (2002). The two columns biostimulated with ethanol were fed 2.8 uL/h 100% ethanol (Aaper Alcohol, Shelbyville, Kentucky), also corresponding to the equivalents required to reduce 50% of the feed sulfate. The ethanol was delivered via a syringe pump (kd Scientific, Holliston, MA) injected into the feed line between the peristaltic pump and the columns.

8.3.3 Column and Effluent Sampling

Liquid exited the columns from the top effluent port into Nalgene bottles via ¼" ID vinyl tubing connected to an 18G needle; the needle tip was maintained under the liquid level to prevent the backflow of oxygen into the column. Liquid samples were collected in acid washed, anaerobically sealed serum bottles using the same vinyl tubing and needle apparatus. To prevent oxygen backflow during sampling, a three-way valve was placed inline between the effluent port and the needle, with flow to the needle stopped temporarily while transferring the needle to the serum bottles. The samples were stored anaerobically sealed at 4 °C prior to chemical analysis to prevent oxidation of sulfides present.

8.3.4 Chemical Analyses

Sulfates were quantified by ion chromatography (IC) using a Metrohm 861 Advanced Compact IC with MSM and CO2 Suppressor and a 250 mm Metrospec A Supp 5 High Resolution Anion Column (Houston, TX). The IC NET Chromatography Control and Data Acquisition System was used to calibrate the instrument and to collect and analyze chromatograms. Effluent samples were diluted 1:10 with deionized water to achieve a concentration within the detection range of 1-100 mg/L. Diluted samples were filtered via an inline filter. A four-point calibration curve (5, 10, 50, and 100 mg/L) was prepared in house via dilution from a 1000 g/L stock solution. Fresh standards were prepared for each analysis set, with one prepared in triplicate for use as a quality control.

Total sulfur and metals were analyzed using inductively coupled plasma absorbance emission spectroscopy (ICP-AES) (Thermo Jarrell Ash IRIS Advantage) following US EPA Method 3015 (1994), as described by Pereyra et al. (2008). Samples were digested according to EPA Method 3015 (1994) prior to analysis. Detection limits were 0.01 mg/L for zinc, 0.005 mg/L for cadmium, and 0.01 mg/L for iron.

The pH was measured with an Accumet® AB15 Basic pH meter (Fisher Scientific, Pittsburgh, PA) immediately upon opening the anaerobically stored samples.

8.3.5 Inocula

8.3.5.1 Anaerobic Cellulose-Degrading Enrichment Culture

A mixed culture was enriched for anaerobic cellulose degraders. The initial inoculum consisted of ~50 g fresh sheep manure and ~70 g of sediment collected from the Cache la Poudre River in Fort Collins, CO, and slurried with 500 mL of sterile DI water. Six replicate serum bottle (60 mL) enrichments were prepared anaerobically with 50 mL of the slurry, 5 g/L crystalline cellulose (J.T. Baker, Phillipsburg, NJ), 2.5 g/L 2-bromoethane sulfonic acid (BESA) to inhibit methanogenic activity (Cabirol, Perrier et al. 1995), and 1.4 g/L sodium molybdate to inhibit SRB activity (Yadav and Archer 1989). The enrichments were maintained at 37 °C at 100 RPM for eight days and subsequently transferred and maintained anaerobically as described in Table 8.2. After 16 days of cultivation and two transfers, solid cellulosic material in the form of 12 g/L of beechwood (<0.841 mm), 5 g/L of pine shavings (0.074 – 2.362 mm) was also included to encourage adaptation to more complex lignocellulose-based carbon sources. M9 minimal salts medium (Fisher Scientific) was substituted for anaerobic cellulolytic medium (ACM) (Atlas 1997) at Day 32 to ensure that adequate growth factors were present for the cellulose degraders. For the final transfer (Day 74), 125 mL serum bottles were used to increase the volume available for column inoculation. Visual degradation of the wood chips was observed beginning Day 60, indicating cellulose degradation was occurring.

Table 8.2 – Media and amendments used for the enrichment of a mixed cellulose-degrading culture.

Day	°C	RPM	Culture Transfer Volume, mL	Medium		Additions	
				Type*	mL	BESA and Na_2MoO_4	Beechwood & Pine Shavings
0	37	100	50	-	-	X	
8	37	100	25	M9	25	X	
16	30	100	4	M9	50	X	X
24	30	100	4	M9	50	X	X
32	20	100	4	ACM	50	X	X
60	20	100	1.25	ACM	25	X	X
74	20	100	8	ACM	100	X	X
102	20	100		*Harvested for Column Inoculation*			

* M9 - M9 minimal salts medium, ACM - Anaerobic Cellulolytic Medium

8.3.5.2 Anaerobic Cellulose-Degrading Pure Cultures

Three pure cultures of cellulose-degrading bacteria were also used for bioaugmentation: *Clostridium cellulovorans* (ATCC #35296), *Ruminococcus flavefaciens* (ATCC #4994), and *Fibrobacter succinogenes* (ATCC #51214). All three are known to be highly efficient anaerobic cellulose degraders (Cunningham, McPherson et al. 1991; Weimer and Odt 1995; Han, Yukawa et al. 2003). Cultures of all three species used as inocula were cultivated anaerobically overnight from freezer stocks with CMC as their sole carbon source prior to inoculating the columns.

8.3.5.3 Sulfate-Reducing Enrichment Culture

An SRB enrichment culture was developed using inoculum collected from an ethanol-fed sulfate-reducing bioreactor (SRBR) treating AMD at the National Tunnel site (see Chapter 5). The organic material obtained from the SRBR was anaerobically slurried with prior to inoculating the enrichment cultures. A modified Postgate C medium

(Postgate 1984) and ATCC Medium 1249 Modified Baar's medium was implemented as described in Table 8.3. Initially, 1.2 mL of the slurry was added to 25 mL of the mixed SRB culture medium anaerobically and maintained for 24 h at 20 °C and 100 RPM. Cultures (1.2 mL) were anaerobically transferred daily to 25 mL of medium for 48 days. Multiple transfers of 2.4 mL culture and 50 mL of medium were performed the day before column inoculation to ensure an adequate volume.

8.3.5.4 Inocula Preparation

Fresh dairy manure (DM) was collected from a local dairy near Fort Collins, CO and stored at 4 °C until use. A 2032.5 g portion of manure was slurried with 1098 mL sterile deionized water. This DM slurry was used as a baseline inoculum for all columns, except the uninoculated control columns. Inocula were prepared anaerobically using sterile 2 L Nalgene bottles. The same mass of DM slurry was added to each bottle, with a target biomass concentration of 1.0 x 10^9 cells/g substrate (dry weight) as determined by 16S Q-PCR. Additional inocula were added to the bioaugmented columns, with a target biomass concentration of an additional 1.0 x 10^9 cells/g substrate (2.0 x 10^9 cells/g total) in both columns. In the case of the CD columns, each of the three pure cultures contributed 1/3 of this biomass target. The biomass of the mixed culture cellulose-degrading enrichment culture was not quantified prior to inoculation, thus the total cell count of the inoculum used in the CD columns exceeded 2.0 x 10^9 cells/g.

Table 8.3 – Medium used for enrichment of sulfate-reducing bacteria.

Component I	
Magnesium sulfate (MgSO4), g	1.00
Sodium citrate dihydrate ($Na_3C_6H_5O_7$*$2H_2O$), g	2.85
Calcium sulfate dihyrdate ($CaSO_4$*$2H_2O$), g	0.63
Ammonium chloride (NH_4Cl), g	0.50
Cysteine ($C_3H_7NO_2S$), g	0.08
Resazurin (1 g/L), mL	0.25
Total volume (with deionized water), mL	200
Component II	
Dipotassium phosphate (K_2HPO_4), g	0.25
Total volume (with deionized water), mL	100
Component III	
60% sodium lactate syrup, mL	1.13
Yeast extract, g	0.50
Total volume (with deionized water), mL	200
Component IV	
Ferrous ammonium sulfate hexahydrate ($Fe(NH_{4})_2(SO_{4})_2$*$6H_2O$), g	0.67
Total volume (with deionized water), mL	10
Component V	
2-bromoethanesulfonic acid sodium salt (C2H4BrNaO3S), g	0.55
Total volume (with deionized water), mL	5
Adjust pH of Components I, II, and III to 7.5 (HCl or NaOH) and autoclave. Cap and seal components immediately after autoclaving. Filter sterilize Components IV and V before use.	
For ~100 mL of Medium	
Under an anaerobic atmosphere (3% H_2, 97% N_2)	
Component I, mL	40.0
Component II, mL	20.0
Component III, mL	40.0
Component IV, mL	2.0
Component V, mL	1.0
200 proof ethanol, mL	1.0
Inoculum	3-5 %

8.3.6 Column Preparation and Inoculation

Dry materials used as column packing were weighed aerobically, placed in Ziploc bags, then mixed and stored for 36 h in an anaerobic chamber under an atmosphere of 97% nitrogen and 3% hydrogen. The dry materials consisted of (per bag): 232 g beechwood (3.33 – 4.75 mm), 112 g pine shavings (3.33 – 4.75 mm), 17 g ground alfalfa, 51 g of limestone sand, and 454 g of playground sand. The dry materials were inoculated with

743 mL of liquid inoculum (Table 8.4), sealed and homogenized, then opened slightly to avoid gas build up and incubated for 24 h to enhance microbial attachment. Samples of the inoculated bags were collected as column starting materials in sterile 50 mL conical tubes, snap frozen in liquid nitrogen, and stored at -80 °C for biomolecular analyses. The total wet weight of each bag was adjusted to 1.4 kg, then double-sealed in an additional Ziploc bag and transferred immediately to a nitrogen-filled glove box for long term housing of the columns.

The columns were packed anaerobically by transferring ~ ½ of the Ziploc contents onto the bottom layer of gravel (separated by nylon mesh) and gently packing by tamping with a sterile Nalgene bottle bottom. The remaining ½ of the bag contents were added, the column material packed again, and then the top layer of gravel added, again separated by nylon mesh. The columns were saturated with simulated AMD at 8.5 mL/min and then allowed to equilibrate for 20 h with no flow. Thus, the inocula were provided ~45 h of total attachment time before being exposed to continuous flow. All columns were maintained covered with aluminum foil throughout operation to inhibit photolithotrophic bacterial growth (Waybrant, Ptacek et al. 2002).

Table 8.4 – Cultures used for column inoculation.

			Enrichment Cultues, mL		**Pure Cultures, mL		
Column	*DM Slurry, g	Sterile Deionized Water, mL	*Sulfate Reducers	Cellulose Degraders	*Clostridium celluvorans*	*Ruminococcus flavefaciens*	*Fibrobacter succinogenes*
Control #1	-	743	-	-	-	-	-
Control #2	-	743	-	-	-	-	-
DM #1	230	662	-	-	-	-	-
DM #2	230	662	-	-	-	-	-
EtOH #1	230	662	-	-	-	-	-
EtOH #2	230	662	-	-	-	-	-
CMC #1	230	662	-	-	-	-	-
CMC #2	230	662	-	-	-	-	-
SRB #1	230	628	34	-	-	-	-
SRB #2	230	628	34	-	-	-	-
CD #1	230	-	-	448	85	29	100
CD #2	230	-	-	448	85	29	100

* Target concentration of 1.0×10^9 cells/g substrate (dry weight)

** Target concentration of 3.33×10^8 cells/g substrate (dry weight)

8.3.7 Sampling for Biomolecular Analyses

Substrate samples for biomolecular analysis were collected aerobically from the top, middle, and bottom sampling port of each column. The liquid level in the column was allowed to drain from the bottom until the top sampling port became unsaturated. Drainage from the column was then stopped, and 3.0 g of packing material was extracted from the sampling port using sterile tweezers in a 50 mL conical and snap frozen in liquid nitrogen. The process was repeated for the middle and bottom ports, with 3.0g g of packing material being added to the same conical tube at each port and snap frozen between ports, for a total of 9.0 g of sample. Samples were stored at -80 °C until biomolecular analyses.

8.3.8 Biomolecular Analyses

8.3.8.1 DNA Extraction and Treatment

Total genomic DNA was extracted from the column materials was performed using the PowerMax™ Soil DNA Isolation Kit (MoBIO, Carlsebad, CA) according to the manufacturer's recommended protocol. A single DNA extraction was performed on the pooled sample of each column collected at steady-state operation after homogenization. A small portion of the extracted genomic DNA was treated for RNA contamination with RNase ONE Ribonuclease (Promega, Madison, WI). For each extract, 4 uL of genomic DNA was mixed with 4 uL of the RNase, 1 uL of nuclease free water, and 1 uL of 10X reaction buffer and incubated for 45 min at 37 °C.

Genomic DNA extractions were also performed on the cellulose-degrading and sulfate-reducing enrichment cultures and the dairy manure slurry using the UltraClean™

Soil DNA Isolation Kit (MoBio, Carlsebad, CA) according to the manufacturer's protocol. Genomic DNA from the three pure cultures was also extracted using the UltraClean™ Microbial DNA Isolation Kit (MoBio, Carlsebad, CA) according to the manufacturer's protocol.

The 16S gene was PCR amplified from the dairy manure slurry genomic DNA, the two enrichment cultures, and the starting dry column packing material using the universal bacterial primer set 8F (5'-AGA GTT TGA TCM TGG CTC AG-3') and 1492R (5'-TAC GGH TAC CTT GTT ACG ACT T-3') (Weisburg, Barns et al. 1991). For each 25 uL reaction, the PCR master mix included: 11.9 uL sterile deionized water, 5.0 uL 5x TaqMaster PCR Enhancer (5 Prime, Gaithersburg, MD), 2.5 uL 10X Taq buffer (5 Prime), 1.5 uL Mg^{2+} (25 mM, 5 Prime), 0.5 uL dNTPs (10 mM, 5 Prime), 1.0 uL 8f primer (5 mM), 1.0 uL 1492r primer (5 mM), 0.25 uL formamide, and 0.35 uL Taq DNA polymerase (5 U/uL, 5 Prime). The PCR thermal cycler program was as follows: initial denaturation step of 3 min at 94 °C, 25 amplification cycles of 30 s at 94 °C, 30 s at 50 °C, 90 s at 72 °C, and a final elongation step of 7 min at 72 °C. PCR products were visualized on 1.2 wt% agarose gels to verify products of the appropriate size.

The 16S PCR products were cloned using the TOPO TA Cloning Kit (Invitrogen, Carlsbad, CA) according to the manufacturer's protocol. Amplified rDNA restriction analysis (ARDRA) was performed visually from MspI restriction enzyme (Promega, Madison, WI)-digested PCR-amplified (using vector-specific primers) inserts. Unique ARDRA patterns from the three cloning reactions were sequenced at the Proteomics and Metabolomics Facility at Colorado State University (Fort Collins, CO).

8.3.8.2 RNA Extraction and Treatment

Total RNA was extracted from the column materials using the RNA PowerSoil™ Total RNA Isolation Kit (MoBIO, Carlsebad, CA) according to the manufacturer's recommended protocol with the addition of two freeze-thaw steps added to the mechanical lysis. A single RNA extraction was performed on the pooled sample of each column collected at steady-state operation after homogenization. A small portion of the extracted total RNA was treated with RQ1 RNase-Free DNase (Promega, Madison, WI) for DNA contamination. For each extract, 4 uL of total RNA was mixed with 4 uL of the DNase, 1 uL of nuclease free water, and 1 uL of 10X reaction buffer and incubated for 30 min at 37 °C. After incubation, each reaction received 1 uL of DNase stop solution and was incubated for an additional 10 min at 65 °C to destroy the enzyme.

This DNase-treated RNA was reverse transcribed using AMV Reverse Transcriptase (Promega, Madison, WI). Each reaction received 3 uL of the treated RNA, 2 uL of nuclease free water, and 1 uL of the W104R (5 mM) (Brosius, Dull et al. 1981) labeled with the 5`-6FAM fluorescien (Applied Biosystems, Foster, CA) ([6FAM]-5`-TTA CCG CGG CTG GCT GGCAC-3`). The mixture was incubated at 70 °C for 5 minutes for primer annealing, followed by 5 min at 4 °C, and the 6 uL was added to the reverse transcription mix that included: 5 uL of 5X reaction buffer, 2.5 uL of dNTPs (10 uM), 2.5 uL of $Na_4P_2O_7^+$ (40 mM, at 42 °C), 7.5 uL nuclease free water, and 1.5 uL of AMV reverse transcriptase. The solution was incubated at 50 °C for 60 min for first strand cDNA synthesis.

8.3.8.3 Active Community Profiling

PCR and CE-SSCP for ACP was performed as described in Chapter 7. Electropherograms were exported as .bmp files and converted to digital format using DigitizeIt v1.4 software (Eden Prairie, MN). Baseline noise, determined as fluorescence intensity signal less than 20, was manually removed before correcting the intensity for dilutions (PCR template, D/RNase treatment, reverse transcription, and CE-SSCP template) and normalizing to the 220 bp peak of the ROX internal standard. The 16S rRNA and the 16S rDNA values were manually binned into 1 bp bins (containing 11 or 12 points each) and the ratio calculated for each bin.

8.4 Results

8.4.1 Remediation Performance

The removal of sulfate from the bioaugmented (Figure 8.2a) and biostimulated (Figure 8.2b) columns was similar to non-inoculated and the dairy manure (DM) baseline control columns over the over the entire 42 d of treatment. For all columns, the effluent sulfate concentrations fluctuated near the feed concentration for the first 15 days (3.5 pore volumes) of operation. This is consistent with an acclimation period where the microbial communities were adapting to the column environment. After the initial acclimation period, the effluent sulfate concentrations decreased steadily for another 7 d (Days 15 – 22) until reaching their steady-state levels near 400 mg/L. This steady-state effluent concentration was maintained for an additional 20 d (4.5 pore volumes). The effluent sulfate concentrations were comparable to other lab-scale column experiments using a similar simulated AMD formulation (Pruden, Messner et al. 2007).

As with the sulfate removal, the iron removal was similar for all columns over the course of the experiment. The effluent iron concentrations (Figure 8.3a) of all the columns was significantly higher than the feed through the first 8 d of operation, after which they rapidly decreased to near feed level concentrations. Considering the extremely low feed concentration of iron (< 2 mg/L) and the consistent effluent profiles, the elevated effluent concentrations were likely due to iron associated with the column packing materials being washed out of the system.

Cadmium (Figure 8.3b) and zinc (Figure 8.3c) effluent concentrations were also similar for all columns except those biostimulated with CMC, and remained significantly below the feed concentrations throughout the experiment. The effluent concentrations of the CMC-stimulated columns were similar to those from the other five columns for the first 15 d of operation, at which point they began to increase. Both cadmium and zinc effluent concentrations from the CMC-fed columns peaked at Day 30 at levels ten times higher than those of all other columns, and then decreased steadily through the end of the experiment. The spike in effluent metal concentrations for the CMC columns did not correlate with a decrease in the other performance-determining metrics (pH or sulfate removal). Because the CMC columns received a separate AMD feed, it is possible that the metal concentrations of the CMC feed was elevated during this time period; further ICP analyses are required to make this determination.

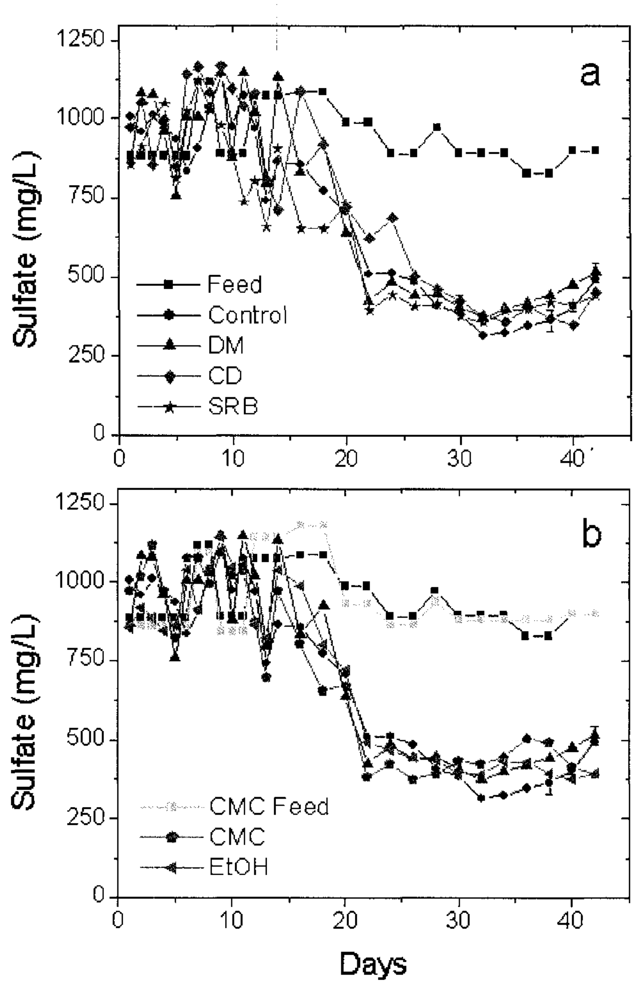

Figure 8.2 – Effluent sulfate concentrations for (a) bioaugmented and (b) biostimulated SRBRs as determined from IC analysis. Feed data was adjusted by 4 d to account for the HRT of the columns. Data points represent the average of two biological replicates. Error bars represent the standard deviation of independently prepared technical replicates.

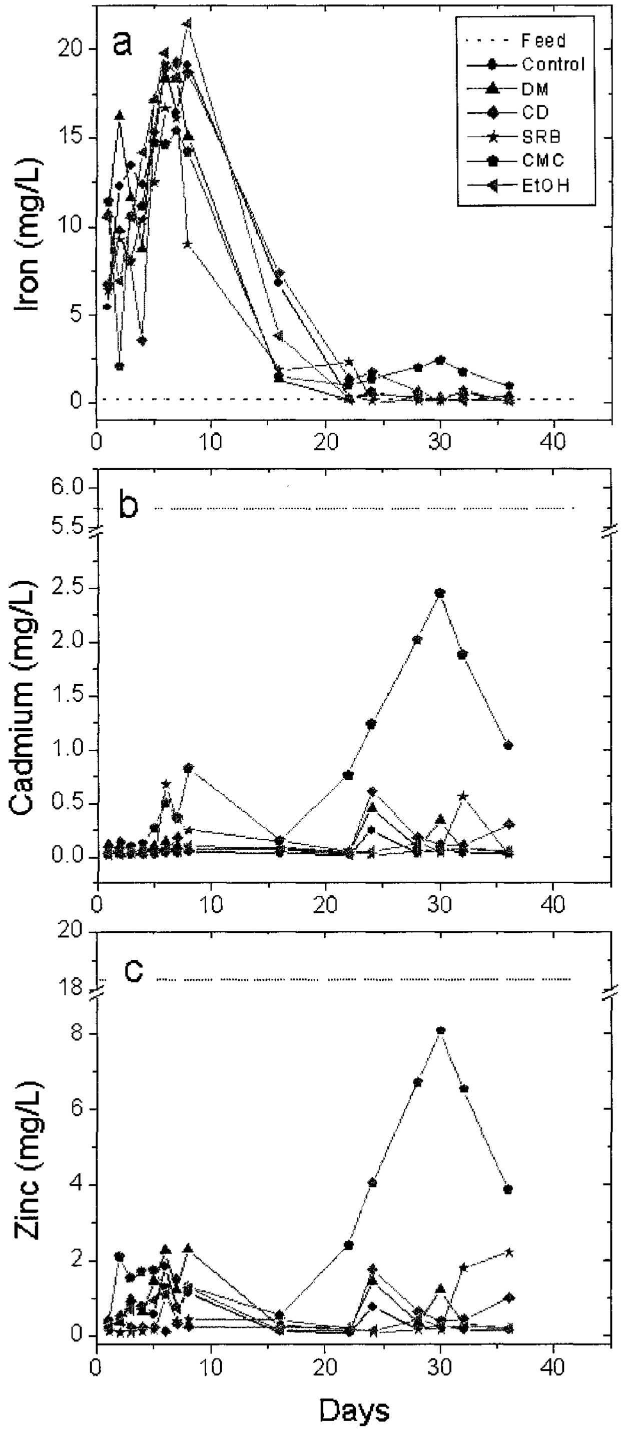

Figure 8.3 – Effluent concentrations of (a) iron, (b) cadmium, and (c) zinc from all SRBRs as determined from ICP-AES analysis. The feed concentrations traces are averages of three measurements taken over the course of the experiment.

The effluent pH levels of all columns were similar (Figure 8.4) and fluctuated near the feed pH for the first 10 d of operation before increasing to steady-state, neural levels by Day 20. It is interesting that the acclimation period, as determined by pH, was ~1 pore volume shorter than that observed in the metal and sulfate removals. It is possible that mechanisms responsible for metal and sulfate removal, in this case SRB activity, was inhibited by the lower pH. However, most SRB are capable of metabolic activity at pH levels at or above 5.5 (Postgate 1984), which was the pH of the synthetic AMD fed to the columns. In addition, limestone sand was included in the column packing material to aid in initial buffering of the column environment, so it is unlikely the pH was the limiting factor in the column startup time.

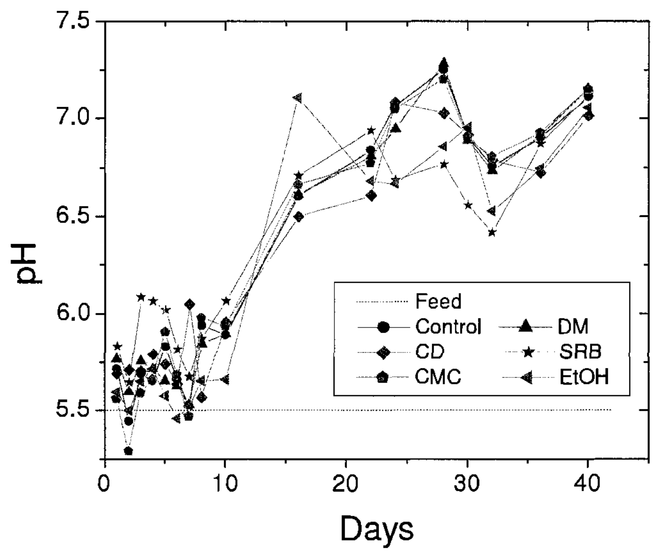

Figure 8.4 - Effluent pH of all SRBRs. The feed trace represents the feed to all columns (with and without CMC amendment).

8.4.2 16S rRNA:16S rDNA Ratio Profiles

The binning approach used to determine the 16S rRNA:16S rDNA ratio for the community profiles adequately captures the relative trends of the rRNA and rDNA (Figure 8.5). Manual noise removal of the nucleic acid signals prevents meaningless 'ghost' peaks in the ratio profiles near the x-axis profile extremes. Because of mathematical constraints, 16S rRNA peaks without corresponding 16S rDNA peaks (i.e., the peak near 175 bp of Figure 8.5) cannot be quantified with the ratio. Bin sizes of 0.5, 1.0, 2.5, and 5.0 bp were evaluated in an attempt to minimize this problem, with the 1.0 bp bin size determined to be appropriate so as to avoid missed rRNA peaks while maintaining overall peak resolution (data not shown). The replicates for each starting column pair had some variability in their 16S rRNA:16S rDNA profiles (Figure 8.6). The largest differences between the biological replicates were observed for the non-bioaugmented columns. The observed differences are attributed to heterogeneities in the dairy manure slurry and the organic substrate used to pack the columns.

8.4.3 Control and Baseline Dairy Manure Columns

The starting 16S rRNA:16S rDNA ratio profile for the uninoculated control column (Control 1) was much less diverse than its steady-state profile (Figure 8.7). All of the dominant peaks in the starting profile persisted through the six weeks of experiment and aligned well with dominant peaks of the steady-state profile. Considering that any microorganisms associated introduced into the Control columns would have come from the column packing materials (all dry), it is not surprising that the diversity of the active species would increase when the materials became saturated. The aqueous environment greatly improves the transport and availability of nutrients, facilitating the growth and activity of species that were dormant or nutrient-limited under dry conditions. The clone library developed from the 16S gene of the starting dry material used as packing material for all of the columns (Table 8.5) was relatively simple and was comprised completely of clone sequences related to the family Enterobactereaceae, predominately *Enterobacter spp.*. Although this is a large taxonomical group with a wide variety of functions, *Enterobacter*-like spp. are generally considered to be facultative anaerobes commonly associated with the degradation of polymeric compounds and fermentation (Holt 1984; Kaufhold and Ferrieri 1991), which is in keeping with their presence on the wood chips used in this study.

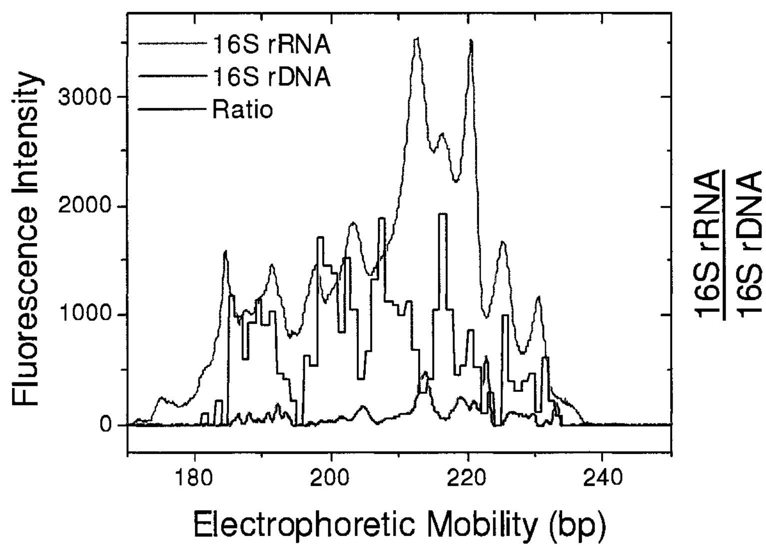

Figure 8.5 – The 16S rRNA and 16S rDNA profiles for the CMC 1 column, along with 16S rRNA:16S rDNA ratio profile determined using 1 bp bin sizes.

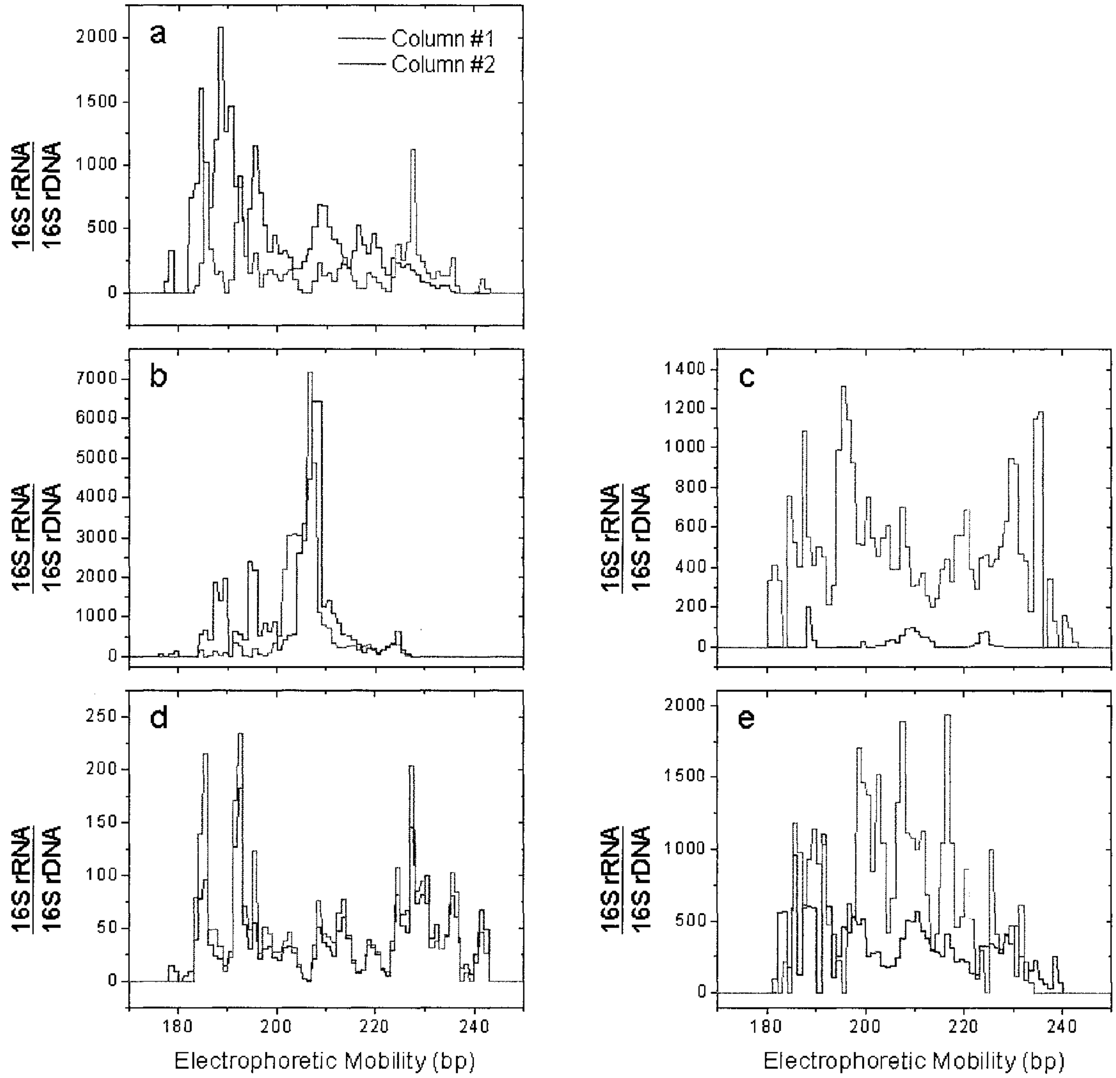

Figure 8.6 – The 16S rRNA:16S rDNA profiles of the starting material from the biological replicate columns (a) DM, (b) SRB, (c) EtOH, (d) CD, and (e) CMC.

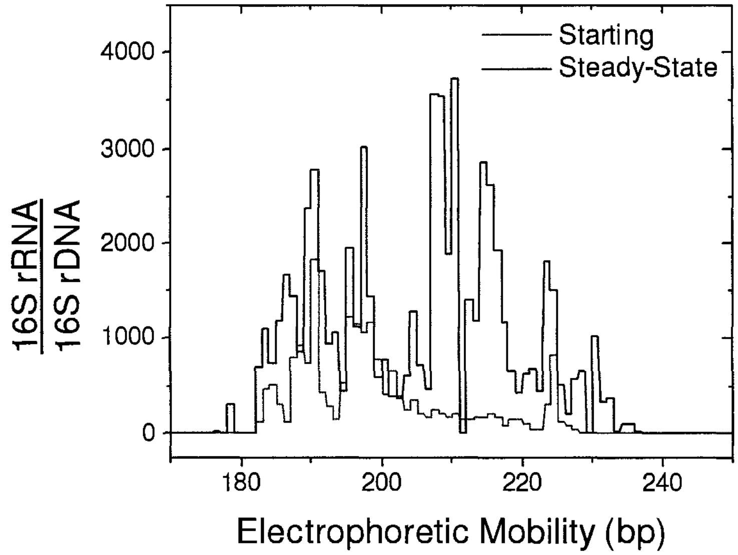

Figure 8.7 - Starting and steady-state 16S rRNA:16S rDNA profile for a uninoculated control column (Control 1).

The starting 16S rRNA:16S rDNA ratio profiles of the two columns inoculated only with DM were very similar to each other (Figure 8.8) and, as expected were much more diverse than the starting profiles of the Control columns (Figure 8.7). The clone library developed from the 16S gene of the DM slurry was extremely diverse (Table 8.6); nearly 300 clones were required to exceed 60% coverage as determined by ARDRA (data not shown). As expected, the DM slurry clone sequences matched well with microorganisms with a wide variety of functions, including the three main functions associated with AMD remediation: cellulose degradation, fermentation, and sulfate reduction. A large proportion of the clone sequences matched poorly (<90%) with the sequences from cultured species in the BLAST database, but matched well with uncultured bacterium sequences obtained from bovine rumen. Several clone sequences also matched well with clones sequences obtained from a field sulfate-reducing bioreactor treating AMD that was also inoculated with dairy manure (Hiibel, Pereyra et al. 2008).

Despite attempts with multiple template dilutions and run conditions, a 16S rRNA profile was not obtained for either steady-state DM column, consequently preventing the ratio profile from being determined.

Table 8.5 - Electrophoretic mobility and nearest cultured BLAST match for 16S gene clones derived from the dry materials used as column substrate.

Clone ID	*Fraction of Community	Electrophoretic Mobility (bp)	Nearest Cultured BLAST Result Match (Accession #)	% Match
OM_01	2%		*Enterococcus mundtii* (AF061013)	96
OM_05	7%	200.32	*Enterobacter hormaechei* (EU047556)	96
OM_16	2%		*Enterobacter sp. TUT1390* (AB308444)	97
OM_19	5%		*Pantoea sp. NJ-32* (AM421978)	97
OM_21	2%		*Pantoea agglomerans* (AY691543)	96
OM_06	31%	198.72	*Enterobacter cloacae* (DQ202394)	93
OM_37	2%		*Enterobacter sp. GW31-6* (EF471901)	96
OM_40	2%		*Enterococcus mundtii* (EF428246)	94
OM_43	2%		*Staphylococcus sp. An21* (AJ551159)	94
OM_50	2%		*Enterobacter sp. CMG24314* (EU162036)	95
OM_51	22%	199.48	*Klebsiella oxytoca* (AF543296)	96
OM_52	22%		*Enterobacter hormaechei* (AY995561)	98

* Based on ARDRA of harvested clones

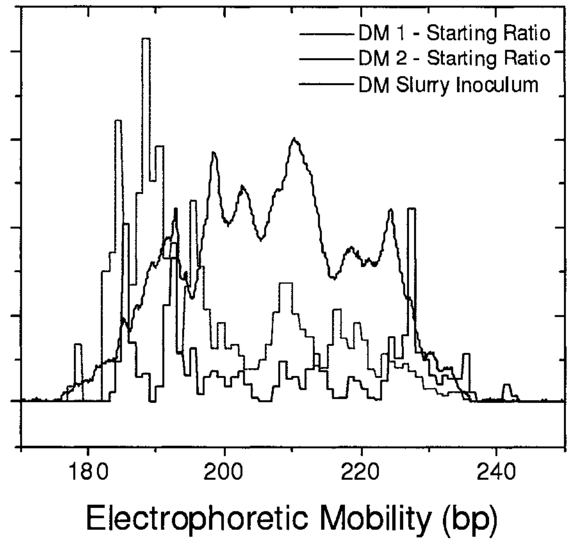

Figure 8.8 - Profile of the dairy manure slurry used as the inoculum for all columns overlain on the starting 16S rRNA:16S rDNA ratio profiles of the columns inoculated with dairy manure only (DM 1 and DM 2).

Table 8.6 - Electrophoretic mobility and nearest cultured BLAST match for 16S gene clones derived from the dairy manure slurry used as the baseline inoculum.

Clone ID	*Fraction of Community	Electrophoretic Mobility (bp)	Nearest Cultured BLAST Result Match (Accession #)	% Match
DM_001	0.4%		*Lysobacter sp. SB-K88* (AB190258)	92
DM_002	0.7%	189.98	*Corynebacterium sp. QKT1393-078* (AB010906)	93
DM_003	0.4%		*Alkaliflexus imshenetskii* (AJ784993)	90
DM_004	1.1%	230.20	*Haliea sp. MOLA 104* (AM990878)	90
DM_005	1.1%	199.21	*Sphingobacterium spiritivorum* (AJ878852)	91
DM_006	0.7%		*Ruminobacillus xylanolyticum* (DQ178248)	93
DM_007	0.4%		*Sphingomonas sp. S11-S-1* (EU016172)	95
DM_008	1.8%	190.17	*Kribbia sp. JL1069* (DQ985060)	94
DM_009	0.4%		*Cytophaga sp. Dex80-64* (AJ431235)	86
DM_010	0.4%		*Microbulbifer sp. CMC-5* (EU121671)	91

DM_011	0.4%		*Anabaena sp. BIR348* (EF568893)	80
DM_012	0.7%		*Ruminobacillus xylanolyticum* (DQ178248)	91
DM_013	0.4%		*Ruminobacillus xylanolyticum* (DQ178248)	92*
DM_014	0.7%	200.54	*Aequorivita ferruginea* (AY027804)	93
DM_015	1.1%	192.12	*Cytophaga sp. AN-BI4* (AM157648)	90
DM_017	0.7%	177.72	*Acidimicrobium ferrooxidans* (EF621760)	87
DM_018	0.4%		*Eubacterium sp. F1* (EU281854)	84
DM_019	2.6%	228.52	*Pseudomonas sp. 117S1* (EU370415)	94
DM_020	0.4%		*Sedimentibacter sp. JN18_V27_I* (EF059533)	100
DM_021	1.1%	226.87	*Persicirhabdus sediminis* (AB331886)	88
DM_022	2.2%	182.92	*Thermodesulfobium narugense* (AB077817)	79
DM_023	1.1%	226.75	*Pseudomonas sp. 117S1* (EU370415)	95
DM_024	0.4%		*Pseudomonas sp. MACL14* (EF198250)	93
DM_025	0.4%		*Clostridium hastiforme* (X80841)	92
DM_026	0.4%		*Ruminococcus sp. DJF_VR67* (EU728791)	88
DM_027	0.4%		*Devosia sp. 6_4V* (EF540476)	94
DM_028	1.1%	217.01	*Microbulbifer sp. MY05* (AY862188)	95
DM_029	0.4%		*Methylophaga thalassica* (X95460)	95
DM_030	0.4%		*Desulfonosporus thiosulfogenes* (Y18214)	90
DM_033	3.3%	194.12	*Sphingomonas sp. S11-S-6* (EU016177)	97
DM_035	0.7%	210.49	*Flavobacteriaceae bacterium JJC* (EU523664)	94
DM_037	0.7%	195.83	*Cyclobacterium linum* (DQ534063)	92
DM_038	0.4%		*Dasania marina* (AY771747)	90
DM_041	0.4%		*Truepera radiovictrix* (DQ022077)	88
DM_042	0.4%		*Opitutaceae bacterium TAV1* (AY587231)	92

DM_043	1.5%	199.48	*Haliscomenobacter hydrossis* (AJ784892)	86
DM_044	1.5%	220.00	*Xanthomonadaceae bacterium NML 93-0792*	95
DM_046	0.4%		*Actinomycetales bacterium SSCS15* (AB211026)	95
DM_047	2.6%	189.33	*Chelatobacter sp. Pht-3B* (DQ659453)	94
DM_048	1.5%	196.59	*Planctomycete str. 543* (AJ231173)	91
DM_049	0.4%	193.29	*Janibacter sp. NSA5-4* (AB177881)	94
DM_050	1.8%	208.94	*Sphingobacterium sp. 44/35* (AY571816)	94
DM_051	0.7%	214.53	*Cibimonas vasta* (DQ846687)	93
DM_053	1.5%	208.79	*Pedobacter sp. An13* (AJ551152)	88
DM_054	0.7%	224.23	*Cellvibrio sp. R4069* (AJ289162)	90
DM_055	0.7%	204.34	*Gemmatimonas aurantiaca* (AB072735)	84
DM_059	0.7%	214.21	*Luteimonas sp. TUT1238* (AB188220)	91
DM_061	0.4%	192.95	*Clostridium fallax* (AY208919)	78
DM_062	0.4%		*Erythrobacter litoralis* (AF465836)	94
DM_064	0.7%	198.06	*Paenibacillus sp. Aek31* (EU741009)	80
DM_066	0.4%	212.72	*Clostridium hastiforme* (X80841)	89
DM_067	0.4%		*Owenweeksia hongkongensis* (AB125062)	86
DM_071	0.4%		*Devosia sp. 4_C16_46* (EF540511)	94
DM_073	0.7%	193.97	*Clostridium jejuens* (AY494606)	89
DM_074	0.4%		*Lyngbya majuscula* (EU315909)	85
DM_075	0.4%		*Aequorivita marinus* (EU290153)	93
DM_076	0.4%		*Kribbia sp. JL1069* (DQ985060)	96
DM_078	1.8%	194.34	*Sphingomonas sp. S11-S-6* (EU016177)	96
DM_079	0.4%		*Xanthomonadaceae bacterium NML 93-0792*	91
DM_080	2.2%	221.07	*Luteimonas sp. S22-40* (AM932272)	94

DM_081	0.7%	190.50	*Antarcticicola litoralis* (EU016198)	89
DM_083	0.7%	212.10	*Ruminobacillus xylanolyticum* (DQ178248)	90
DM_085	0.4%		*Clostridium sp.* (AY949857)	93
DM_086	0.4%		*Lysobacter sp. 3070* (AM111012)	95
DM_087	0.4%	189.93	*Desulfuromusa succinoxidans* (X79415)	77
DM_090	0.7%	195.49	*Erythrobacter sp. R14* (EF177676)	93
DM_092	0.4%		*Vitellibacter sp. JC2436* (EU642844)	91
DM_093	0.7%	191.78	*Leifsonia sp. 3_1K* (EF540446)	93
DM_096	0.4%		*Alterierythrobacter sp. H32* (EU726272)	94
DM_097	0.4%		*Clostridium lituseburense* (M59107)	94
DM_098	0.4%		*Planctomycete str. 116* (AJ231181)	96
DM_105	0.7%	220.49	*Lewinella cohaerens* (EU371937)	84
DM_106	0.7%	223.14	*Bacillus sp. PML14* (EF165014)	92
DM_108	1.1%	211.47	*Verrucomicrobia bacterium 05IJR53-1* (AB372855)	84
DM_110	0.7%	212.74	*Flavobacteriaceae bacterium 3519-10* (EU523664)	92
DM_111	0.7%	205.09	*Vitellibacter sp. JC2436 (EU642844)*	92
DM_112	0.4%		*Pirellula sp.* (X81942)	87
DM_113	0.4%		*Rikenellaceae bacterium JAM-BA0501* (AB362265)	93
DM_114	0.4%	213.24	*Cibimonas vasta* (DQ846687)	92
DM_125	0.4%		*Granulosicoccus antarcticus* (EF495228)	84
DM_128	0.7%	200.39	*Synechocystis PCC6308* (AB039001)	
DM_129	0.7%	182.12	*Caulobacter sp.* (AB016847)	93
DM_131	0.4%		*Alkalibacterium indicireducens* (AB268551)	99
DM_132	0.4%		*Anaerovorax odorimutans* (AJ251215)	92
DM_134	0.4%		*Porphyrobacter sp. KK351* (AB033326)	93

DM_136	0.4%		*Pusillimonas terrae* (DQ466075)	94
DM_137	0.7%	228.34	*Denitromonas indolicum* (AY972852)	88
DM_138	0.4%		*Luteimonas sp. TUT1238 (AB188220)*	92
DM_139	0.4%		*Bellia baltica* (AJ564643)	89
DM_141	0.4%		*Yeosuana yeosuensis* (AY682383)	91
DM_143	0.4%		*Cyclobacterium linum* (DQ534063)	90
DM_144	0.7%	214.87	*Lysobacter sp. 3070 (AM111012)*	91
DM_145	1.8%	227.57	*Pseudomonas sp. HY-14* (EU620679)	95
DM_147	0.4%		*Alcaligenes sp. Ic4* (DQ421393)	96
DM_148	0.4%		*Truepera radiovictrix (DQ022077)*	85
DM_150	0.4%		*Bacillus sp. CHNTR52* (EF551863)	94
DM_156	0.4%		*Sphingomonas sp. JQ1-11* (AB425062)	93
DM_157	0.4%		*Coprococcus eutactus* (EF031543)	78
DM_158	0.4%		*Methylacidiphilum infernorum V4* (CP000975)	76
DM_160	0.4%		*Stenotrophomonas sp. KC-5* (AM400231)	92
DM_162	0.4%	211.17	*Halomonas organivorans* (AJ616910)	94
DM_163	1.5%	219.91	*Alcaligenes sp. R-21939* (AJ786800)	91
DM_164	0.4%		*Alcaligenes sp. R-21939 (AJ786800)*	94
DM_166	0.4%		*Devosia sp. 6_4V* (EU196329)	93
DM_167	0.4%		*Bacteroidetes bacterium M-phe-1* (AY766096)	97
DM_169	0.4%		*Stenotrophomonas sp. KC-5* (AM400231)	94
DM_170	0.4%		*Lysobacter pocheonensis* (EU273938)	95
DM_171	0.7%	205.60	*Rikenellaceae bacterium JAM-BA0501 (AB362265)*	90
DM_173	0.4%		*Desulfobacterium autotrophicum* (AF418177)	93
DM_177	0.4%		*Devosia neptuniae* (AF469072)	89

DM_178	0.4%		*Pseudoxanthomonas mexicana* (AB246798)	93
DM_180	0.4%		*Truepera radiovictrix (DQ022077)*	86
DM_181	0.4%		*Cytophaga sp. Dex80-64 (AJ431235)*	85
DM_182	0.4%		*Alcaligenes sp. H* (AJ412685)	93
DM_183	0.4%		*Roseovarius aestuarii* (FM180527)	90
DM_187	0.4%		*Ruminofilibacter xylanolyticum* (DQ141183)	88
DM_195	0.4%		*Leucobacter sp. Ch1* (EF362778)	92
DM_197	0.4%		*Clavibacter michiganensis* (EU685335)	95
DM_198	1.8%	194.38	*Sphingomonas sp. NP31* (EU196324)	94
DM_200	1.1%	211.25	*Lysobacter sp. YIM C734* (EU135665)	93
DM_209	0.4%		*Desulfonosporus sp. AAN04* (AB436739)	88
DM_210	0.4%	186.22	*Clostridium sp. D3RC-2* (DQ852338)	95
DM_215	0.4%		*Rikenellaceae bacterium JAM-BA0501* (AB362265)	92
DM_217	0.4%	208.71	*Devosia sp. BD-c194* (EF575560)	93
DM_219	0.4%	221.16	*Clostridium sp.* (AY949859)	89
DM_221	0.4%	225.99	*Sphingomonas sp. S11-S-6 (EU016177)*	93
DM_224	0.7%	192.18	*Pedobacter sp. An13* (AJ551152)	88
DM_225	1.1%		*Ruminobacillus xylanolyticum* (DQ178248)	91
DM_226	0.4%		*Parvibaculum lavamentivorans* (CP000774)	92
DM_227	0.7%		*Cellvibrio sp. KY-CR-1* (EF692633)	92
DM_228	0.4%		*Xanthomonadaceae bacterium NML 93-0792*	94
DM_229	0.4%		*Acidimicrobidae bacterium YM22-133* (AB360343)	89
DM_230	0.4%		*Alcaligenes sp. C4M17* (DQ089749)	94
DM_232	0.7%		*Rhodobacteraceae bacterium 216* (AJ810846)	94
DM_240	0.4%		*Pseudomonas sp. Hg4-08* (EU304254)	88

DM_242	0.4%		*Clostridiaceae bacterium DJF_LS40* (EU728744)	89
DM_254	0.4%		*Acidimicrobidae bacterium YM22-133* (AB360343)	86
DM_255	0.4%		*Lysobacter spongiicola* (AB299978)	92
DM_256	0.4%		*Vitellibacter sp. JC2436* (EU642844)	92
DM_259	0.4%		*Actinomycetales bacterium SSCS15* (AB211026)	90
DM_260	0.4%		*Coprococcus eutactus* (EF031543)	78
DM_263	0.4%		*Marinobacter lutaoensis* (AF288157)	89
DM_268	0.4%		*Sphingobacterium spiritivorum* (AJ878852)	90
DM_269	0.4%		*Devosia neptuniae* (AF469072)	93
DM_270	0.4%		*Ruminobacillus xylanolyticum* (DQ178248)	94
DM_273	1.1%		*Truepera radiovictrix* (DQ022077)	89
DM_274	0.4%		*Truepera radiovictrix* (DQ022077)	85
DM_275	0.7%	213.36	*Lysobacter pocheonensis* (EU273938)	95
DM_277	0.4%		*Janibacter anophelis* (AY837752)	96
DM_283	0.4%		*Brevundimonas sp. N5* (EU567032)	91
DM_290	0.4%		*Sphingomonas sp. S11-S-6* (EU016177)	95
DM_294	0.4%		*Marinobacter bacchus* (DQ282120)	96
DM_299	0.4%		*Persicirhabdus sediminis* (AB331886)	89
DM_302	0.4%		*Lewinella cohaerens* (EU371937)	84
DM_303	0.4%		*Clostridium alkalicellum* (AY959944)	90
DM_304	0.4%		*Clostridiaceae bacterium SK061* (AB298753)	85

* Baed on ARDRA of harvested clones

8.4.4 Enrichment Cultures

8.4.4.1 Cellulose Degraders

The cellulose-degrader enrichment culture included both cellulose degraders and fermentative species, based on the developed clone library (Table 8.7). The dominant peak in the electropherogram (Figure 8.9) aligned with clones CD_01 and CD_06, which were closely related to *Citrobacter* spp.. Other dominant peaks of the enrichment culture aligned with clones that were similar to *Shigella boydii* and *Sporobacter termiditis*. Several clone sequences were also found to match well with *Clostridium* spp.. *Citrobacter, Clostridium,* and *Shigella* spp. are all capable of fermentation, and some *Citrobacter* and *Clostridium* spp. can degrade cellulose (Holt 1984). *S. termiditis* is an obligate anaerobe that was isolated from termite gut and is capable of growth on a limited range of methylated aromatic compounds (GrechMora, Fardeau et al. 1996), and thus is likely to have grown on the CMC. The presence of fermentative species was expected, as no effort was made in the enrichment process to inhibit fermentation. Because the enrichment was performed in batch fashion, the presence of fermenters was necessary to prevent product inhibition by the cellulose degraders (Mandenius, Nilsson et al. 1988). In addition, fermenters are a key functional group of the AMD-remediation microbial community.

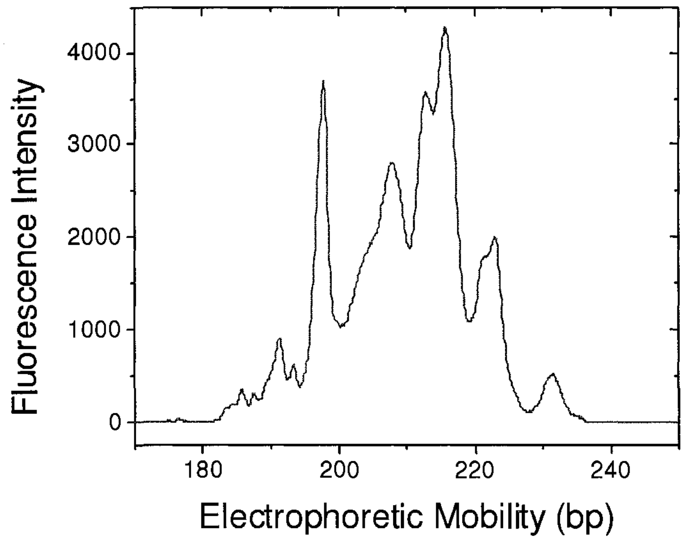

Figure 8.9 – Electropherogram of the cellulose-degrading enrichment culture.

Table 8.7 – Electrophoretic mobility and nearest cultured BLAST match for 16S gene clones derived from the cellulose-degrading enrichment culture.

Clone ID	*Fraction of Community	Electrophoretic Mobility (bp)	Nearest Cultured BLAST Result Match (Accession #)	% Match
CD_01	17%	214.32	*Citrobacter freundii* (DQ444289)	96
CD_04	13%	209.01	*Shigella boydii* (CP001063)	97
CD_06	4%	214.49	*Citrobacter braakii* (AF025368)	95
CD_07	2%		*Clostridium propionicum* (X77841)	94
CD_10	2%		*Enterobacter hormaechei* (EU047556)	98
CD_12	4%	187.98	*Sporobacterium olearium* (AF116854)	96
CD_13	2%		*Oscillibacter valericigenes* (AB238598)	94
CD_16	2%		*Klebsiella sp. IS-J3* (EF599758)	97
CD_18	4%	186.4	*Clostridium aminobutyricum* (X76161)	92
CD_20	2%		*Dysgonomonas gadei* (Y18530)	97
CD_26	2%		*Sporobacterium olearium* (AF116854)	91
CD_31	4%	191.79	*Sporobacter termitidis* (Z49863)	88
CD_34	23%		*Klebsiella oxytoca* (AF543296)	98
CD_44	4%		*Clostridiales bacterium DJF_B152* (EU728715)	93
CD_02	4%	225.87	Unknown	
CD_30	6%	204.03	Unknown	
CD_41	4%	211.7	Unknown	

* Based on ARDRA of harvested clones

8.4.4.2 Sulfate Reducers

No SRB species were found in the sulfate-reducing enrichment cultures based on the 16S gene clone library developed from the culture (Table 8.8), although one small peak of the enrichment profile (Figure 8.10) corresponded to an SRB, *Desulfuromusa succinoxidans*, which was detected in the DM inoculum clone library. The dominant peaks of the enrichment profile corresponded to clones related to *Shigella spp.*, *Trichococcus spp.*, and a *Klebsiella sp*. Clones related to *Clostridium spp.* also aligned with several of the less dominant peaks of the enrichment culture profile. The clone library results were in direct contrast with observations of the enrichment cultures, namely blackening of the culture media and a distinctive hydrogen sulfide odor were observed in all of the enrichment transfers and in the final culture used to inoculate the columns. The clone library result also contradicts previous biomolecular analysis of the bioreactor the initial inoculum was obtained from, where both 16S and *apsA* gene cloning and Q-PCR indicated a SRB-dominant microbial community (Reactor ETOH 2, Chapter 5). The prevalence of clones closely related to *Shigella* spp. would indicate either contamination from the recombinant *Taq* DNA polymerase used for the clone insert amplification PCR or an error associated with the transformation step of the cloning process.

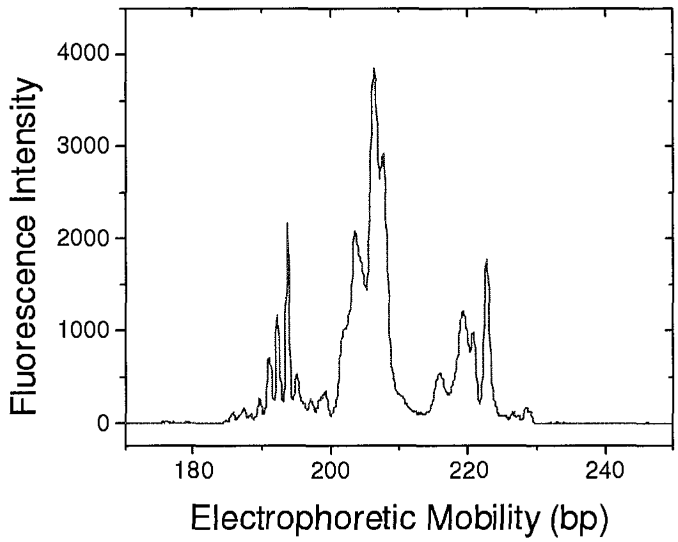

Figure 8.10 - Electropherogram of the sulfate-reducing enrichment culture.

Table 8.8 - Electrophoretic mobility and nearest cultured BLAST match for 16S gene clones derived from the sulfate-reducing enrichment culture.

Clone ID	*Fraction of Community	Electrophoretic Mobility (bp)	Nearest Cultured BLAST Result Match (Accession #)	% Match
SRB_01	11%	194.12	*Clostridium amygdalinum* (AY353957)	97
SRB_02	8%	206.63	*Klebsiella sp. F51-1-2* (DQ277701)	98
SRB_03	19%	206.75	*Trichococcus pasteurii* (X87150)	95
SRB_05	6%	208.38	*Shigella boydii* (CP001063)	98
SRB_06	6%	208.00	*Shigella sonnei* (EU723822)	97
SRB_07	6%	195.19	*Oscillibacter valericigenes* (AB238598)	97
SRB_10	8%	207.84	*Trichococcus pasteurii* (X87150)	91
SRB_11	3%	191.35	*Clostridium methoxy-benzovorans* (AF067965)	92
SRB_14	3%		*Trichococcus collinsii* (AJ306612)	97
SRB_18	3%		*Shigella sonnei* (EU009199)	98
SRB_20	17%		*Shigella boydii* (CP001063)	95
SRB_25	6%	207.84	*Anaerofilum pentosovorans* (X97852)	90
SRB_29	3%	191.35	*Clostridium sp. BL-3* (DQ196627)	98
SRB_36	3%		*Acidaminococcus fermentans* (X78017)	92

* Based on ARDRA of harvested clones

8.4.5 Active Community Profiling of Bioaugmented Columns

8.4.5.1 Cellulose Degraders

The starting 16S rRNA:16S rDNA ratio profiles of the columns bioaugmented with cellulose degraders were considerably simpler than the steady-state ratio profile (Figure

8.11). The three dominant peaks of the starting profile persist throughout the experiment and are present in the steady-state sample. The three pure culture cellulose-degrading bacteria used in the bioaugmentation do not align with significant peaks in the starting ratio profile (Figure 8.12a), but after six weeks of operation, each of the three pure cultures aligns with a dominant peak in the steady-state ratio profile (Figure 8.12b). A similar trend is seen with the cellulose-degrader enrichment culture. None of the dominant peaks of the enrichment profile align with peaks of in the ratio profile at the start of the experiment, while several of the enrichment peaks align with dominant peaks of the steady-state ratio profile (Figure 8.13). The results for the initial samples were unexpected because the three pure cultures used for bioaugmentation were inoculated at a level intended to be 50% of the total population and the inocula came from actively growing overnight cultures. The most likely explanation of this behavior is that the activity of the bioaugmented species decreased during the time between inoculation and sampling, approximately 24 h, as they were acclimating to the solid substrate environment.

The apparent survival of the bioaugmented species during the course of the experiment, based on the 16S rRNA:16S rDNA ratio profiles of the steady-state columns, was encouraging as bioaugmentation failure is often associated with the rapid loss of added species (Bouchez, Patureau et al. 2000; El Fantroussi and Agathos 2005). That the activity of the added cellulose degraders increased in the columns indicates that the species were able to adapt to the AMD environment and contribute to the microbial community. Considering their location at the top of the carbon flow (Figure 1.4), it is assumed that the activity of the bioaugmented cellulose degraders added to the available metabolite pool of the entire community.

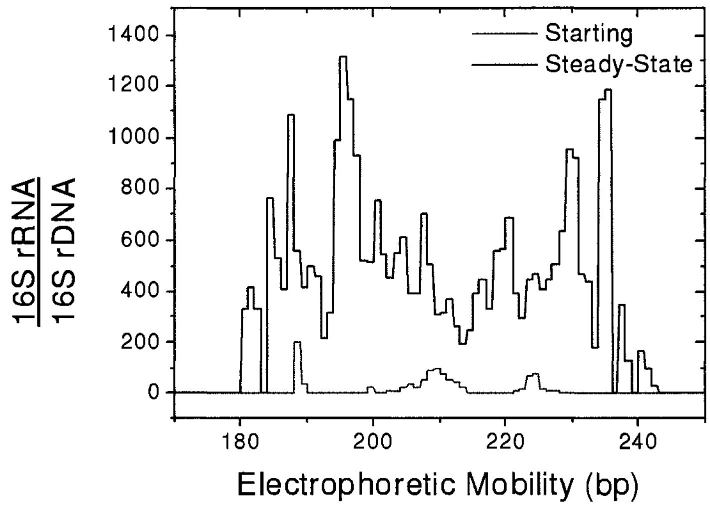

Figure 8.11 – Starting and steady-state 16S rRNA:16S rDNA profile for a column (CD2) bioaugmented with cellulose degraders.

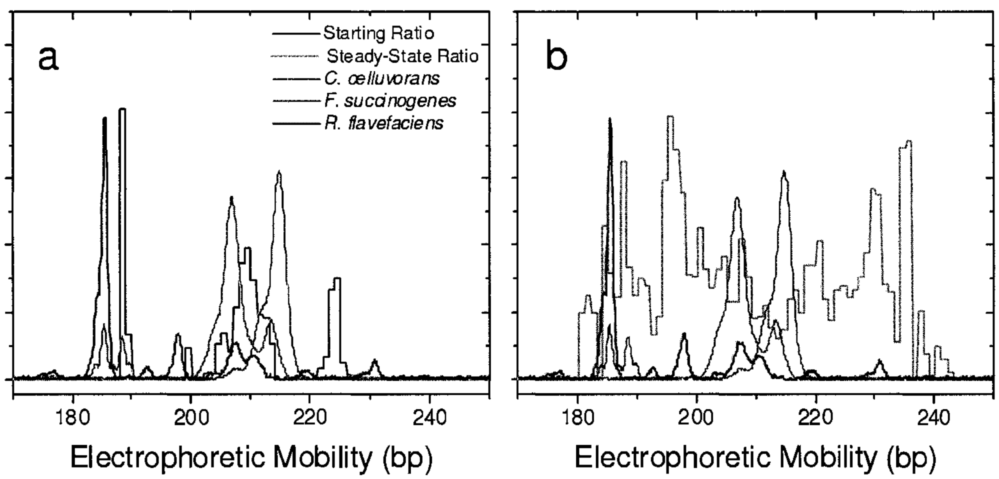

Figure 8.12 – Cellulose-degrading pure culture profiles overlain on the (a) starting and (b) steady-state 16S rRNA:16S rDNA ratio profiles of a column (CD2) bioaugmented with cellulose-degrading bacteria.

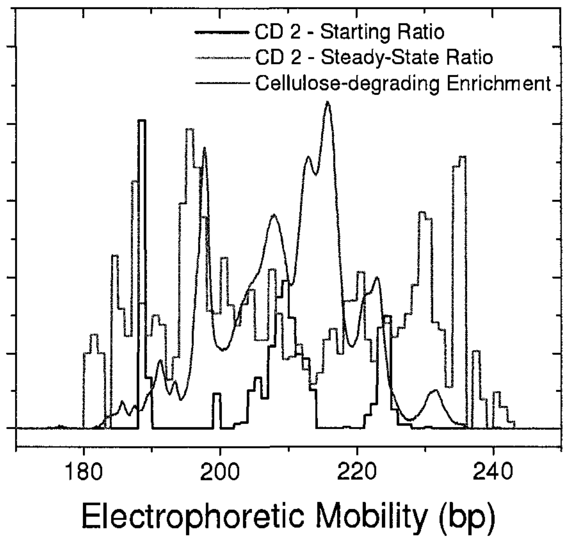

Figure 8.13 – Profile of the cellulose-degrader enrichment overlain on the starting and steady-state 16S rRNA:16S rDNA ratio profiles of a column (CD 2) bioaugmented with cellulose-degrading bacteria.

8.4.5.2 Sulfate Reducers

The starting 16S rRNA:16S rDNA ratio profiles of columns bioaugmented with SRB aligned very well with the enrichment culture profile (Figure 8.14). As expected, the dominant peak in the ratio profile of both columns aligned with the dominant peak of the enrichment culture. Based on these profiles, it can be assumed that the acclimation time required for the SRB enrichment culture was shorter than the CD enrichment culture. Considering the species identified in the SRB clone library, the shorter acclimation period would be expected considering their relative growth rates compared to those of most cellulose degraders (Holt 1984). It is also of note that the peak corresponding to *D. succinoxidans* (EM = 189.9 bp), identified from the DM clone library, was elevated in the SRB 1 column starting material 16SrRNA:16SrDNA ratio profile.

Despite attempts with multiple template dilutions and run conditions, a 16S rRNA profile was not obtained for either steady-state SRB bioaugmented column, consequently preventing the ratio profile from being determined.

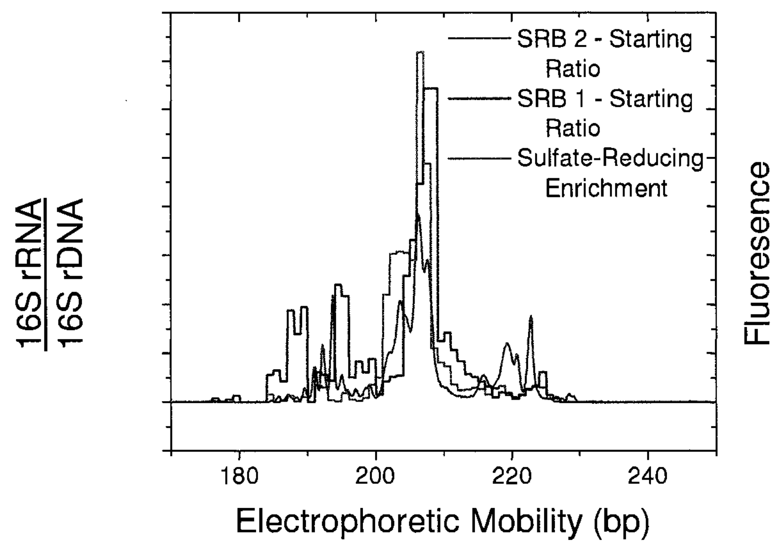

Figure 8.14 – Profile of the sulfate-reducer enrichment overlain on the starting 16S rRNA:16S rDNA ratio profiles of the two columns bioaugmented with sulfate-reducing bacteria.

8.4.6 Active Community Profiling of Bioaugmented Columns

8.4.6.1 CMC

The active species in the columns biostimulated with carboxymethyl cellulose remained consistent through the course of the experiment, based on the CMC columns' rRNA:16S rDNA ratio profiles (Figure 8.15). It was surprising that the starting profiles of these columns were much different than the DM or EtOH columns. Because the starting samples were collected prior to the addition of any CMC, ethanol, or AMD, the microbial communities of the three columns were expected to be very similar. The differences between the starting profiles of the duplicate CMC columns were also unexpected. Initially, two *Clostridium* spp. (*C jejuens*, EM = 193.97 bp; *C. sp. D3RC-2*, EM 186.22 bp) had significantly elevated 16S rRNA:16S rDNA ratios in CMC 1 compared to CMC 2. At steady-state the behavior was reversed, especially for *C. sp. D3RC-2*, which had a higher ratio in CMC 2 compared to CMC 1.

The maintenance of a diverse, active community throughout the experiment is consistent with a nutrient stimulation applied at the top of the carbon flow, as was the case with the CMC. Because the products from CMC metabolism can be used by other members of the community, the addition of the one nutrient results in an increase of available metabolites for the functional groups downstream in the carbon flow. Directly stimulating one group of microorganisms indirectly stimulates many other groups, and thus the diversity of active species remains high.

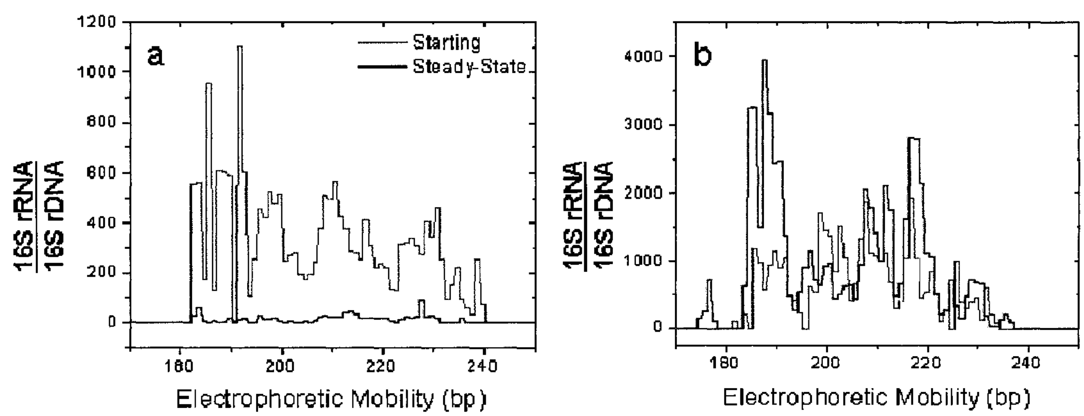

Figure 8.15 – Starting and steady-state 16S rRNA:16S rDNA profile for the (a) CMC 1 and (b) CMC 2 columns biostimulated with carboxymethyl cellulose.

8.4.6.2 Ethanol

The starting 16S rRNA:16S rDNA ratio profile for the columns biostimulated with ethanol (Figure 8.16) were very similar to the starting profiles for the DM columns (Figure 8.8). As mentioned above, the microbial communities of the EtOH and DM columns were expected to be the same. Unlike the CMC-stimulated columns, the active microbial community appears to simplify over the course of the experiment, as the steady-state ratio profile has fewer total and dominant peaks than the starting profiles. This behavior is consistent with the biostimulation of a group of microorganisms at the bottom of the carbon flow (Figure 1.4), such as the SRB in the AMD community, where the added nutrient does not result in a cascade of metabolites for use by other community members.

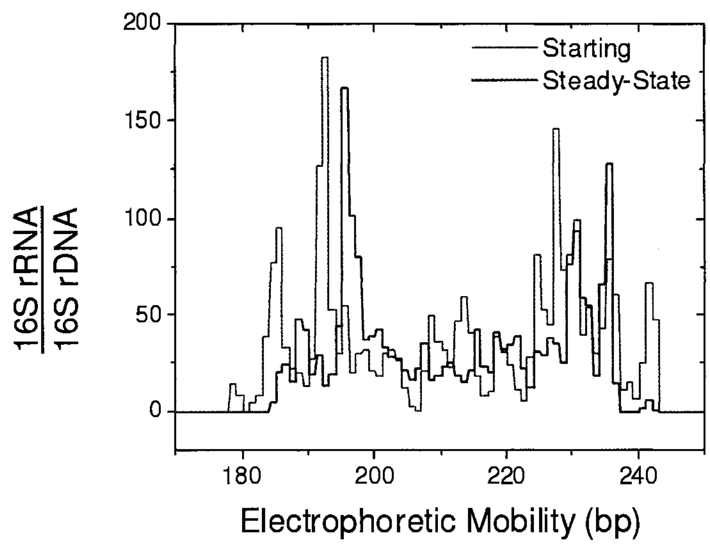

Figure 8.16 - Starting and steady-state 16S rRNA:16S rDNA profile for a column biostimulated with ethanol (EtOH 1).

8.5 Discussion

The similarity between the remediation performances of all the columns was quite surprising. Previous lab-scale SRBRs demonstrated a strong correlation between performance and the starting microbial inoculum (Pruden, Messner et al. 2007; Pereyra, Hiibel et al. 2008), so some performance differences were expected between the various columns of this experiment. One possible explanation for the observed behavior is that the removal of sulfate and metals is primarily a result of abiotic mechanisms, such as sorption, and that the biological remediation in all the columns was negligible during this period. If only metal removal was considered, this explanation may be plausible as the effluent metal concentrations were near zero for the first ~15 days of the experiment before increasing slightly. This behavior would indicate that the metals were adsorbed onto the organic material of the columns. However, the effluent concentrations never reached the feed levels of zinc or cadmium, thus some additional removal continued to occur throughout the course of the experiment. Sorption also fails to explain the pH increases or the sulfate removal, and is thus it is unlikely that this was the sole remediation mechanism.

Another possible explanation for the similarity in performance is that the solid substrate material used to pack the columns had a microbial population that was well suited for the AMD environment and that neither the addition of microorganisms or nutrients was required or necessary for remediation to occur. Although this would also seem an unlikely scenario based on the demonstrated complexity of the microbial communities required for remediation of AMD in other solid substrate-based SRBR (Hallberg and Johnson 2005; Hallberg and Johnson 2005; Logan, Reardon et al. 2005;

Pruden, Messner et al. 2007; Pereyra, Hiibel et al. 2008), it is a possibility. The majority of bacterial species identified in the clone library of the starting dry materials were related to *Pantoea* and *Enterobacter* spp. (Table 8.5), which are known to have cellulolytic (Delalibera, Handelsman et al. 2005) and fermentative capabilities (Holt 1984; Kaufhold and Ferrieri 1991), respectively. It is possible that microbes capable of sulfate reduction were also present in the organic material, but at levels below the detection limits of the methods employed for this work. Other systems treating AMD, SRB have observed to represent a relatively low proportion of the overall microbial community (Johnson and Hallberg 2003; Hallberg and Johnson 2005; Moraeles 2005), so it is conceivable that all of the species necessary for remediation were present, just not detected.

8.6 Conclusions

This study evaluated the effects of bioaugmentation and biostimulation on biological AMD remediation and the microbial community associated with the treatment. Despite the differences in fed organic materials and the starting microbial communities, the remediation performance of all the columns was nearly identical. At steady-state, each column removed more than 50% of the fed sulfate, cadmium, and zinc, and all columns increased the pH to near neutral.

Although the columns all had similar remediation performances, the overall structure and the active species of their microbial communities at steady-state were significantly different, as determined by ACP. The diversity and number of active species in the columns augmented with cellulose degraders and stimulated with carboxymethyl cellulose were much greater after six weeks of operation than in the starting communities. The opposite trend was observed in columns stimulated with sulfate reducers, where the number of active species in the starting community was much larger than at the end of the experiment. These results demonstrate that targeting the top level of the ecological carbon chain via either biostimulation or bioaugmentation can increase the activity of a larger portion of the microbial community than can be achieved by targeting the lower levels of the carbon chain. The increase in diversity may offer redundancy of functional groups within the bioreactor, and thus improved resilience to system perturbations and stresses. Additional tests are currently underway to evaluate the robustness of the twelve columns to oxygen exposure (Chapter 10), which will give additional insight into potential benefits of bioaugmentation or biostimulation for the biological AMD remediation systems.

ACP analysis also indicated that the majority of the species bioaugmented into the columns flourished in the bioreactors and were dominant members of the active community after six weeks. The proliferation of the augmented species under AMD conditions is a critical finding, considering most bioaugmentation failures are due to low survival rates of added species. It is also important to note that the ability to easily differentiate the biostimulated species from the rest of the microbial community and to characterize them as active members of the community in a single assay is unique to ACP, demonstrating the utility of this method for complex microbial systems.

This work is the first systematic examination of the relationships between bioreactor remediation performance, the active microbial community, and the parallel use of bioaugmentation and biostimulation in AMD bioremediation systems. Although no correlations could be made to bioremediation performance, bioaugmentation and biostimulation had dramatic effects on the structure of the active microbial communities. The applied research approach may be beneficial to advancing the understanding of other microbially driven systems, thereby progressing towards the integration of microbial community dynamics with bioreactor design.

8.7 Acknowledgements

Financial assistance was provided by the National Science Foundation Award CBET-0651947. Additional funding was provided by the EPA Office of Research and Development's Engineering Technical Support Center, under contract with Golder Associates, Inc., Contract # GS-10F00130N DO #1101 (David Reisman, Project Officer; reisman.david@epa.gov); and by the Water Research Experience for Undergraduates program at CSU sponsored by the National Science Foundation. The authors wish to thank B. Crimi and M.V. Prieto for their assistance in with the CE-SSCP analysis and the clone library construction, respectively.

8.8 References

(1994). "Method 3015: Microwave Assisted Acid Digestion of Aqueous Samples and Extracts." Test Methods for Evaluating Solid Waste, Physical/Chemical Methods. Retrieved November 16, 2005, from http://www.epa.gov/epaoswer/hazwaste/test/pdfs/3015.pdf.

(1996). Hardrock Mining Framework: Final Draft, United States Environmental Protection Agency, Washington DC: 66.

(1998). "Cleaning up Abandon Mines: A Western Partnership." Retrieved October 16, 2005, 2005, from http://www.westgov.org/wga/publicat/miningre.pdf.

Atlas, R. M. (1997). Handbook of Microbiological Media. Boca Raton, FL, CRC Press.

Badger, P. C. (2002). Ethanol From Cellulose: A General Review. Trends in New Crops and New Uses. J. J. a. A. Whipkey. Alexandria, VA, ASHS Press: 17-21.

Benner, S. G., D. W. Blowes, et al. (1997). "A full-scale porous reactive wall for prevention of acid mine drainage." Ground Water Monitoring and Remediation **17**(4): 99-107.

Bouchez, T., D. Patureau, et al. (2000). "Ecological study of a bioaugmentation failure." Environmental Microbiology **2**(2): 179-190.

Brosius, J., T. J. Dull, et al. (1981). "Gene Organization and Primary Structure of a Ribosomal-Rna Operon from Escherichia-Coli." Journal of Molecular Biology **148**(2): 107-127.

Cabirol, N., J. Perrier, et al. (1995). "Role of Methanogenic and Sulfate-Reducing Bacteria in the Reductive Dechlorination of Tetrachloroethylene in Mixed Culture." Bulletin of Environmental Contamination and Toxicology **56**: 817-824.

Christensen, B., M. Laake, et al. (1996). "Treatment of Acid Mine Water by Sulfate-Reducing Bacteria: Results from Bench Scale Experiments." Water Research **30**(7): 1617-1624.

Cunningham, C., C. A. McPherson, et al. (1991). "Sequence of a Cellulase Gene from the Rumen Anaerobe Ruminococcus-Flavefaciens 17." Molecular & General Genetics **228**(1-2): 320-323.

Da Silva, M. L. B. and P. J. J. Alvarez (2004). "Enhanced anaerobic biodegradation of benzene-toluene-ethylbenzene-xylene-ethanol mixtures in bioaugmented aquifer columns." Applied and Environmental Microbiology **70**(8): 4720-4726.

Delalibera, I., J. Handelsman, et al. (2005). "Contrasts in Cellulolytic Activities of Gut Microorganisms Between the Wood Borer, *Saperda vestita* (Coleoptera; Cerambycidae), and the Bark Beetles, *Ips pini* and *Dendroctonus frontalis* (Coleoptera: Curculionidae)." Environmental Entomology **34**(3): 541-547.

El Fantroussi, S. and S. N. Agathos (2005). "Is bioaugmentation a feasible strategy for pollutant removal and site remediation?" Current Opinion in Microbiology **8**(3): 268-275.

Engelstad, O.P. and G. L. Terman (1966). "Fertilizer Nitrogen - Its Role in Determining Crop Yield Levels." Agronomy Journal **58**(5): 536-&.

EPA, U. S. (2005). Mine Waste Technology Program 2005 Annual Report, U.S. Environmental Protection Agency National Risk Management Research Laboratory and U.S. Department of Energy Environmental Management Consolidated Business Center. **DW89939897-01-0**.

Fageria, N. K., V. C. Baligar, et al. (2008). "The role of nutrient efficient plants in improving crop yields in the twenty first century." Journal of Plant Nutrition **31**(6): 1121-1157.

Flynn, S. J., F. E. Loffler, et al. (2000). "Microbial community changes associated with a shift from reductive dechlorination of PCE to reductive dechlorination of *cis*-DCE and VC." Environmental Science & Technology **34**(6): 1056-1061.

GrechMora, I., M. L. Fardeau, et al. (1996). "Isolation and characterization of *Sporobacter termitidis* gen nov sp nov, from the digestive tract of the wood-feeding termite *Nasutitermes lujae*." International Journal of Systematic Bacteriology **46**(2): 512-518.

Hallberg, K. B. and D. B. Johnson (2005). Microbial Populations of Compost Wetlands Constructed To Remediate Acidic Coal Spoil Drainage. 16th International Biohydrometallurgy Symposium (IBS), Cape Town, South Africa.

Hallberg, K. B. and D. B. Johnson (2005). "Microbiology of a Wetland Ecosystem Constructed to Remediate Mine Drainage from a Heavy-Metal Mine." Science of the Total Environment **338**: 53-66.

Han, S. O., H. Yukawa, et al. (2003). "Regulation of expression of cellulosomal cellulase and hemicellulase genes in *Clostridium cellulovorans*." Journal of Bacteriology **185**(20): 6067-6075.

Hiibel, S. R., L. P. Pereyra, et al. (2008). "Microbial Community Analysis of Two Field-Scale Sulfate-Reducing Bioreactors Treating Mine Drainage." Environmental Microbiology **10**(8): 2087-2097.

Holt, J. H., ed. (1984). Bergey's Manual of Systematic Bacteriology Baltimore, Williams & Wilkins.

Johnson, D. B. and K. B. Hallberg (2003). "The Microbiology of Acidic Mine Waters." Research in Microbiology **154**(7): 466-473.

Jong, T. and D. L. Parry (2006). "Microbial sulfate reduction under sequentially acidic conditions in an upflow anaerobic packed bed bioreactor." Water Research **40**(13): 2561-2571.

Kaufhold, A. and P. Ferrieri (1991). "Isolation of *Enterococcus mundtii* from Normally Sterile Body Sties in Two Patients." Journal of Clinical Microbiology **29**(5): 1075-1077.

Lendvay, J. M., F. E. Loffler, et al. (2003). "Bioreactive barriers: A comparison of bioaugmentation and biostimulation for chlorinated solvent remediation." Environmental Science & Technology **37**(7): 1422-1431.

Loffler, F. E., Q. Sun, et al. (2000). "16S rRNA gene-based detection of tetrachloroethene-dechlorinating *Desulfuromonas* and *Dehalococcoides* species." Applied and Environmental Microbiology **66**(4): 1369-1374.

Logan, M. V., K. F. Reardon, et al. (2005). "Microbial Community Activities During Establishment, Performance, and Decline of Bench-Scale Passive Treatment Systems for Mine Drainage." Water Research **39**: 4537-4551.

Lyon, J. S., T. J. Hilliard, et al. (1993). Burden of Gilt: The legacy of environmental damage from abandoned mines, and what America should do about it. Washington, D.C., Mineral Policy Center.

Mandenius, C. F., B. Nilsson, et al. (1988). "Kinetic models for enzymatic cellulose degradation in aqueous two-phase systems." Biotechnology and Bioengineering **31**(3): 203-207.

MaymoGatell, X., Y. T. Chien, et al. (1997). "Isolation of a bacterium that reductively dechlorinates tetrachloroethene to ethene." Science **276**(5318): 1568-1571.

Moraeles, T. A., M.,Dopson, R., Athar, and R.B., Herbert Jr. (2005). "Analysis of Bacterial Diversity in Acidic Pond Water and Compost After Treatment of Artificial Acid Mine Drainage for Metal Removal." Biotechnology and Bioengineering **90**(5): 543-551.

Pereyra, L. P., S. R. Hiibel, et al. (2008). "Comparison of Microbial Community Inocula Composition and Activity in Sulfate-Reducing Batch Systems Remediating Mine Drainage." Biotechnology and Bioengineering ***In Press,*** **DOI: 10.1002/bit.21930**.

Postgate, J. R. (1984). The sulphate-reducing bacteria. Cambridge, Cambridge University Press.

Pruden, A., N. Messner, et al. (2007). "The effect of inoculum on the performance of sulfate-reducing columns treating heavy metal contaminated water." Water Research **Volume 41**(4): 904-914.

Rousseaux, S., A. Hartmann, et al. (2003). "Inoculation of an atrazine-degrading strain, *Chelatobacter heintzii Citl*, in four different soils: effects of different inoculum densities." Chemosphere **51**(7): 569-576.

Singer, P. C. and W. Stumm (1970). "Acidic Mine Drainage: The Rate-Determining Step." Science **167**(3921): 1121-1123.

Smith, A. E., K. Hristova, et al. (2005). "Comparison of biostimulation versus bioaugmentation with bacterial strain PM1 for treatment of groundwater contaminated with methyl tertiary butyl ether (MTBE)." Environmental Health Perspectives **113**(3): 317-322.

Tsukamoto, T. K. and G. C. Miller (1999). "Methanol as a Carbon Source for Microbiological Treatment of Acid Mine Drainage." Water Research **33**(6): 1365-1370.

van Veen, J. A., L. S. van Overbeek, et al. (1997). "Fate and Activity of Microorganisms Introduced into Soil." Microbiology and Molecular Biology Reviews **61**(2): 121-135.

Waybrant, K. R., C. J. Ptacek, et al. (2002). "Treatment of Mine Drainage Using Permeable Reactive Barriers: Column Experiments." Environmental Science and Technology **36**: 1349-1356.

Weimer, P. J. and C. L. Odt (1995). "Cellulose degradation by ruminal microbes: Physiological and hydrolytic diversity among ruminal cellulolytic bacteria." Enzymatic Degradation of Insoluble Carbohydrates **618**: 291-304.

Weisburg, W. G., S. M. Barns, et al. (1991). "16S Ribosomal DNA Amplification for Phylogenetic Study." Journal of Bacteriology **173**(2): 697-703.

Yadav, V. K. and D. B. Archer (1989). "Sodium molybdate inhibits sulphate reduction in the anaerobic treatment of high-sulphate molasses wastewater." Applied Microbiology and Biotechnology **31**: 103-106.

Chapter 9 Conclusions

This results of the research projects presented in this dissertation have emphasized the importance of the microbial community associated with acid mine drainage (AMD) remediation and have furthered the understanding of these communities.

Using 16S rDNA-based profiling, a relationship between the choice of microbial inoculum and remediation performance was first identified in laboratory-scale columns treating AMD. A separate, systematic follow-up analysis examining the relationship between microbial community composition and remediation capabilities confirmed that the community of sulfate-reducing bioreactors (SRBRs) affected remediation performance. Further 16S rDNA-based analyses also established that SRBRs that performed well all contained a common set of three key functional groups in their microbial communities: cellulose degraders, fermenters, and sulfate-reducing bacteria (SRB). Despite the SRB's direct involvement in the remediation reactions, and thus their importance to SRBR performance, quantitative methods revealed that they were present at concentrations near or below detection limits of traditional 16S profiling techniques. It was therefore determined that a more appropriate biomolecular target was necessary to accurately profile the sulfate reducers in the overall microbial community.

In subsequent analyses of pilot- and field-scale SRBRs, both the 16S gene and the *apsA* functional gene were targeted. The *apsA* gene catalyzes the reduction of sulfate to sulfite and is found in all SRB. The analysis of the specific functional gene allowed for higher resolution of an important but numerically small subset of the overall community. Multivariate statistical analyses were used to compare *apsA* and 16S gene clone sequences obtained from the bioreactors, which allowed for objective and statistically valid conclusions. Although the 16S gene analyses did not reveal obvious differences between the overall microbial communities of the two field-scale bioreactors, the *apsA* gene-containing portions of the two SRBR were significantly different from each other. Examination of the *apsA* clone library revealed the presence of *Thiobacillus* spp., which are capable sulfide oxidation and thus reversal of the remediation process, at the field-scale SRBR with poor remediation performance. While these studies confirmed the utility using a functional gene to target a subset of the overall microbial community, it was also clear that the conclusions that could be drawn varied depending on the choice of biomolecular target.

Although the identification studies were important first steps to understanding the microbial ecology of AMD bioremediation, they did not provide information regarding which species were actively involved in the remediation process. Knowledge of the active community members is critical from an engineering perspective, and thus a novel biomolecular method was developed to identify those active species.

Active community profiling (ACP) takes advantage of the correlation between a cell's growth rate and its ratio of cellular rRNA to rDNA to determine which members of a mixed culture are actively growing and which microorganisms are dormant. ACP has application well beyond AMD remediation, and can be used to study any type of mixed microbial community. Because of its high throughput nature, ACP can also be used to track a mixed community at a biologically relevant time-scale to determine how the activated members change in response to environmental factors. When coupled with traditional physiochemical analysis, the method offers a powerful new tool to help understand the community dynamics at the microbial scale.

ACP was employed to explore the effect of bioaugmentation and biostimulation on the performance and microbial communities of laboratory-scale SRBRs treating AMD. Columns were bioaugmented with two different groups of microorganisms and two different carbon sources were used to stimulate the microbial community. The results were unexpected in that all of the columns performed similarly from a remediation perspective. However, ACP analysis revealed that the active members of the columns' microbial communities were distinctive. It was determined that stimulation or augmentation at the top of the microbial carbon chain resulted in increased diversity of the active microbial species, which can potentially result in a more robust community. In an ongoing study, the columns were been exposed to oxygen to simulate an environmental stress to evaluate whether the increased diversity observed in this study results in improved resistance to the stress.

The research projects presented in this dissertation have emphasized the role of the microbial community associated with AMD remediation. Characterization of these microbial communities with a multitude of biomolecular tools at several scales has significantly advanced the understanding of the community's structure, function, and activity. The coupling of this microbial-level understanding with macro-level remediation performance information has also furthered the integration of microbial community dynamics with bioreactor design. The research approaches and methodologies developed in this dissertation have a wide range of application, and have provided unique and valuable contributions to the body of scientific knowledge of AMD treatment specifically and to microbial ecology and bioremediation in general.

Chapter 10 Opportunities for Future Work

Future research efforts should continue to improve the understanding of the microbial community of acid mine drainage (AMD) bioremediation with the ultimate goal of predictive design and operation of high-performance sulfate-reducing bioreactors (SRBRs). The column experiment discussed in Chapter 8 offers a unique opportunity towards this goal. For remediation treatment such as SRBRs to be viable and truly passive options, they must be robust enough to withstand the perturbations and stresses likely to be experience in a field employment. A current, yet untested hypothesis regarding such stress events is that increased phylogenetic diversity levels in the microbial community will correspond to functional redundancies and thus an increased tolerance to withstand system perturbations. Two common stresses that AMD remediation sites are frequently subjected to, and that can be easily simulated with the column setup of Chapter 8, are periods of oxygen exposure and elevated metals loading. Thus, the response of the column microbial communities to an oxygen stress or metals loading would be a valuable next study. Chemical and ACP analyses, as described in Chapter 8, of the existing columns after the stress would provide the information necessary to determine several parameters that are central to the proper design of SRBRs: the time required to return to a steady-state remediation level, how the new steady-state remediation compares to pre-stress performance, and the effect of the stress on the structure and active members of the microbial community. It is conceivable that the same stress event could be repeated with the given columns to evaluate the effects of repetitive stresses, or else a different stress could be applied.

Another area of future research involves the further development of the ACP method. The results of Chapters 5 and 6 indicate that the use of multiple biomolecular targets can improve the resolution of specific subsets of the microbial community and gives additional information that can factor into the conclusions drawn from an experiment. Thus, a logical next step in the evolution of ACP would be its application to functional genes of interest, which in the context of AMD remediation would include genes associated with or directly catalyzing cellulose degradation, fermentation, and sulfate reduction. When performed in parallel with the 16S gene-based ACP described in Chapters 7 & 8, functional gene ACP could be used to identify the active members of the overall microbial community and of specific subsets therein. An extension to the hypothesis that increased phylogenetic diversity correlates with robustness is that the increased diversity of specific functional groups dictates the overall community's ability to tolerate stress. Because cellulose degradation is considered the rate-limiting step in lignocellulosic SRBRs, a reasonable hypothesis would be that increased phylogenetic diversity of the cellulose-degrading portion of the SRBR community will result in an increased tolerance to stress. The functional gene-based ACP approach, in parallel with chemical performance data, would provide the necessary information to evaluate this extended hypothesis and others like it. Because the CE instrument uses fluorescence for detection, it is plausible that the 16S and multiple functional genes could be simultaneously targeted using different primer pairs and then analyzed simultaneously, although primer pair compatibility would be a challenge. This multi-plex approach would allow for an even higher throughput of sample analyses, making the ACP an even more attractive method for evaluating complex microbial communities.

The final area of future research also involves further improvement of the resolution of ACP, especially for the 16S-based evaluation of complex environmental samples. Traditional methods for improving CE resolutions typically involve the optimization of parameters such as the composition of the polymer mixture and buffers or adjusting the temperature and voltage profiles throughout the analysis run time. While the exploration of these parameters should be considered, it is unlikely that any single CE method will be capable of adequately resolving the number of species commonly found in environmental samples. As with any analytical technique, the utility of ACP is dramatically affected by its detection limitations, thus improving its resolution is an important goal. A potential approach to improving resolution is to couple the CE instrument with mass spectrometer (MS). With this approach, CE would be used as a preliminary separation technique and the downstream MS would be used to distinguish co-eluting species. Similar couplings between liquid chromatography (LC) systems and MS are currently available, thus CE-MS is logistically feasible. Because the current size of the single-stranded DNA fragments that are eluted from the CE instrument (~220 bp) is on the upper bounds for most MS systems, inconsistent ionization and fragmentation of the nucleic acids may render spectra analysis challenging.

Appendix A Detailed Protocols and Methods

A.1 DNA Extraction

A.1.1 PowerMax™ Soil DNA Isolation Kit

MoBio Catalog # 12988-10

1. Add 15 mL of PowerBead Solution to a PowerBead Tube.
2. Add approximately 5 g of sample to the PowerBead Tube and vortex vigorously for 1 min.
   Note: Record mass of sample is used.
3. Add 1.2 mL of Solution C1 to the PowerBead Tube and vortex vigorously for 30 sec.
   Note: Check Solution C1 – if it is precipitated, heat the solution at 60°C until the precipitate has dissolved.
4. Place PowerBead Tube on the MoBio vortex adapter and vortex for 5 min at the maximum speed (10).
5. Centrifuge tubes at 2500 x *g* for 3 min at room temperature.
6. Transfer supernatant to a clean Collection Tube.
   Note: The supernatant may still contain some soil particles and color.
7. Add 5 mL of Solution C2 and invert twice to mix. Incubate at 4 °C for 10 min.
8. Centrifuge tubes at 2500 x g for 4 min at room temperature.
   Note: Centrifuge longer if pellet does not appear stable.
9. Avoiding pellet, transfer supernatant to a clean Collection Tube.
10. Add 4 mL of Solution C3 and invert twice to mix. Incubate at 4 °C for 10 min.
11. Centrifuge tubes at 2500 x *g* for 4 min at room temperature.
    Note: Centrifuge longer if pellet does not appear stable.
12. Avoiding pellet, transfer supernatant to a clean Collection Tube.
13. Add 30 mL of Solution C4 to supernatant and invert twice.
14. Fill Spin Filter with solution from Step 13. Centrifuge at 2500 x *g* for 2 min at room temperature. Discard flow through and add second volume of supernatant to same Spin Filter and centrifuge at 2500 x *g* for 2 min at room temperature. Discard flow through. Repeat until entire volume has been processed.
15. Add 10 mL of Solution C5 to Spin Filter and centrifuge at 2500 x *g* for 3 min at room temperature. Discard flow through.
16. Centrifuge Spin Filter at 2500 x *g* for 5 min at room temperature.
17. Carefully place Spin Filter in a new Collection Tube.
    Note: Avoid splashing Solution C5 onto Spin Filter.
18. Add 5 mL of Solution C6 to the center of Spin Filter membrane. Let sit at room temperature for 2 min. Centrifuge at 2500 x *g* for 3 min at room temperature

19. Discard Spin Filter. The DNA in the tube is now ready for any downstream application.
20. Using filter tips in the laminar flow hood, aliquot out the DNA extract into five 2-mL O-ring tubes. Also transfer 100 uL aliquots into two 0.5-mL O-ring tubes for use as working stock.
21. Store in -80 °C freezer.

A.1.2 UltraClean™ Soil DNA Isolation Kit

MoBio Catalog # 12800-50

1. Add 0.25 – 1 gm of sample to the 2mL Bead Solution tubes provided
   Note: Typically use ~0.5 gm/mL. Record mass of sample used.
2. Gently vortex to mix.
3. Add 60 uL of Solution S1 and invert several times or vortex briefly.
   Note: Check Solution S1 – if it is precipitated, heat solution to 60 °C until dissolved before use.
4. Add 200 uL of Solution IRS (Inhibitor Removal Solution).
5. Bead beat for 3 min at 'homogenize' setting
6. Centrifuge tubes at 10,000 x *g* for 30 sec.
   Note: Do not to exceed 10,000 x g or tubes may break.
7. Transfer the supernatant to a clean microcentrifuge tube.
8. Add 250 uL of Solution S2 and vortex for 5 sec. Incubate 4 °C for 5 min.
9. Centrifuge the tubes for 1 min at 10,000 x g.
10. Avoiding the pellet, transfer entire volume of supernatant to a clean microcentrifuge tube.
11. Add 1.3mL of Solution S3 to the supernatant and vortex for 5 sec.
    Note: Use 15 mL conical tubes if there is not enough room in the small tube.
12. Load 700 uL onto a spin filter and centrifuge at 10,000 x *g* for 1 min. Discard the flow through, add the remaining supernatant to the spin filter, and centrifuge at 10,000 x *g* for 1 min. Repeat until all supernatant has passed through the spin filter.
13. Add 300 uL of Solution S4 and centrifuge for 30 sec at 10,000 x *g*. Discard the flow through.
14. Centrifuge at 10,000 x *g* for 1 min.
15. Carefully place spin filter in a new clean tube.
    Note: Avoid splashing any Solution S4 onto the spin filter.
16. Add 50 uL of Solution S5 to the center of the white filter membrane and allow to sit for 1 min.
17. Centrifuge for 30 sec.
18. Discard the spin filter. DNA in the tube is now application ready.
19. Using filter tips in the laminar flow hood transfer DNA into a 0.5-mL O-ring tube. From there, transfer one 10-uL aliquots to a 0.5-mL O-ring tubes tube for use as working stock.
20. Store in -80 °C freezer.

A.1.3 UltraClean™ Microbial DNA Isolation Kit

MoBio Catalog # 12224-50

1. Using filter tips in the laminar flow hood, add 1.8 mL of liquid culture to a 2 mL Collection Tube.
   Note: Make sure that the cultures are well mixed before taking sample. Record the volume of culture added.
2. Centrifuge at 10,000 x *g* for 5 min at room temperature. Decant the supernatant and spin the tubes at 10,000 x *g* for 1 min at room temperature and completely remove the media supernatant with a pipette tip.
   Note: Depending on the type of microbial culture, it may be necessary to centrifuge longer.
3. Resuspend the cell pellet in 300 uL of MicroBead Solution and gently vortex to mix. Transfer resuspended cells to MicroBead Tube.
4. Add 50 uL of Solution MD1 to the MicroBead Tube.
5. Bead beat for 3 min at 'homogenize' setting.
6. Centrifuge the tubes at 10,000 x *g* for 30 sec at room temperature.
   Note: Do not exceed10,000 x *g* or tubes may break.
7. Transfer all the supernatant to a clean 2 mL Collection Tube.
8. Add 100 uL of Solution MD2 to the supernatant, vortex for 5 sec to mix, then incubate at 4 °C for 5 min.
9. Centrifuge the tubes at room temperature for 1 min at 10,000 x *g*.
10. Avoiding the pellet, transfer the entire volume of supernatant to a clean 2 mL Collection Tube.
11. Add 900 uL of Solution MD3 to the supernatant and vortex 5 sec.
12. Load about 700 uL into the Spin Filter and centrifuge at 10,000 x *g* for 30 sec at room temperature. Discard the flow through, add the remaining supernatant to the Spin Filter, and centrifuge at 10,000 x *g* for 30 sec at room temperature.
    Note: A total of 2 - 3 loads for each sample processed are required. Discard all flow through liquid.
13. Add 300 uL of Solution MD4 and centrifuge at room temperature for 30 sec at 10,000 x *g*. Discard the flow through.
14. Centrifuge at room temperature for 1 min at 10,000 x *g*.
15. Being careful not to splash liquid on the spin filter basket, place Spin Filter in a new 2 mL Collection Tube.
16. Add 50 uL of Solution MD5 to the center of the white filter membrane allow to sit for 1 min.
17. Centrifuge at room temperature for 30 sec at 10,000 x *g*.
18. Discard Spin Filter.
21. Using filter tips in the laminar flow hood transfer DNA into a 0.5-mL O-ring tube. From there, transfer one 10-uL aliquots to a 0.5-mL O-ring tubes tube for use as working stock.
22. Store in -80 °C freezer.

A.2 RNase Treatment

Use RNase ONE Ribonuclease (Promega Catalog # 74104)

- Master mix
    - 1 uL Nuclease free water
    - 1 uL 10X Buffer
    - 4 uL RNase
- Add to Master mix
    - 4 uL DNA extract
- Incubate at 37 °C for 45 min

A.3 RNA Extraction

A.3.1 RNeasy Mini Kit

Qiagen Catalog # M4261

1. Prepare TE buffer with 2.5 mg/mL lysozyme
2. Prepare Buffer RLT with 10 uL/mL beta-mercaptoethanol
   Note: Add 4 volumes of 200 proof ethanol to Buffer RPE the first kit use
3. 1.8 mL sample – centrifuge at 5,000 g for 10 min – decant supernatant and blot tube
4. Add 200 uL of TE buffer (with lysozyme)
5. Vortex for 5 min at 1,250 rpm
6. Add 700 uL of Buffer RLT (with □-mercaptoethanol) – vortex
   - Centrifuge and use only supernatant if particulate material present
7. Add 500 uL of ethanol - vortex
8. Load 700 uL into spin column
9. Centrifuge at 8,000 g for 15 sec – repeat as necessary
10. Add 700 uL of Buffer RW1 - centrifuge at 8,000 g for 15 sec
11. Transfer to new collection tube
12. Add 500 uL of Buffer RPE - centrifuge at 8,000 g for 15 sec
13. Add 500 uL of Buffer RPE - centrifuge at 8,000 g for 2 min
14. Transfer to 1.5 mL tube
15. Add 50 uL of RNase-free water to center of filter membrane
16. Centrifuge at 8,000 g for 1 min
17. Discard filter membrane and transfer to 0.2 mL O-ring tube for storage at -80 °C

A.3.2 RNA PowerSoil™ Total RNA Isolation Kit Protocol

MoBio Catalog # 12866-25

Phenol:chloroform:isoamyl alcohol solution

- 25 parts purified phenol
- 24 parts chloroform
- 1 part isoamyl alcohol

Solution can be stored under TE buffer (or 0.1M Tris, pH 8. 0) for up to 3 months at 4 °C in an amber bottle.

1. Add 1.0 – 2.0 g of soil to the 15 mL Bead Tube.
2. Add 2.5 mL of Bead Solution to the Bead Tube and vortex to mix.
3. Add 0.25 mL of Solution SR1 to the Bead Tube and vortex to mix.
4. Add 0.8 mL of Solution SR2 to the Bead Tube and vortex at maximum speed for 5 min.
5. Remove the Bead Tube and add 3.5 mL of phenol:chloroform:isoamyl alcohol solution.
6. Vortex to mix until the biphasic layer disappears.
7. Vortex the Bead Tube at maximum speed for an additional 10 min.
8. Remove the Bead Tube and centrifuge at 2500 x *g* for 10 min at room temperature.
9. Transfer the upper aqueous phase (avoiding the interphase and lower phenol layer) to a clean 15 mL collection tube.
    a. Discard the phenol:chloroform:isoamyl alcohol in an approved waste receptacle.
    b. The biphasic layer will be thick and firm in soils high in organic matter and may need to be pierced to remove the bottom phenol layer.
10. Add 1.5 mL of Solution SR3 to the aqueous phase and vortex to mix.
11. Incubate at 4 °C for 10 min.
12. Centrifuge at 2500 x g for 10 min at room temperature.
13. Transfer the supernatant (without disturbing the pellet) to a new 15 mL collection tube.
14. Add 5 mL of Solution SR4 to the collection tube containing the supernatant, vortex to mix, and incubate at -20 °C for 30 min.
15. Centrifuge at 2500 x *g* for 30 min at room temperature.
16. Decant the supernatant and invert the 15 mL collection tube on a sterile paper towel for 5 min.
    a. Depending on soil type, the pellet may be large and/or dark in color.
17. Add 1 mL of Solution SR5 to the 15 mL collection tube and resuspend the pellet completely.
    a. Resuspension may be aided by placing the tubes in a heat block or water bath at 45 °C for 10 min, followed by vortexing. Repeat until the pellet is resuspended.
18. Prepare one RNA Capture Column for each RNA Isolation Sample:
    a. Remove the cap of a 15 mL collection tube and place the RNA Capture Column inside the 15 mL collection tube. The column will hang in the 15 mL tube.

   b. Add 2 mL of Solution SR5 to the RNA Capture Column and allow it to gravity flow through the column and collect in the 15 mL Collection tube. Allow Solution SR5 to completely flow through the column
      i. Do NOT allow the column to dry out prior to loading the RNA isolation sample.
19. Add the RNA Isolation Sample from Step 15 onto the RNA Capture Column and allow it to gravity flow through the column.
   a. Collect the flow through in the 15 mL Collection Tube.
20. Wash the column with 1 mL of Solution SR5.
   a. Allow it to gravity flow and collect the flow through in the 15 mL Collection tube.
21. Transfer the RNA Capture Column to a new 15 mL collection tube and add 1 mL of Solution SR6 to the RNA Capture Column to elute the bound RNA into the 15 mL Collection tube.
22. Allow Solution SR6 to gravity flow into the 15 mL Collection Tube.
23. Transfer the eluted RNA to a 2.2 mL collection tube and add 1 mL of Solution SR4.
24. Invert to mix and incubate at -20 °C for 10 min.
25. Centrifuge the 2.2 mL collection tube at 13,000 x g for 15 min at room temperature to pellet the RNA.
26. Decant the supernatant and invert the 2.2 mL collection tube onto a sterile paper towel for 10 min to air dry the pellet.
27. Resuspend the RNA pellet in 100 µL of Solution SR7.

A.4 DNase Treatment

Using RQ1 RNase-Free DNase (Promega Catalog # M6101)

1. Master mix (per sample)
   - 1 uL of nuclease free water
   - 1 uL of 10X Rq1 DNase Buffer
   - 4 uL of DNase
2. Add to master mix
   - 4 uL of RNA extract
3. Incubate at 37 °C for 30 min.
4. Add 1 uL of Stop Solution.
5. Incubate at 65 °C for 10 min.

A.5 Reverse Transcription

Using AMV Reverse Transcriptase (Promega Catalog # M5101)

1. Pre-warm the Na4P2O7 to 42 °C
2. Master mix #1
   - 2 uL of nuclease free water
   - 1 uL of W104R-6FAM primer

3. Add to master mix #1
    - 3 uL of DNase treated RNA
4. In thermal cycler
    - 70 °C for 5 min
    - 4 °C for 5 min
    - Hold at 4 °C
5. Master mix #2
    - 5 uL of 5X Buffer
    - 2.5 uL of dNTPs
    - 2.5 uL of $Na_4P_2O_7^+$
    - 7.5 uL of nuclease free water
6. Add 17.5 uL of master mix #2 to RNA mixture
7. Add 1.5 uL of AMV RT
8. In thermal cycler
    - 50 °C for 60 min
    - Hold at 4 °C

A.6 Polymerase Chain Reaction

The primers and thermal cycler programs used for PCR amplification of nucleic acids are listed in Tables A.1 and A.2, respectively. With two exceptions (M13f/M13r and W49f/W104r-6FAM), the reaction included:

- 5.0 uL 5X TaqMaster PCR Enhancer (5 Prime, Gaithersburg, MD)
- 2.5 uL 10X Taq buffer (5 Prime)
- 5 pM of each dNTP (5 Prime)
- 0.25 pM of each primer
- 0.25 uL formamide
- 1.75 U *Taq* DNA polymerase (5 Prime)
- Magnesium (25 mM as Mg^{2+}, 5 Prime), as needed
- Sterile deionized water to 24 uL
- 1 uL nucleic acid template

The magnesium was often added as a cofactor for the *Taq* DNA polymerase to aid in the amplification process of samples with PCR inhibitors.

The master mix for the M13f/M13r PCR included:

- 15.9 uL sterile deionized water
- 5.0 uL 5X TaqMaster PCR Enhancer (5 Prime)
- 2.5 uL 10X reaction buffer (GenScript)
- 0.5 uL dNTP mix (10 mM, 5 Prime)
- 0.25 uL M13r primer
- 0.25 uL M13f primer
- 0.25 uL formamide
- 0.35 uL *Taq* DNA polymerase (5 U/uL, GenScript)

- 1 clone colony (harvested with sterile pipette tip)

The master mix for the W49f/W104r-6FAM PCR included:

- 12.4 uL sterile deionized water
- 2.0 uL 10X *Pfu* Turbo Buffer
- 0.4 uL dNTP mix (10 mM, 5 Prime)
- 2.0 uL W49f (5 uM)
- 2.0 uL W104r-6FAM (5 uM)
- 0.2 uL *Pfu Turbo*® DNA polymerase (2.5 U/uL, Stratagene)

Table A.1 – Names, sequences, and targets of primers used.

Primer	Sequence 5' to 3'	Target	Reference
1492r	GGT TAC CTT GTT ACG ACT T	Bacteria 16S gene	Weisburg et al. (1991)
8f	AGA GTT TGA TCC TGG CTC AG	Bacteria 16S gene	Weisburg et al. (1991)
M13F	GTA AAA CGA CGG CCA GT	Cloning Plasmid Insert	Lau and Spencer (1982)
M13R	AAC AGC TAT GAC CAT G	Cloning Plasmid Insert	Lau and Spencer (1982)
U341F	CCT ACG GGR SGC AGC AG	Universal 16S gene	Hansen et al. (1998); Baker and Cowen (2004); Klocke et al. (2007)
U515F	GTG CCA GCM GCC GCG GTA A	Universal 16S gene	Reysenbach et al. (1992); Baker and Cowen (2004)
DGGEf (341fGC)	CGC CCG CCG CGC GCG GCG GGC GGG GCG GGG GCA CGG GGG GCC TAC GGG AGG CAG CAG	Bacteria 16S gene	Muyzer et al. (1993)
DGGEr (533r)	ATT ACC GCG GCT GCT GG	Bacteria 16S gene	Muyzer et al. (1993)
I-341fGC	CGC CCG CCG CGC GCG GCG GGC GGG GCG GGG GCA CGG GGG GCC TAC GGG IGG CIG CA	Bacteria 16S gene	Watanabe et al. (2001)
I-533r	TIA CCG III CTI CTG GCA C	Bacteria 16S gene	Watanabe et al. (2001)
W104r-6FAM	[6-FAM] TTA CCG CGG CTG CTG GCA C	Universal 16S gene	Delbes et al. (2001)
W49f	ACG GTC CAG ACT CCT ACG GG	Bacteria 16S gene	Delbes et al. (2001)
apsA-7f	GGG YCT KTC CGC YAT CAA YAC	adenosine 5'-phosphosulfate reductase (*apsA*)	Friedrich (2002)
apsA-8r	GCA CAT GTC GAG GAA TCT TC	adenosine 5'-phosphosulfate reductase (*apsA*)	Friedrich (2002)
mcrA1035f	GGT GGT GTM GGA TTC ACA CAR TAY GCW ACA GC	methyl coenzyme-M reductase (*mcrA*)	Luton et al. (2002)
mcrA1530r	TTC ATT GCR TAG TTW GGR TAG TT	methyl coenzyme-M reductase (*mcrA*)	Luton et al. (2002)

Table A.2 – Thermal cycler programs used for primers described in Table A.1.

Primer Set		Initial	Amplifiction					Final
		Denaturation,	Denaturation	Annealing		Elongation		Elongation,
Forward	Reverse	94 °C (min)	94 °C (sec)	°C	sec	72 °C (sec)	Cycles	72 °C (min)
341f	533r	2	15	52 *	15	20	30	7
8f	1492r	3	30	50	30	90	25	7
apsA-7f	apsA-8r	3	30	63	30	60	35	7
M13f	M13r	3	20	55	30	90 **	35	7
W49f	W104r-6FAM	2	30	61	30	30	25	10
341f	1492r	2	15	53 *	15	70	35	7

* Touchdown every two cycles to 47 °C

** Elongation time varies depending on size of insert

A.7 Cloning

Using TOPO TA Cloning Kit for Sequencing (Invitrogen Catalog # K4575-01) with pCR 4-TOPO vector and One Shot TOP 10 chemically competent cells

A.7.1 LB Agar Plates

1. Autoclave LB agar mixture
    a. 250 mL deionized water with 10.0 grams of LB agar
2. Cool until bottle can comfortably be held against your skin (50-55 °C)
3. In the laminar hood:
    a. Add 250 uL of fresh kanamycin (25 mg/mL)
        i. Final concentration in agar should be 50 ug/mL
        ii. Kanamycin can be stored in the -20 °C freezer for *up to 1 month*
    b. Swirl gently to mix
4. Pour plates and allow to cool in a stack until agar solidifies
    a. Should have 10 to 12 plates from 250 mL of agar
5. Move to incubator, 37 °C, and place them upside down with so that any condensation is removed
6. Store in refrigerator in a *sealed* plastic bag

A.7.2 Ligation/Cloning

1. Pre-warm plates and incubator before starting
2. Remove tube of competent cells from -80 °C freezer and place on/in ice immediately
   Note: The competent cells are very sensitive! Have as much of the tube touching an ice cube as possible so that the thawing process is slow. Never hold the tube by the bottom as your body heat will affect their transformation efficiency
3. Ligation recipe (in a PCR tube)
    a. 0.5 – 4.0 uL PCR product (uncleaned)
       Note: Amount to add is dependant on strength of original PCR product band. Typical volume is 2-3 uL.
    b. 1 uL Salt Solution
    c. Sterile water to a total of 5 uL
    d. 1 uL pCR 4-TOPO vector
4. Gently flick the tube to mix the components, then tap to get all liquid to the bottom
5. Let stand at room temperature for 20-25 minutes
6. Add 2 uL of ligation product to thawed competent cells
    a. Retain remaining ligation product and store at -4 °C until cloning reaction verified
7. Incubate on ice for 25-30 minutes
8. Shock at 42 °C for 30 seconds in a hot water bath
9. Add 250 uL S.O.C. medium *gently* to the side of the tube and *gently* mix by swirling

10. Incubate horizontally at 37 °C for 1 hour at 225 rpm
    Note: Alternatively, tube can be rotated by hand every 10 minutes
    a. Incubate plates at 37 °C for 16-18 hours until colonies are clearly visible and large enough to harvest with pipette tip

A.8 ARDRA

Using MspI Restriction Enzyme (Promega Catalog # R6401)

1. Restriction digest master mix
    - Sterile DI water 15.3 uL
    - 10X Buffer B 2.0 uL
    - Bovine serum albumin 0.2 uL
    - MspI Enzyme 0.5 uL
2. Aliquot 18 uL into 0.5 mL tubes
3. Add 2 uL of M13 PCR product per tube
4. Incubate at 37 °C for 4 hours at 100 rpm
    - Incubation time and agitation rates must be constant when comparing samples digested at different times
5. Run 3.0% agarose gel on digestion products
    - o For each digestion product, mix
        - ▪ 1.5 uL 1:1000 SYBRGreen:DMSO mix
        - ▪ 3.0 uL loading dye
        - ▪ Entire digest product (~20 uL)
    - o Load 20 uL of mixture per well
        - ▪ Suggested gel loading pattern

Lad	1	2	3	4	5	6	7	8	9	10	Empty	Lad	11	12	13	14	15	16	17	18	19	20

6. Suggested comparison method
    - o Cut gel into pieces corresponding to ladder and 10 samples
    - o Take individual pictures of each piece
        - ▪ Make sure gels are straight horizontally
        - ▪ Make sure zoom is same for each picture
    - o Copy pictures into PowerPoint
    - o Line up the ladder of each picture and then put all pictures in a single row
    - o Compare banding patterns either with lines for each band in a given well or by copying each lane and moving it across the row of pictures

A.9 CE-SSCP

A.9.1 Preparing Polymer and Buffer

Do not use chemicals (polymer or buffer) presenting a precipitate at room temperature. Always measure the components of the polymer and buffer by weight.

A.9.2 CE-SSCP Polymer

- 1X TBE
- 10% Glycerol
- 5.6% GeneScan Polymer

To make ~4 mL of the polymer, weigh the following in a 15 mL centrifuge tube:
- 0.4 gm 10X TBE (filtered with 0.22 um syringe filter)
- 0.4 gm UltraPure glycerol
- 3.2 gm 7% GeneScan polymer

Combine, vortex, and allow any bubbles to settle out for a minimum of 4 hr at 4 °C.
Before use, allow polymer to warm to room temperature for 15-30 min.
Polymer can be stored for up to 1 month at 4 °C.

A.9.3 CE-SSCP Buffer

- 80% Water
- 1X TBE
- 10% Glycerol

To make ~40 mL of the buffer, weigh the following in a 50 ml centrifuge tube:
- 32 gm NanoPure deionized water (filtered with 0.22 um syringe filter) (
- 4.0 gm 10X TBE (filtered with 0.22 um syringe filter)
- 4.0 gm UltraPure glycerol

Combine and vortex to mix. Buffer can be stored for up to 3 months at 4 °C.

A.9.4 Adding Polymer to the Syringe

The polymer only needs to be added if there is not enough polymer for flushing the block (0.05 – 0.1 mL), filling the capillary, and completing the runs (10 uL each).
1. In the data collection software, open the Manual Control Window from the Window drop down menu.
2. Select and execute Home Syringe from the Function menu list.
3. Flip the drive toggle to the left once it is done moving.
4. Remove the syringe from the block by unscrewing it at the metal base.
   Note: Do not unscrew the syringe by the glass barrel.
5. Slowly draw ~0.05 mL of polymer into the syringe and use it to coat the inside of the barrel; discard after coating.
6. Slowly draw the necessary amount of polymer into the syringe.
   1. Remove any air bubbles from the syringe by inverting, gently tapping the syringe barrel, and pushing the bubbles out.
   2. Wipe down the syringe with a damp Kimwipe to remove any polymer on the outside. Dry the outside of the syringe with another Kimwipe.

3. Re-attach they syringe to the pump block by screwing in the syringe (finger tight) at the base.
4. Flip the drive toggle back to the right.
5. Select Syringe Down from the Function menu list. Enter 50 into the value box and click Execute. Repeat until the drive toggle touches the top of the syringe plunger.
6. Click Execute one additional time to flush the block and remove any bubbles in the block.

A.9.5 Filing Buffer and Water Reservoirs

The solutions in the buffer and water reservoirs should be changed at the beginning of each run. For runs longer than 24 hours, the buffer and water reservoirs should be filled with fresh solutions every 24 hours.

1. Press the Tray button.
2. Remove the anode buffer reservoir by pulling and twisting gently on the jar.
3. Fill the anode buffer reservoir with buffer to the red line and place the reservoir back on the pump block.
4. Remove the glass vials and plastic tube from the autosampler (positions 1 – 3) and discard liquid in the sink.
5. Rinse the vials, caps, septa, and tube thoroughly with NanoPure water. Dry all components thoroughly with a Kimwipe.
6. Refill one vial with buffer to the line and replace the cap and septa. Place buffer filled vial back in position 1 on the autosampler.
7. Refill the other vial with NanoPure water to the line and replace the cap and septa. Place water filled vial back in position 2 on the autosampler.
8. Refill the 1.5 mL plastic tube ¾ full with NanoPure water and place tube in back in position 3 on the autosampler.
9. Press the Tray button again to return the autosampler platform.
10. In the data collection software, open the Manual Control Window from the Window drop down menu.
11. Select Autosampler to Position from the Function menu list, type 1 in the Value cell, and click execute.
12. Select Autosample Up from the Function menu list, type 50 in the Value cell, and click execute. Repeat until the capillary and cathode are submersed ~1 cm in the buffer.

A.9.6 Creating a Sample Sheet

The sample sheet is used to define a sample's location in the 96 sample tray.

1. In the data collection software, choose New from the File menu.
2. Select GeneScan Smpl Sheet 96 Tube.
3. Enter the sample name in its corresponding location in the 96 sample tray.
   Notes: A blank sample with only the ROX standard (called roxonly) should be

included with each run. Two locations in the 96 sample tray should also be left open for the Test CCD module (called testccd) and the capillary fill module (called seqfill). Any comments or notes should be entered in the line corresponding to the blue box.

4. Select Save from the File menu and name the sample sheet.
5. Exit the Sample Sheet.

A.9.7 Creating an Injection List

The injection list defines the order the samples are injected, and allows for additional capillary flushes and detector checks.

1. In the data collection software, choose New from the File menu.
2. Choose GeneScan Injection List.
3. Enter the operator name or initials.
4. From the Sample Sheet box near the top of the screen select the sample sheet corresponding to the samples to be analyzed.
   a. A list of all named samples from the Sample sheet will appear.
5. Highlight the top row of the injection list and then choose Insert Row from the Edit menu. Repeat three times (total of four new rows).
   a. In the Tube and Sample Name cell, choose testccd for the first and third injections.
   b. In the Tube and Sample Name cell, choose seqfill for the second injection.
   c. In the Tube and Sample Name cell, choose roxonly for the fourth injection.
6. Assign the remaining injections using the same method.
   Note: For analyses with a large number of injections, the four injections described in Step 5 should be included approximately every 15 injections.
7. Select SSCP 32 min – GS STR POP4 (1mL)D.md4 in the Module column for all the injections except the testccd and seqfill ones.
8. Select SSCP_MatrixD_updated.mtx in the Matrix column for all the injections except the testccd and seqfill ones.
9. For the testccd injections, choose TestCCD-4color.md4 and Bogus.md4 in the Module and Matrix columns, respectively.
10. For the seqfill injections, choose SeqFill Capillary.md4 and Bogus.md4 in the Module and Matrix columns, respectively.
11. Once the samples are loaded into the instrument, click the green arrow to begin the run.
    Note: Click OK if a warning message appears that reads "The EPA current is zero!"

A.9.8 Sample Preparation

1. Prepare a master mix using Hi-Di Formamide (stored at –20 °C) and the ROX size standard (stored at 4 °C) for the number of samples plus one blank.
   Note: The Hi-Di Formamide cannot be thawed more than once.

a. Master Mix for 1 sample
    - HiDi Formamide 18.8 uL
    - ROX size standard 0.2 uL
2. Combine the needed amount of each reagent in a sterile tube and vortex to ensure homogeneity.
3. Place the MicroAmp sample tray in a 96-well PCR tube rack. Load the sample tubes through the sample tray so that they rest in the PCR tube rack. One tube will be needed for the ROX standard.
4. Place the MicroAmp retainer on top of the MicroAmp sample tray so that the sample tubes are locked into position.
5. Aliquot out 19uL of the master mix into each tube.
6. Add 1uL of each sample.
   Note: Ensure the location in the MicroAmp tray corresponds to the prepared Sample Sheet.
7. Push the Genetic Analyzer Septa Strips into the tubes so that each tube is covered.
   Note: Verify that each septa is open; a sterile 10 uL pipette tip can be used to open the septa if necessary. The septa strips can be cut to fit using a razor blade.
8. With the septa strips in place, denature samples for 5 minutes at 95 °C on the thermocycler.
9. Immediately place samples on ice water for 15 minutes and keep refrigerated until ready to use.
10. Remove any air bubbles from the Sample Tubes by spinning the entire MicroAmp tray in the Salad Spinner.
11. Place a Genetic Analyzer Retainer Clip directly over each Septa Strip; the clip will snap onto the sides of the MicroAmp Tray and will fit into the holes of the Septa Strip.
12. Open the instrument doors and press the Tray button located on left side of the instrument to move the autosampler tray forward.
13. Place the MicroAmp tray on the 96 sample tray Adaptor.
    Note: The PCR tube rack is no longer needed.
14. Press the Tray button again to return the autosampler to its original position.
15. Close the instrument doors.

A.10 Ion Chromatography

A.10.1 Equipment Description

Instrument

Metrohm 861 Advanced Compact IC with MSM and CO2 Suppressor

Column

Metrospec A Supp 5 High Resolution Anion Column, 250 mm (6.1006.530)

Software

IC NET Chromatography Control and Data Acquisition System

Flow: 0.7 mL/min

Minimum/maximum Pressure: 0 MPa / 20 MPa

Instrument configured for EPA Method 300.0

A.10.2 Sample Preparation

1. ~1.5 mL effluent sample removed from anaerobic serum bottle with hypodermic needle and disposable syringe
    a. Syringe and needle vigorously rinsed 5 times with DI water between each sample
2. 1.0 mL (measured with micro-pipette) is added to 9.0 mL of DI (measured with 10 mL pipette) in a IC vial and immediately capped with snap-top lid

A.10.3 Calibration Standard Preparation

1. A 100 mg/L stock solution is prepared via 1:10 dilution with ultrapure DI water of commercially purchased 1000 mg/L solution (Acculon^{TM} Reference Standard Multi-Component Anion Mix 11 – Ion Chromatography Standard, IC-MAN-11-1)
2. 50, 10, and 5 mg/L are prepared via dilution with ultrapure DI water from the 100 mg/L stock solution
    a. A duplicate 50 mg/L standard is also prepared
3. Calibration standards are analyzed in increasing order at the start of each analysis set (12-15 samples).
4. The additional 50 mg/L standard is analyzed at the end of the analysis set

A.10.4 Instrument Calibration

1. The four calibration standards are defined using the IC NET software
2. A manual check of peak integration of each standard chromatogram is performed
    a. Integration is corrected as necessary
3. IC NET software generates calibration curve based on peak areas and defined concentrations of the four standards
    a. A minimum R^2 correlation value of 0.999 is manually verified
4. The calibration curve is applied to the remaining samples in the analysis set using the IC NET software

A.10.5 Startup Procedure

1) Verify that there will be enough eluent, deionized water, suppressor regenerant solution, and autosampler rinse water for the number of samples in question (note: the rate of which the eluent is consumed is about 20 mL per sample).
    1.) Eluent – we typically use bagged eluent.
        - If making from scratch, the eluent consists of:
            - 3.2 mM Na_2CO_3
            - 1.0 mM $NaHCO_3$.
                - 0.678 g of Na_2CO_3 and 0.168 g $NaHCO_3$ in 2 L DI water.

- The suppressor regenerant solution is 100 mM H_2SO_4.
    - 5.6 mL of 37% sulfuric acid to 1 L of ultrapure water.

2) Open program IC Net 2.3.
3) Press icon in the upper right on the tool bar. A new window will open displaying the three components of the IC.
4) From this window select "Startup Hardware (measure baseline)" from the control menu.
5) Double click the IC unit icon from the warm-up window to open the instrument control window. Click the "Step" button. The suppressor should be stepped 3 times with 10-25 minute delays until a stable baseline is reached.
6) During "stepping" procedures (previous step), load sample vials into autosampler tray and set up sample queue (sample queue setup is presented below).
7) When the warm-up is complete it should have reached a steady state and the pressure should read about 10 MPa and the conductivity should read about 1.0 μS/cm, record these values in log book.

A.10.6 Starting a Sample Queue

1) After the warm-up is complete select "Sample Queue" from the system menu. Create a file name for which the data will be stored.
2) Check the "Shut down system after the queue finishes" option. Then click on the "Edit" option - a Queue Editor window will open.
3) For samples, standards and, and blanks the "System" column should read anions.
4) Add the identity of the samples, standards, and blanks to be tested to the Ident column.
5) Add the vial number associated to the identity to the "Vial" column.
6) If a dilution was performed the program will account for this if a number is placed in the "Dilution" column.
    a. e.g. 100 is entered for a 1:100 dilution
7) This queue should be saved by clicking on the second icon from the left.
8) Click the check mark icon (the second icon from the right) and the Queue Editor window will close.
9) Click "Start" to begin the testing.

A.11 Microwave Digestion for Inductively Coupled Plasma Atomic Emission Spectroscopy (from EPA method 3015)

1. Filter ~15 mL of effluent through a 0.2 um filter (Fisher # 09-719-2B).
2. In a graduated cylinder, measure 10 mL of the filtered effluent (a smaller or bigger sample size can be used but the final volume prior to addition of nitric acid has to be 45 mL).
3. Add DI water to 45 mL.
4. Transfer the solution to a digestion vessel.
5. In the fume hood:
    1. Add 5 mL of nitric acid

2. Insert the pressure relief disks in the orange caps.
   Note: If the disks are not broken during the digestion, they can be re-used up to three times.
3. Place each digestion vessel into a microwave vessel and close them tightly. Also tighten the orange caps with the pressure relief disks.

6. Turn on the microwave digester.
7. Press F3 to disable temperature unit.
8. On the outside of the unit, back left, turn the valve counterclockwise to the horizontal (open) position and remove the syringe.
9. Place an empty beaker in the microwave cavity and place the open end of the pressure sensing line in the beaker.
10. Fill the syringe with DI water and remove the air.
11. Attach the syringe back to the open end of the fill tubing.
12. Push the plunger on the syringe to force water into the pressure control system until water begins to come out of the pressure tubing into the beaker. As soon as this happens, turn the valve to the vertical (closed) position.
13. Remove the beaker from the microwave cavity and discard the water.
14. Press F1 System Setup.
15. Press F4 Temp options.
16. Press F2 disable temp unit ("off" on top of panel).
17. Press "O" to exit.
18. Press F1 System Setup.
19. Press F2 calibrate.
20. Press F2 pressure calibrate.
21. Press F2 Zero transducer.
22. Press Enter.
23. Distribute the vessels evenly in the carrousel. When less than 8 samples are digested, fill the remaining vessels with 45 mL of water and 5 mL of nitric acid.
24. Connect pressure line to control vessel.
25. Press "0".
26. Press F4 to use EPA methods.
27. Press 3 (liquids) or 5 (solids) for EPA 3015 or EPA 3051, respectively.
28. Press F1 to start.
29. Press F1 for "yes" correct vessels.
30. After done, wait until pressure drops to at least to 20 psi .
31. Vent the orange caps slowly.
32. Allow vessels to reach 0 psig.
33. Transfer from microwave to fume hood and open slowly
    Note: An orange/yellow vapor will comes out.
34. Allow to cool in hood ~15 minutes or until comfortable temperature to handle.
35. If the digested sample contains particulates which may clog nebulizers or interfere with the injection of the sample into the instrument, the sample may be centrifuged, allowed to settle or filtered.
36. Store ~30 mL of the digested sample in glass containers that have been acid-wash and rinsed in DI water three times.

Appendix B Estimation of Diversity and Richness from DGGE and CE-SSCP Data

B.1 Background

A diversity index can be used to characterize the richness, the total number of species, and evenness, the distribution of those species, of community. These indices have the benefit of distilling a consortium of different species into a single numerical representation, allowing for direct comparisons between consortia. One of the most common indices used in microbial ecology is the Shannon Diversity Index (Equation B.1):

$$H = -\sum\left[\frac{n_i}{N}\log\left(\frac{n_i}{N}\right)\right] \qquad \textbf{Equation B.1}$$

where n_i is the count of species i and N is the total count of the community. Another popular microbial ecology index is the Simpson Index (Equation B.2):

$$D = \frac{\sum_i n_i(n_i - 1)}{N(N-1)} \qquad \textbf{Equation B.2}$$

where ni and N are the same as defined above. There are two other common permutations, the Simpson Reciprocal Index (SRI) (Equation B.3) and the Simpson Index of Diversity (SID) (Equation B.4); it is important to know which form is used when comparing communities.

$$SRI = \frac{1}{D} \qquad \textbf{Equation B.3}$$

$$SID = 1 - D \qquad \textbf{Equation B.4}$$

Many other diversity indices have been developed for both macro- and micro-scale ecology comparisons, and in general, all attempt to incorporate the richness and evenness of a community into a single, representative number. These indices have been developed and modified around count-based data sets, such as clone libraries, and thus their application towards microbial community profiling data, such as DGGE or CE-SSCP profiles, may not be appropriate.

Current application of the diversity indices to DGGE or CE-SSCP data considers only the well-defined peaks (DGGE banding patterns can be converted into intensity profiles with band intensity on the y-axis and distance traveled on the x-axis). This approach is at best a crude estimation of the overall community diversity because only the dominant species are considered. The approach also fails to incorporate all of the information available in typical DGGE/SSCP profiles, namely the profile regions that have a non-zero (or background level) intensity but that are not associated with a defined peak. It is hypothesized that these elevated regions of the profiles correspond to non-dominant species, and thus their incorporation into the diversity index calculation would result in a more accurate estimation of the overall community diversity. Unfortunately, the number of species that contribute to the elevated intensity regions can not be determined in a time and cost effective manner, and thus an estimate of the total number of species in the community (the richness) must be estimated. A wide variety of richness estimators have been developed and many reviewed by Colwell and Coddington (1994) and Chao (2005).

B.2 Concept Status

It is hypothesized that the overall community diversity can be more accurately estimated by including information relating to the non-dominant species. To current conceptual approach for making the diversity index entails:

- Estimating the total number of species in the community via a richness estimator that uses the defined peaks of a DGGE/SSCP profile as its inputs
- The number of non-dominant species is estimated as the difference of the total number of species (step 1) and the number of defined peaks
- The DGGE/SSCP profile intensity which is not attributed to dominant species (in the form of defined peaks) is considered to be the contribution of the non-dominant species, and is distributed between the estimated number of non-dominant species
- The diversity index can be estimated using the peak areas of the dominant-peaks areas/numbers of estimated non-dominant species

To date, the need to include non-dominant species in the diversity estimation has been conclusively validated with simulated data sets (see Example). Diversity index calculations from real DGGE profiles and clone libraries from the same sample also indicate the need to include the non-dominant species based on significantly lower values DGGE-based index values compared to the clone libraries. Using clone library data, several richness estimators have been evaluated: classic Chao1, bias-corrected Chao1, classic Chao2, bias-corrected Chao2, Abundance-based Coverage Estimator (ACE), and Curtis (2002) (Equation B.5); an excellent description of the Chao estimators and ACE can be found in the Appendix B of the EstimateS software manual, available on line at http://viceroy.eeb.uconn.edu/.

$$S(N)=\frac{S_T \cdot a}{\sqrt{\pi}} \cdot \exp\left[-\left(a \cdot \log_2\left(\frac{N}{N_0}\right)\right)^2\right] \qquad \textbf{Equation B.5}$$

where a is related to standard deviation of peaks/bands, ST is total number of taxa (corresponds to the area under S(N) and is a measure of the extent of diversity), and N0 is the modal abundance.

Due to the limited size and coverage of the clone libraries used for evaluation, no particular estimator was identified as being more applicable. Several methods for finding peaks were also evaluated, including simple change of slope requirements, wavelet functions, and expectation-maximization (EM) algorithms. The most promising method evaluated was the Rival-Penalized EM algorithm (RPEM) of Cheung (2005), although the technique was not fully explored due to input parameter issues associated with the author supplied source code.

Example

Assume a simplified DGGE gel has eight distinct bands with intensities of n = {2, 1, 4, 1, 4, 6, 8, 2}. Assume also that the entire lane of the DGGE band has a total intensity of 35, while a blank lane has an intensity of 4.

The sum of the intensities from the defined bands is: $N_{sum} = 28$.

Subtracting the blank lane intensity from the total intensity gives $N_{w\_bg} = 31$.

The intensity which can be attributed to background (or phylotypes which are below the detection limit of DGGE) is: $n_{bg} = 35 - 28 - 4 = 3$.

Ignoring the background, the traditional Shannon Diversity Index is calculated as:

$$D := -\sum_{i=1}^{8} \frac{n_i}{28} \cdot \log\left(\frac{n_i}{28}\right) \qquad D = 0.807$$

If the background intensity is included in the calculation but not attributed to any particular band the SDI is calculated as:

$$D := -\sum_{i=1}^{8} \frac{n_i}{31} \cdot \log\left(\frac{n_i}{31}\right) \qquad D = 0.769$$

If the background intensity is included and is attributed to a single phylotype (band), the SDI is calculated as:

$$D := -\left(\sum_{i=1}^{8} \frac{n_i}{31} \cdot \log\left(\frac{n_i}{31}\right) + \frac{3}{31} \cdot \log\left(\frac{3}{31}\right)\right) \qquad D = 0.867$$

If the background intensity is included and is attributed to 100 different phylotypes, the SDI is calculated as:

$$D := -\left(\sum_{i=1}^{8} \frac{n_i}{31} \cdot \log\left(\frac{n_i}{31}\right) + 100 \cdot \frac{\frac{3}{100}}{31} \cdot \log\left(\frac{\frac{3}{100}}{31}\right)\right) \qquad D = 1.061$$

So the number of phylotypes has a significant effect on the diversity of the system. Plotting the SDI as a function of the number of phylotypes attributed to the background intensity further demonstrates this:

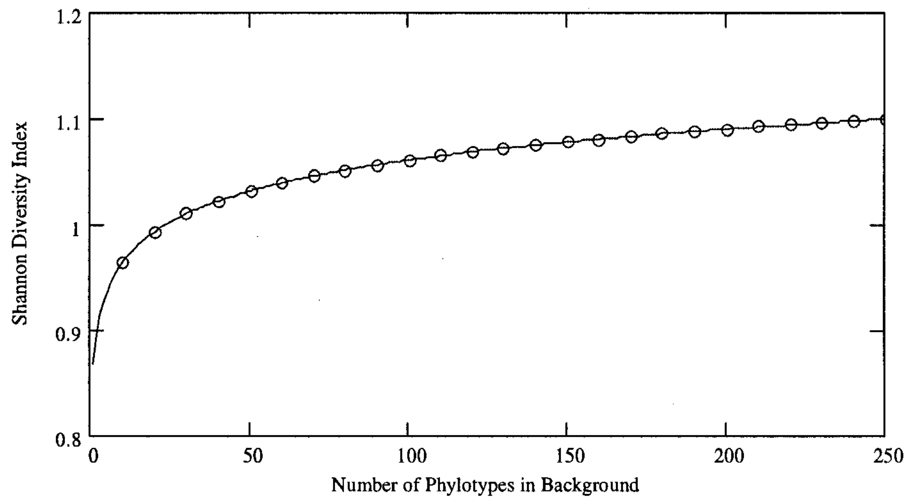

A possible method of approximating the total number of phylotypes is the nonparametric estimator described by Chao. However, this method was developed based on a sample set from which discreet samples can be drawn (for example clones harvested). To apply the method to DGGE, some form of normalization of the intensities must be done. In this simple case, assume that 1 intensity unit correlates to a single organism. Remembering the band intensities from above, n={2, 1, 4, 1, 4, 6, 8, 2} and using the terminology of Kemp and Allen (2004):

The number of phylotypes occurring only once, $F_1 = 2$.

The number of phylotypes occurring 10 or fewer times, $S_{rare} = 8$.

The number of phylotypes occurring more than 10 times, $S_{abund} = 0$.

The total number of individuals in phylotypes occurring 10 or fewer times, N_{rare} = 28.

The sample coverage is estimated as:

$$C_{ACE} := 1 - \frac{F_1}{N_{rare}} \qquad C_{ACE} = 0.929$$

The coefficient of variation is calculated as:

$$\gamma_{ACE} := \max\left[\frac{S_{rare}}{C_{ACE}} \cdot \frac{\sum_{i=1}^{10} \left[i \cdot (i-1) \cdot F_1\right]}{N_{rare} \cdot (N_{rare} - 1)} - 1, 0\right] \qquad \gamma_{ACE} = 6.521$$

The total number of phylotypes is estimated as:

$$S_{ACE} := S_{abund} + \frac{S_{rare}}{C_{ACE}} + \frac{F_1}{C_{ACE}} \cdot \gamma_{ACE} \qquad S_{ACE} = 22.661$$

The total number of phylotypes in the system would be estimated as 23, which includes both those identified as bands and those unidentified that are in the background. The number of phylotypes in the background then is, n_{back} = 23-8 = 15.

Assuming that the background intensity is spread evenly across the background phylotypes, the Shannon Diversity Index is calculated as:

$$D := -\left(\sum_{i=1}^{8} \frac{n_i}{31} \cdot \log\left(\frac{n_i}{31}\right) + 15 \cdot \frac{\frac{3}{15}}{31} \cdot \log\left(\frac{\frac{3}{15}}{31}\right)\right) \qquad D = 0.981$$

Potential concerns:

1. The nonparametric estimator was developed based on most of the information known of the population is focused in the two most prevalent phylotypes identified through sampling. The validity of the estimation isn't known for a system such as DGGE bands where there are more than two dominant species.

2. A more quantitative approach to normalizing the banding intensities than is necessary. This could potentially be connected to the amount of sample loaded in a given lane for DGGE gels, but would be more difficult to quantify for an SSCP injection.

3. The background intensity is almost certainly not distributed equally over the phylotypes not represented by bands. However, because these phylotypes are not dominant enough to have their own band, i.e. less than 1%, perhaps this assumption is acceptable.

B.3 Future Work

A number of questions must be answered to validate the approach described above.

Those questions, along with thoughts regarding them, include:

1. How should peaks be defined?
    a. Visually
    b. Based on the change in slope of the profile trace
2. What criterion should be used to differentiate between major and minor peaks?
    a. User defined on a per sample basis
    b. Some form of distribution function between based on the total area of only defined peaks
3. Can the peaks themselves be resolved sufficiently to the give a direct estimate of the diversity?
    a. Expectation-Maximization algorithms (see PowerPoint slides below)
    b. Wavelet functions
4. Should the "blank" be a PCR blank or an unloaded lane for DGGE (ROX only injection for SSCP)?
    a. A PCR blank would be more representative
    b. Intra-gel variation may require that both types are used for DGGE
2. How should non-blank background noise be accounted for?
    a. Simple subtraction of the total blank intensity from the total non-peak associated signal area
    b. Area between sample and blank along the course of the profile

B.4 References

Chao, A. 2005. Species richness estimation, Pages 7909-7916 in N. Balakrishnan, C. B. Read, and B. Vidakovic, eds. *Encyclopedia of Statistical Sciences*. New York, Wiley.

Cheung, Y. 2005. On rival penalization controlled competitive learning for clustering with automatic cluster number selection. *IEEE Transactions on Knowledge and Data Engineering* 17(6), 1583-1588.

Colwell, R. K., & J. A. Coddington. 1994. Estimating terrestrial biodiversity through extrapolation. *Philosophical Transactions of the Royal Society* (Series B) **345**, 101-118.

Curtis, TP, WT Sloan, & JW Scannell. 2002. Estimating prokaryotic diversity and its limits. *Proceedings of the National Acadamy of Science* **99**(16), 10494-10499.

Kemp PF & Aller JY. 2004. Bacterial diversity in aquatic and other environments: what 16S rDNA libraries can tell us. *FEMS Microbiology Ecology* **47**(2), 161-177.

Cluster Analysis Applied to DGGE Images as a Richness Estimator

Sage Hiibel
KFR Group Meeting
4-26-06

Background

- Traditional methods of comparing different microbial communities are based on the richness and evenness of the community
  - Richness – number of species (not individuals)
  - Evenness – proportion of individuals among the species
- Diversity indices attempt to link and relate both
- Most of the numerical methods developed to date have two major drawbacks
  - Only consider "major" species
  - Sample size sensitivity

Overall Goals

- Develop a method for calculating microbial diversity which incorporates the presence of low-abundance species
- Develop analysis for time-series-like data
  - DGGE
  - CE-SSCP
- Couple diversity index with an appropriate richness estimator

Simplified DGGE Band

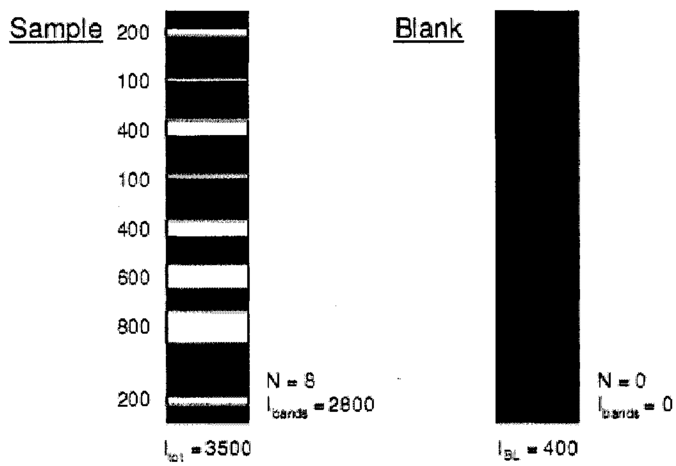

Sample Calculations

- Original Shannon Diversity Index (SDI)

$$D := -\sum_{i=1}^{8} \left(\frac{I_i}{2800} \cdot \log\left(\frac{I_i}{2800} \right) \right) \qquad D = 0.807$$

- SDI including background intensity attributed to 100 different species

$$D := -\left[\sum_{i=1}^{8} \left(\frac{I_i}{3100} \cdot \log\left(\frac{I_i}{3100} \right) \right) + 100 \cdot \frac{\frac{300}{100}}{3100} \cdot \log\left(\frac{\frac{300}{100}}{3100} \right) \right] \qquad D = 1.061$$

SDI vs. Species

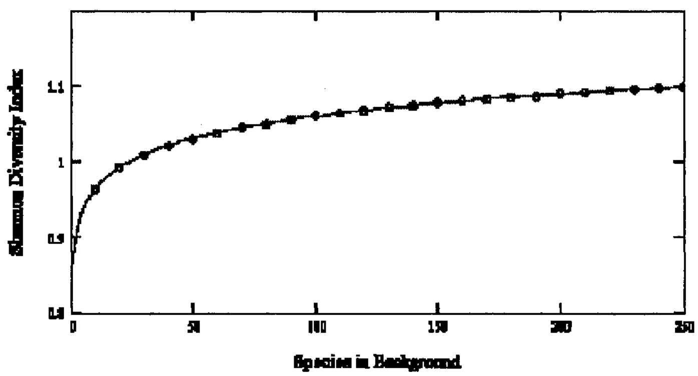

Number of species in background is significant!

Reality

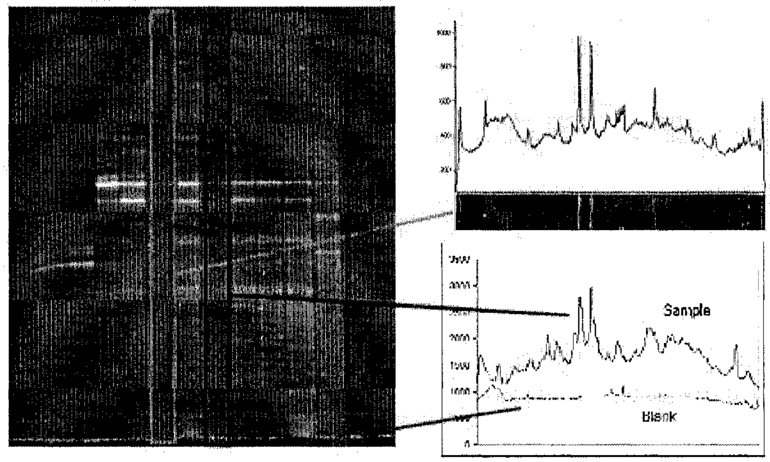

Reality (2)

- Intra- and inter-gel variation
- Blanks
- Estimating number of species challenging
- Many estimators (all claiming to be the best)
  - Extrapolation
  - Parametric
  - Non-parametric

  Require exhaustive sampling and not robust
- Distribution of species over background intensity

Previous Goal List

- Statistical analysis of data
  - Signal processing 101
- Test improved model on simulated data
  - Many bands
  - Few bands
  - High background
  - Low background
- Test improved model on real data from lab
  - DGGE with corresponding clone libraries
- Test and compare model with literature data
- Publication

Statistical Analysis 101

- Changed gears to "Data Fitting 101" after confusing most of the Stats Department
- New idea
  - Why not fit the data and then use the fit parameters as estimates of number of species
  - Expectation-Maximization (EM) algorithm
    - Frequently used for density mixture clustering
    - Originally developed as part of the training step in a neural network

EM Algorithm

- General idea
  - Fit a series of probability distribution functions (pdf) to intensity vs. space data
  - Weighting function on the number of pdfs penalizes model for using too many pdfs
    - Rival Penalized EM (RPEM) algorithm
      - "... makes the components in the density mixture compete with each other, and rivals intrinsically penalized with a dynamic control during learning."*
      - Initially guess too many species and the algorithm will phase out extras

*Cheung, Y. 2005. IEEE Transactions on Knowledge and Data Engineering. 17 (6)

k=k* - Initially

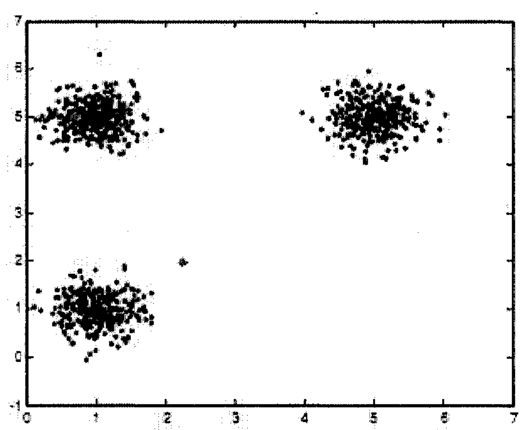

k=k* - 10 Iterations

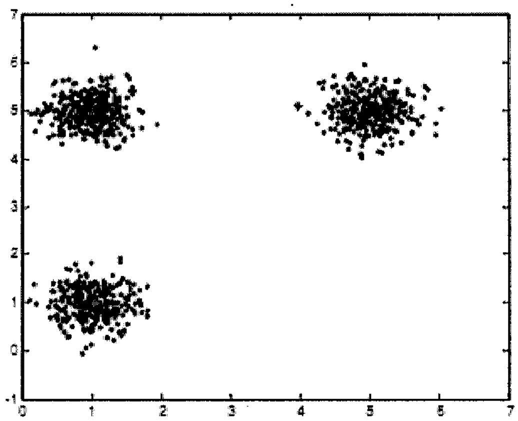

k=k* - 100 iterations

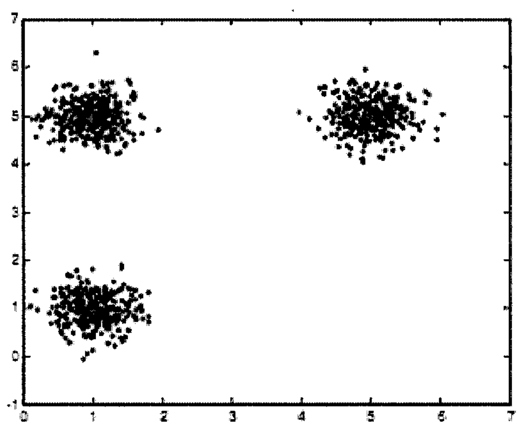

k>k* - Initially

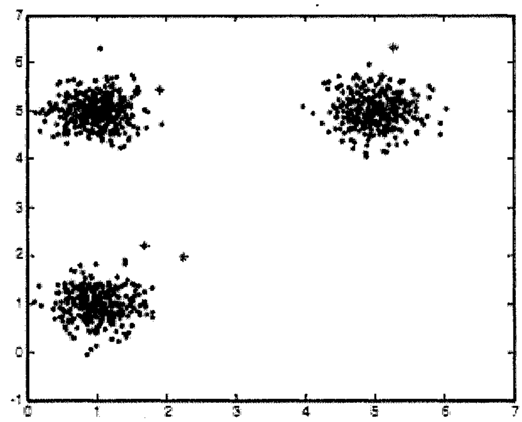

k>k* - 10 iterations

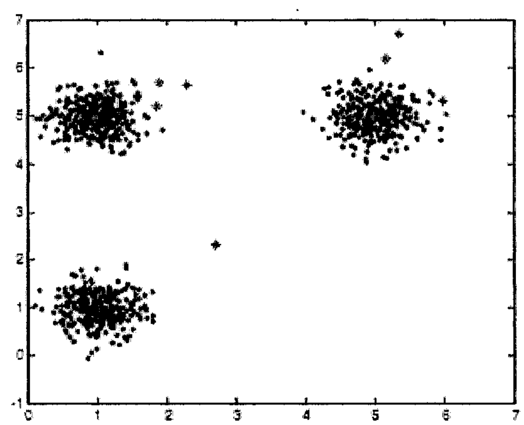

k>k* - 100 iterations

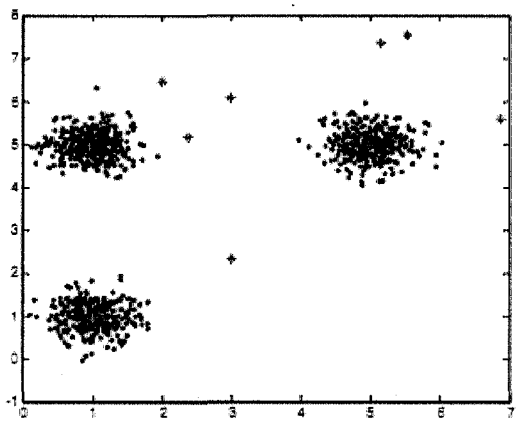

EM Algorithm as Designed

- Algorithm appears to work well with simulated data
  - Over-estimated clusters fade out
  - Mean and covariance estimated accurately
  - Smaller data sets and overlapped clusters not a problem

Simulated Data - Problems

- Finite DGGE data will not cluster as is
  - Data points equidistance on space axis
    - Weighting function necessary

$$\begin{pmatrix} 1 & 2 & 3 & 4 & 5 \\ 1 & 2 & 3 & 2 & 1 \end{pmatrix} \longrightarrow \begin{pmatrix} 1 & 2 & 2 & 3 & 3 & 3 & 4 & 4 & 5 \\ 1 & 2 & 2 & 3 & 3 & 3 & 2 & 2 & 1 \end{pmatrix}$$

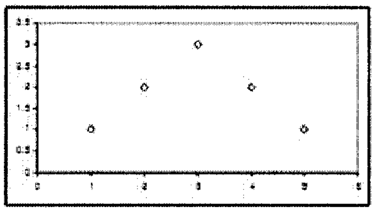

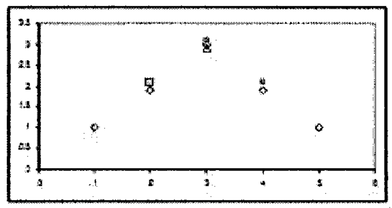

Simulated Data – Problems (2)

- pdfs are easily trapped at local clusters & convergence is slow
  - Means are randomly initialized
    - Equally distributed initial means on 'space'-axis
    - Initialize means at overall mean on y-axis

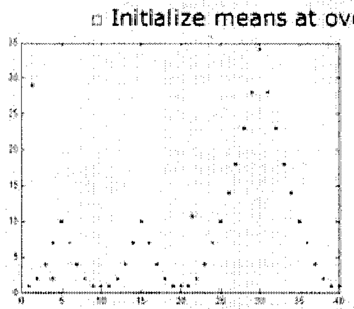

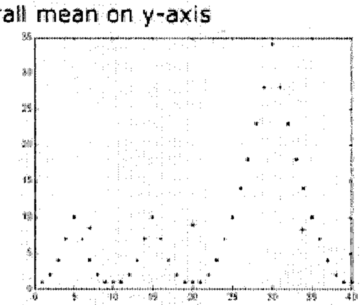

k = k* - Initially

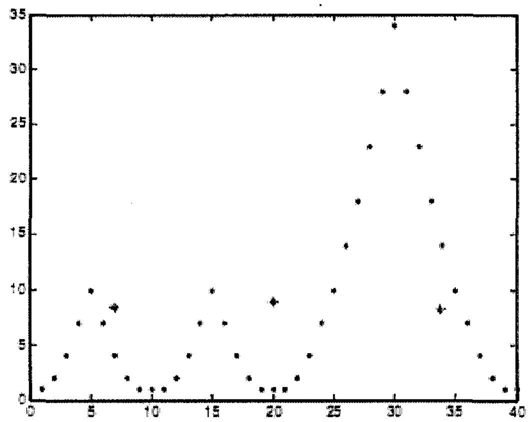

k = k* - 10 iterations

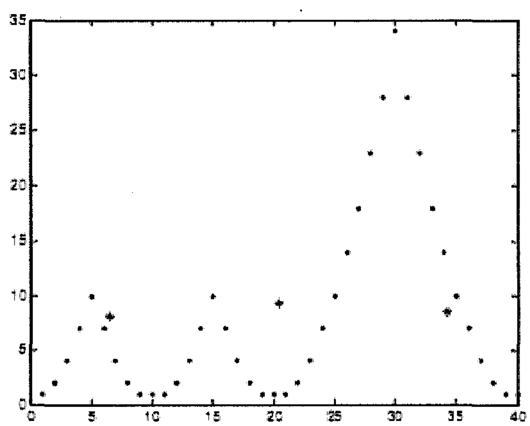

k = k* - 100 iterations

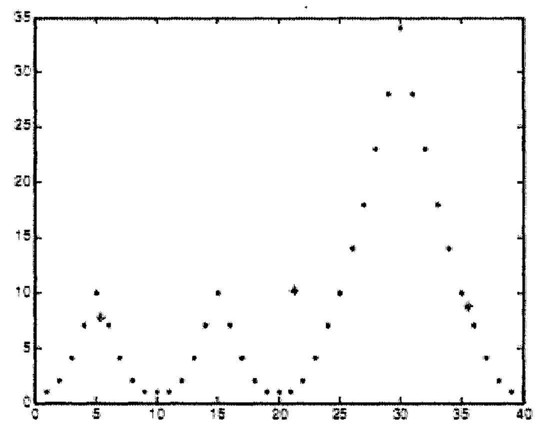

k = k* - 1,000 iterations

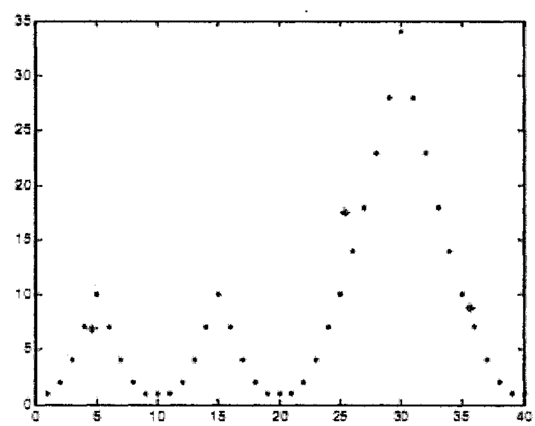

k = k* - 5,000 iterations

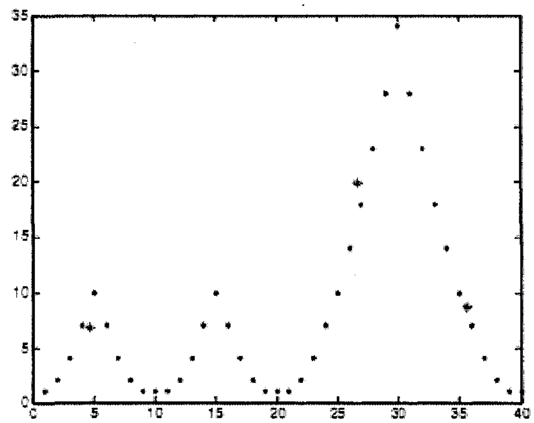

k=k*+1 - Initially

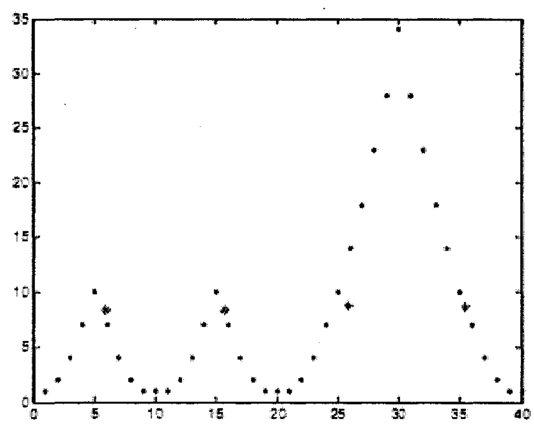

k=k*+1 - 10 iterations

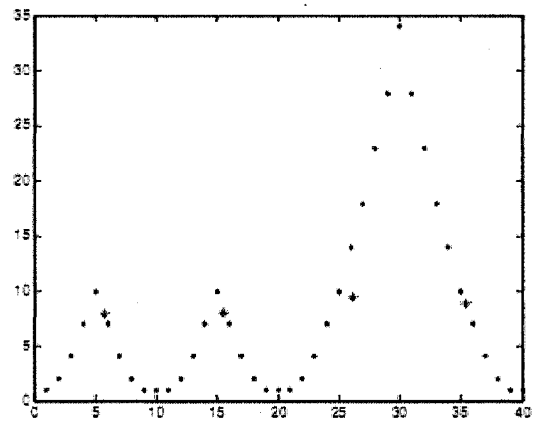

k=k*+1 - 100 iterations

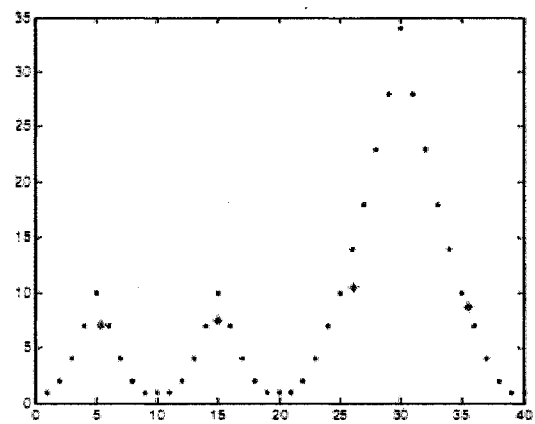

k=k*+1 – 1,000 iterations

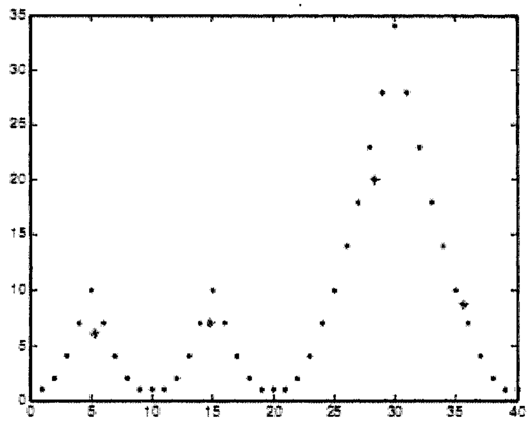

k=k*+1 – 5,000 Iterations

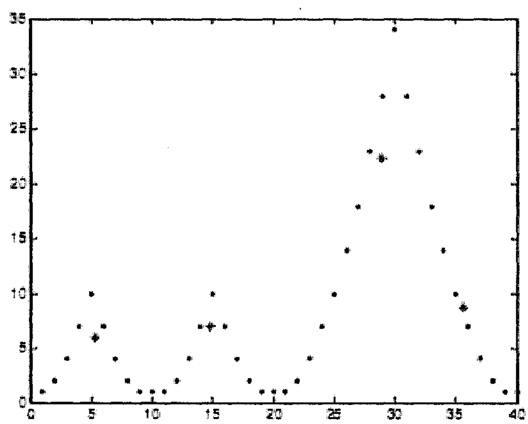

k>k* - Initially

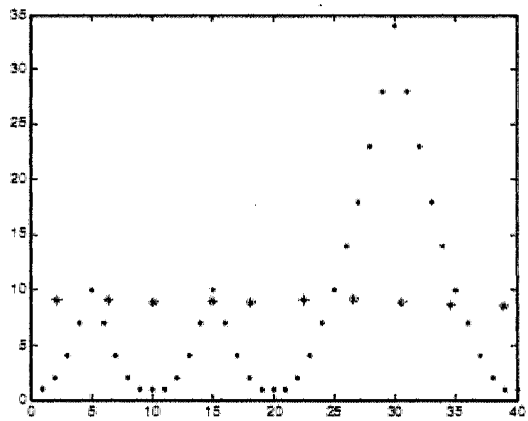

k>k* - 10 iterations

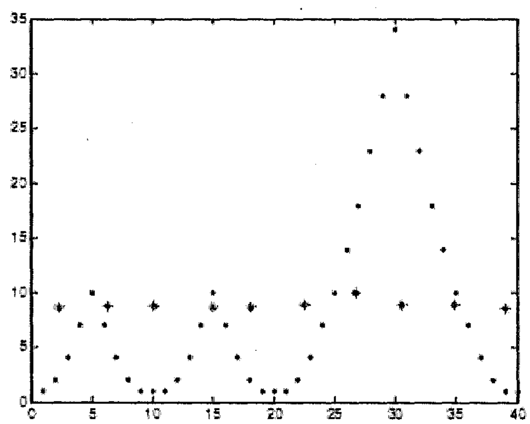

k>k* - 100 iterations

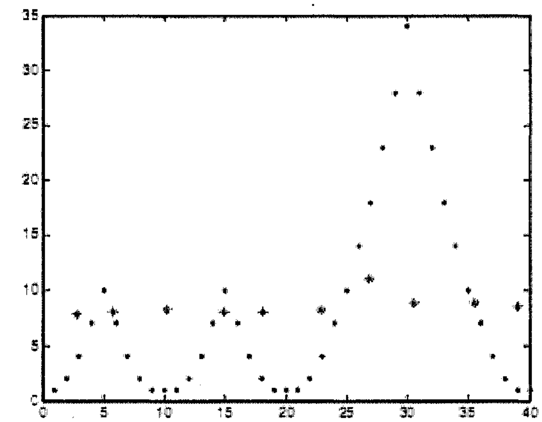

k>k* - 1,000 iterations

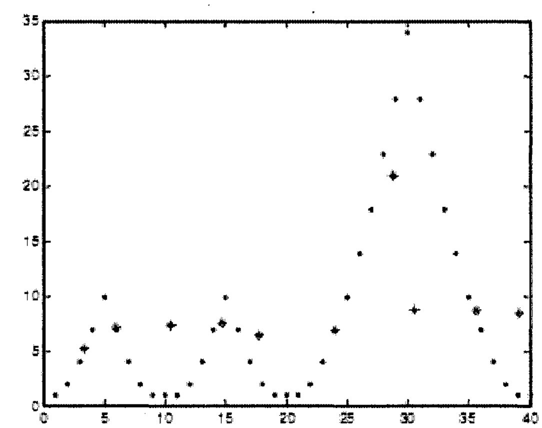

k>k* - 10,000 iterations

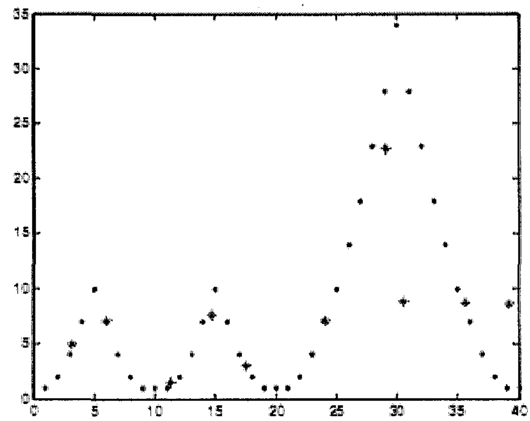

Simulated Data Conclusions

- Weighting function allows algorithm to cluster around peaks
- Spacing initial positions of pdfs minimizes chances of pdfs being trapped at local maxima
- Excess pdfs appear to faze out when k > k*

Real Data (k≈k*) - Initial

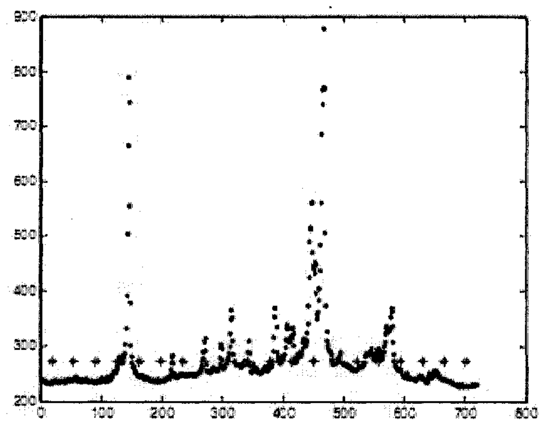

Real Data – 1 iteration

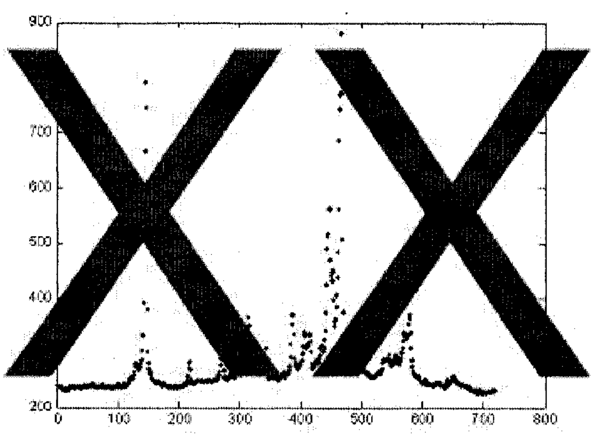

EM Algorithm vs. Real Data

- Matrix operations associated with the algorithm do not agree with real data
  - Convergence to a fit is rare
    - Fit is poor when it is found
- Code troubleshooting in progress

Idea #1

- Algorithm outputs the mean of pdfs
  - X-dimension mean linked to identity
    - Peak/band at a given position in one lane is assumed to be the same species in another lane
  - Y-dimension mean linked to quantity??
    - Compared to an included standard could give additional quantitative aspect

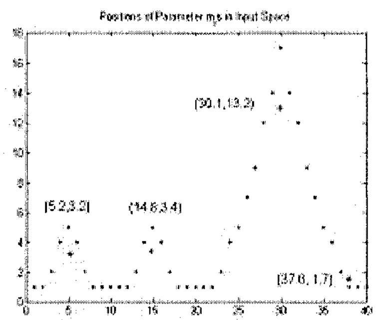

Idea #2

- EM algorithm will (?) accurately predict number of "peaks" and location from DGGE image
  - Still doesn't account for increased baseline in the gel
- Couple the fitting results (#) with a traditional or nonparametric estimator
  - Most require accurate number of observed species in sub-sample as input

Idea #2 (2)